

**LINEAR LOW DENSITY POLYETHYLENE -
BIODEGRADABILITY USING BACTERIA FROM MARINE BENTHIC
ENVIRONMENT AND PHOTODEGRADABILITY USING ULTRAVIOLET LIGHT**

*Thesis submitted to
Cochin University of Science and Technology
in partial fulfilment of the requirements
for the award of the degree of
Doctor of Philosophy
Under the
Faculty of Technology*

By

Anna Dilfi K. F.



**Department of Polymer Science and Rubber Technology
Cochin University of Science and Technology
Kochi- 682 022, Kerala, India**

August 2011

Department of Polymer Science and Rubber Technology
Cochin University of Science and Technology
Kochi – 682 022, India



Dr. Thomas Kurian
Professor

Phone: 0484-2575723 (Off)
0484-2575144 (Res)
Email: drtkurian@gmail.com

Date:.....

Certificate

This is to certify that the thesis entitled “**Linear Low Density Polyethylene-Biodegradability Using Bacteria from Marine Benthic Environment and Photodegradability Using Ultraviolet Light**” which is being submitted by Ms. Anna Dilfi K. F., in partial fulfilment of the requirements of the degree of Doctor of Philosophy, to Cochin University of Science and Technology (CUSAT), Kochi, Kerala, India is a record of the bonafide research work carried out by her under my guidance and supervision.

Ms. Dilfi has worked on the research problem for about 4 years (2007 - 2011) in the Department of Polymer Science and Rubber Technology of CUSAT. In my opinion, the thesis has fulfilled all the requirements according to the regulations. The results embodied in this thesis have not been submitted for any other degree or diploma.

Thomas Kurian
(Supervising Teacher)

Declaration

I hereby declare that the thesis entitled “**Linear Low Density Polyethylene-Biodegradability Using Bacteria from Marine Benthic Environment and Photodegradability Using Ultraviolet Light**” is the original research work carried out by me under the supervision of Dr. Thomas Kurian, Professor, Department of Polymer Science and Rubber Technology, Cochin University of Science and Technology, Kochi, Kerala, India. No part of this thesis has been presented for any other degree from any other institution.

Kochi
Date:

Anna Dilfi K. F.

Acknowledgement

I take this opportunity to express my deep gratitude to my supervisor Dr. Thomas Kurian, Professor, Department of Polymer Science and Rubber Technology, Cochin University of Science and Technology (CUSAT) for his generous, enthusiastic and inspiring guidance throughout the tenure of my research.

I am extremely grateful to Prof. Eby Thomas Thachil, Head, Department of Polymer Science and Rubber Technology, CUSAT for providing me with all laboratory facilities, and for the providence.

I express my sincere gratitude to Prof. K. E. George, Prof. Rani Joseph, Prof. Philip Kurian, Prof. Sunil K. Narayanankutty and Mrs. Jayalatha Gopalakrishnan of the Department of Polymer Science and Rubber Technology, CUSAT for their personal interest, support and valuable advice.

I am grateful to Dr. Sarita G. Bhat, Head, Department of Biotechnology, CUSAT for providing me the opportunity to work in her research group. I am thankful to Mr. Raghul Subin, Research Scholar, and other friends at the Microbial Genetic Laboratory, Department of Biotechnology, CUSAT for their immense help and support during the biodegradation studies.

I would like to thank Mr. S. P. John, Managing Director, and Staff, especially Ms. Sunitha of Jemsons Starch and Derivatives, Aroor, Kerala, India for providing the starch and dextrin samples for the research work.

The co-operation, help and lively environment extended to me by the staff and fellow researchers of the Department of Polymer Science and Rubber Technology, CUSAT are sincerely appreciated. My special thanks are due to Mr. Jineesh, Mr. Deepak and Mr. Anil for their valuable help during my research.

The good wishes, support and encouragement of my family members, especially my parents, parents-in-law, sister, brother, sisters-in-law, brothers-in-law and my husband Mr. Rijo Mathew are gratefully acknowledged.

Above all, I thank God Almighty for showering His abundant grace on me throughout the course of the research work.

Anna Dilji K. F.

Preface

The modern society in which we live in the 21st century provides enormous improvements in quality of human life. The plastics produced from petroleum resources is one of the materials, which contribute to a comfortable and convenient life style. However, as with any development, the developments in plastics production and processing technology too have resulted in unanticipated negative secondary effects. The persistence of plastics in the environment, shortage of landfill space, concerns over emissions resulting from incinerations and hazards to human health, as well as hazards to animals, birds and fish from entrapment or ingestion of plastic packaging materials have motivated materials scientists and engineers to develop novel eco-friendly materials.

Worldwide approximately 30% of the plastics are used for packaging applications. Polyethylenes, especially linear low density polyethylene (LLDPE), are one of the most commonly used plastics in packaging because of their special properties, such as toughness, flexibility, strength, ease of processing, relatively low cost, lightweight, and resistance to water and most water-borne microorganisms. LLDPE consists of molecules with linear polyethylene backbone to which short alkyl groups are attached at random intervals.

Biodegradation is a process whereby bacteria, fungi, yeasts and their enzymes consume a substance as a food source so that its original form disappears. Under appropriate conditions of moisture, temperature and oxygen availability, biodegradation is a relatively rapid process. Biodegradation for limited periods is a reasonable technique to initiate

the complete assimilation and disappearance of an article leaving no toxic or environmentally harmful residue. In recent years the development of biodegradable polymeric materials, that will have a very powerful impact on our lives, has emerged as a subject of great research challenge in materials science. The blending of biodegradable polymers, such as starch, with inert polymers, like polyethylene, has received considerable attention recently because of the possible application of this technique in the waste disposal of plastics. The logic behind this approach is that if the biodegradable component is present in sufficient amount, and if it is removed by microorganisms in the waste disposal environment, then the base inert plastic should slowly disintegrate and disappear. Addition of transition metals such as iron and cobalt is believed to promote the oxidation of polyethylenes thereby facilitating the degradation.

There has been no systematic study on the effect of bio-fillers, such as starch and dextrin, on the biodegradability of LLDPE using amylase producing vibrios, which were isolated from marine benthic environment. The effect of pro-oxidants, such as metal oxides and stearate, on the photodegradation of LLDPE too has not been systematically studied so far.

The present study aims at the preparation of biodegradable and photodegradable blends based on LLDPE. Consisting of seven chapters, the thesis portrays an introduction and literature survey in the first chapter, and describes the materials and experimental procedures employed for the study in the second chapter.

Third chapter focuses on the preparation and characterisation of LLDPE-biofiller blends. The results of investigations on the role of

various pro-oxidants on the photodegradation of LLDPE are reported in chapter 4. Chapter 5 deals with the results of the studies on the combined effect of bio-fillers and pro-oxidants on the degradation of LLDPE. Chapter 6 has been divided into two parts. The first part deals with the effect of maleation of LLDPE on the compatibility of LLDPE and the bio-fillers. The role of pro-oxidants on the photodegradation of the compatibilised blends is discussed in the second part. The conclusion of the present investigations constitutes the last chapter of the thesis.

.....❧.....

Abstract

Various compositions of linear low density polyethylene (LLDPE) containing bio-filler (either starch or dextrin) of various particle sizes were prepared. The mechanical, thermal, FTIR, morphological (SEM), water absorption and melt flow (MFI) studies were carried out. Biodegradability of the compositions were determined using a shake culture flask containing amylase producing bacteria (vibrios), which were isolated from marine benthic environment and by soil burial test. The effect of low quantities of metal oxides and metal stearate as pro-oxidants in LLDPE and in the LLDPE-biofiller compositions was established by exposing the samples to ultraviolet light. The combination of a bio-filler and a pro-oxidant improves the degradation of linear low density polyethylene. The maleation of LLDPE improves the compatibility of the blend components and the pro-oxidants enhance the photodegradability of the compatibilised blends. The reprocessability studies on the partially biodegradable LLDPE containing bio-fillers and pro-oxidants suggest that the blends could be repeatedly reprocessed without deterioration in mechanical properties.

Keywords: Linear low density polyethylene, biodegradability, photodegradability, soil burial, bio-fillers, pro-oxidants, ultraviolet light, vibrios, maleation, compatibilisation, starch, dextrin, thermogravimetry, differential scanning calorimetry, fourier transform infrared spectroscopy, scanning electron microscopy, melt flow index, water absorption, reprocessability

.....✂.....

CONTENTS

Preface
Abstract

Chapter 1

General introduction.....01 - 46

1.1	Introduction -----	01
1.2	Modern trends in plastics-----	04
1.3	Polyethylene -----	06
1.4	Polymer degradation-----	10
1.5	Modes of polymer degradation-----	11
1.6	Biodegradation -----	13
1.6.1	Biodegradable additives -----	15
1.6.2	The role of microorganisms-----	18
1.6.3	Nutritional requirements of microorganisms -----	19
1.6.4	Starch based polymers-----	20
1.6.4.1	Biodegradation of starch -----	23
1.6.4.2	Starch hydrolysis-----	23
1.7	Photodegradation-----	24
1.8	Compatibilisation of polyethylene and bio-fillers -----	28
1.9	Scope and objectives of the work -----	32
	References-----	34

Chapter 2

Experimental techniques47 - 59

2.1	Materials-----	47
2.1.1	Polymer-----	47
2.1.2	Bio-fillers-----	47
2.1.3	Pro-oxidants-----	48
2.1.4	Other chemicals -----	48
2.2	Methods -----	48
2.2.1	Sample preparation-----	48
2.2.2	Preparation of test specimens-----	50
2.2.3	Mechanical properties -----	50

2.2.4	Thermal studies	50
2.2.4.1	Thermogravimetric analyses	50
2.2.4.2	Differential scanning calorimetry	51
2.2.5	Biodegradation studies	52
2.2.5.1	Bacterial strains	52
2.2.5.2	Purification of vibrios	53
2.2.5.3	Screening for amylase producers	53
2.2.5.4	Medium for biodegradation studies	54
2.2.5.5	Preparation of consortia of amylase producers for biodegradation studies	54
2.2.5.6	Biodegradation studies on blends using the consortium	54
2.2.5.6.1	Preparation of blends	54
2.2.5.6.2	Preparation of inoculum & shake flask culture	55
2.2.6	Soil burial test	55
2.2.7	Photodegradation studies	56
2.2.8	Melt flow indices	56
2.2.9	FTIR	57
2.2.10	Scanning electron microscopic analyses (SEM)	57
2.2.11	Water absorption	58
2.2.12	Reprocessability	58
	References	58

Chapter 3

Biodegradability studies on LLDPE using bio-fillers61 - 93

3.1	Introduction	62
3.2	Results and discussion	64
3.2.1	Mechanical properties	64
3.2.2	Thermal studies	68
3.2.2.1	Thermogravimetric analyses	68
3.2.2.2	Differential scanning calorimetry	70
3.2.3	Biodegradation studies	72
3.2.3.1	In shake culture flask	72
3.2.3.2	Soil burial test	76
3.2.4	Scanning electron microscopic studies	79
3.2.5	Melt flow test	81
3.2.6	Infrared spectroscopic analyses	83

3.2.7	Water absorption studies -----	87
3.2.8	Reprocessability -----	89
3.3	Conclusion -----	90
	References -----	91

Chapter 4

Photodegradation of LLDPE using metal oxides and a metal stearate95 - 124

4.1	Introduction -----	96
4.2	Results and discussion -----	97
4.2.1	Mechanical properties -----	97
4.2.2	Thermal studies -----	99
4.2.2.1	Thermogravimetric analyses -----	99
4.2.2.2	Differential scanning calorimetry -----	100
4.2.3	Photodegradability studies -----	102
4.2.3.1	Variation in mechanical properties -----	103
4.2.3.2	Infrared spectroscopic analyses -----	110
4.2.4	Melt flow test -----	115
4.2.5	Water absorption studies -----	117
4.2.6	Reprocessability -----	118
4.3	Conclusion -----	121
	References -----	122

Chapter 5

Combined effect of bio-fillers and pro-oxidants on the degradation of LLDPE 125 - 177

5.1	Introduction -----	126
5.2	Results and discussion -----	127
5.2.1	Mechanical properties -----	127
5.2.2	Thermal studies -----	129
5.2.2.1	Thermogravimetric analyses -----	129
5.2.2.2	Differential scanning calorimetry -----	131
5.2.3	Biodegradation studies -----	134
5.2.3.1	In shake culture flask -----	134

5.2.3.2	Soil burial test -----	139
5.2.3.3	Scanning electron microscopic analyses -----	144
5.2.3.4	Infrared spectroscopic analyses -----	147
5.2.4	Photodegradability studies -----	155
5.2.4.1	Variation in tensile strength -----	155
5.2.4.2	FTIR -----	160
5.2.5	Melt flow test -----	167
5.2.6	Reprocessability -----	170
5.3	Conclusion -----	174
	References -----	175

Chapter 6

Effect of maleation on the compatibility of LLDPE-biofiller blends and the photodegradability of the compatibilised blends in presence of pro-oxidants 179 - 223

6.1	Introduction -----	180
-----	--------------------	-----

Part A

Effect of maleation on the compatibility of LLDPE and bio- fillers

6A.1	Results and discussion -----	181
6A.1.1	Mechanical properties -----	181
6A.1.2	Thermal studies -----	184
6A.1.2.1	Thermogravimetric analyses -----	184
6A.1.2.2	Differential scanning calorimetry -----	186
6A.1.3	Biodegradation studies -----	189
6A.1.3.1	In shake culture flask -----	189
6A.1.3.2	Soil burial test -----	191
6A.1.3.3	Scanning electron microscopic analyses --	192
6A.1.3.4	Infrared spectroscopic analyses -----	194
6A.1.4	Water absorption studies -----	197

Part B

Photodegradability of the compatibilised blends

6B.1	Results and discussion -----	198
------	------------------------------	-----

6B.1.1	Mechanical properties -----	198
6B.1.2	Photodegradability studies -----	201
6B.1.3	Biodegradation studies -----	207
	6B.1.3.1 In shake culture flask -----	207
	6B.1.3.2 Soil burial test-----	213
6B.1.4	Scanning electron microscopic analyses -----	217
6.2	Conclusion -----	220
	References-----	221

Chapter 7

Conclusion.....	225 - 227
List of symbols and abbreviations -----	229 - 231
Publications -----	232 - 236
Resume -----	237 - 238

.....

GENERAL INTRODUCTION

<i>Contents</i>	1.1 Introduction
	1.2 Modern trends in plastics
	1.3 Polyethylene
	1.4 Polymer degradation
	1.5 Modes of polymer degradation
	1.6 Biodegradation
	1.7 Photodegradation
	1.8 Compatibilisation of polyethylene and bio-fillers
	1.9 Scope and objectives of the work

1.1 Introduction

Plastic materials accumulate in the environment at the rate of 25 million metric tons per annum. Polyethylenes represent 64% of plastic materials used as packaging and bottles, which are discarded usually after a very brief use [1]. Among the packaging materials, plastic carry bags are the most visible due to their large surface area and attractive colours. They accumulate in the environment due to their low degradability. Recycling of these materials is not very economic as they have very low mass [2-3]. The degradation of the plastic packaging materials at the waste composting plants is not complete. Therefore, fragments of the plastic packaging in the compost usually require screening or other processes for their removal.

The use of biodegradable plastics as packaging materials is a solution to reduce the accumulation of plastic packaging waste in the environment and visual pollution [4-5]. The biodegradable plastic materials may be divided into two groups:

- (i). The materials in the first group are intrinsically biodegradable. The materials of this group may be further divided into two classes: (a) the materials whose chemical structure allows for the direct action of enzymes (such as amylase and cellulase), and (b) the materials that become biodegradable after the action of one or more physical and/or chemical processes, like hydrolysis, photolysis or pyrolysis [3,6].

- (ii). Materials of the second group are also of two classes: (a) hydro-biodegradable polymers, such as poly (lactic acid) and aliphatic–aromatic polyesters, which need chemical hydrolysis prior to biodegradation [3,7], and (b) the polymeric materials containing pro-oxidant (or prodegrading) substances, which are known as oxo-biodegradable polymers. These materials require oxidative degradation (normally by the action of ultraviolet radiation and/or heat) in order to reduce the molar mass and to form oxygenated groups, which are more easily metabolized by microorganisms [8-9]. A pro-oxidant structure may also be incorporated into the polymeric chain [5]. Pro-oxidant additives are added at low concentrations in the formulation of conventional polymers, or even of

hydro-biodegradable resins, without changing their original mechanical and optical properties. These pro-oxidant activated materials have been used as mulch films, in agriculture [10], and as retail shopping bags and garbage bags [5,11], among many other applications. The earlier research on the degradation of polyethylene have shown that the biodegradation of polyethylene is affected by preliminary irradiation from a UV source [12-13], the presence of photodegradative enhancers [12-13], morphology, surface area [14-15], additives [16-17], antioxidants, and its molecular weight [18].

Biodegradable polymers derived from renewable sources (plants and microorganisms) are suitable for land filling. However, they are 2.5–10 times more expensive than conventional polymers and often show physical or chemical properties that restrict their use. Oxo-biodegradable materials consist of a modification of conventional plastics obtained from non-renewable resources (oil, natural gas, or coal) and renewable resources (sugar cane or corn). Currently, they constitute a more economical alternative, raising the final cost by only about 10–20% [19], as they are based on pro-oxidant additives added to polyethylenes, polypropylene, polystyrene, or other polymers. Among the substances added to the polymers as pro-oxidant additives are the compounds of cobalt, manganese and iron, as well as substances formed by polyunsaturated molecules. The composting of

the oxo-biodegradable polymers do not exhibit ecotoxicity in applied whole organism tests [6,11].

1.2 Modern trends in plastics

Plastics are among the most complex engineering materials with amazing properties that revolutionized the way in which products are manufactured. They are in almost every walk of life, ranging from the ordinary to high end application in which no other materials could serve as replacement.

Plastic materials differ from metals in respect of mechanical and other properties. These differences can be attributed to the molecular structural characteristics of the polymer base materials forming the plastics. The characteristic properties of plastic materials are responsible for their applications in many areas in preference to metals. Moreover, their unique properties make them the indispensable choice in many instances.

The key growth segment in plastics is “packaging” which accounts for over 30% of the global consumption. Amongst the individual plastics materials polyolefin accounts for 53% of the total consumption of plastics (PE 33.5%, PP 19.5%) [20].

In recent years, significant aspect of plastics material growth globally has been the innovation of newer application areas for plastics such as increasing plastics application in automotive field, rail, transport, etc. The present global per capita consumption of plastics (in kgs) is shown in table 1.1 [20].

Table 1.1 Global Per capita consumption of Plastics (in Kgs)

World Average	26
North America	90
West Europe	65
East Europe	10
China	12
India	5
South East Asia	10
L. America	18

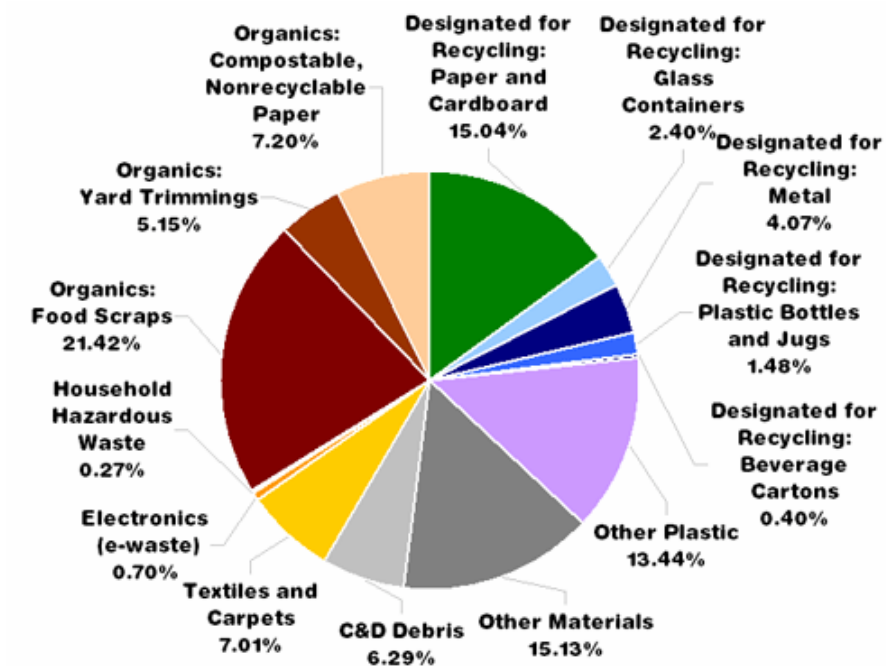
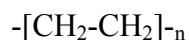


Figure 1.1 Pie chart showing the percentage of various types of plastics waste

The percentages of various plastics waste are shown in figure 1.1. The wide use of plastics causes serious environmental problems and thus demands are put on using degradable materials as well as increasing the possibilities of recycling [21].

1.3 Polyethylene

Polyethylene (PE) is the simplest hydrocarbon polymer and has the following structure:



Polyethylene is classified into several different categories based mostly on its density and branching. The mechanical properties of PE depend significantly on variables such as the extent and type of branching, the crystal structure and the molecular weight. With regard to sold volumes, the most important polyethylene grades are HDPE, LLDPE and LDPE.

- Ultra high molecular weight polyethylene (UHMWPE)
- Ultra low molecular weight polyethylene (ULMWPE or PE-WAX)
- High molecular weight polyethylene (HMWPE)
- High density polyethylene (HDPE)
- High density cross-linked polyethylene (HDXLPE)
- Cross-linked polyethylene (PEX or XLPE)
- Medium density polyethylene (MDPE)

- Linear low density polyethylene (LLDPE)
- Low density polyethylene (LDPE)
- Very low density polyethylene (VLDPE)
- Ethylene vinyl acetate co-polymer
- Ethylene ionomers

UHMWPE is polyethylene with a molecular weight numbering in millions, usually between 3.1 and 5.67 million. The high molecular weight makes it a very tough material, but results in less efficient packing of the chains into the crystal structure as evidenced by densities of less than high density polyethylene (for example, 0.930–0.935 g/cm³). UHMWPE can be made through any catalyst technology, although Ziegler catalysts are most common. Because of its outstanding toughness and its cut, wear and excellent chemical resistance, UHMWPE is used in a diverse range of applications. These include can and bottle handling machine parts, moving parts on weaving machines, bearings, gears, artificial joints, edge protection on ice rinks and butchers' chopping boards.

HDPE is defined by a density of greater or equal to 0.941 g/cm³. HDPE has a low degree of branching and thus stronger intermolecular forces and tensile strength. HDPE can be produced by chromium/silica catalysts, Ziegler-Natta catalysts or metallocene catalysts. The lack of branching is ensured by an appropriate choice of catalyst (for example, chromium catalysts or Ziegler-Natta catalysts) and reaction conditions [22-26]. HDPE is used in products and packaging such as

milk jugs, detergent bottles, margarine tubs, garbage containers and water pipes. One third of all toys are manufactured from HDPE. In 2007, the global HDPE consumption reached a volume of more than 30 million tons [27].

PEX is a medium- to high-density polyethylene containing cross-link bonds introduced into the polymer structure, changing the thermoplast into an elastomer. The high-temperature properties of the polymer are improved, its flow is reduced and its chemical resistance is enhanced. PEX is used in some potable-water plumbing systems because tubes made of the material can be expanded to fit over a metal nipple and it will slowly return to its original shape, forming a permanent, water-tight, connection.

MDPE is defined by a density range of 0.926–0.940 g/cm³. MDPE can be produced by chromium/silica catalysts, Ziegler-Natta catalysts or metallocene catalysts. MDPE has good shock and drop resistance properties. It is also less notch sensitive than HDPE, stress cracking resistance is better than HDPE. MDPE is typically used in gas pipes and fittings, sacks, shrink film, packaging film, carrier bags and screw closures.

LLDPE is defined by a density range of 0.915–0.925 g/cm³. LLDPE is a substantially linear polymer with significant numbers of short branches, commonly made by copolymerization of ethylene with short-chain alpha-olefins (for example, 1-butene, 1-hexene and 1-octene). LLDPE has higher tensile strength than LDPE, it exhibits higher

impact and puncture resistance than LDPE. Lower thickness (gauge) films can be blown, compared with LDPE, with better environmental stress cracking resistance. LLDPE is used in packaging, particularly film for bags and sheets. Lower thickness may be used compared to LDPE. Cable covering, toys, lids, buckets, containers and pipe. While other applications are available, LLDPE is used predominantly in film applications due to its toughness, flexibility and relative transparency [28-31]. LLDPE films can be treated, printed, and sealed by using the same equipment used for LDPE [32-42]. Product examples range from agricultural films, and bubble wrap, to multilayer and composite films [27].

LDPE is defined by a density range of 0.925–0.940 g/cm³. LDPE has a high degree of short and long chain branching, which means that the chains do not pack into the crystal structure as well. It has, therefore, less strong intermolecular forces as the instantaneous-dipole induced-dipole attraction is less. This results in a lower tensile strength and increased ductility. LDPE is created by free radical polymerization. The high degree of branching with long chains gives molten LDPE unique and desirable flow properties. LDPE is used for both rigid containers and plastic film applications such as plastic bags and film wrap [27].

VLDPE is defined by a density range of 0.880–0.915 g/cm³. VLDPE is a substantially linear polymer with high levels of short-chain branches, commonly made by copolymerization of ethylene with short-chain alpha-olefins (for example, 1-butene, 1-hexene and

1-octene). VLDPE is most commonly produced using metallocene catalysts due to the greater co-monomer incorporation exhibited by these catalysts. VLDPEs are used for hose and tubing, ice and frozen food bags, food packaging and stretch wrap as well as impact modifiers when blended with other polymers.

Recently much research activity has focused on the nature and distribution of long chain branches in polyethylene. In HDPE a relatively small number of these branches, perhaps 1 in 100 or 1,000 branches per backbone carbon, can significantly affect the rheological properties of the polymer.

1.4 Polymer degradation

Polymer degradation is the collective name given to various processes, which degrade polymer, i.e. deteriorate their properties or ruin their outward appearance. Conventionally, the term ‘degradation’ is taken to mean a reduction in the molecular weight of the polymer.

The degradation of polymers is provoked by exposure to various environmental factors, e.g., heat, UV radiation, ozone, chemical attack, mechanical stress and microbes, resulting in embrittlement, cracks, discoloration, etc. [43-46].

Degradation may happen during every phase of a polymer’s life, i.e. during its synthesis, processing, and use. Plastics are subjected to environmental degradation to various extents by the action of ultraviolet light from the sun or microorganisms in the soil. Heat, oxygen and moisture too accelerate the degradation.

The preparation of environmentally degradable/biodegradable polymeric systems and assessment of their propensity to degradation /biodegradation under different environmental conditions [47-50] are still going on.

1.5 Modes of polymer degradation

a) Thermal degradation:

All plastics can be chemically degraded by the influence of heat. As majority of the plastics are melt processed, heat is applied during polymer processing. Many of the plastic components experience heat during their service too. Long-term exposure to an elevated temperature condition causes a deleterious effect on the mechanical and thermal properties, as well as surface morphology of polyethylene based plastic products due to thermal degradation [43, 45, 46, 55, 57, 58, 60-68].

b) Photo oxidative degradation:

Chemical bonds in polymers can be broken by the highest energy UV waves of the solar spectrum, leading to their photodegradation.

c) Hydrolytic degradation:

Hydrolysis of a polymer can also result in the degradation of the main chain scission. Polymers such as polycarbonates, polyamides, and polyacetals can be degraded by hydrolysis

under acidic conditions present in the environment. Hydrolytic degradation takes place when polymers containing hydrolysable groups are exposed to moisture. If hydrolysis is achieved enzymatically, then the process is usually considered to be biodegradation [69-70].

d) Degradation due to environmental stress cracking (ESC):

When polymeric materials develop crazes as they are attacked by an applied stress in the presence of an external environment (detergent, polar vapours of liquids etc.) it is termed as environmental stress cracking.

e) Chemical degradation:

Chemical degradation caused by corrosive liquids and gases can affect most polymers except poly tetra fluoro ethylene (PTFE) and poly ether ether ketone (PEEK). Ozone, atmospheric pollutants (such as sulphuric oxides) and acids like, sulphuric, nitric and hydrochloric will attack and degrade most polymers.

f) Mechano chemical degradation:

Owing to their molecular chain length, polymers have the ability to convert mechanical energy applied in shear into main chain bond energy resulting in bond scission. When polymers are subjected to shear, as during processing in a screw extruder, micro alkyl radicals are formed that lead to accelerated oxidation.

g) Radiation induced degradation:

X-rays, gamma rays, alpha rays and beta rays are among the most well known high energy radiations. Like UV, gamma rays are electromagnetic radiations, but their energy level is much higher than that of UV rays. Degradation by the high energy radiations is more than that by the lower energy (UV) radiation.

h) Degradation due to weathering:

All plastics subjected to long term exposure to weather degrade to different extents depending on their composition. Weathering encompasses the effects of almost all types of degradation.

i) Biodegradation:

Biodegradation is a process by which bacteria, fungi, yeasts, and enzymes consume a substance. While synthetic polymers are not attacked by microorganisms, some additives incorporated in the plastics may act as hosts. Enhanced photo-oxidation of polymers may also increase their biodegradability.

1.6 Biodegradation

In many of the surveys on the biological degradation of synthetic polymers, it is fairly clearly stated that polyethylene is an inert polymer with good resistance to microorganisms.

Polyethylenes are easily molded into complex shapes, and have high chemical resistance. They can be formed into fibers or thin films. These properties have made them popular in many durable or disposable goods and for packaging materials. Excessive molecular size seems to be mainly responsible for the resistance of polyethylenes to biodegradation and their persistence in soil environment for a long time [22-26, 71-72]. Several reports mention, however, that fungal growth can occur on the surface of polyethylene [73-74]. Connolly and Dolezel [73] have also reported a change in tensile strength for polyethylene exposed to a biotic environment, and Kestelman *et al.* [75] have demonstrated a higher water uptake in polyethylene.

Since degradation is a chemical process, it affects not only chemical composition of the polymer but also various physical parameters such as chain conformation, molecular weight, molecular weight distribution, crystallinity, chain flexibility, cross-linking and branching. These parameters correlate with the properties of the material, hence their alteration due to degradation will produce a corresponding alteration in properties.

Koutny *et al.* have reported two types of approaches to test the biodegradability of polymers [11, 76].

One of the approaches is to evaluate the biodegradability of pro-oxidant activated polyethylene in complex media like soil, waste water sludge or compost. As this approach makes use of diverse microbial inoculums, it is apparently comparable to the real conditions

in the nature and/or in waste treatment processes. This approach was used by Chiellini et al. [47] who showed 50-80% mineralization of a pre-oxidized film incubated under compost conditions after approximately one and a half year of incubation. Jakubowicz [9] claimed about 60% mineralization during six months of incubation. Recently, Ojeda et al. [77] reported about 12% mineralization after 90 days in compost.

The second approach is to use controlled experimental conditions, i.e. experiments with identified microbial strains in a medium formulated from defined chemical compounds. This type of experiments allows a better understanding of the process fundamentals, while it could also become the basis of standardised, easy to reproduce tests. Biodegradation with defined microbial strains was evaluated in several studies, most recently with *Pseudomonas aeruginosa* strain [78-79]. In these research papers, the authors brought rather qualitative evidences that bacteria used some substances from polyethylene to support their metabolism. Koutny, et al. [80] proposed a new methodology to assess the biodegradability of polyethylene films containing pro-oxidants. In this methodology, thermo and photo-oxidized films were incubated in mineral media containing the polymer as sole carbon source in the presence of pure microbial strains previously tested for oxidized polyethylene degradation [7, 81].

1.6.1 Biodegradable additives

Polymer compounds for practical use are made by including additives such as plasticizers, lubricants, and stabilizers in the formulations. In general, these additives have a great influence on the

degradability of the final product, in both a positive and a negative respect. Scott [82], Mishi and Hagiwara [83], and Griffin [84] have used different additives to increase the degradation of polyethylene. Colin et. al. [85-86] showed that polyolefins were biodegradable, and their embrittlement data is an evidence for biodegradation. Dolezel [73], on the other hand, has shown that the tensile strength of polyethylene changes in a biotic environment.

One way by which the biodegradation of polyethylene can be accelerated, is by the incorporation of biodegradable fillers such as starch into the polymer matrix [87-89]. Among the biomaterials tested for their suitability as biodegradable fillers, only raw starch meets the requirements of high thermal stability, minimum interference with flow properties, and absence of toxicity [90]. Secondly, starch is inexpensive, of high purity, produced in large quantities and easily available throughout the year. Corn and wheat starches are produced in abundance in America and Europe, while tapioca and sweet potato starches are produced in Africa. In Asia, sago and sweet potato starches are predominant. The production of sago starch is reported to be higher than that of corn or wheat starches [91]. Plastic films containing various percentages of corn and potato starches have been commercialised. Malaysia is one of the countries with a large cultivation of sago palm (*Metroxylon Sago*) in Asia, where the starch is commonly used in many food formulations. The structures of starch and dextrin are shown in figures 1.2 and 1.3.

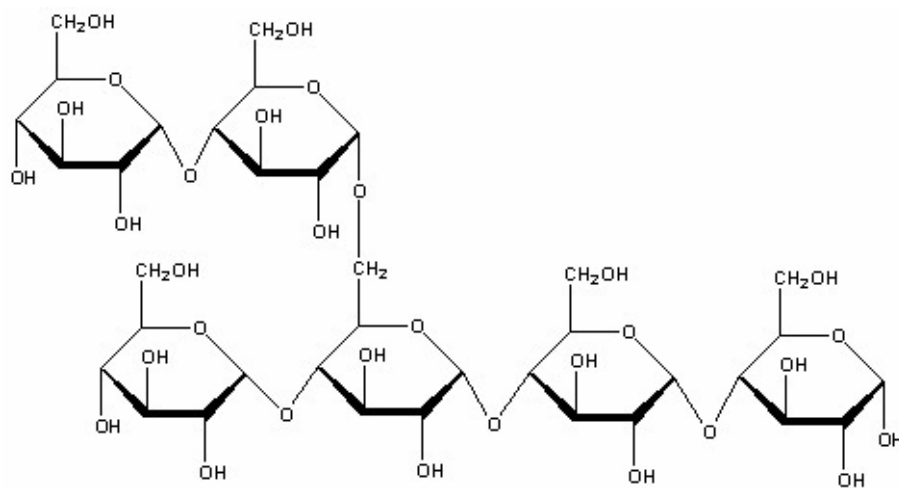


Figure 1.2 Structure of starch

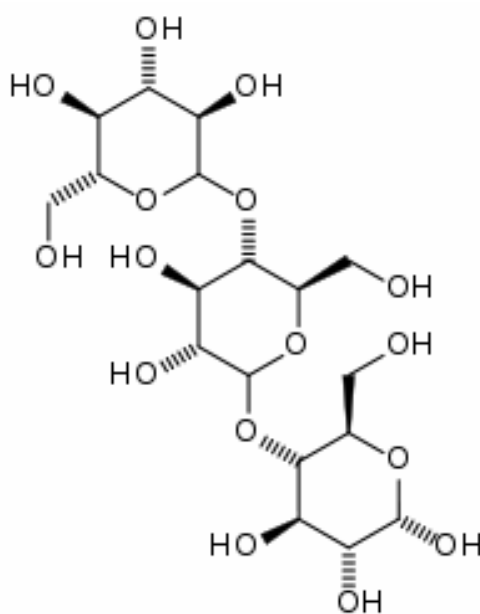


Figure 1.3 Structure of dextrin

Low molecular weight additives, usually containing various reactive groups, are much more sensitive to microbial attack than the polymer molecules. The biodegradable additives function as a nutrient, “luring” the microorganisms into the plastic and serving as a good medium for their growth, thus promoting their attack on a polymer molecule, which is otherwise “unattractive to them”. When a biodegradable additive is employed, microorganisms can easily utilize the additive. The porosity of the material is thereby increased and a mechanically weakened film is obtained. The surface area will be increased, and this film will be more susceptible than the original film to all degradation factors including biodegradation [92].

1.6.2 The role of microorganisms

Microorganisms occur nearly everywhere in nature. They occur most abundantly, where they find food, moisture, and a temperature suitable for their growth and multiplication. Some microorganisms, the bacteria in particular, are able to utilize a great variety of chemical substances as their energy source ranging from simple inorganic substances to complex organic substances [83].

Microorganisms involve viruses, bacteria, many algae, fungi and protozoa.

- Viruses are very small non-cellular parasites or pathogen of plants, and animals. These can be cultivated only in living cells.

- Algae are relatively simple organisms, the cell of which contain chlorophyll and capable of photosynthesis. These are found most commonly in aquatic environments and damp soil.
- Fungi are eukaryotic lower plants devoid of chlorophyll. They are usually multicellular but are not differentiated into stems, roots and leaves.
- Protozoa are unicellular eukaryotic organisms, which are differentiated based on morphological, nutritional, and physiological characteristics. The best known protozoa are the few that cause disease in human beings and animals.
- Bacteria are unicellular prokaryotic organisms or simple association of similar cells.

Comparing the above microorganisms, bacteria play a major role in the process of biodegradation. Cell multiplication is usually by binary fission. Bacteria have different morphological structure. They are found in soil, water, air etc. They have so many applications in the welfare of human health even though some are pathogens [85].

1.6.3 Nutritional requirements of microorganisms

As in the case of all other organisms, microorganisms too require certain basic nutrients and physical factors for the existence of their life. However, the specific nutritional requirements of various types of microorganisms vary to a great extent. Environmental factors such as temperature, oxygen levels and the osmotic concentration of the medium are critical in the successful cultivation of the microorganisms.

Analysis of microbial cell composition show that over 95% of cell dry weight is made up of a few major elements C, O, H, N, S, P, K, Ca, Mg and Fe. These are called macro elements or macro nutrients because they are required by microorganisms in relatively large amounts. Microorganisms require several trace elements also (micro elements or micro nutrients).

The requirements for C, H and O often are satisfied together. Carbon is needed for the skeleton or backbone of all organic molecules, and molecules serving as carbon sources usually contribute both oxygen and hydrogen atoms. Probably all microorganisms can fix CO₂. The reduction of CO₂ is a very energy expensive process. Thus, many microorganisms cannot use CO₂ as their sole carbon source but rely on the presence of more reduced complex molecules such as glucose for the supply of carbon [84-86].

1.6.4 Starch based polymers

Starch exists as a major carbohydrate storage product in all plants containing chlorophyll. Starch has been widely considered as a raw material in film production because of increasing prices and decreasing availability of conventional film-forming resins [93]. It finds a wide variety of uses based on its thickening, gelling, adhesive, and film-forming properties, as well as its low cost. The characteristics of the starch can be modified by chemical, physical, and/or enzyme treatment to enhance or repress its intrinsic properties or to impart new ones. This capability for modification has been a necessary factor for developing new uses for starch and maintaining old markets.

Starch has been used for many years as an additive to plastic for various purposes [94-95]. Starch was added as a filler [96] to various resin systems to make films that are impermeable to water but permeable to water vapour. Starch as a biodegradable filler in LDPE was reported [97-98]. Gelatinized starch [99-102], modified starch [88], oxidized polyethylene and dry granular starch [103] have been used as fillers to improve the biodegradability of plastics.

A starch-filled polyethylene film was prepared [103], which becomes porous after the extraction of the starch. This porous film can be readily invaded by microorganisms and rapidly saturated with oxygen, thereby increasing polymer degradation by biological and oxidative pathways. Otey *et al.* [100] in a study on starch-based films found that a starch–polyvinyl alcohol film could be coated with a thin layer of water-resistant polymer to give a degradable agricultural mulching film. Starch-based polyethylene films were formulated [101, 104] and consisted of up to 40% starch, and other additives such as urea, and poly (ethylene-*co*-acrylic acid) (EAA). The EAA acted as a compatibiliser, forming a complex between the starch and the polyethylene. The resulting blend could be cast or blown into films, and had physical properties approaching those of polyethylene.

Chemical modification of starches could improve the interfacial contact between starch granule and polymer. Griffin [88] proposed a process for making low-density polyethylene (LDPE) blown films containing native or modified starches. Swanson, Westhoff, and Doane [105] examined the effect of starch modification on LDPE

films and found that the mixture of LDPE and poly (ethylene-co-acrylic acid) (EAA) polymers filled with hydroxypropyl or acetyl derivatives of starch had a higher elongation and often had a higher tensile strength than native starch-filled films. Otey, Westhoff, and Russell [106] used a mixture of polyvinyl alcohol (PVA) and modified starch to develop water-soluble packaging plastics.

Chemically starch is a polymer of anhydroglucose units. Starch can be considered to be a condensation polymer of glucose, and yields glucose when subjected to hydrolysis by acids and/or certain enzymes. Tapioca starch granules vary in diameter from 5 to 35 μm , potato starch from 15-100 μm , while rice starch granules are only about 3-8 μm in diameter.

The shapes vary from near perfect spheres to flattened ovoids, elongated discs, polygons, and many others. The granule is not just a loose agglomeration of glucose polymers, but it is systematically structured with the starch molecules oriented in specific crystalline patterns. Although the starch granules are physically strong, they can be disorganised quite easily [96-99].

The properties of starch granules are dependent upon the arrangement of the anhydroglucose units within the starch molecule itself. The starch molecule is a homopolymer of repeating anhydroglucose units joined by an α -glucosidic linkage, the aldehyde group of one unit being chemically bound to a hydroxyl group in the next unit through an hemiacetal linkage. In most starches, the α -1,4 linkage yield straight chain molecules called amylose, while the 1,6

linkages serve as the branching point in the branched chain starch molecules called amylopectine [87].

1.6.4.1 Biodegradation of starch

Starch is a biodegradable natural polymer. It acts as a source of carbon for the metabolic activities of bacterial cells. Due to its complex structure and high molecular mass, it cannot be transported into a bacterial cell for energy production. These high molecular weight macromolecules must be hydrolysed by specific extra cellular enzymes into their respective basic building blocks. These low molecular weight substances can be then transported into the cells and used for the synthesis of protoplasmic requirements and energy production [89].

There are various types of bacteria with different properties and characteristics, which can use starch as a sole source of carbon. Therefore, addition of particular bacteria is very important for selective degradation of starch. To select suitable consortia of bacteria, starch hydrolysis test is conducted.

1.6.4.2 Starch hydrolysis

Starch degradation requires the presence of the extracellular enzyme amylase for its hydrolysis into shorter polysaccharides namely dextrans and ultimately into maltose molecules. The final hydrolysis of this saccharide, which is catalysed by maltase yields low molecular weight soluble glucose molecules that can be transported into the cell and used for energy production through the process of glycolysis [100].

In the experimental procedure starch agar is used to demonstrate the hydrolytic activities of these exoenzymes. The medium is composed of nutrient agar supplemented with starch, which serves as the polysaccharide substrate. The detection of the hydrolytic activity following the growth period is made up performing the starch test to determine the presence or absence of starch in the medium. Starch in the presence of iodine will impart a blue-black colour to the medium, indicating the absence of starch supplying enzymes and representing a negative result. If the starch has been hydrolysed, a clear zone of hydrolysis will surround the growth of the organism, which implies a positive result.

1.7 Photodegradation

Most polyolefins are insensitive to sunlight exposure in their pure state. [107-108]. A number of studies have been performed for improving thermal and UV stability of polymers by incorporating different kinds of stabilizers [109].

The actual absorption spectra of commercial polyolefins are rather complicated and they exhibit weak absorptions in the near ultraviolet region. The reasons behind this include crystallinity and thermal history of the polymer. All the polyolefins may be subjected to heat treatment in the presence of air. These operations increase the susceptibility of the polyolefins to sunlight through the formation of chromophores such as carbonyl groups, hydroperoxide and unsaturation. Metallic impurities such as iron and titanium incorporated into polymers during processing also act as chromophores. Some

chromophoric impurities are absorbed from the atmosphere during storage of polymers [110]. Oxygen-polymer charge-transfer (CT) complexes are also light-absorbing species [111-112]. When polyolefins containing such chromophores absorb photoenergy, some of their electrons in the ground state are raised to higher energy states. Since these latter states are unstable, they discharge excitation energy by various photophysical and photochemical processes. In photophysical processes, the excitation energy is spent in emitting longer wavelength light (fluorescence and phosphorescence). The energy may also be consumed as heat and Raman vibrations of electrons, atoms and molecules. If the excitation energy is not completely used in the photophysical processes, the excess energy will lead photochemical processes to dissociate polymer bonds. The bond energies in polymers generally have a strength of about 40-90 kcal/mol corresponding to a photoenergy of 300-700nm. The photophysical and photochemical processes bring about discolouration, crazing, loss of gloss, erosion, cracking, reduction in tensile strength and extensibility in polymers.

In order to produce photodegradable polyolefins, therefore, these chromophores are intentionally introduced into the polyolefin structure or mixed with the polyolefins. There are two ways of achieving this. One is to copolymerise olefin monomers with carbonyl-group-containing monomers such as carbon monoxide and vinyl ketones. The other is to mix polyolefins with chromophoric substances such as metal oxides, salts, organometallic compounds, polynuclear aromatic compounds, carbonyl compounds, etc.

Researchers have attempted several techniques to promote the photodegradation of polyethylene in presence of pro-oxidants [6, 9, 47, 77, 80, 113-114]. Polyethylene films containing transition metal complexes such as dithiocarbamates as pro-oxidants to induce photo or thermal oxidation have been manufactured. The presence of these complexes in polyethylene is believed to produce peroxides and hydroperoxides on exposure to light, oxygen and temperature, through the generation of free radicals [115-117].

Main chain scission and cross-linking are the major consequences of thermal oxidation of polyolefins [118-120]. Several studies have reported the significant reduction of molecular weight after thermal degradation of polyethylene samples containing pro-oxidants [121], as well as on the identification of oxidation products including carboxylic acids, ketones, lactones and low molecular weight hydrocarbons [120]. Rate and extent of free radical oxidation of polyolefins are also affected by structural parameters such as chain defects (unsaturation) and branching, the latter being representative of relatively weak links susceptible to oxygen uptake to give hydroperoxides and bond cleavage. It has been reported that the hierarchy in the oxidation susceptibility of polyolefins is in the order PP > LDPE > LLDPE > HDPE [122-123].

A fine balance of antioxidant and pro-oxidant contents in a plastic product may promise relatively fast abiotic oxidation after a preset period of service life. As a result of the abiotic oxidation the plastic product may lose its mechanical properties and disintegrates

into small fragments. This technique may provide a perspective solution to the problems of “visual pollution” by plastic litter that are constantly in the centre of public attention. On the molecular level, the abiotic oxidation may result in polymer chain fragmentation, dramatic reduction of molecular weight, introduction of polar groups and increase of hydrophilicity. Such an oxidation process is thought to make the material much more vulnerable to microbial attack, which in the longer term could reduce the accumulation of such micro-fragments in the environment [9, 47, 124-129].

It is generally accepted that hydroperoxides are the key compounds in the mechanism of photo-oxidation of LLDPE. Their production is generally followed by their photochemical decomposition. Under UV exposure, the quantum yield of hydroperoxide decomposition is recognized to be high. Their decomposition may lead to several photo-products such as carboxylic acid, alcohol, ketone, etc [130].

Photodegradation (or transformation) occurs under the influence of solar radiation in the atmosphere, and to a lesser extent in the hydrosphere and on soil surfaces. New developments in environmental risk assessment have given photodegradation a new significance [9, 47, 114, 125-129]. Photodegradability is an intrinsic property of a chemical substance. Reactive species, which degrade a chemical substance in the atmosphere, are the hydroxyl radical, ozone and the nitrate radical. As these species are produced via solar radiation, this mechanism of

degradation is known as “indirect”, in order to distinguish it from the direct photolysis by solar radiation [131-132].

Environmental chemists and national governments are interested in the capacity of solar radiation to degrade, destroy and finally eliminate man-made chemical substances from the atmosphere. Atmospheric distribution of a chemical substance is critical because it can potentially lead to world-wide dissemination, if it is long-lived (persistent) and not destroyed [133].

1.8 Compatibilisation of polyethylene and bio-fillers

Polyethylenes are of high commercial interest due to their wide range of physical and chemical properties. However, their use in polymer blends of technological interest has been limited due to their typical non-polar character leading to poor adhesion. To overcome this deficiency and to facilitate compatibilization with polar polymers, polyethylenes have been chemically modified through functionalization or grafting. This process introduces polar groups onto the polymer main chain as pendant units or short-chain branching [134]. It can be achieved by copolymerization of new monomers or by modification or blending of existing polymers [135].

Grafting of preformed polymer is an important method for preparation of polymers with suitable functional groups [136]. Grafting involves covalent coupling of species, usually monomers or chain extenders, onto an existing polymer backbone. Reactive sites for grafting can be generated by mechanical processing, by chemical

initiation, by photochemical activation (UV-radiation) and by high-energy radiation (electron beam or gamma radiation). Grafting processes may be carried out under simultaneous treatment conditions, with all components being present during the creation of reactive sites. Alternatively, grafting can be performed via pre-activation process. Reactive sites are generated in the absence of the modifying species, but subsequently exposed to modifying species under some predetermined and controlled condition [137]. Recently, other methods have been developed such as atom transfer radical polymerization [138-139] or “living” radical polymerization [140-141]. These methods allow in controlling the length of grafts since they act more efficiently on the kinetics of the chain growth.

Starches from various botanical sources are among the most abundant, renewable, and inexpensive natural biopolymers. The use of starch to partially replace synthetic plastics reduces the dependence on petroleum and minimises the plastic waste. Biodegradable plastics from starch cannot compete with conventional petroleum-based plastics because of their poor mechanical properties. However, starch may be combined with synthetic plastic materials, to achieve satisfactory mechanical properties [142]. Two major technologies for starch addition to plastics have been developed. These are the use of thermoplastic starch (gelatinized starch), and the use of native starch (granular starch). During the last 30 years, various synthetic plastics have been combined with starches to prepare more biodegradable plastics [134, 135, 143-145].

Most research on the blends of starch and synthetic plastics has been focused on common plastics such as polyethylenes as the base materials. However, polyethylenes and starch are immiscible because of their differences in polarity; that is, starch is hydrophilic whereas polyethylene is hydrophobic. To improve their compatibility, various attempts have been made to modify either starch or polyethylenes [136, 137]. It was found that plasticizers, coupling agents, or modified starch only partially improved the dispersion of starch in PE and their interfacial properties because of their limited interaction. Another approach was to use poly (ethylene-co-acrylic acid), poly (ethylene-co-vinyl alcohol), or oxidized polyethylene as a compatibilizer in polyethylene–starch composites, but the composites show inadequate mechanical properties [140-141,146]. The inferior mechanical properties may be due to the result of weak interaction (e.g., hydrogen bonding) between starch and compatibilizer and limited opportunities for compatibilizer to interact with polyethylene.

More recently, an increased interest has been noticed in the use of polymers containing reactive groups (e.g., maleic anhydride) as compatibilizers [147-156]. Considerable studies have been carried out on maleic anhydride [146-150,157] grafting of polyethylene. It has been reported that anhydride groups could react with the hydroxyl groups in starch to produce chemical bonding, thus improving the dispersion of starch, the interfacial adhesion, and, subsequently, the mechanical properties of the resultant blends. It is believed that the

polar character of the anhydride causes affinity for the starch particles such that the maleated polyolefin can serve as a ‘compatibilizer’ between the matrix and filler [158-177].

Maleic anhydride grafted polyolefins are generally produced using maleic anhydride (MA) in the presence of peroxide in a melt polymer processing process [146, 147]. Maleic anhydride is, however, very volatile, toxic and strongly corrosive to the metallic equipment used in the polymer melt processing [148]. It is generally accepted that the grafting of maleic anhydride (MA) on polyolefins proceeds via a free radical mechanism [178]. The free radicals produced from the thermal decomposition of a peroxide (e.g. DCP) abstract hydrogen atoms from the polyethylene backbones, thus the polymer free radicals are generated. The polymer radicals then attack the monomer MA resulting in the grafting of the monomer on the polymer backbones. Heinen et al. performed the grafting using ¹³C-enriched MA and found that MA attaches to the HDPE and LDPE backbones in the form of single succinic anhydride as well as short oligomers [178].

Most research involving blending starch with PE employs thermoplastic starch [148-150] that consists of reactive groups because thermoplastic starch has been shown to improve processing properties [178]. In recent studies, Sailaja and Chanada concluded that PE-plasticized starch blends performed better than dry starch blends [148-149], however, the dry starch blends exhibited a greater tensile strength than the plasticized starch blends.

1.9 Scope and objectives of the work

Plastics continue to be an exciting class of materials to use, and a dynamic area for research. New application areas are being developed continually to utilize more fully the unique properties of this class of materials. In addition, new processing techniques are emerging to exploit the versatility of plastics and to take advantage of their ease of manufacture into all types of end products.

Polyethylene is one of the most widely used plastics in the world. There are seven principle variants of polyethylene. They are high density polyethylene, low density polyethylene, linear low density polyethylene, very low density polyethylene, ethylene vinyl acetate co-polymer, crosslinked polyethylene and ethylene ionomers. Linear low density polyethylene is a copolymer of ethylene and 1-alkene. By varying the level of co-monomer from approximately 2 to 8 mol %, it is possible to produce LLDPE with densities ranging from approximately 0.94 down to 0.90 g/cm³. Transparency, flexibility and resilience of LLDPE increase as density decreases. LLDPE products exhibit outstanding toughness, both as films and moulded items. Films have excellent tear and puncture resistance, which suits them for bulk packaging of heavy and irregular shaped items.

The production of plastics materials requires large quantities of crude oil as the main ingredient. Increasing oil prices and depleting oil sources gradually increases the cost of producing plastics. Though plastics are an ideal solution as a material for many applications they

are a permanent problem after their disposal. The blending of biodegradable polymers, such as starch, with inert polymers, like polyethylene, has received considerable attention recently because of the possible application of this technique in the waste disposal of plastics. The logic behind this approach is that if the biodegradable component is present in sufficient amount, and if it is removed by microorganisms in the waste disposal environment, then the base inert plastic should slowly disintegrate and disappear.

Polyolefins show very low degree of degradation when exposed to sunlight (photodegradation). Although photodegradation is undesirable in the case of plastic products where durability is important, it is ecologically desirable in the case of disposable containers and agricultural mulching films. Pro-oxidants have been mixed with LLDPE to accelerate degradation on exposure to sunlight.

The main objective of the present investigation is to evaluate in detail the possibility of biodegradability and photodegradability of LLDPE by blending with bio-fillers such as starch and dextrin, and by the incorporation of small quantities of pro-oxidants such as metal oxides and metal stearate. The use of bio-fillers such as starch and dextrin in polymer blends of technological interest has been limited due to their typical non-polar character leading to poor compatibility. To overcome this deficiency and to facilitate the compatibilization of LLDPE with bio-fillers, LLDPE has been chemically modified by grafting with maleic anhydride.

The management and recovery of plastic waste has become an increasingly important issue since the closing decades of 20th century, as awareness of the environment and the need to conserve petroleum based raw materials has grown considerably. One of the objectives of the investigation is to establish the reprocessability of LLDPE containing bio-fillers and pro-oxidants.

References

- [1] Sudhakar M, Doble M, Murthy PS, Venkatesan R, *International Journal of Biodeterioration and Biodegradation*, **61**, [2008], 203.
- [2] Scott G, *Polymers and the environment*. Cambridge, UK: RSC Paperbacks; [1999], 20.
- [3] Scott G, *Polymer Degradation and Stability*, **68**, [2000], 1.
- [4] Gross RA, Kalra B, *Science*, **297**, [2002], 803.
- [5] Botelho G, Queiro SA, Machado A, Frangiosa P, Ferreira J, *Polymer Degradation and Stability*, **86**, [2004], 493.
- [6] Chiellini E, Corti A, D'Antone S, *Polymer Degradation and Stability*, **92**, [2007], 1378.
- [7] Bonhomme S, Cuer A, Delort AM, Lemaire J, Sancelme M, Scott G, *Polymer Degradation and Stability*, **81**, [2003], 441.
- [8] Chiellini E, Corti A, D'Antone S, Baciú R, *Polymer Degradation and Stability*, **91**, [2006], 2739.
- [9] Jakubowicz I, *Polymer Degradation and Stability*, **80**, [2003], 39.
- [10] Billingham NC, Wiles DM, Cermak BE, Gho JG, Hare CWJ, Tung JF, In: *Proceedings Addcon world 2000*. Basel: RAPRA Publishing, [2000], Paper 6.

- [11] Koutny M, Lemaire J, Delort AM, *Chemosphere*, **64**, [2006], 1243.
- [12] Albertsson AC and Rfinby B, *Proceedings of the 3rd International Biodegradation Symposium*, (Sharpley JM and Kaplan KM (Eds)), Applied Science, London, 743 [1976].
- [13] Albertsson AC, *European Polymer Journal*, **16**, [1980], 623.
- [14] Albertsson AC, *Journal of Applied Polymer Science*, **22**, [1978], 3419.
- [15] Albertsson AC, Banhidi ZG and Beyer-Ericsson LL, *Journal of Applied Polymer Science*, **22**, [1978], 3435.
- [16] Albertsson AC and Rfinby B, *AppL Polym. Symp.*, **35**, [1979], 4243.
- [17] Albertsson AC, *Eighth Annual Conference on Advances in the Stabilization and Controlled Degradation of Polymers*, Lucerne, May [1986].
- [18] Albertsson AC and Banhidi ZG, *Journal of Applied Polymer Science*, **25**, [1980], 1655.
- [19] Stevens ES, *Biocycle*, [2003], 24.
- [20] www.cipet.gov.in, CIPET – Plastic Industry Statistics, [2011].
- [21] Van Os G, *The European plastic industry - a sunset industry. EPF special Issue*, [2001]. 19.
- [22] Ali S, Garforth AA, Harris DH, Rawlence DY, Uemichi Y, *Catalysis Today*, **75**, [2002], 247.
- [23] Uddin A, Koizumi K, Murata K, Sakata Y, *Polymer Degradation and Stability*, **56**, [1997], 37.
- [24] Ukei H, Hirose T, Horikawa T, Takai Y, Taka M, and Azuma N, *Catalysis Today*, **62**, [2000], 67.
- [25] Murata K, Hirano Y, Sakata Y, and Uddin A, *Journal of Analytical and Applied Pyrolysis*, **65**, [2002], 71.

- [26] Grieken R, Serrano DP, Aguado J, Garcia R, and Rojo C, *Journal of Analytical and Applied Pyrolysis*, **58-59**, [2001], 127.
- [27] Andrew. J. Peacock, Handbook of Polyethylene: Structures, Properties and Applications, CRC Press, [2000], 2.
- [28] Kuwabara K, Kaji H, Horii F, Bassett DC, and Olley RH, *Macromolecules*, **30**, [1997], 7516.
- [29] Gabriel C, Lilge D, *Polymer*, **42**, [2001], 297.
- [30] Chiu FC, Fu Q, Peng Y, and Shin HH, *Journal of Polymer Science Part B: Polymer Physics*, **40**, [2002], 325.
- [31] Puig CC, Aviles MV, Joskowicz P, Diaz A, *Journal of Applied Polymer Science*, **79**, [2001], 2022.
- [32] Crist B, and Hill MJ, *Journal of Polymer Science Part B: Polymer Physics*, **35**, [1997], 2329.
- [33] Akpalu Y, Kielhorn L, Hsiao BS, Stein RS, Russell TP, van Egmond J, and Muthukumar M, *Macromolecules*, **32**, [1999], 765.
- [34] Graessley WW, Krishnamoorti R, Balsara NP, Butera RJ, Fetters LJ, Lohse DJ, Schulz DN, and Sissano JA, *Macromolecules*, **27**, [1994], 3896.
- [35] Alamo RG, Londono JD, Mandelkern L, Stehling FC, and Wignall GD, *Macromolecules*, **27**, [1994], 411.
- [36] Mandelkern L, Alamo RG, Wignall GD, and Stehling FC, *TRIP*, **4**, [1996], 377.
- [37] Gupta AK, Rana SK, and Deopura BL, *Journal of Applied Polymer Science*, **44**, [1992], 719.
- [38] Gupta AK, Rana SK, and Deopura BL, *Journal of Applied Polymer Science*, **51**, [1994], 231.

- [39] Rana SK, *Journal of Applied Polymer Science*, **69**, [1998], 2599.
- [40] Drummond KM, Hopewell JL, and Shanks RA, *Journal of Applied Polymer Science*, **78**, [2000], 1009.
- [41] Prasad A, *Polymer Engineering Science*, **38**, [1998], 1716.
- [42] Wignall GD, Alamo RG, Londono JD, Mandelkern L, Kim MH, Lin JS, and Brown GM, *Macromolecules*, **33**, [2000], 551.
- [43] Osawa Z, Kurisu N, Nagashima K, Nakano K, *Journal of Applied Polymer Science*, **23**, [1979], 3583.
- [44] Andersson U, In: *Proceedings of plastic pipes XI*, [2001], 311.
- [45] Ifwarson M, Aoyama K, In: *Proceedings of Plastic Pipes X*, [1998], 691.
- [46] Gugumus F., *Polymer Degradation and Stability*, **63**, [1999], 41.
- [47] Chiellini E, Corti A, Swift G, *Polymer Degradation and Stability*, **81**, [2003], 341.
- [48] Chiellini E, In: Ziad S, Chiellini E, editors, *Proceeding of ICS-UNIDO conference on environmentally degradable polymers - plastic materials and the environment*, **1**, Doha (Qatar), [2000], 1.
- [49] Chiellini E, Corti A, Solaro R, *Polymer Degradation and Stability*, **64**, [1999], 305.
- [50] Chiellini E, Corti A, D'Antone S, Solaro R, *Progress in Polymer Science*, **28**, [2003], 963.
- [51] Hassinen J, Lundback M, Ifwarson M, Gedde UW, *Polymer Degradation and Stability*, **84**, [2004], 261.
- [52] Dear JP, Mason NS, *Polymers & Polymer Composites*, **9**, [2001], 1.
- [53] Gedde UW, Viebke J, Leijstronm H, Ifwarson M, *Polymer Engineering Science*, **34**, [1994], 1773.

- [54] Viebke J, Gedde UW, *Polymer Engineering Science*, **37**, [1997], 896.
- [55] Viebke J, Hedenqvist M, Gedde UW, *Polymer Engineering Science*, **36**, [1996], 2896.
- [56] Viebke J, Elble E, Ifwarson M, Gedde UW, *Polymer Engineering Science*, **34**, [1994], 1354.
- [57] Karlsson K, Smith GD, Gedde UW, *Polymer Engineering Science*, **32**, [1992], 649.
- [58] Smith GD, Karlsson K, Gedde UW, *Polymer Engineering Science*, **32**, [1992], 658.
- [59] Gedde UW, Ifwarson M, *Polymer Engineering Science*, **30**, [1990], 202.
- [60] Potyrailo RA, Wroczynski RJ, Morris WG, Bradtke GR, *Polymer Degradation and Stability*, **83**, [2004], 375.
- [61] Audisio G, Bertini F, *Journal of Analytical and Applied Pyrolysis*, **24**, [1992], 61.
- [62] Malhotra SL, Hesse L, Blanchard LP, *Polymer*, **16**, [1975], 81.
- [63] Boyd RH, *Polymer*, **26**, [1985], 323.
- [64] Krishnaswamy RK, *Polymer Engineering Science*, **47**, [2007], 516.
- [65] Hoàng EM, Lowe D, *Polymer Degradation and Stability*, **93**, [2008], 1496.
- [66] Weon JI, Chung YK, Shin SM, Choi KY, *Polymer Korea*, **32**, [2008], 440.
- [67] Ragnarsson L, Albertsson AC, *Biomacromolecules*, **4**, [2003], 900.
- [68] Albertsson AC, Andersson SO and Karlsson S, *Polymer Degradation and Stability*, **18**, [1987], 73.
- [69] Mumtaz T, Khan MR and Mohd Ali Hassan, *Micron*, **41**, 2010, 430.

- [70] Albertsson AC and Ljungquist O, *Journal of Macromolecular Science - Chemistry*, **A23**, [1986], 411.
- [71] Breen C, Last PM, Taylor S, Komadel P, *Thermochimica Acta*, **363**, [2000], 93.
- [72] Miranda R, Yang J, Roy C, Vasile C, *Polymer Degradation and Stability*, **72**, [2001], 469.
- [73] Dolezel B, *British Plastics*, **49**, [1967], 105.
- [74] Yoshito Ohtake, Tomoko Kobayashi, Hitoshi Asabe and Nobunao Murakami, *Polymer Degradation and Stability*, **60**, [1998], 79.
- [75] Kestelman VN, Yaravenko VL, and Melnikova EI, *International Biodeterioration Bulletin*, **8**, [1972], 15.
- [76] Koutny M, Delort AM, In: *Environmental Biodegradation Research Focus*, Nova Publishers, New York, [2008], 239.
- [77] Ojeda T, Dalmolin E, Forte M, Jacques R, Bento F, Camargo F, *Polymer Degradation and Stability*, **94**, [2009], 965.
- [78] Reddy MM, Deighton M, Gupta RK, Bhattacharya SN, Parthasarathy R, *Journal of Applied Polymer Science*, **111**, [2008], 1426.
- [79] Reddy MM, Deighton M, Gupta RK, Bhattacharya SN, Parthasarathy R, *Journal of Applied Polymer Science*, **113**, [2009], 2826.
- [80] Koutny M, Sancelme M, Dabin C, Pichon N, Delort AM, Lemaire J, *Polymer Degradation and Stability*, **91**, [2006], 1495.
- [81] Arnaud R, Dabin P, Lemaire J, Al-Malaika S, Chohan S, Coker M, *Polymer Degradation and Stability*, **46**, [1994], 211.
- [82] Scott G, *Polymer Age*, **6**, [1975], 54.

- [83] Omishi H and Hagiwara M, *Polymer Photochemistry*, **1**, [1981], 15.
- [84] Griffin GJL, *Pure and Applied Chemistry*, **52**, [1980], 399.
- [85] Colin G., Cooney JD, Carlsson DJ and Wiles DM, *Journal of Applied Polymer Science*, **26**, [1981], 509.
- [86] Colin G, Cooney JD and Wiles DM, *International Biodeterioration Bulletin*, **12**, [1976], 67.
- [87] Griffin GJL, US Patent 4,016, 117 [1977]
- [88] Griffin GJL, US Patent 4,021, 388 [1977]
- [89] Griffin GJL, US Patent 4,125,495 [1978]
- [90] Aminabhavi TM, Balundgi RH, Cassidy PE, *Polymer Plastic Technology and Engineering*, **29**, [1990], 235.
- [91] Nagato K, Shimoda H, *Japanese Journal of Tropical Agriculture*, **23**, [1979], 160.
- [92] Kawai F, Watanabe M, Shibata M, Yokoyama S, Sudate Y, *Polymer Degradation and Stability*, **76**, [2002], 129.
- [93] Otey FH, Westhoff RP and Russell CR, *Industrial Engineering Chemistry Production Research and Development*, **16**, [1977], 305.
- [94] Wei S, and Nikolov ZL, *Industrial Engineering Chemistry and Research*, **31**, [1992], 2332.
- [95] Gage P, *Tappi Journal*, **73**, [1990], 161.
- [96] Shulman J and Howarth JT, US Patent 3,137,664, June [1964].
- [97] Nadejzda Haider and Sigbritt Karlsson, *Polymer Degradation and Stability*, **64**, [1999], 321.
- [98] Griffin GJL and Turner RD, *International Biodeterioration Conference*, Berlin, [1978].

- [99] Otey FH and Westhoff RP, *Industrial Engineering Chemistry Production Research and Development*, **23**, [1984], 284.
- [100] Otey FH, Mark AM, Mehlretter CL and Russell CR, *Industrial Engineering Chemistry Production Research and Development*, **13**, [1974], 90.
- [101] Otey FH, Westhoff RP and Doane WM, *Industrial Engineering Chemistry Production Research and Development*, **19**, [1980], 592.
- [102] Otey FH, Westhoff RP, & Doane WM, *Industrial Engineering Chemistry and Research*, **26**, [1987], 1659.
- [103] Griffin GJL, *Advances in Chemistry Series*, **134**, [1974], 159.
- [104] Otey FH and Doane WM, in *Proceedings of Society of the Plastic Industry, Symposium on Degradable Plastics*, Washington, DC, [1987], 39.
- [105] Swanson CL, Westhoff RP and Doane WP, *Proceedings of the Corn Utilization Conference*, Columbus, OH: National Corn Growers Association, [1988].
- [106] Otey FH, Westhoff RP and Russell CR, *Industrial Engineering Chemistry Production Research and Development*, **16**, [1977], 305.
- [107] Baum B and Deanin RD, *Polymer Plastic Technology and Engineering*, **2**, [1973], 1.
- [108] Rabek JB, *Photodegradation Mechanisms and Experimental Methods*, Chapman and Hall, London, [1995].
- [109] Rabek JB, *Photostabilization of Polymers Principles and Applications*, Elsevier Science and Publishers Ltd., England, [1990].
- [110] Carlsson DJ, Garton A and Wiles DM, *Macromolecules*, **9**, [1976], 695.
- [111] Mckellar JF and Allen NS, *Photochemistry of man-made polymers*, Applied Science Publishers Ltd, London, [1979].

- [112] Allen NS, *Polymer Degradation and Stability*, **2**, [1980], 155.
- [113] Sudhakar M, Trishul A, Doble M, Suresh KK, Syed JS, Inbakandan D, et al., *Polymer Degradation and Stability*, **92**, [2007], 1743.
- [114] Roy PK, Surekha P, Rajagopal C, Choudhary V, *Polymer Degradation and Stability*, **91**, [2006], 1980.
- [115] Lee B, Pometto III AL, Fratzke A, Bailey TB, *Applied and Environmental Microbiology*, **57**, [1991], 678.
- [116] Khabbaz F, Albertsson AC, Karlsson S, *Polymer Degradation and Stability*, **63**, [1999], 127.
- [117] Gugumus F, *Polymer Degradation and Stability*, **74**, [2001], 327.
- [118] Erlandsson B, Karlsson S, Albertsson AC, *Polymer Degradation and Stability*, **55**, [1997], 237.
- [119] Burman L, Albertsson AC, *Polymer Degradation and Stability*, **89**, [2005], 50.
- [120] Khabbaz F, Albertsson AC, Karlsson S, *Polymer Degradation and Stability*, **63**, [1999], 127.
- [121] Karlsson S, Hakkarainen M, Albertsson AC, *Macromolecules*, **30**, [1997], 7721.
- [122] Iring M, Foldes E, Barabas K, Kelen T, Tudos F, *Polymer Degradation and Stability*, **14**, [1986], 319.
- [123] Winslow FH, *Pure and Applied Chemistry*, **49**, [1977], 495.
- [124] Kawai F, Shibata M, Yokoyama S, Maeda S, Tada K, Hayashi S, *Macromolecular Symposia*, **144**, [1999], 73.
- [125] Scott G, Wiles DM, *Biomacromolecules*, **2**, [2001], 615.
- [126] Kyrikou I, Briassoulis D, *Journal of Polymers and the Environment*, **15**, [2007], 125.

- [127] Roy PK, Titus S, Surekha P, Tulsi E, Deshmukh C, Rajagopal C, *Polymer Degradation and Stability*, **93**, [2008], 1917.
- [128] Ojeda TFM, Dalmolin E, Forte MMC, Jacques RJS, Bento FM, Camargo FAO, *Polymer Degradation and Stability*, **94**, [2009], 965.
- [129] Albertsson AC, Barenstedt C, Karlsson S, *Acta Polymerica*, **45**, [1994], 97.
- [130] Adams Tidjani, *Polymer Degradation and Stability*, **68**, [2000], 465.
- [131] Finlayson-Pitts BJ, Pitts Jr JN, *Atmospheric Chemistry – Fundamentals and Experimental Techniques*, Wiley, New York [1986].
- [132] Finlayson-Pitts BJ, Pitts Jr JN, *Chemistry of the Upper and Lower Atmosphere: Theory, Experiment, and Application*, Academic Press, San Diego [2000].
- [133] Atkinson R, *Chemical Reviews*, **85**, [1985], 69.
- [134] Hawker CJ, Mecerreyes D, Dao J, Hedrick J, Barakat I, Duboise P, Jerome R, Volkson W, *Macromolecular Chemistry and Physics*, **198 (1)**, [1997], 155.
- [135] Miwa Y, Yamamoto K, Sahaguchi M, Shimada S, *Macromolecules*, **32**, [1999], 8234.
- [136] Stehling UM, Malmstron EE, Waymouth RW, Hawker CJ, *Macromolecules*, **31**, [1998], 4396.
- [137] Roper H, Koch H, *Starch*, **42**, [1990], 123.
- [138] Bhattacharya M, Vaidya UR, Zhang D, Narayan R, *Journal of Applied Polymer Science*, **57**, [1995], 539.
- [139] Odusanya OS, Ishiaku US, Azemi BMN, *Polymer Engineering Science*, **40**, [2000], 1298.

- [140] Arvanitoyannis I, Psomiadou E, Biliaderis CG, *Starch*, **49**, [1997], 306.
- [141] Ke T, Sun X, *Cereal Chemistry*, **77**, [2000], 761.
- [142] Villarreal N, Pastor JM, Perera R, Rosales C, Merino JC, *Macromolecular Chemistry and Physics*, **203 (1)**, [2002], 238.
- [143] Machado AV, Covas JA, Van Duin M, *Polymer*, **42 (8)**, [2001], 3649.
- [144] Guthrie JT, *Surface Coatings International Part B: Coatings Transactions*, **85 (B1)**, [2002], 27.
- [145] Paik HJ, Gaynor SG, Matyjaszewski K, *Macromolecular Rapid Communications*, **19 (1)**, [1998], 47.
- [146] Kollengode ANRS, Bhatnagar S, Hanna MA, *Cereal Chemistry*, **73**, [1996], 539.
- [147] Evangelista RL, Nikolov NL, Sung W, Jane J, Gelina RJ, *Industrial & Engineering Chemistry Research*, **30**, [1991], 1841.
- [148] Parandoosh S, Hudson M, *Journal of Applied Polymer Science*, **48**, [1993], 787.
- [149] Sagar AG, Merril EW, *Journal of Applied Polymer Science*, **58**, [1995], 1647.
- [150] Aburto J, Thiebaud S, Alric I, Borredon E, Bikiaris D, Prinos J, Panayiotou C, *Carbohydrate Polymers*, **34**, [1997], 101.
- [151] Wang KH, Choi MH, Koo CM, Choi YS, Chung IJ, *Polymer*, **42**, [2001], 9819.
- [152] Hotta S, Paul DR, *Polymer*, **45**, [2004], 7639.
- [153] Lee JH, Jung D, Hong CE, Rhee KY, Advani SG, *Composites Science and Technology*, **65**, [2005], 1996.
- [154] Morawiec J, Pawlak A, Slouf M, Galeski A, Piorkowska E, Krasnikowa N, *European Polymer Journal*, **41**, [2005], 1115.

- [155] Wang Y, Chen FB, Wu KC, *Journal of Applied Polymer Science*, **97**, [2005], 1667.
- [156] Ranade A, Nayak K, Fairbrother D, D'Souza NA, *Polymer*, **46**, [2005], 7323.
- [157] Jane J, Gelina RJ, Nikolov Z, Evangelista RL, US Patent 5,059,642 [1991].
- [158] Reichert P, Nitz H, Klinke S, Brandsh R, Thomann R, Mulhaupt R, *Macromolecular Materials and Engineering*, **8**, [2000], 275.
- [159] Wang ZM, Nakajima H, Manias E, Chung TC, *Macromolecules*, **36**, [2003], 8919.
- [160] Galgali G, Ramesh C, Lele A, *Macromolecules*, **34**, [2001], 852.
- [161] Kawasumi M, Hasegawa N, Kato M, Usuki A, Okada A, *Macromolecules*, **30**, [1997], 6333.
- [162] Hasegawa N, Kawasumi M, Kato M, Usuki A, Okada A, *Journal of Applied Polymer Science*, **67**, [1998], 87.
- [163] Ellis TS, D'Angelo JS, *Journal of Applied Polymer Science*, **90**, [2003], 1639.
- [164] Svoboda P, Zeng C, Wang H, Lee LJ, Tomasko DL, *Journal of Applied Polymer Science*, **85**, [2002], 1562.
- [165] Koo CM, Kim MJ, Choi MH, Kim SO, Chung IJ, *Journal of Applied Polymer Science*, **88**, [2003], 1526.
- [166] Garc'ia-Lo'pez D, Picazo O, Merino JC, Pastor JM, *European Polymer Journal*, **39**, [2003], 945.
- [167] Chen L, Wong SC, Pisharath S, *Journal of Applied Polymer Science*, **88**, [2003], 3298.

- [168] Hasegawa N, Okamoto H, Kato M, Tsukigase A, Usuki A, *Macromolecular Materials and Engineering*, **280/281**, [2000], 76.
- [169] Kato M, Okamoto H, Hasegawa N, Tsukigase A, Usuki A, *Polymer Engineering Science*, **43(6)**, [2003], 1312.
- [170] Wang KH, Koo CM, Chung IJ, *Journal of Applied Polymer Science*, **89**, [2003], 2131.
- [171] Wang KH, Choi MH, Koo CM, Xu M, Chung IJ, Jang MC, Sun Choi W, Song HH, *Journal of Polymer Science Part B: Polymer Physics*, **40**, [2002], 1454.
- [172] Wang KH, Choi MH, Koo CM, Choi YS, Chung IJ, *Polymer*, **42**, [2001], 9819.
- [173] Gopakumarm TG, Lee JA, Kontopoulou M, Parent JS, *Polymer*, **43**, [2002], 5483.
- [174] Koros WJ, Paul DR, Rocha AA, *Journal of Polymer Science Part B: Polymer Physics*, **14**, [1976], 687.
- [175] Yoon PJ, Hunter DL, Paul DR, *Polymer*, **44**, [2003], 5323.
- [176] Shah RK, Paul DR, *Polymer*, **45**, [2004], 2991.
- [177] Fornes TD, Paul DR, *Polymer*, **44**, [2003], 4993.
- [178] Vaidya UR, Bhattacharya M, *Journal of Applied Polymer Science*, **52**, [1994], 617.

.....*RCR*.....

EXPERIMENTAL TECHNIQUES

Contents
2.1 Materials**2.2 Methods**

The materials used for the study and the experimental procedures are discussed in this chapter.

2.1 Materials

2.1.1 Polymer

The film grade linear low density polyethylene (LLDPE 20FS010) used in this study was provided by Reliance Industries Limited, Mumbai, India.

Density (23°C) – 0.92 gm/cm³

Melt flow index (190°C/2.16 kg) – 1.0 gm/10 min

2.1.2 Bio-fillers

The bio-fillers used in this study were starch (100 and 300 mesh) and dextrin (100, 200 and 300 mesh). These fillers were supplied by Jemsons Starch and Derivatives, Aroor, Alapuzha, Kerala. As these fillers were hygroscopic in nature these were oven dried at 120°C for 1 hour prior to mixing.

2.1.3 Pro-oxidants

The pro-oxidants used in this study include metal oxides and a metal stearate. The iron oxide was supplied by Merck Specialities Pvt. Ltd., Mumbai, India. Manganese dioxide was supplied by Qualigens Fine Chemicals, Mumbai, India. Titanium dioxide (anatase and rutile grades) were supplied by Associated Chemicals, Edappally, Kerala, India and Cobalt stearate was supplied by Alfa Aesar, Lancaster.

2.1.4 Other chemicals

The maleic anhydride was supplied by Loba Chemie Pvt. Ltd., Mumbai and the dicumyl peroxide was supplied by Associated Chemicals, Edappally, Kochi, Kerala.

2.2 Methods

2.2.1 Sample preparation

Blends were prepared by melt mixing [1] in a Thermo Haake Rheometer (Rheocord 600p) (Figure 2.1) using roller type rotors. The mixing chamber has a volumetric capacity of 69 cm³.

A mixing time of 8 minutes was given for all the compounds at a rotor speed of 30 rpm at 150°C. LLDPE was first melted for 2 minutes followed by the addition of filler. Mixing was continued for another 6 min.

In the case of maleated blends, initially the LLDPE was melted for 2 minutes and then grafted with maleic anhydride (1%) using dicumyl peroxide (0.25%) as the initiator. The bio-filler was then

added and mixing was continued for a total duration of 8 minutes. Different compositions for each filler were prepared. The neat LLDPE was also masticated under the same conditions.



Figure 2.1 Thermo HAAKE polylab system. (Mixing chamber and the rotors are also shown)

2.2.2 Preparation of test specimens

The test specimens were prepared from neat LLDPE and the compounds by moulding in an electrically heated hydraulic press for 5 minutes at 150°C under a pressure of 20 MPa.

2.2.3 Mechanical properties

The stress-strain properties were evaluated as per ASTM D-882 [2] in a Shimadzu Autograph AG-I series Universal Testing Machine at a crosshead speed of 50 mm/min using a load cell of 10 kN capacity. An average of at least five measurements was taken to represent each data point.

2.2.4 Thermal studies

2.2.4.1 Thermogravimetric analyses

Thermogravimetric analysis (TGA) is a technique by which the mass of the sample is monitored as a function of temperature or time, while the substance is subjected to a controlled temperature program [3]. Thermogravimetric analysis is used to investigate thermal degradation and thus the thermal stability of the samples.

Thermo gravimetric analyses of the samples were carried out in a TGA Q-50 thermal analyzer (TA Instruments) or Perkin Elmer, Diamond TG/DTA under nitrogen atmosphere. The samples were heated from room temperature to 800°C at a heating rate of 20°C/min. The chamber (furnace) was continuously swept with nitrogen at a rate of 90 mL/min. Sample weight varied from 10-15 mg. The weight changes were noted with the help of an ultra sensitive microbalance.

The data of weight loss versus temperature and time was recorded online using the TA Instrument's Q Series Explorer software. The analysis of the thermogravimetric (TG) and derivative thermogravimetric (DTG) curves were done using TA Instrument's Universal Analysis 2000 software version 3.3 B. Thermograms were recorded from room temperature to 800°C. The temperature at which weight loss is maximum (T_{\max}) was evaluated.

2.2.4.2 Differential scanning calorimetry

Differential Scanning Calorimetry (DSC) is a technique for studying the thermal behavior of a material as a function of temperature as they go through physical or chemical changes with absorption or evolution of heat. It is used to investigate thermal transitions, including phase changes, crystallization, melting, and glass transition of a material as a function of temperature [4, 5, 6]. Heat flow, i.e., heat absorption (endothermic) or heat emission (exothermic), is measured as a function of time or temperature of the sample and the result is compared with that of a thermally inert reference. DSC directly gives a recording of heat flow rate (C_p) against temperature. The degree of crystallinity (X) can be measured as function of time.

$$X = \Delta H_f (\text{observed}) / \Delta H_f (100\% \text{ crystalline})$$

The crystallinity of the samples were studied using a TA Q-100 thermal analyzer (TA Instruments) performed under nitrogen with a heating rate of 10°C/min. Samples of 5-10mg were heated from -50°C

to 170°C at a heating rate of 10°C/min, and kept at 170°C for 3 min in order to erase thermal history. Then a cooling was performed at a rate of 10°C/min from 170 to -50°C followed by a second heating from -50 to 170°C at the same rate. Polymer crystallinity was calculated from the melting enthalpy obtained by endothermic peak integration and the melting enthalpy of a perfect LLDPE crystal (289J/g) as reference. The melting and crystallization parameter, such as melting point (T_m), heat of fusion (ΔH_f), temperature of crystallization (T_c), and heat of crystallization (ΔH_c) were used for the comparison of samples.

2.2.5 Biodegradation studies

The biodegradation studies on the blends were carried out according to ASTM D 6691 [7].

2.2.5.1 Bacterial strains

Bacterial cultures were obtained from the culture collections of *Microbial Genetic Lab, Department of Biotechnology, Cochin University of Science and Technology*. These cultures were isolated from sediment samples collected from different locations of Cochin backwaters and Mangalavanam mangroves, Kerala, India. These cultures were previously identified as genus *Vibrionacea* based on their morphological and biochemical characteristics outlined in Bergey's Manual of Systematic Bacteriology [8]. They were preserved in 10mL glass bottles employing paraffin oil overlay method.

2.2.5.2 Purification of Vibrios

A loopful of these preserved cultures were transferred by spread plated onto Thiosulphate Citrate Bile salt Sucrose (TCBS) agar plates (Himedia) and was incubated at 37°C for 24 hours. Isolated yellow and green colored single colonies were picked, purified on nutrient agar plates (quadrant streaking), sub cultured on nutrient agar slants with 1% NaCl and was kept at 4°C for further studies.

The isolates were identified as *Vibrios* based on their morphological and biochemical characteristics outlined in Bergey's Manual of Systematic Bacteriology [8] which include Gram staining, oxidation/fermentation reaction with glucose (MOF test) and oxidase test. The isolates that are gram negative rods, fermentative in MOF test and behaved positive in oxidase test were streaked onto nutrient agar slants containing 1% NaCl for further studies. They were stocked at 4°C for further studies.

2.2.5.3 Screening for amylase producers

Plate assay method was employed for the screening of amylase producers. Nutrient agar medium supplemented with 1% starch and 1% NaCl was used for the plate preparation [9]. All the isolates were spot inoculated onto the nutrient plates and incubated at 37°C for 2 days. After incubation, the plates were flooded with Grams iodine for visualizing the zone of clearance around the colony. The clearing zones indicate the production of amylase enzyme by the isolates. From the results, potential amylase producers were selected based on the diameter of zone of clearance around colonies.

2.2.5.4 Medium for biodegradation studies

Minimal medium was used for testing the degradation of the blends. The composition and pH of 1L of amylase minimal medium [10] is given below.

Table 2.1 Composition and pH of amylase minimal medium

Peptone	6.0 g
MgSO ₄	0.5 g
KCl	0.5 g
Starch	1 g
NaCl	1 g
pH	7±0.3

2.2.5.5 Preparation of consortia of amylase producers for biodegradation studies

The isolates with largest zones of clearance in the primary screening for starch degradation were selected to make up the consortium to study the degradation of starch/dextrin plastic blended films. 15 isolates of Vibrios which were optimum producers based on the plate assay were selected and were grown to OD₆₀₀=1.00. The culture suspension was centrifuged to harvest the cells and the cells were resuspended in physiological saline for using as inoculums. 1mL of each culture was aseptically transferred to the minimal media.

2.2.5.6 Biodegradation studies on blends using the consortium

2.2.5.6.1 Preparation of blends

The blends were prepared by melt mixing in a Thermo HAAKE PolyLab system. The moulding was done using an electrically heated

hydraulic press. The test specimens for checking the biodegradation were cut from the samples according to ASTM D-882 [2].

2.2.5.6.2 Preparation of inoculum & shake flask culture

To prepare the inoculum the individual isolates of the consortium were grown overnight at 37°C at 120 rpm on an Orbitek shaker (Scigenics Pvt. Ltd, Chennai, India) in a nutrient broth (Himedia, Mumbai) of pH 7.0 ±0.3 with 1% NaCl. The cells were harvested by centrifugation at 5000 rpm (2292g) for 20 minutes, washed with physiological saline and then pooled. 5 ml of this pooled culture ($OD_{660} = 1$) was used to inoculate 50mL amylase minimal medium [10] lacking starch. The samples prepared from the blends previously wiped with 70% alcohol were added to this medium and these strips acted as the sole source of carbon. Incubation was in the Orbitek environmental shaker at 37°C and 120 rpm for a total period of 3 months with regular sampling. The medium without the inoculum with corresponding starch/dextrin-plastic blends and subjected to the same treatment as above were used as controls.

2.2.6 Soil burial test

The soil burial test was also carried out for evaluating the biodegradability of the blends. The soil was taken in pots and the plastic strips were placed in it. The bacterial culture was supplied to the soil. Care was taken to ensure that the samples were completely covered with soil. The pot was then kept at room temperature. The loss in weight and tensile strength was measured after thorough

washing with water and drying in oven until constant weight to determine the extent of biodegradability.

2.2.7 Photodegradation studies

Disinfection lamps (TUV lamps) are low pressure mercury-vapour discharge lamps consisting of a tubular glass envelope, emitting shortwave ultraviolet radiation with a radiation peak at 253.7nm (UV-C) for germicidal action. The glass filters out the 185nm ozone-forming line. A protective coating on the inside limits the depreciation of the useful UV-C radiation output (Longlife lamps). They are applied in a variety of photochemical processes.

In the present study, the plastic film samples were cut to 8x1 cm size and exposed under a 30-watt shortwave UV lamp at a distance of 30 cm. The plastic films were then taken out at different time intervals, viz., 48, 120 and 240 hours to determine tensile strength using a universal testing machine. The FTIR was used for the characterisation and monitoring for the functional group changes in samples during irradiation.

2.2.8 Melt flow indices

An extrusion plastometer was used for measuring the melt flow index of polymer melts according to ASTM D-1238 [11]. The rate of extrusion through a die of specified length and diameter was measured under prescribed conditions of temperature and load as a function of time. Melt index is calculated and reported as g/10min. This index is inversely related to molecular weight.

The melt flow index (MFI) of each blend of LLDPE with filler was measured using a CEAST Modular Line Melt Flow Indexer in accordance with ASTM method D-1238 using a 2.16 kg load at a melt temperature of 190°C.

2.2.9 FTIR

Fourier transform infrared spectra (FTIR) are generated by the absorption of electromagnetic radiation in the frequency range 400 to 4000 cm^{-1} by organic molecules. Different functional groups and structural features in the molecules absorb energy at characteristic frequencies. The frequency and intensity of absorption are the indication of the bond strength and structural geometry in the molecule. The FTIR spectra of the samples were recorded in the transmittance mode using a Thermo Nicolet, Avatar 370 FTIR spectrophotometer in the spectral range of 4000–400 cm^{-1} .

2.2.10 Scanning electron microscopic analyses (SEM)

SEM is used to investigate the morphology of fractured surfaces [12]. In SEM, the electron beam incident on the specimen surface causes various phenomena of which the emission of secondary electrons is used for the surface analysis. Emitted electron strikes the collector and the resulting current is amplified and used to modulate the brightness of the cathode ray tube. There is one-to-one correspondence between the number of secondary electrons collected from any particular point on the specimen surface and the brightness of the analogous point on the screen and thus an image of the surface is progressively built up on the screen.

In the present study, morphological characterisation of the fractured surfaces of the tensile test specimens was carried out using scanning electron microscope (JEOL Model JSM - 6390LV) after sputter coating the surface with platinum.

2.2.11 Water absorption

Water absorption of the samples was measured using plastic film strips of <1mm thickness according to the ASTM D 570-81 [13] method. The measurements were performed by soaking the samples in distilled water. The water absorption was calculated as the weight difference and is reported as percent increase of the initial weight.

2.2.12 Reprocessability

The reprocessability of the samples was studied by masticating the moulded samples in a Thermo HAAKE PolyLab System equipped with roller type rotors for 6 minutes at a rotor speed of 30 rpm at 150°C. The samples were remoulded in an electrically heated hydraulic press for 5 minutes at 150°C under a pressure of 20MPa. The process of masticating and moulding was repeated up to 3 cycles. The stress-strain properties of the moulded specimens after each cycle were measured.

References

- [1] Wei S, Shiyi G, Changshui F, Dong X, Quan R, *Journal of Materials Science*, **34**, [1999], 5995.
- [2] Annual Book of ASTM Standards, D 882, **08.01**, [2004].

- [3] Neil CM, Allen G, Editor, *Comprehensive Polymer Science*, Pergamon press, New York, **5**, [1989].
- [4] Busigin C, Lahtinern R, Thomas G, Woodharms RT, *Polymer Engineering Science*, **24**, [1984], 169.
- [5] Zhu WP, Zhang GP, Yu JY, Dai G, *Journal of Applied Polymer Science*, **91**, [2004], 431.
- [6] Labour T, Vigier G, Segeula R, Gauthier C, Orange G, Bomal Y, *Journal of Polymer Science Part B: Polymer Physics*, **40**, [2002], 31.
- [7] Annual Book of ASTM Standards, D 6691, **08.03**, [2004].
- [8] Buchanan RE and Gibbons NE, *Bergey's Manual of Systematic Bacteriology* (Eighth edition), The Williams and Wilkins Co., Baltimore, [1974], 747.
- [9] Furniss BS, Hannaford AJ, Rogersm V, Smith PWG and Tatchell AR (eds), *Vogel's Textbook of Practical Organic Chemistry*, Longman publishing, England, **4**, [1978], 497.
- [10] Bernfed PC, *Enzymes of Starch degradation and synthesis*, *Advanced Enzymology*, **12**, [1951], 379.
- [11] Annual Book of ASTM Standards, D 1238, **08.01**, [2004].
- [12] Arthur WE, *Atlas of Polymer Morphology*, Hanser, New York, [1989].
- [13] Annual Book of ASTM Standards, D 570, **08.01**, [2004].

.....✂.....

BIODEGRADABILITY STUDIES ON LLDPE USING BIO-FILLERS

Contents	3.1 Introduction
	3.2 Results and Discussion
	3.3 Conclusion

.....

Linear low density polyethylene (LLDPE) was blended with starch (100 and 300 mesh size) and dextrin (100, 200 and 300 mesh size). Various compositions were prepared and their mechanical, thermal, FTIR, morphological (SEM), and reprocessability studies have been carried out. The melt flow indices (MFI) of the blends were studied. The percentage of water absorption of each composition was calculated. Biodegradability of the samples has been verified using shake culture flask containing Vibrios - an amylase producing bacteria, which were isolated from marine benthic environment. Soil burial test too of the samples was conducted. The biodegradability tests on the blends indicate that the blends are partially biodegradable. Scanning electron photomicrographs confirm the biodegradability in LLDPE-starch and LLDPE-dextrin blends. The reprocessability studies suggest that the blends are reprocessable without sacrificing much of their mechanical properties.

.....

3.1 Introduction

Petrochemical based plastics such as polyolefins, are one of the largest groups of polymeric materials, which are formed into useful shapes by application of heat and pressure [1-5]. These have been increasingly used as packaging materials because of their availability in large quantities at low cost and favourable properties such as good tensile and tear strength, good barrier properties to oxygen and heat sealability [6]. These materials are not degraded by the microorganisms present in the environment, which contributes to their long lifetime of hundreds of years, thus causing serious environmental pollution.

The resistance of polyethylene to its biological attack is related to its hydrophobicity, high molecular weight, and lack of functional groups recognizable by microbial enzymatic systems. These properties restrict the applications of polyethylene in which biodegradability is a desirable attribute [7]. Therefore, the development of modified plastics and substitutes that could be degraded by microorganisms has been emphasized. The blending of biodegradable polymers, such as starch, with inert polymers, like polyethylene, has received considerable attention recently because of the possible application of this technique in the waste disposal of plastics. The logic behind this approach is that if the biodegradable component is present in sufficient amount, and if it is removed by microorganisms in the waste disposal environment, then the base inert plastic should slowly disintegrate and disappear [8]. The advantage of biodegradable plastic is that, under proper conditions

(sunlight, moisture, oxygen, etc.), the plastic degrades to the point where organisms are able to digest them. This reduces problems with litter and minimizes the harmful effects on wildlife.

Linear low density polyethylene (LLDPE) consists of molecules with linear polyethylene backbone to which short alkyl groups are attached at random intervals. These materials are produced by the copolymerization of ethylene with 1-alkenes. The branches most commonly encountered are ethyl, butyl or hexyl groups, but can also be a variety of other alkyl groups, both linear and branched. The branches hinder crystallization to some extent, reducing density relative to high density polyethylene. The result is a density range of approximately 0.915–0.925 g/cm³ [9].

Starch is a polymer of glucose. Starch consists of two components namely amylose (water soluble component) and amylopectin (water insoluble). Amylose is a linear polymer chain of α -D glucose units, linked in the 1, 4 positions. Amylopectin (β -amylose) has a branched chain structure also composed of α -D glucose units. The chains of α -D-glucose units are linked with 1,4 linkages, with chains branching off at every 24–30 glucose units through 1, 6 linkages [10,11].

Dextrins are prepared by degrading starch in various ways, e.g., acid hydrolysis at low temperatures or at high temperatures. The dextrins formed under different conditions differ in structure [12]. Dextrin and starch have the general formula $[C_x (H_2O)_y]_n$, $y = x-1$, in

which glucose units are joined to one another usually head-to-tail, but dextrin has a smaller and less complex molecule than starch.

This chapter focuses on the preparation of LLDPE-biofiller [starch (100 and 300 mesh) and dextrin (100, 200 and 300 mesh)] blends and evaluation of various properties. Three compositions (5, 10 and 15 weight %) with each filler grade were prepared and characterized by evaluating their mechanical properties, thermal properties, biodegradability, SEM, FTIR spectra, MFI, water absorption and reprocessability.

3.2 Results and Discussion

3.2.1 Mechanical properties

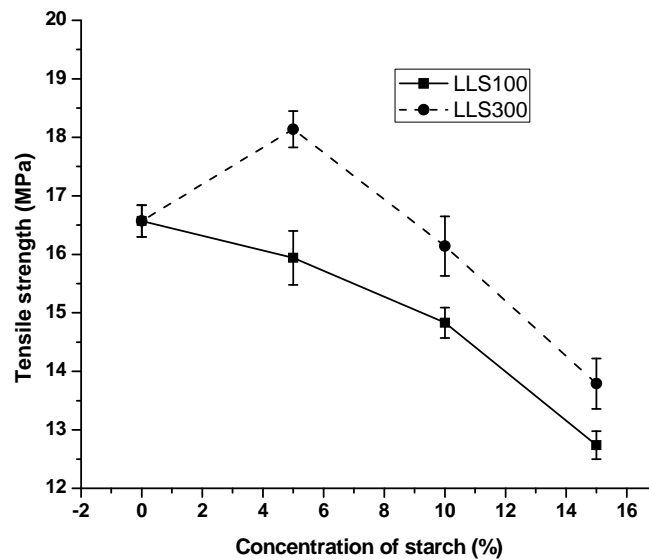


Figure 3.1a. Variation of tensile strength with concentration of starch in LLDPE-starch blends (LLS100 = LLDPE-starch 100 mesh; LLS300 = LLDPE-starch 300 mesh)

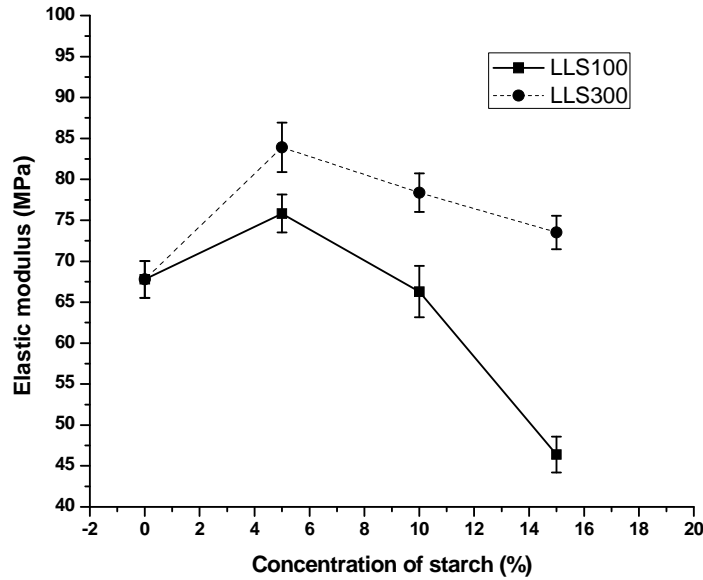


Figure 3.1b. Variation of elastic modulus with concentration of starch in LLDPE-starch blends (LLS100 = LLDPE-starch 100 mesh; LLS300 = LLDPE-starch 300 mesh)

Figures 3.1a and 3.1b show the variation of tensile strength and elastic modulus of LLDPE-starch blends. In the case of LLS300 blends tensile strength shows a marginal increase at a loading of 5% starch. Further increase in starch content leads to decrease in tensile strength. For LLS100 blends, tensile strength decreased as the loading of starch increased indicating that starch behaves as a non-reinforcing filler.

The elastic modulus values of LLDPE-starch blends also decreased for higher concentrations of starch. A marginal increase in elastic modulus was observed for lower concentration of starch. i.e., 5 weight % compositions.

Figures 3.1c and 3.1d show the variation of tensile strength and elastic modulus of LLDPE-dextrin blends. As the concentration of dextrin in the blends increases, the tensile strength of LLDPE-D100 and LLDPE-D200 blends decreased while LLDPE-D300 blend showed a marginal increase. The magnitude of elastic modulus increased for 5% concentration of dextrin for all the blends and then it decreased slightly.

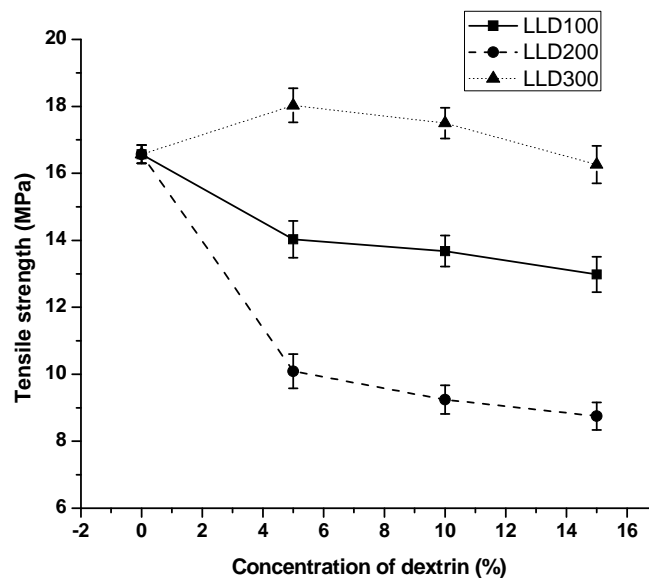


Figure 3.1c. Variation of tensile strength with concentration of dextrin in LLDPE-dextrin blends (LLD100 = LLDPE-dextrin 100 mesh; LLD200 = LLDPE-dextrin 200 mesh; LLD300 = LLDPE-dextrin 300 mesh)

The decrease in tensile strength and elastic modulus may be due to the weakness of interfacial adhesion of the hydrophilic fillers with hydrophobic matrix of LLDPE leading to mechanical rupture at the blend interface.

As the filler concentration increases, there is less effective cross-sectional area of LLDPE matrix towards the spherical beads of starch and dextrin. The tensile strength and elastic modulus of LLS100 blends is lower compared to LLS300 blends. In the case of LLDPE-dextrin blends, the maximum values for tensile strength and elastic modulus were observed for the lowest particle size blend, i.e., LLD300 blend. As the particle size of filler decreases, there is effective interfacial adhesion, which causes an increase in tensile strength of LLD300 and LLS300 blends. The mechanical properties of the blends suggest that like starch, dextrin too has no reinforcing effect on LLDPE.

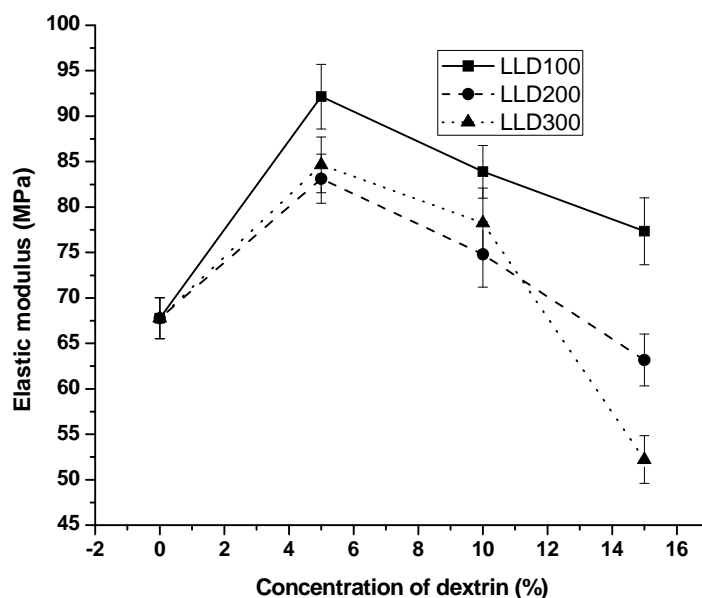


Figure 3.1d. Variation of elastic modulus with concentration of dextrin in LLDPE-dextrin blends (LLD100 = LLDPE-dextrin 100 mesh ; LLD200 = LLDPE-dextrin 200 mesh; LLD300 = LLDPE-dextrin 300 mesh)

Starch and dextrin exhibit hydrophilic properties and strong intermolecular association through hydrogen bonding due to hydroxyl groups on the surface. The hydrophilic nature and strong intermolecular hydrogen bonding make these fillers less compatible with the hydrophobic LLDPE [10]. The dextrin and starch have similar structure and their behavior in the LLDPE matrix too is apparently similar. These observations show good agreement with the results presented by other researchers [13, 14].

3.2.2 Thermal studies

3.2.2.1 Thermogravimetric analyses

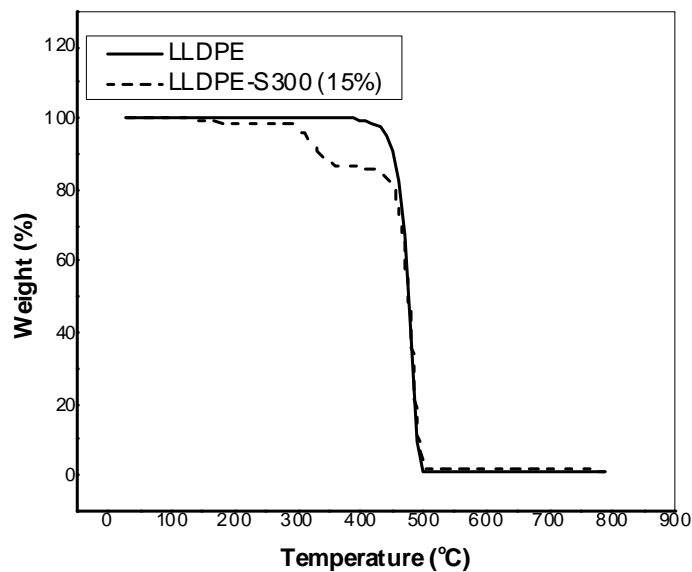


Figure 3.2a. Thermograms of LLDPE and LLDPE-starch (LLDPE-S300, 15%) blends

In thermogravimetry, the mass change of a substance is measured as a function of temperature while the substance is heated under a

controlled temperature program. It has been widely used for studying thermal stability of materials. Since mass is so fundamental to a material, any mass change is more likely to be associated with a chemical change which, in turn, may reflect a compositional change.

Thermograms of LLDPE, LLDPE-S300 (15 weight%) and LLDPE-D300 (15 weight%) blends are shown in figure 3.2a and figure 3.2b. For LLDPE-S300, there is considerable decrease in weight in the temperature range of 250-350°C. For LLDPE-D300 blend also similar weight loss was observed in the same temperature range.

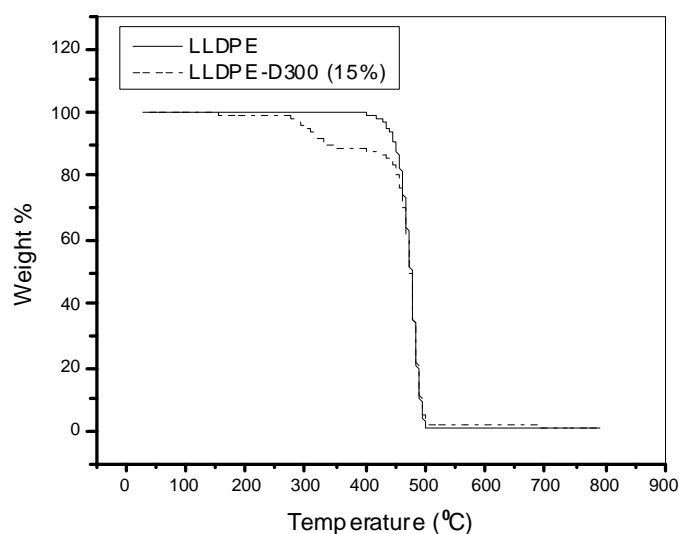


Figure 3.2b Thermograms of LLDPE and LLDPE-dextrin (LLDPE-D300, 15%) blends

Table 3.1 Results of thermogravimetric analyses

Sample	T_{\max} ($^{\circ}\text{C}$)
LLDPE	482
LLDPE-S100 (15%)	482
LLDPE-S300 (15%)	481
LLDPE-D100 (15%)	482
LLDPE-D200 (15%)	481
LLDPE-D300 (15%)	482

The weight change in the temperature range of 250-350 $^{\circ}\text{C}$ corresponds to the loss of fillers, as this is the decomposition temperature for these fillers. Above this temperature, a gradual loss in weight occurs. The temperature at which weight loss is maximum (T_{\max}) is given in table 3.1. There is no significant change in T_{\max} , which indicates that the presence of fillers doesn't adversely affect the thermal stability of LLDPE.

3.2.2.2 Differential scanning calorimetry

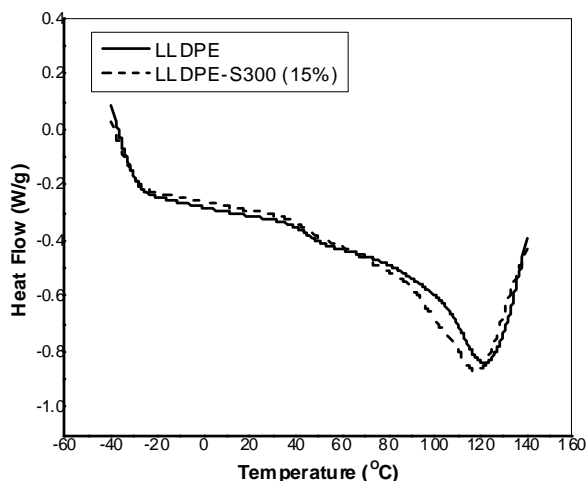


Figure 3.3a DSC thermograms of LLDPE and LLDPE-starch (LLDPE-S300, 15%) blends

Figure 3.3a shows DSC heating curves of LLDPE and LLDPE-S300 (15 weight%) blends. Table 3.2 shows the average values for the melting temperature (T_m), crystallisation temperature (T_c), enthalpy of fusion (ΔH_f), enthalpy of crystallization (ΔH_c) and % crystallinity for LLDPE, LLDPE-S300 (15 weight %) and LLDPE-D300 (15 weight %) blends. DSC thermograms of LLDPE and LLDPE-D300 (15 weight %) blend are shown in figure 3.3b.

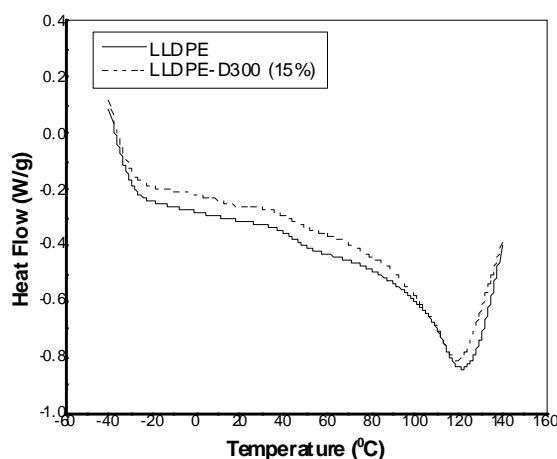


Figure 3.3b DSC thermograms of LLDPE and LLDPE-dextrin (LLDPE-D300, 15%) blends

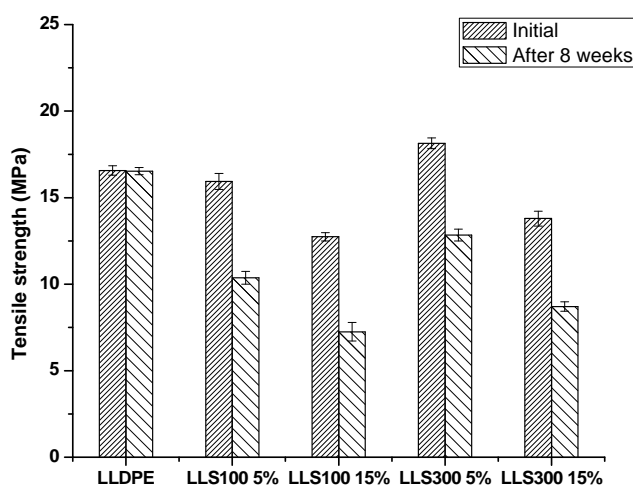
ΔH_f and ΔH_c values for the blends are almost similar as compared to the virgin LLDPE. This suggests that the blends have almost similar degree of crystallinity. There is no significant decrease in crystallinity of LLDPE in the blends, which indicates that LLDPE and fillers are incompatible. i.e., LLDPE-starch and LLDPE-dextrin interactions are weak. The melting and crystallization temperature of LLDPE and blends were almost similar. This also suggests the incompatibility of LLDPE and the fillers [15, 16].

Table 3.2 Results of differential scanning calorimetry

Sample	T_m (°C)	ΔH_f (J/g)	T_c (°C)	ΔH_c (J/g)	% Crystallinity
LLDPE	126	58	106	59	20
LLDPE-starch (S300, 15%)	125	57	107	53	19
LLDPE-dextrin (D300, 15%)	126	55	107	48	19

3.2.3 Biodegradation studies

3.2.3.1 In shake culture flask



[LLS100 5% = LLDPE-starch 100 mesh (5 weight%), LLS100 15% = LLDPE-starch 100 mesh (15 weight%), LLS300 5% = LLDPE-starch 300 mesh (5 weight%), LLS300 15% = LLDPE-starch 300 mesh (15 weight%)]

Figure 3.4a Biodegradation of LLDPE-starch blends after immersion in shake culture flask for 8 weeks (Evident from tensile strength)

The figure 3.4a shows the decrease in tensile strength of LLDPE-starch blends after immersing the strips in shake culture flask [17] for 8 weeks. There is significant variation in tensile strength of the samples

after 8 weeks of immersion in the shake culture flask indicating higher degree of biodegradation. During the incubation of plastic strips in shake culture flask, the mechanical damage of LLDPE macrochain might have caused by swelling and bursting of the growing cells of the invading micro-organisms or the micro-organisms in the shake culture flask [18].

Table 3.3a Percentage decrease in tensile strength of LLDPE-starch blends after biodegradation in shake culture flask for 8 weeks

Sample	Initial tensile strength (MPa)	Tensile strength after 8 weeks (MPa)	% decrease in tensile strength
LLDPE	16.57	16.53	0.24
LLS100 5%	15.94	10.37	34.94
LLS100 15%	12.74	7.25	43.09
LLS300 5%	18.14	12.84	29.22
LLS300 15%	13.79	8.71	36.84

[LLS100 5% = LLDPE-starch 100 mesh (5 weight%), LLS100 15% = LLDPE-starch 100 mesh (15 weight%), LLS300 5% = LLDPE-starch 300 mesh (5 weight%), LLS300 15% = LLDPE-starch 300 mesh(15 weight%)]

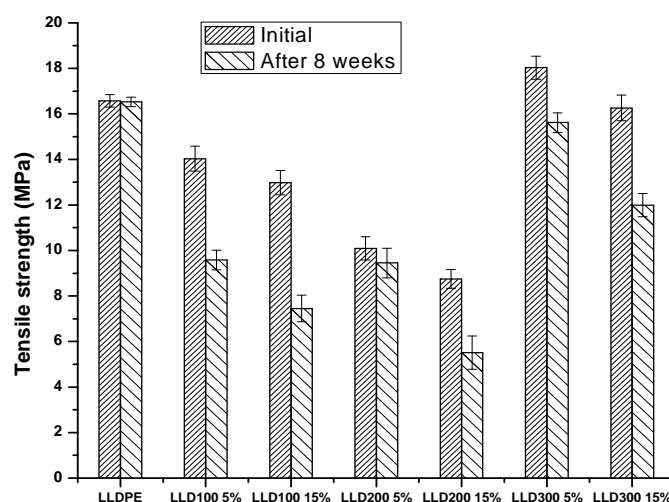
Table 3.3b Weight loss of LLDPE-starch blends after biodegradation in shake culture flask for 8 weeks

Sample	Initial weight (g)	Weight after 8 weeks (g)	% Weight loss
LLDPE	0.2022	0.2021	0.05
LLS100 5%	0.225	0.2191	2.62
LLS100 15%	0.1892	0.1797	5.02
LLS300 5%	0.1662	0.1628	2.05
LLS300 15%	0.1912	0.1838	3.87

[LLS100 5% = LLDPE-starch 100 mesh (5 weight%), LLS100 15% = LLDPE-starch 100 mesh (15 weight%), LLS300 5% = LLDPE-starch 300 mesh (5 weight%), LLS300 15% = LLDPE-starch 300 mesh(15 weight%)]

Tables 3.3 and 3.4 show the percentage decrease in tensile strength and weight of LLDPE-starch blends after biodegradability test in shake culture flask. The tensile strength of these blends was lowered after biodegradability studies in shake culture flask for 8 weeks. For blends containing higher concentrations of starch, the percentage decrease in tensile strength is higher suggesting a higher degree of biodegradation for these blends.

There is considerable loss of weight for these blends after immersing the strips in shake culture flask for 8 weeks. This also is in agreement with increased biodegradation of LLDPE in presence of starch.



[LLD100 5% = LLDPE-dextrin 100 mesh (5 weight%), LLD100 15% = LLDPE-dextrin 100 mesh (15 weight%), LLD200 5% = LLDPE-dextrin 200 mesh (5 weight%), LLD200 15% = LLDPE-dextrin 200 mesh (15 weight%), LLD300 5% = LLDPE-dextrin 300 mesh (5 weight%), LLD300 15% = LLDPE-dextrin 300 mesh (15 weight%)]

Figure 3.4b Biodegradation of LLDPE-dextrin blends after immersing the plastic strips in shake culture flask for 8 weeks (As evident from tensile strength)

The figure 3.4b shows the decrease in tensile strength of LLDPE-dextrin blends after immersing the strips prepared from the blends in shake culture flask for 8 weeks. There is significant variation in tensile strength of the blends indicating higher degree of biodegradation.

Table 3.4a Percentage decrease in tensile strength of LLDPE-dextrin blends after immersion of plastic strips in shake culture flask for 8 weeks

Sample	Initial tensile strength (MPa)	Tensile strength after 8 weeks (MPa)	% decrease in tensile strength
LLDPE	16.57	16.53	0.24
LLD100 5%	14.03	9.58	31.71
LLD100 15%	12.98	7.45	42.6
LLD200 5%	10.09	9.45	6.34
LLD200 15%	8.75	5.51	37.03
LLD300 5%	18.03	15.62	13.37
LLD300 15%	16.26	11.99	26.26

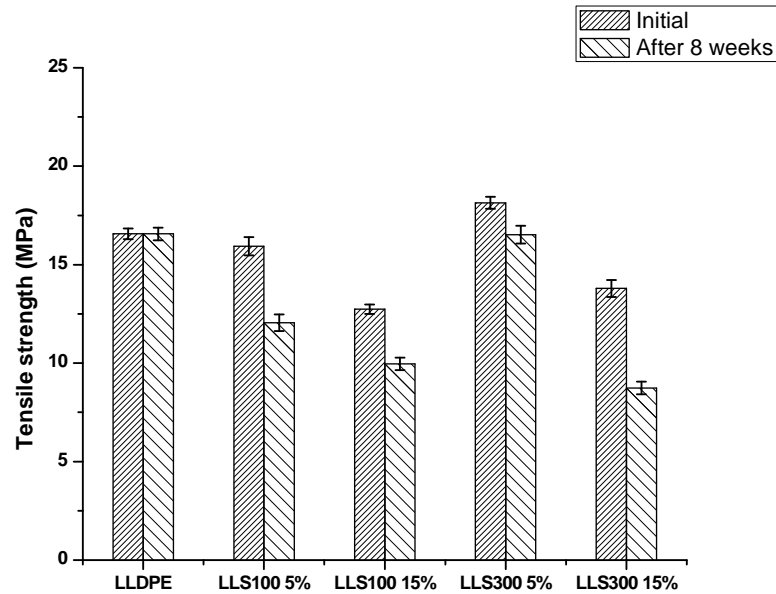
[LLD100 5% = LLDPE-dextrin 100 mesh (5 weight%), LLD100 15% = LLDPE-dextrin 100 mesh (15 weight%), LLD200 5% = LLDPE-dextrin 200 mesh (5 weight%), LLD200 15% = LLDPE-dextrin 200 mesh (15 weight%), LLD300 5% = LLDPE-dextrin 300 mesh (5 weight%), LLD300 15% = LLDPE-dextrin 300 mesh (15 weight%)]

Table 3.4b Weight loss of LLDPE-dextrin blends after immersion of plastic strips in shake culture flask for 8 weeks

Sample	Initial weight (g)	Weight after 8 weeks (g)	% Weight loss
LLDPE	0.2022	0.2021	0.05
LLD100 5%	0.2602	0.2586	0.61
LLD100 15%	0.2382	0.2283	4.16
LLD200 5%	0.2212	0.2187	1.13
LLD200 15%	0.2596	0.245	5.62
LLD300 5%	0.1637	0.1567	4.28
LLD300 15%	0.1993	0.1841	7.62

[LLD100 5% = LLDPE-dextrin 100 mesh (5 weight%), LLD100 15% = LLDPE-dextrin 100 mesh (15 weight%), LLD200 5% = LLDPE-dextrin 200 mesh (5 weight%), LLD200 15% = LLDPE-dextrin 200 mesh (15 weight%), LLD300 5% = LLDPE-dextrin 300 mesh (5 weight%), LLD300 15% = LLDPE-dextrin 300 mesh (15 weight%)]

3.2.3.2 Soil burial test



[LLS100 5% = LLDPE-starch 100 mesh (5 weight%), LLS100 15% = LLDPE-starch 100 mesh (15 weight%), LLS300 5% = LLDPE-starch 300 mesh (5 weight%), LLS300 15% = LLDPE-starch 300 mesh (15 weight%)]

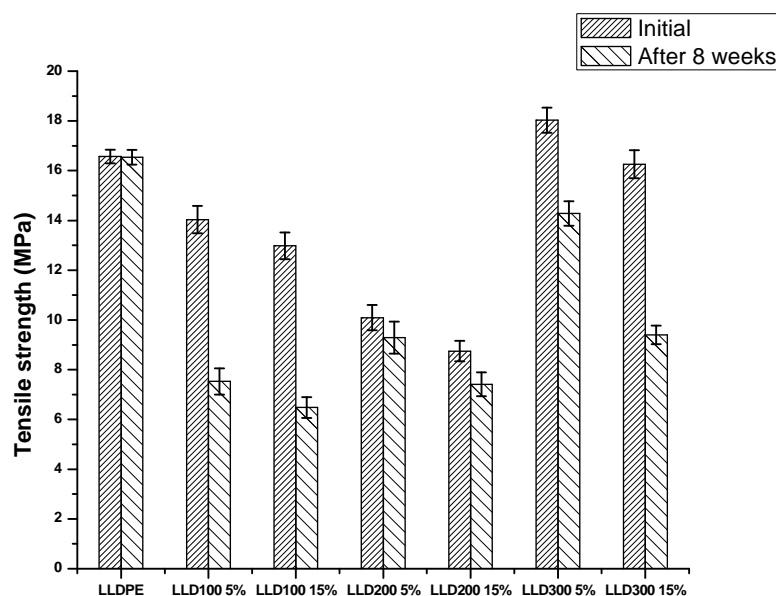
Figure 3.5a Variation of tensile strength of LLDPE-starch blends after soil burial test

Figure 3.5a shows the variation in tensile strength of LLDPE-starch blends after the soil burial test. Tensile strength decreases considerably on increasing the filler content indicating an increase in rate of biodegradation. The variation in tensile strength of LLDPE-dextrin blends after soil burial test is shown in figure 3.5b. The decrease in tensile strength is considerable for the blends as compared to the neat LLDPE suggesting an increase in the rate of biodegradation.

Table 3.5a % weight loss of LLDPE-starch blends after soil burial test

Sample	Initial weight (g)	Weight after 8 weeks (g)	% Weight loss
LLDPE	2.77	2.77	0
LLS100 5%	0.8272	0.8257	0.18
LLS100 15%	0.9837	0.9788	0.50
LLS300 5%	0.6366	0.6365	0.02
LLS300 15%	0.9338	0.9311	0.29

[LLS100 5% = LLDPE-starch 100 mesh (5 weight%), LLS100 15% = LLDPE-starch 100 mesh (15 weight%), LLS300 5% = LLDPE-starch 300 mesh (5 weight%), LLS300 15% = LLDPE-starch 300 mesh(15 weight%)]



[LLD100 5% = LLDPE-dextrin 100 mesh (5 weight%), LLD100 15% = LLDPE-dextrin 100 mesh (15 weight%), LLD200 5% = LLDPE-dextrin 200 mesh (5 weight%), LLD200 15% = LLDPE-dextrin 200 mesh(15 weight%), LLD300 5% = LLDPE-dextrin 300 mesh (5 weight%), LLD300 15% = LLDPE-dextrin 300 mesh (15 weight%)]

Figure 3.5b Variation of tensile strength of LLDPE-dextrin blends after soil burial test

Table 3.5b % weight loss of LLDPE-dextrin blends after soil burial test

Sample	Initial weight (g)	Weight after 8 weeks (g)	% Weight loss
LLDPE	2.77	2.77	0
LLD100 5%	0.7058	0.7018	0.57
LLD100 15%	0.5483	0.5419	1.17
LLD200 5%	0.764	0.7614	0.34
LLD200 15%	0.5614	0.5523	1.62
LLD300 5%	0.5942	0.5936	0.10
LLD300 15%	0.4695	0.4622	1.55

[LLD100 5% = LLDPE-dextrin 100 mesh (5 weight%), LLD100 15% = LLDPE-dextrin 100 mesh (15 weight%), LLD200 5% = LLDPE-dextrin 200 mesh (5 weight%), LLD200 15% = LLDPE-dextrin 200 mesh (15 weight%), LLD300 5% = LLDPE-dextrin 300 mesh (5 weight%), LLD300 15% = LLDPE-dextrin 300 mesh (15 weight%)]

Tables 3.5a and 3.5b show the percentage weight loss of LLDPE-starch and LLDPE-dextrin blends after burial in the soil for 8 weeks. Both LLDPE-starch and LLDPE-dextrin blends show weight loss indicating that these blends are partially biodegradable.

3.2.4. Scanning electron microscopic studies

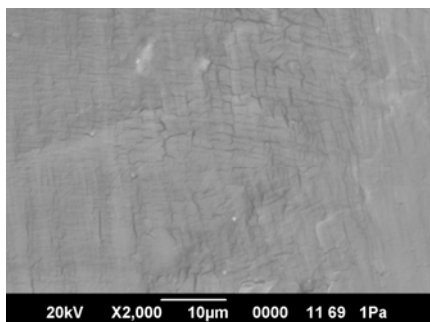


Figure 3.6a LLDPE -Before biodegradation

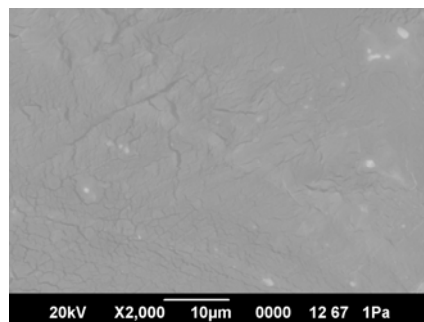


Figure 3.6b LLDPE- After biodegradation

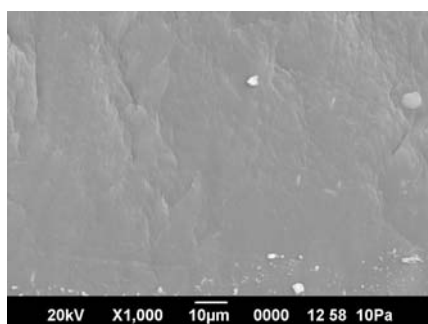


Figure 3.7a LLDPE-starch (S300) blend- Before biodegradation

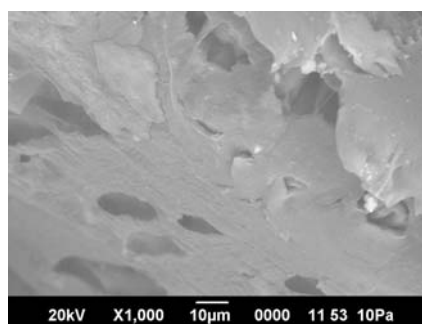


Figure 3.7b LLDPE- starch (S300) blend- After biodegradation

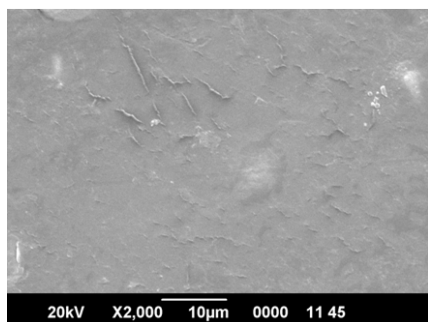


Figure 3.8a LLDPE-dextrin (D300) blend – Before biodegradation

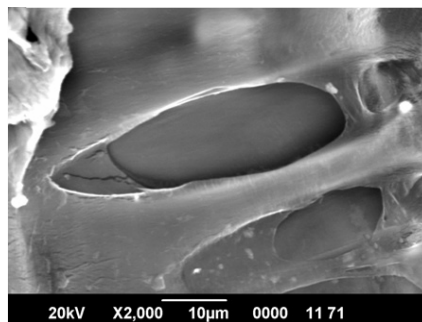
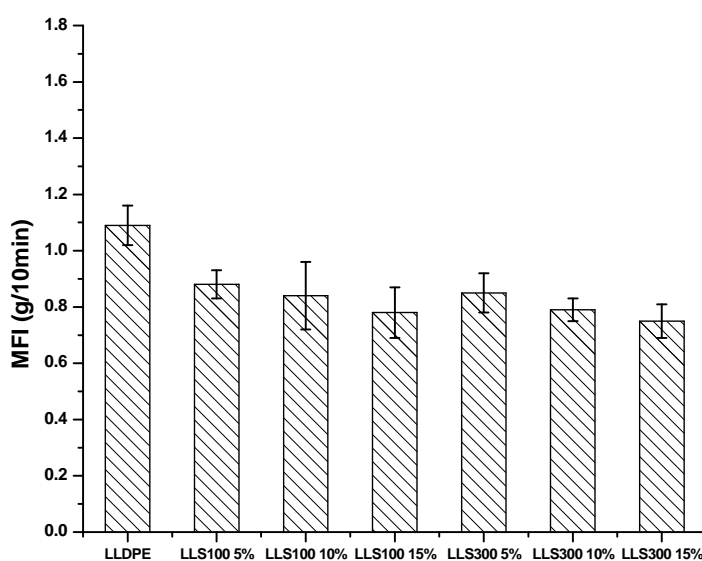


Figure 3.8b LLDPE- dextrin (D300) blend – After biodegradation

SEM is a significant and reliable tool to measure the morphological changes of a degraded polymer. The scanning electron photomicrographs of LLDPE, before and after biodegradation studies in shake culture flask for 8 weeks are shown in figures 3.6a and 3.6b. As seen in the SEM images, the LLDPE has not undergone any degradation after immersing the strips in shake culture flask for 8 weeks. The surface of LLDPE after 8 weeks immersion in shake culture flask was smooth, without cracks and defects. The scanning electron photomicrographs of LLDPE-starch blends, before and after biodegradation studies in shake culture flask for 8 weeks are shown in figures 3.7a and 3.7b. Figures 3.8a and 3.8b represent the scanning electron photomicrographs of LLDPE-dextrin blends, before and after incubation in shake culture flask. During the incubation period, the degradation of LLDPE-starch and LLDPE-dextrin blends occurred and the change in morphology was observed in scanning electron photomicrographs. The formation of cavities in the blends after biodegradation is due to the removal of bio-fillers by the microorganisms. In the case of LLDPE-starch blends, the cavities are numerous and small in size whereas in LLDPE-dextrin blends the cavities are less in number and bigger in size. It shows that the bio-fillers in the blend favours the microbial accumulation throughout the surface [19]. The scanning electron photomicrographs of LLDPE-starch and LLDPE-dextrin reveal two-phase morphology indicating that these are immiscible. The LLDPE acts as the continuous phase and the filler acts as the dispersed phase. From the scanning electron photomicrographs, it can be seen that the dispersion of filler particles in the LLDPE matrix is almost uniform.

3.2.5 Melt flow test

The MFI of a polymer is related to its molecular weight distribution and is often used to characterize processability [20]. The melt flow indices (MFI) of all blends were determined according to ASTM D- 1238 [21].

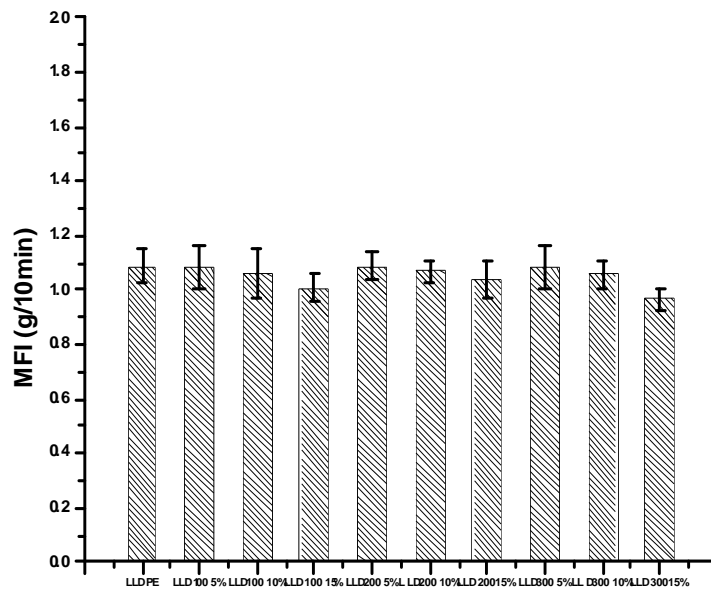


[LLS100 5% = LLDPE-starch 100 mesh (5 weight%), LLS100 10% = LLDPE-starch 100 mesh (10 weight%), LLS100 15% = LLDPE-starch 100 mesh (15 weight%), LLS300 5% = LLDPE-starch 300 mesh (5 weight%), LLS300 10% = LLDPE-starch 300 mesh (10 weight%), LLS300 15% = LLDPE-starch 300 mesh (15 weight%)]

Figure 3.9a Melt flow indices of LLDPE-starch blends

The melt flow indices of LLDPE-starch and LLDPE-dextrin blends are shown in figures 3.9a and 3.9b. Incorporation of starch and dextrin to LLDPE decreased the MFI values of the blends. The MFI decreased with increasing starch and dextrin content. Since the MFI is an indirect measure of viscosity, the results show that both starch and dextrin act as rigid fillers, because the main effect of rigid

fillers is to increase the elastic modulus of a composite or the viscosity of a fluid suspension [22]. When solid particles are present in the matrix, they restrict the melt movement by increasing viscosity, which implies the hardening effect of filler [23]. The melt flow index gives information about the degree of chain entanglement of polymer chains by chemical or physical crosslinks [24]. The low melt flow indices at higher concentration of the fillers are apparently due to increased entanglement of the polymer chains of LLDPE and the fillers.



[LLD100 5% = LLDPE-dextrin 100 mesh (5 weight%), LLD100 10% = LLDPE-dextrin 100 mesh (10 weight%), LLD100 15% = LLDPE-dextrin 100 mesh (15 weight%), LLD200 5% = LLDPE-dextrin 200 mesh (5 weight%), LLD200 10% = LLDPE-dextrin 200 mesh (10 weight%), LLD200 15% = LLDPE-dextrin 200 mesh (15 weight%), LLD300 5% = LLDPE-dextrin 300 mesh (5 weight%), LLD300 10% = LLDPE-dextrin 300 mesh (10 weight%), LLD300 15% = LLDPE-dextrin 300 mesh (15 weight%)]

Figure 3.9b Melt flow indices of LLDPE-dextrin blends

3.2.6 Infrared spectroscopic analyses

Representative FTIR spectra of starch, dextrin, LLDPE (before and after biodegradation), LLDPE-starch (before and after biodegradation) and LLDPE-dextrin (before and after biodegradation) are shown in figures 3.10a, 3.10b, 3.10c, 3.10d and 3.10e in the range of 4000-400 cm^{-1} .

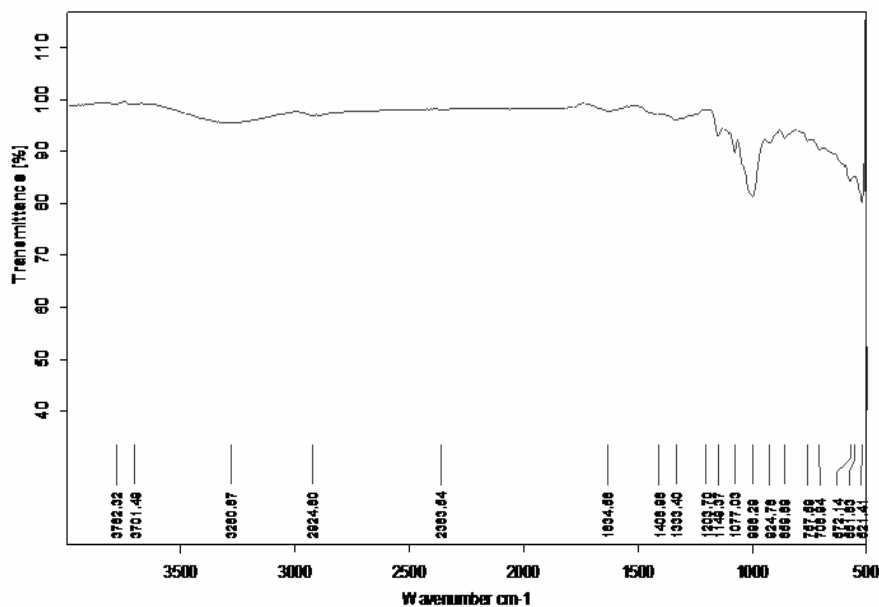


Figure 3.10a FTIR spectrum of starch

The characteristic peak assignments are shown in table 3.6. For starch, three peaks corresponding to C-O stretching and O-H deformation were observed. For dextrin the peaks obtained correspond to O-H stretching, C-H bending, C-O stretching and O-H deformation. All the characteristics peaks of pure LLDPE, pure starch and pure dextrin can be seen in the spectra of LLDPE-starch and LLDPE-dextrin

blends which shows that the whole spectrum is the superposition of the spectra of pure polymers. This reveals that IR spectral bands are not affected by the compositions of blends, which indicates that there is no specific interaction between LLDPE and starch, as well as LLDPE and dextrin. The incompatibility of LLDPE and the bio-fillers can be explained by FTIR spectra of the polymer and the blends.

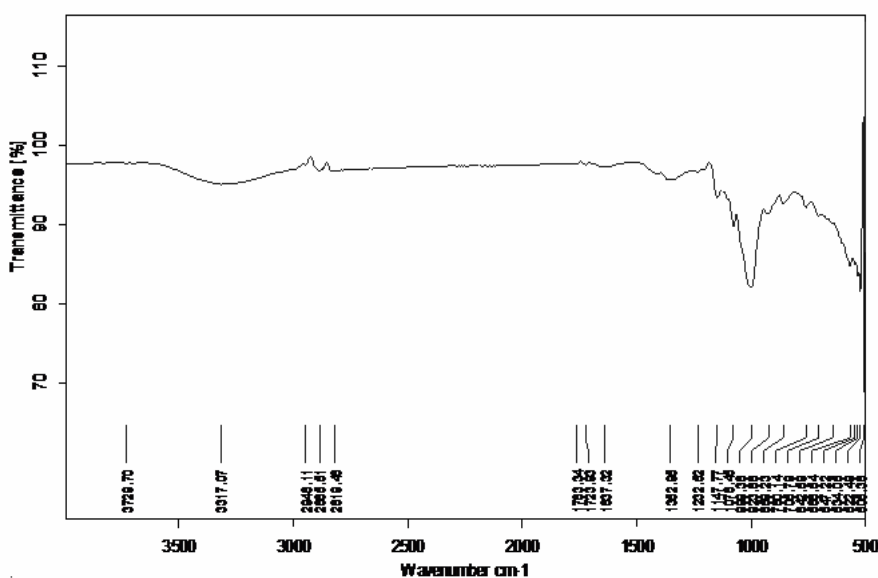


Figure 3.10b FTIR spectrum of dextrin

Two peaks at 3317 cm^{-1} and 999 or 1000 cm^{-1} were observed which correspond to the O-H stretching vibrations of starch and dextrin. A typical IR spectrum of the dextrin presents bands at 3365 cm^{-1} (O-H), $2851\text{-}2940\text{ cm}^{-1}$ (C-H), $1040\text{-}1110\text{ cm}^{-1}$ (C-O) [25].

Information about different stages of degradation can be obtained by subtracting the spectrum of the pure polymer from the spectrum of the degraded sample [26, 27].

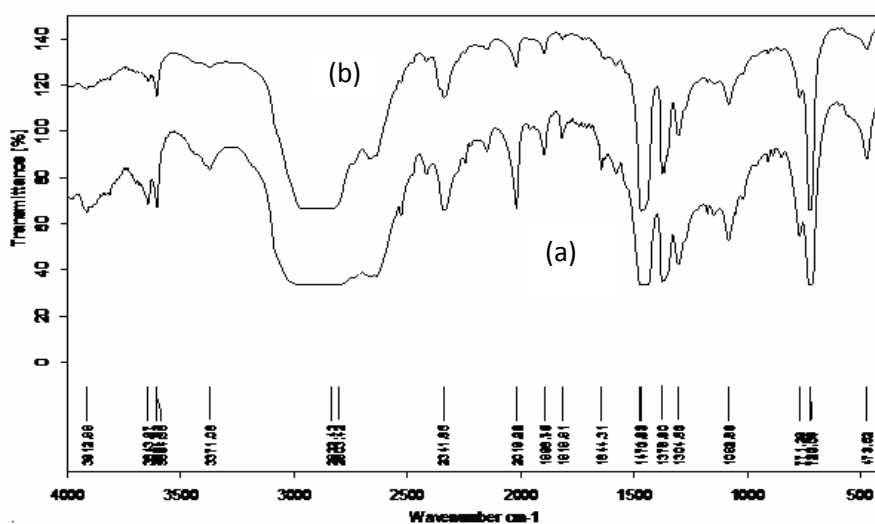


Figure 3.10c FTIR spectra of LLDPE: (a) before biodegradation, (b) after biodegradation in shake culture flask for 8 weeks

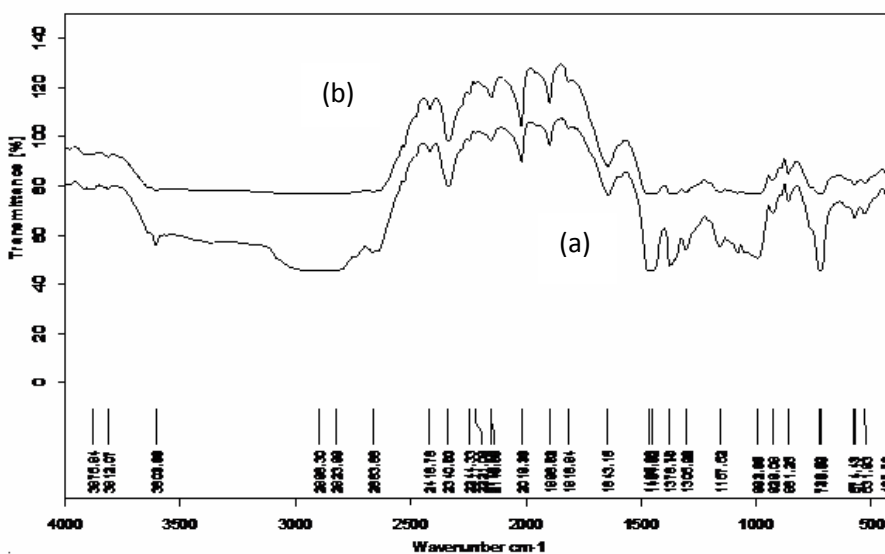


Figure 3.10d FTIR spectra of LLDPE-S300 blends: (a) before biodegradation, (b) after biodegradation in shake culture flask for 8 weeks

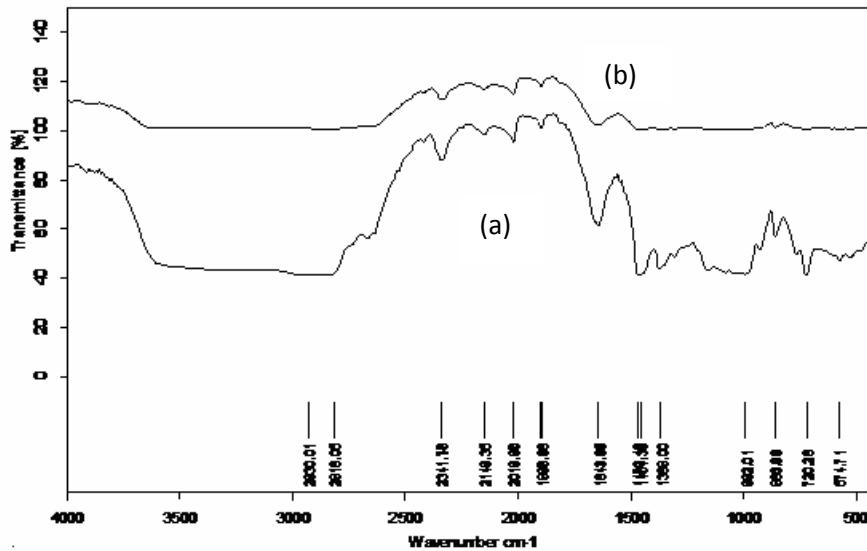


Figure 3.10e FTIR spectra of LLDPE-D300 blends: (a) before biodegradation, (b) after biodegradation in shake culture flask for 8 weeks

Comparison of spectra of LLDPE-starch (before and after biodegradation) shows notable differences in intensities at 1454 cm^{-1} (H-C-OH deformation), 1376 cm^{-1} (C-H bending), 991 cm^{-1} (O-H deformation) and 719 cm^{-1} (CH_2 vibration). The difference in peak intensities at 1454 cm^{-1} and 991 cm^{-1} reveals the removal of starch by the microorganism. There is slight difference in the intensity of peaks at 1376 cm^{-1} and 719 cm^{-1} which could be due to the removal of LLDPE also. The pores generated by the removal of starch act as a feasible site for oxygen and microbes to enhance the degradation process.

In case of LLDPE-dextrin blends, the comparison of the spectra, before and after biodegradation, shows notable differences in peak intensities at 1648 cm^{-1} (O-H band of absorbed water), 1470 cm^{-1}

(CH₂ bending), 1368 cm⁻¹ (C-H bending), 992 cm⁻¹ (O-H deformation) and 720 cm⁻¹ (CH₂ vibration). The difference in peak intensities at 1648 cm⁻¹ and 992 cm⁻¹ of LLDPE-dextrin blends after biodegradation indicates the removal of dextrin by microorganisms. Here too slight differences for CH₂ bending, C-H bending and CH₂ vibration were observed. This could be explained as the removal of LLDPE by microorganism when dipped in shake culture flask for 8 weeks.

Table 3.6 Characteristic FTIR spectral peaks (cm⁻¹) in starch, dextrin and LLDPE

	Peak position (cm⁻¹)	Characteristic group
Starch	1149	C-O stretching
	1077	C-O stretching
	998	O-H deformation
Dextrin	3317	O-H stretching
	1352	C-H bending
	1147	C-O stretching
	1076	C-O stretching
	999	O-H deformation
LLDPE	1644	δ (O-H) band of absorbed water
	1470	CH ₂ bending
	720	skeletal vibration CH ₂

3.2.7 Water absorption studies

The uptake of water by LLDPE-starch and LLDPE-dextrin blends was determined according to ASTM D-570 [28]. Tables 3.7a

and 3.7b show the percentage water absorption values for the blends. The uptake of water by pure LLDPE was only 0.25% whereas for blends an enhancement in water uptake was observed.

Table 3.7a Water absorption values of LLDPE-starch blends

Sample	Initial weight (g)	Weight after 8 weeks (g)	% Water absorption
LLDPE	0.0394	0.0395	0.25
LLS100 5%	0.1055	0.1084	2.75
LLS100 10%	0.1354	0.1398	3.25
LLS100 15%	0.0573	0.061	6.46
LLS300 5%	0.0406	0.0417	2.71
LLS300 10%	0.0774	0.0803	3.75
LLS300 15%	0.0474	0.05	5.49

[LLS100 5% = LLDPE-starch 100 mesh (5 weight%), LLS100 10% = LLDPE-starch 100 mesh (10 weight%), LLS100 15% = LLDPE-starch 100 mesh (15 weight%), LLS300 5% = LLDPE-starch 300 mesh (5 weight%), LLS300 10% = LLDPE-starch 300 mesh (10 weight%), LLS300 15% = LLDPE-starch 300 mesh(15 weight%)]

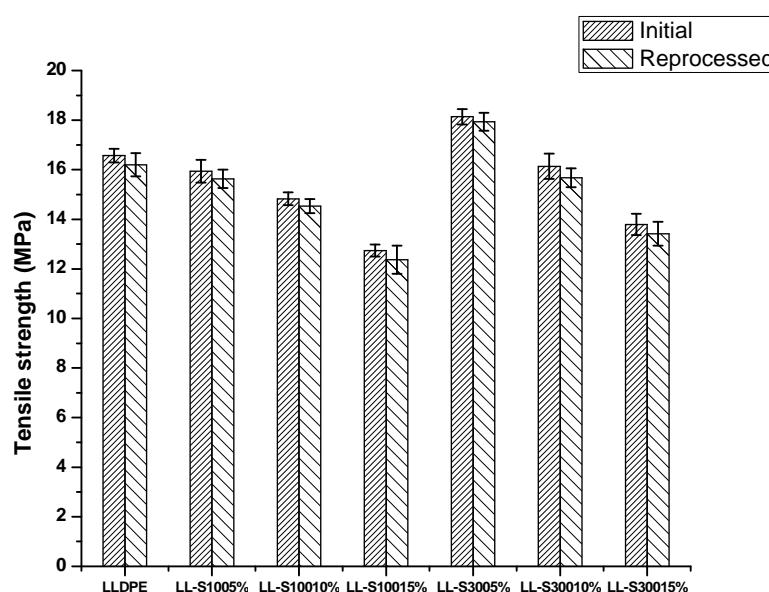
Table 3.7b Water absorption values of LLDPE-dextrin blends

Sample	Initial weight (g)	Weight after 8 weeks (g)	% Water absorption
LLDPE	0.0394	0.0395	0.25
LLD100 5%	0.1096	0.1128	2.92
LLD100 10%	0.0875	0.0922	5.37
LLD100 15%	0.0519	0.0552	6.36
LLD200 5%	0.0982	0.1032	5.09
LLD200 10%	0.045	0.0475	5.56
LLD200 15%	0.1155	0.1232	6.67
LLD300 5%	0.0441	0.0479	8.61
LLD300 10%	0.0679	0.074	8.98
LLD300 15%	0.0417	0.0459	10.07

[LLD100 5% = LLDPE-dextrin 100 mesh (5 weight%), LLD100 10% = LLDPE-dextrin 100 mesh (10 weight%), LLD100 15% = LLDPE-dextrin 100 mesh (15 weight%), LLD200 5% = LLDPE-dextrin 200 mesh (5 weight%), LLD200 10% = LLDPE-dextrin 200 mesh (10 weight%), LLD200 15% = LLDPE-dextrin 200 mesh(15 weight%), LLD300 5% = LLDPE-dextrin 300 mesh (5 weight%), LLD300 10% = LLDPE-dextrin 300 mesh (10 weight%), LLD300 15% = LLDPE-dextrin 300 mesh (15 weight%)]

For higher concentrations of fillers, the water absorption values increased. This may be the reason for improved susceptibility of these blends to microbial attack and more degradation observed after immersing the blends in shake culture flask and also after soil burial.

3.2.8 Reprocessability

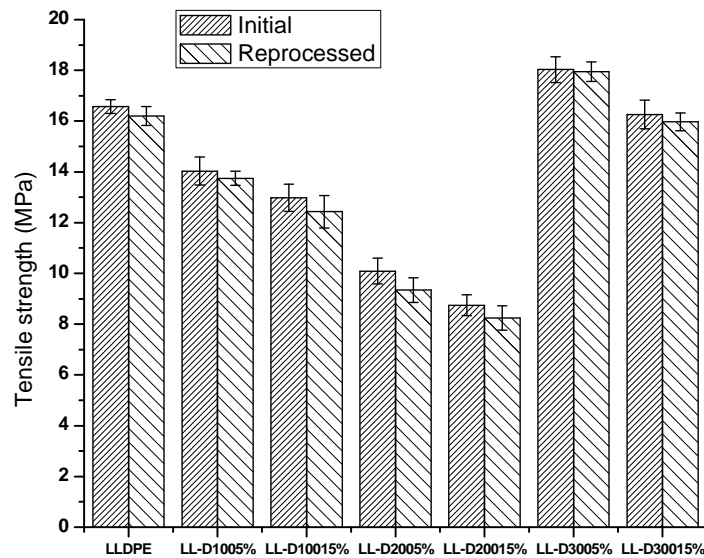


[LLS100 5% = LLDPE-starch 100 mesh (5 weight%), LLS100 10% = LLDPE-starch 100 mesh (10 weight%), LLS100 15% = LLDPE-starch 100 mesh (15 weight%), LLS300 5% = LLDPE-starch 300 mesh (5 weight%), LLS300 10% = LLDPE-starch 300 mesh (10 weight%), LLS300 15% = LLDPE-starch 300 mesh (15 weight%)]

Figure 3.11a Reprocessability of LLDPE-starch blends with respect to tensile strength

The reprocessability of LLDPE-starch and LLDPE-dextrin blends are shown in figures 3.11a and 3.11b. It was observed that the stress-strain properties of the LLDPE-starch and LLDPE-dextrin blends remained almost constant after repeated mixing in a Thermo HAAKE polylab system and moulding in an electrically heated

hydraulic press up to three cycles. This shows that the LLDPE-starch and LLDPE-dextrin blends could be reprocessed by mechanical recycling without deterioration in properties.



[LLD100 5% = LLDPE-dextrin 100 mesh (5 weight%), LLD100 15% = LLDPE-dextrin 100 mesh (15 weight%), LLD200 5% = LLDPE-dextrin 200 mesh (5 weight%), LLD200 15% = LLDPE-dextrin 200 mesh (15 weight%), LLD300 5% = LLDPE-dextrin 300 mesh (5 weight%), LLD300 15% = LLDPE-dextrin 300 mesh (15 weight%)]

Figure 3.11b Reprocessability of LLDPE-dextrin blends with respect to tensile strength

3.3 Conclusion

The comparison of the mechanical properties of neat LLDPE and the blends suggest that the fillers have no reinforcing effect on LLDPE. The thermogravimetric studies indicate that the thermal stability of the blends are unaffected by the addition of fillers. The percentage crystallinity of the blends and the neat LLDPE are almost similar suggesting that the fillers and the LLDPE are incompatible. The results of FTIR studies also support the incompatibility of LLDPE

and the fillers. The reduction in tensile properties and the loss of weight of the samples after biodegradability studies in shake culture flask and also after soil burial test for 8 weeks suggest that these blends are partially biodegradable. The scanning electron photomicrographs of LLDPE-starch and LLDPE-dextrin blends confirm the biodegradability of the blends in shake culture flask. The differences in the characteristic FTIR peak intensities of LLDPE-starch and LLDPE-dextrin blends before and after biodegradation studies in shake culture flask reveal the biodegradation of the samples in presence of amylase producing vibrios. The blends show lower melt flow indices as compared to neat LLDPE. The lower melt flow indices at higher concentrations of the fillers are apparently due to increased entanglement of the polymer chains of LLDPE and the fillers. The water absorption values of the blends were higher indicating an enhanced affinity for microbial attack. The reprocessability studies on the blends suggest that the blends could be repeatedly reprocessed without deterioration in mechanical properties.

References

- [1] Kim M, and Lee S, *Carbohydrate Polymers*, **50**, [2002], 331.
- [2] Soundararajan S, Palanivelu K, and Sharma SK, *Popular Plastics and Packaging*, **47**, [2002], 80.
- [3] Kim M, *Carbohydrate Polymers*, **54**, [2003], 173.
- [4] Ke T, Sun S, and Seib P, *Journal of Applied Polymer Science*, **89**, [2003], 3639.

- [5] Bhattacharya M, and Mani R, *Journal of Applied Polymer Science*, **90**, [2003], 1545.
- [6] Tharanathan RN, *Trends in Food Science and Technology*, **14**, [2003], 71.
- [7] Chiellini E, Corti V, Swift G, *Polymer Degradation and Stability*, **81**, [2003], 341.
- [8] Chandra R, Rustgi R, *Progress in Polymer Science*, **23**, [1998], 1273.
- [9] Peacock AJ, *Handbook of Polyethylene: Structure, Properties and Applications*, CRC Press, [2000], 2-24.
- [10] Garg S and Jana AK, *Indian Chemical Engineer*, Section A, Vol. 48, No.3, [2006], 185.
- [11] Baldev Raj, Udaya Sankar K., Siddaramaiah, *Advances in Polymer Technology*, **23**, [2004], 32.
- [12] Finar IL, *Organic Chemistry Vol 2: Stereochemistry and the Chemistry of Natural Products (Fifth Edition)*, Pearson Education (Singapore) Pte. Ltd., [1973], 339.
- [13] Thakore IM, Iyer S, Desai A, Lele V and Devi S, *Journal of Applied Polymer Science*, **74**, [1999], 2791.
- [14] Ahamed NT, Singhal RS, Kulkarni PR, Kale DD and Pal M, *Carbohydrate Polymers*, **31**, [1996], 157.
- [15] Pedroso AG and Rosa DS, *Carbohydrate Polymers*, **59**, [2005], 1.
- [16] Aburto J, Thiebaud S, Alric I, Borredon E, Bikiaris D, Prinos J & Panayiotou C, *Carbohydrate Polymers*, **34**, [1997], 101.
- [17] *Annual Book of ASTM Standards*, D 6691, **08.03**, [2004].

- [18] Rutkowska M, Heimowska A, Krasowska K, Janik H, *Polish Journal of Environmental Studies*, **11**, [2002], 267.
- [19] Pratheep Kumar A, Jitendra K. Pandey, Bijendra Kumar, Singh RP, *Journal of Polymers and the Environment*, **14**, [2006], 203.
- [20] Bremner T, Rudin A and Cook DG, *Journal of Applied Polymer Science*, **41**, [1990], 1617.
- [21] Annual Book of ASTM Standards, D 1238, **08.01**, [2004].
- [22] Nielsen LE., *Mechanical Properties of Polymers and Composites*, Vol. 1., Marcel Dekker: New York, [1974], 255.
- [23] Albano C, Karam A, Dominguez N, Sanchez Y, Gonzalez J, Aguirre O, Catano L, *Composite Structures*, **71**, [2005], 282.
- [24] Jang BC, Huh SY, Jang JG, Bae YC, *Journal of Applied Polymer Science*, **82**, [2001], 3313.
- [25] Wang HR, Chen KM, *Colloids and Surfaces A: Physicochemical and Engineering Aspects*, **281**, [2006], 190.
- [26] Lin SC, Bulkin BJ, Pearce EM, *Journal of Polymer Science Polymer Chemistry*, Ed **17**, [1979], 3121.
- [27] Coleman MM, Painter PC, *Fourier Transform Infra-red Spectra of Macromolecules*. In: Brame Jr EG (ed) *Applications of Polymer Spectroscopy*, Academic Press, New York, [1978], 135.
- [28] Annual Book of ASTM Standards, D 570, **08.01**, [2004].

.....❧.....

PHOTODEGRADATION OF LLDPE USING METAL OXIDES AND A METAL STEARATE

<i>Contents</i>	4.1 Introduction
	4.2 Results and Discussion
	4.3 Conclusion

.....

Various metal oxides [iron oxide, manganese dioxide, titanium dioxide (rutile and anatase grades)] and a metal stearate (cobalt stearate) have been mixed with linear low density polyethylene to enhance its photodegradability. The studies include the evaluation of mechanical properties, thermal properties, measurement of melt flow indices, water absorption and reprocessability. For assessing the effect of metal oxides and the stearate on the photodegradability of LLDPE, the test specimens were exposed under a 30 watt shortwave UV lamp and were retrieved at different time intervals. The mechanical properties and changes in FTIR spectra of the specimens were noted before and after exposure to ultraviolet light. The results of the study show that the presence of metal oxides and the stearate enhances the photodegradation of LLDPE.

.....

4.1 Introduction

Polyolefins are widely used in the manufacture of disposable containers for food and beverages, and films for agricultural mulching. Polyolefins show very low degree of degradation when exposed to sunlight (photodegradation) [1]. Although photodegradation is undesirable in the case of plastic products where durability is important, it is ecologically desirable in the case of disposable containers and agricultural mulching films. Pro-oxidants have been mixed with plastic materials to accelerate degradation on exposure to sunlight, thereby facilitating the disposal of the plastic products [1-6].

The effect of pro-oxidants on the photodegradation of linear low density polyethylene has not been systematically studied so far. This chapter reports the results of investigations on the role of various pro-oxidants on the photodegradation of LLDPE.

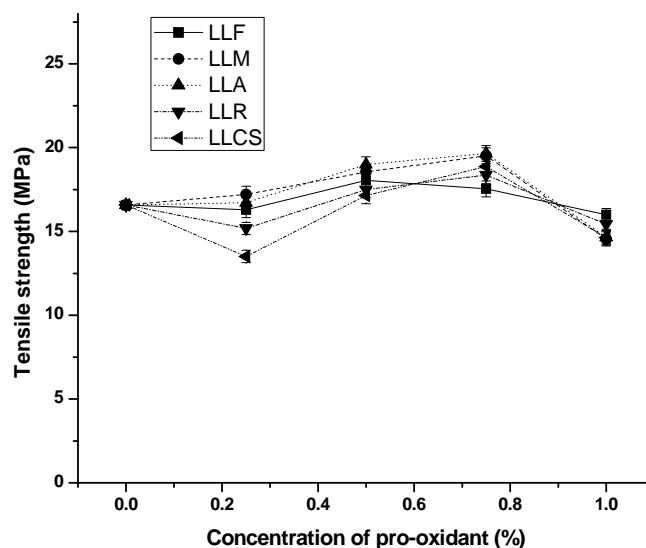
The natural photodegradation of polyolefins is reported to be a very slow process [7-10]. Typical pro-oxidants used with the plastics include the oxides or stearates of metals such as manganese, iron, zinc, zirconium, cerium, titanium and cobalt [11-15]. Due to its superb characteristics such as inexpensiveness, non-toxicity, stability and high photoactivity, titanium dioxide has become the popular choice as photocatalyst [16,17].

Linear low density polyethylene containing various compositions (0.25, 0.5, 0.75 and 1 weight %) of pro-oxidants, viz., iron oxide, manganese dioxide, titanium dioxide (rutile and anatase grade) and cobalt

stearate were prepared by melt mixing [18]. These compositions were exposed to UV light for 240 hours. The mechanical properties, thermal properties, FTIR spectra, melt flow characteristics, water absorption and reprocessability [19-21] of the pro-oxidant mixed LLDPE were compared with those of the neat LLDPE.

4.2 Results and Discussion

4.2.1 Mechanical properties

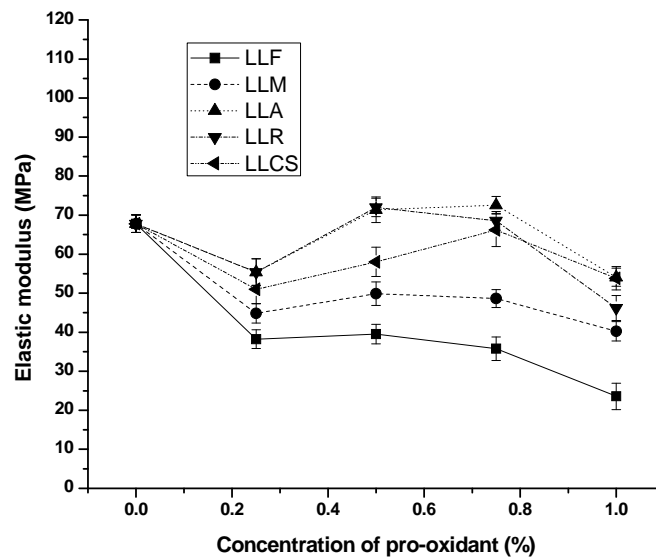


[LLF = LLDPE-Fe₂O₃, LLM = LLDPE-MnO₂, LLA = LLDPE-TiO₂ (Anatase), LLR = LLDPE- TiO₂ (Rutile), LLCS = LLDPE-Cobalt stearate]

Figure 4.1a Variation of tensile strength of LLDPE on addition of various pro-oxidants

The variation of tensile strength with concentration of various pro-oxidants are shown in figure 4.1a. The tensile strength of all the mixes was found to increase marginally for higher dosages of pro-oxidants as compared to neat LLDPE.

For LLDPE-Fe₂O₃, the maximum tensile strength was observed in the case of the composition containing 0.5 weight % of iron oxide. Further increase in the iron oxide content decreased the tensile strength. In case of LLDPE-MnO₂, the maximum tensile strength was obtained for the mix containing 0.75 weight % MnO₂. Similar results were observed in the case of the mixes containing TiO₂ (Anatase), TiO₂ (Rutile) and cobalt stearate.



(LLF = LLDPE-Fe₂O₃, LLM = LLDPE-MnO₂, LLA = LLDPE-TiO₂ (Anatase), LLR = LLDPE- TiO₂ (Rutile), LLCS = LLDPE-Cobalt stearate)

Figure 4.1b Variation of elastic modulus of LLDPE on addition of various pro-oxidants

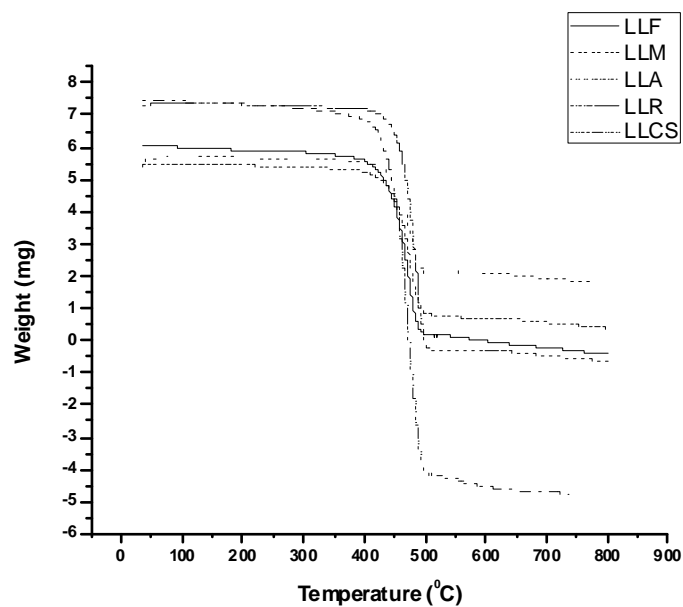
Figure 4.1b shows the variation of elastic modulus with concentration of pro-oxidants. The compositions containing titanium dioxide and cobalt stearate show marginal improvement in elastic modulus at optimum dosage of the pro-oxidant (based on tensile

strength) whereas all other compositions show lower elastic modulus compared to the neat LLDPE.

The stress-strain properties of the LLDPE-prooxidant compositions suggest that the pro-oxidants do not affect the tensile strength of LLDPE adversely, apparently due to the poor polymer-filler interaction.

4.2.2 Thermal studies

4.2.2.1 Thermogravimetric analyses



(LLF = LLDPE-Fe₂O₃, LLM = LLDPE-MnO₂, LLA = LLDPE-TiO₂ (Anatase), LLR = LLDPE- TiO₂ (Rutile), LLCS = LLDPE-Cobalt stearate)

Figure 4.2a TGA thermograms of LLDPE-prooxidant compositions

Table 4.1a Results from thermogravimetric analyses

Sample	T _{max} (°C)
LLDPE	482
LLDPE-Fe ₂ O ₃ (0.5%)*	471
LLDPE-MnO ₂ (0.75%)*	471
LLDPE-Rutile (0.75%)*	472
LLDPE-Anatase (0.75%)*	470
LLDPE-Cobalt stearate (0.75%)*	471

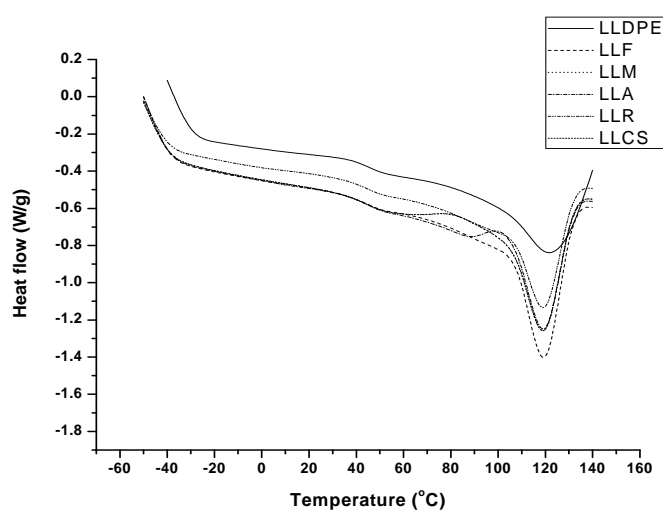
(* Based on the optimum tensile strength)

Figure 4.2a shows the degradation behaviour observed from the thermogravimetric analyses (TGA) of LLDPE and LLDPE-prooxidant compositions. The samples were heated from room temperature to 800°C at a heating rate of 20°C/min under nitrogen atmosphere. For all the mixes the thermograms show similar trend. The thermal degradation above 400°C was caused by the thermal decomposition of LLDPE. The temperature at which maximum weight loss occurs (T_{max}) is given in table 4.1a. All the compositions show lower T_{max} as compared to neat LLDPE which suggests that the thermal stability of LLDPE is decreased by the addition of pro-oxidant. The pro-oxidant in the mix apparently accelerates the thermal oxidation of LLDPE and thus reducing its thermal stability.

4.2.2.2 Differential scanning calorimetry

Differential scanning calorimetry (DSC) provides an easy means of determining the crystallization behaviour of polymers. This is done by melting the polymer and holding it under isothermal conditions to

fully melt out the existing crystalline structure. The molten polymer is then rapidly cooled to an isothermal temperature which is between the sample's glass transition event (T_g) and its melting point (T_m). The crystallization of the polymer is monitored as a function of time under isothermal conditions. An exothermic peak will be obtained and the peak maximum represents the sample's maximum rate of crystallization.



(LLF = LLDPE-Fe₂O₃, LLM = LLDPE-MnO₂, LLA = LLDPE-TiO₂ (Anatase), LLR = LLDPE- TiO₂ (Rutile), LLCS = LLDPE-Cobalt stearate)

Figure 4.2b DSC thermograms (heating) of LLDPE-prooxidant compositions

Table 4.1b Results of differential scanning calorimetry

Sample	T _m (°C)	ΔH _f (J/g)	T _c (°C)	ΔH _c (J/g)	% Crystallinity
LLDPE	126	58	106	59	20
LLF	123	50	109	52	17
LLM	122	54	109	54	18
LLR	123	50	109	52	17
LLA	123	57	109	53	19
LLCS	124	54	107	55	18

(LLF = LLDPE-Fe₂O₃, LLM = LLDPE-MnO₂, LLA = LLDPE-TiO₂ (Anatase), LLR = LLDPE- TiO₂ (Rutile), LLCS = LLDPE-Cobalt stearate)

The DSC thermograms of LLDPE and the compounds are shown in figure 4.2b. Table 4.1b shows the average values for the melting temperature (T_m), crystallisation temperature (T_c), enthalpy of fusion (ΔH_f), enthalpy of crystallization (ΔH_c) and percentage crystallinity for LLDPE and the LLDPE-prooxidant compositions.

The LLDPE-prooxidant compositions show very minor decrease in melting temperature and crystallisation temperature as compared to neat LLDPE. The heat of fusion (ΔH_f) and percentage crystallinity of LLDPE and the mixes are almost similar. The results indicate that the interactions between LLDPE and the pro-oxidants are insignificant. The LLDPE and the pro-oxidants are apparently incompatible.

4.2.3 Photodegradability studies

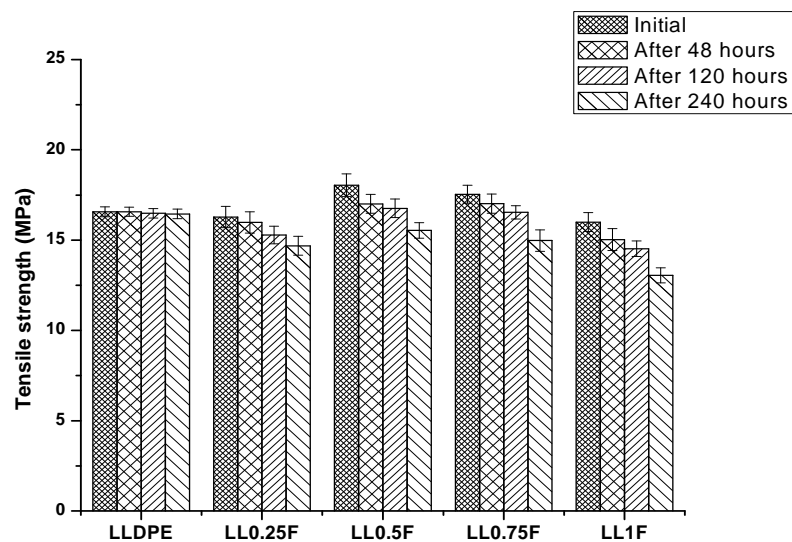
Photodegradation is the degradation of a photodegradable molecule caused by the absorption of photons, particularly those wavelengths found in sunlight, such as infrared radiation, visible light, and ultraviolet light. Other forms of electromagnetic radiation too can cause photodegradation. Photodegradation includes photodissociation, and the breakup of molecules into smaller pieces by photons. It also includes the change of a molecule's shape to make it irreversibly altered, such as the denaturing of proteins, and the addition of other atoms or molecules. A common photodegradation reaction is oxidation. Photooxidation increases the amount of low molecular weight material by breaking bonds and increasing the surface area through

embrittlement. The effects of photooxidation promote the degradation of polymers. UV irradiation generates free radicals in LLDPE [22,23].

Initially, UV radiation is absorbed which leads to radical formation. Eventually, oxygen is absorbed and hydroperoxides are formed, the end products being carbonyl groups. Additional exposure to UV radiation causes the carbonyl groups to undergo the Norrish type I and/or II degradation (Schemes 1&2) [24]. The photooxidation can be initiated by the presence of pro-oxidants. UV degradation can also begin at locations of trace hydroperoxide or ketone groups, introduced during the manufacturing, processing or fabrication.

4.2.3.1 Variation in mechanical properties

Evaluation of mechanical properties after exposure to UV radiation is a significant tool for determining the extent of degradation. The variation in tensile properties after exposing the samples to UV light for various time intervals are shown in figures 4.3a, 4.3b, 4.3c, 4.3d and 4.3e. The loss in tensile strength (%) after exposure to UV radiation for 240 hours is shown in tables 4.2a, 4.2b, 4.2c, 4.2d and 4.2e.



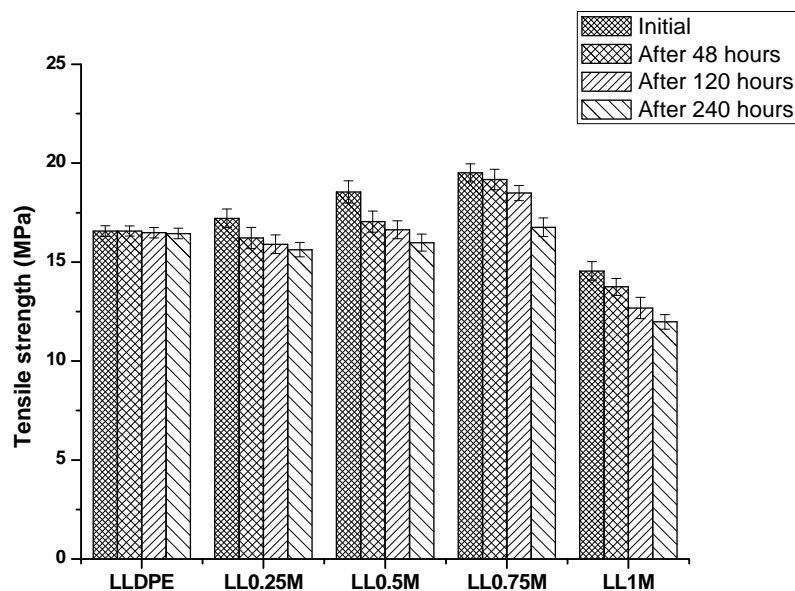
(LL0.25F = LLDPE-0.25% Fe₂O₃, LL0.5F = LLDPE-0.5% Fe₂O₃, LL0.75F = LLDPE-0.75% Fe₂O₃, LL1F = LLDPE-1% Fe₂O₃)

Figure 4.3a Variation in tensile strength of LLDPE-Fe₂O₃ after UV irradiation for various durations

Table 4.2a Percentage decrease in tensile strength of LLDPE-Fe₂O₃ after UV exposure for 240 hours

Sample	Initial tensile strength (MPa)	Tensile strength after 240 hours of UV irradiation (MPa)	% decrease in tensile strength
LLDPE	16.57	16.45	0.72
LL0.25F	16.28	14.69	9.77
LL0.5F	18.04	15.54	13.86
LL0.75F	17.54	14.98	14.6
LL1F	16	13.05	18.44

(LL0.25F = LLDPE-0.25% Fe₂O₃, LL0.5F = LLDPE-0.5% Fe₂O₃, LL0.75F = LLDPE-0.75% Fe₂O₃, LL1F = LLDPE-1% Fe₂O₃)



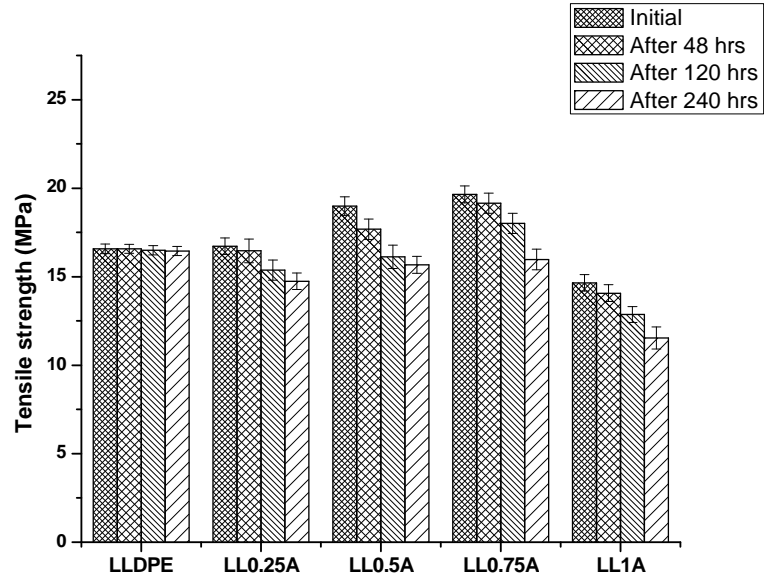
(LL0.25M = LLDPE-0.25% MnO₂, LL0.5M = LLDPE-0.5% MnO₂, LL0.75M = LLDPE-0.75% MnO₂, LL1M = LLDPE-1% MnO₂)

Figure 4.3b Variation in tensile strength of LLDPE-MnO₂ after UV irradiation for various durations

Table 4.2b Percentage decrease in tensile strength of LLDPE-MnO₂ after UV exposure for 240 hours

Sample	Initial tensile strength (MPa)	Tensile strength after 240 hours of UV irradiation (MPa)	% decrease in tensile strength
LLDPE	16.57	16.45	0.72
LL0.25M	17.21	15.63	9.18
LL0.5M	18.55	15.98	13.85
LL0.75M	19.51	16.76	14.09
LL1M	14.55	11.98	17.66

(LL0.25M = LLDPE-0.25% MnO₂, LL0.5M = LLDPE-0.5% MnO₂, LL0.75M = LLDPE-0.75% MnO₂, LL1M = LLDPE-1% MnO₂)



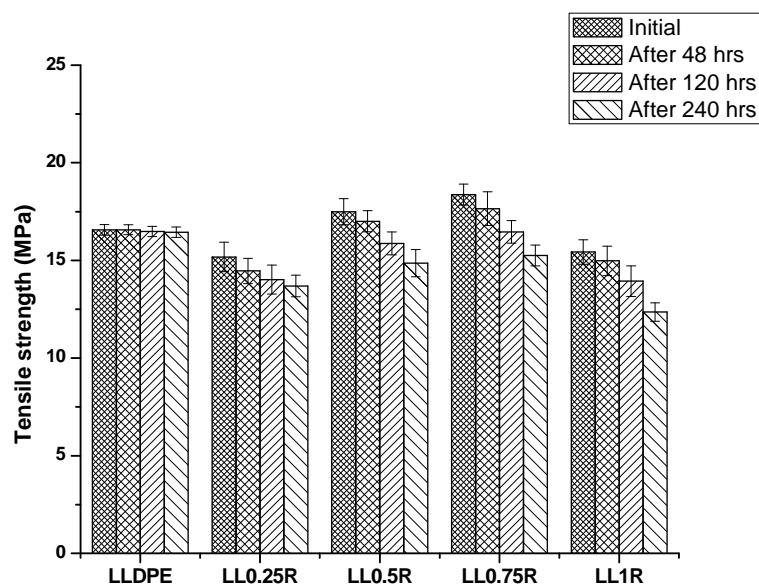
(LL0.25A = LLDPE-0.25% TiO₂ (Anatase), LL0.5A = LLDPE-0.5% TiO₂ (Anatase), LL0.75A = LLDPE-0.75% TiO₂ (Anatase), LL1A = LLDPE-1% TiO₂ (Anatase))

Figure 4.3c Variation in tensile strength of LLDPE- TiO₂ (anatase) after UV irradiation for various durations

Table 4.2c Percentage decrease in tensile strength of LLDPE- TiO₂ (anatase) after UV exposure for 240 hours

Sample	Initial tensile strength (MPa)	Tensile strength after 240 hours of UV irradiation (MPa)	% decrease in tensile strength
LLDPE	16.57	16.45	0.72
LL0.25A	16.72	14.74	11.84
LL0.5A	18.99	15.67	17.48
LL0.75A	19.65	15.97	18.73
LL1A	14.65	11.54	21.23

(LL0.25A = LLDPE-0.25% TiO₂ (Anatase), LL0.5A = LLDPE-0.5% TiO₂ (Anatase), LL0.75A = LLDPE-0.75% TiO₂ (Anatase), LL1A = LLDPE-1% TiO₂ (Anatase))



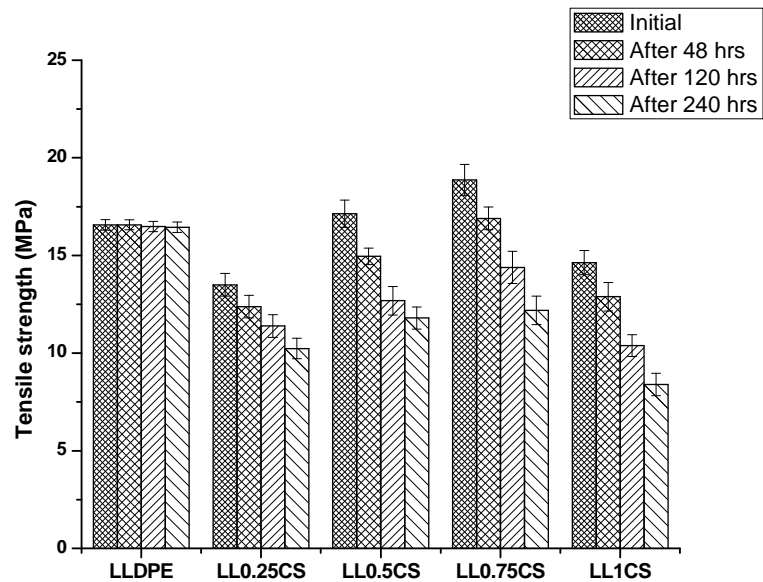
[LL0.25R = LLDPE-0.25% TiO₂ (Rutile), LL0.5R = LLDPE-0.5% TiO₂ (Rutile), LL0.75R = LLDPE-0.75% TiO₂ (Rutile), LL1R = LLDPE-1% TiO₂ (Rutile)]

Figure 4.3d Variation in tensile strength of LLDPE- TiO₂ (rutile) after UV irradiation for various durations

Table 4.2d Percentage decrease in tensile strength of LLDPE- TiO₂ (rutile) after UV exposure for 240 hours

Sample	Initial tensile strength (MPa)	Tensile strength after 240 hours of UV irradiation (MPa)	% decrease in tensile strength
LLDPE	16.57	16.45	0.72
LL0.25R	15.18	13.69	9.82
LL0.5R	17.49	14.86	15.04
LL0.75R	18.37	15.26	16.93
LL1R	15.43	12.36	19.9

[LL0.25R = LLDPE-0.25% TiO₂ (Rutile), LL0.5R = LLDPE-0.5% TiO₂ (Rutile), LL0.75R = LLDPE-0.75% TiO₂ (Rutile), LL1R = LLDPE-1% TiO₂ (Rutile)]



(LL0.25CS = LLDPE-0.25% Cobalt stearate, LL0.5CS = LLDPE-0.5% Cobalt stearate, LL0.75CS = LLDPE-0.75% Cobalt stearate, LL1CS = LLDPE-1% Cobalt stearate)

Figure 4.3e Variation in tensile strength of LLDPE-cobalt stearate after UV irradiation for various durations

Table 4.2e Percentage decrease in tensile strength of LLDPE-cobalt stearate after UV exposure for 240 hours

Sample	Initial tensile strength (MPa)	Tensile strength after 240 hours of UV irradiation (MPa)	% decrease in tensile strength
LLDPE	16.57	16.45	0.72
LL0.25CS	13.5	10.24	24.15
LL0.5CS	17.14	11.8	31.16
LL0.75CS	18.87	12.19	35.4
LL1CS	14.63	8.39	42.65

(LL0.25CS = LLDPE-0.25% Cobalt stearate, LL0.5CS = LLDPE-0.5% Cobalt stearate, LL0.75CS = LLDPE-0.75% Cobalt stearate, LL1CS = LLDPE-1% Cobalt stearate)

The tensile strengths of all the LLDPE-prooxidant compositions decreased after 240 hours of exposure to UV radiation. It seems that the presence of metal oxides and stearate in the mix accelerates the photodegradation of LLDPE. The neat LLDPE showed 0.72% loss in tensile strength after exposure to ultraviolet radiation. The loss in tensile strength after exposure to UV radiation was significant in the case of all the LLDPE-prooxidant mixes. Among various metal oxides used, the maximum reduction in tensile strength was observed in the case of the mix containing TiO₂ (anatase grade) [25]. The results show that the cobalt stearate is more effective than the metal oxides.

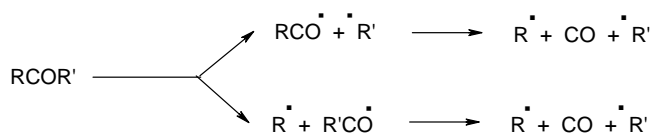
The initiation of photodegradation due to pro-oxidants can be attributed to the presence of oxidation products which are formed as a result of heat treatment. Hydroperoxides are commonly the major products of oxidative degradation and are potentially powerful initiators for further degradation. Other functionalities introduced include carbonyl groups, which are formed as a result of hydroperoxide decomposition. The carbonyl groups absorb UV radiation readily and get excited to singlet and triplet states which further decompose via Norrish reactions of type I, II and III [26].

Norrish type I reaction (Scheme 1) is the radical cleavage of the bond between the carbonyl group and a carbon atom (α -scission), and is followed by formation of CO.

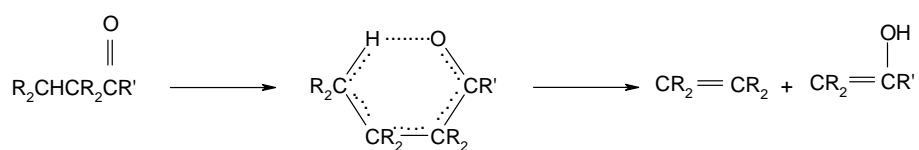
Norrish type II reaction (Scheme 2) is a non-radical, intramolecular process that occurs through the formation of a six

membered cyclic intermediate. Abstraction of hydrogen atom from the γ -carbon results in its subsequent decomposition into an unsaturated polymer chain end, and a polymer chain with an end carbonyl group [26].

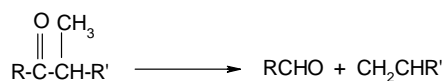
Norrish type III reaction (Scheme 3) is also a non-radical chain scission. However, it involves the transfer of β -hydrogen atom and leads to the formation of an olefin and an aldehyde.



Scheme 1. Norrish Type I



Scheme 2. Norrish Type II



Scheme 3. Norrish Type III

4.2.3.2 Infrared spectroscopic analyses

Representative FTIR spectra (in the range 4000-400 cm^{-1}) of LLDPE- Fe_2O_3 , LLDPE- MnO_2 , LLDPE- TiO_2 (anatase), LLDPE- TiO_2 (rutile) and LLDPE-cobalt stearate (before and after exposure to ultraviolet light) are shown in figures 4.4a, 4.4b, 4.4c, 4.4d and 4.4e.

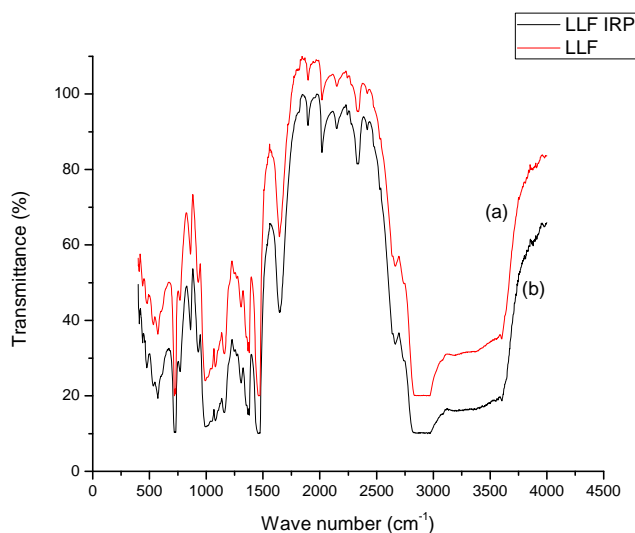


Figure 4.4a FTIR spectra of LLDPE-Fe₂O₃ [LLF]: (a) before exposure to UV light [LLF] and (b) after exposure to UV light [LLF IRP]

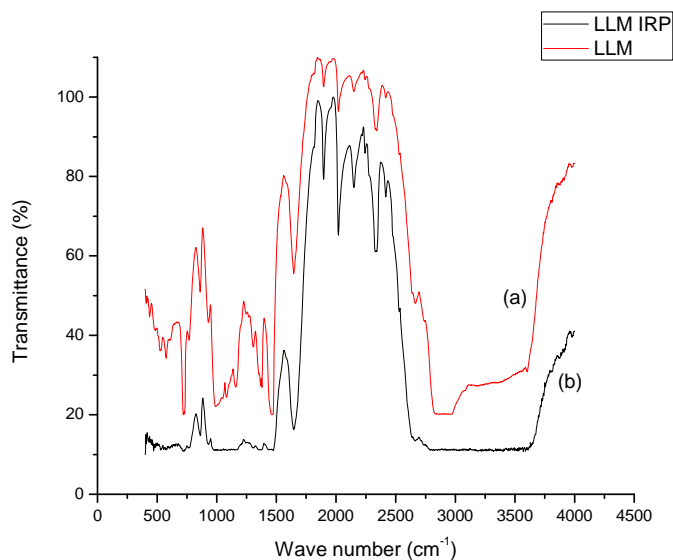


Figure 4.4b FTIR spectra of LLDPE-MnO₂ [LLM]: (a) before exposure to UV light [LLM] and (b) after exposure to UV light [LLM IRP]

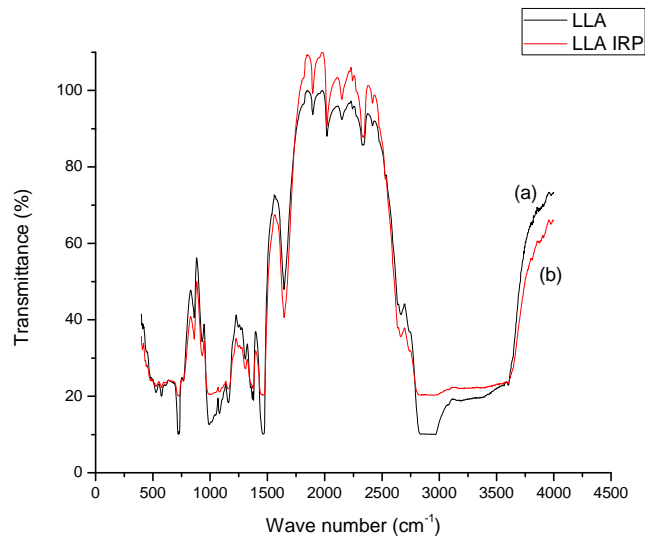


Figure 4.4c FTIR spectra of LLDPE-TiO₂ (anatase) [LLA]: (a) before exposure to UV light [LLA] and (b) after exposure to UV light [LLA IRP]

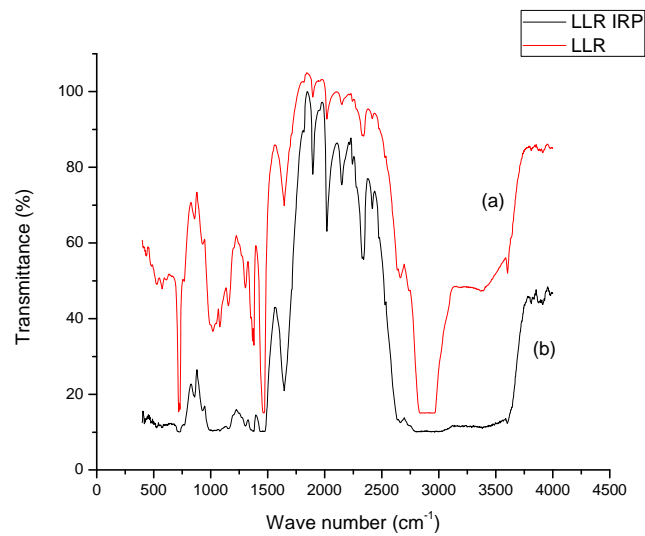


Figure 4.4d FTIR spectra of LLDPE- TiO₂ (rutile) [LLR]: (a) before exposure to UV light [LLR] and (b) after exposure to UV light [LLR IRP]

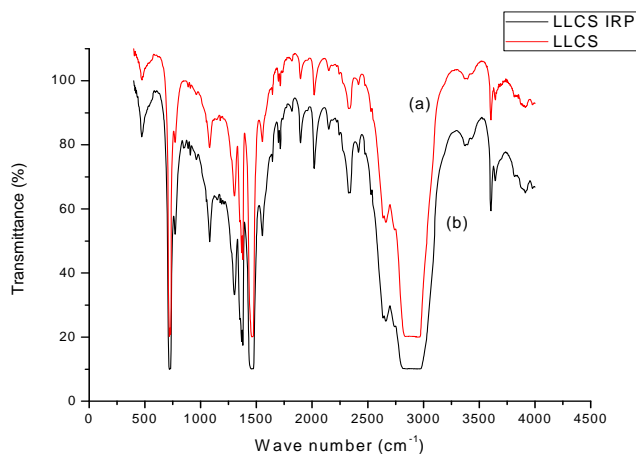


Figure 4.4e FTIR spectra of LLDPE-cobalt stearate [LLCS]: (a) before exposure to UV light [LLCS] and (b) after exposure to UV light [LLCS IRP]

Table 4.3 Data obtained from FTIR spectrograms of LLDPE and LLDPE-prooxidant compositions (Peaks at cm^{-1})

	Peak position (cm^{-1})	Characteristic group
LLDPE	1644	δ (O-H) band
	1470	CH_2 bending
	720	skeletal vibration of CH_2
	473	O-H deformation (broadening by water, C-O-C ring vibration)
LLDPE- Fe_2O_3	2901	C-H stretching
	998	C-H bending
LLDPE- MnO_2	2912	C-H stretching
	1459	CH_2 bending
	998	C-H bending
	720	skeletal vibration of CH_2
LLDPE- TiO_2 (Rutile)	2901	C-H stretching
	1450	CH_2 bending
	998	C-H bending
	720	skeletal vibration of CH_2
LLDPE- TiO_2 (Anatase)	2900	C-H stretching
	998	C-H bending
	720	skeletal vibration of CH_2
LLDPE-Cobalt stearate	2903	C-H stretching

The characteristic peak assignments are shown in table 4.3. Information about different stages of degradation can be obtained by subtracting the spectrum of the neat LLDPE from the spectra of the degraded LLDPE-prooxidant mixes. The major types of molecular vibrations are stretching and bending. Infrared radiation is absorbed and the associated energy is converted into these types of motions [27-31].

Comparison of spectra of LLDPE-Fe₂O₃ before and after UV exposure shows notable decreases in intensities at 2901 cm⁻¹ which corresponds to C-H stretching and at 998 cm⁻¹ which corresponds to C-H bending. The decreases in peak intensities in LLDPE-MnO₂ composition before and after exposure to ultraviolet light include the peaks at 2912 cm⁻¹, 1459 cm⁻¹, 998 cm⁻¹ and 720 cm⁻¹ which corresponds to C-H stretching, CH₂ bending, C-H bending and skeletal vibration of CH₂. In the case of LLDPE-TiO₂(anatase) composition, the peaks at 2900 cm⁻¹ (C-H stretching), 998 cm⁻¹ (C-H bending) and 720 cm⁻¹ (skeletal vibration of CH₂) showed decreases in peak intensities. These decreases in peak intensities were observed in the case of LLDPE-TiO₂ (rutile) also. In addition, a decrease in peak intensity at 1450 cm⁻¹ (CH₂ bending) was also observed in the case of LLDPE-TiO₂ (rutile) composition. For the LLDPE-cobalt stearate composition, only the C-H stretching vibration at 2903 cm⁻¹ showed notable decrease.

The decrease in peak intensities at 2903 cm⁻¹, 1450 cm⁻¹, 998 cm⁻¹ and 720 cm⁻¹ reveals the auto-oxidation of LLDPE in presence of pro-oxidants. This shows that the presence of pro-oxidants enhances the auto-oxidation of LLDPE and thus accelerates the

photodegradation process. The metal oxides and the stearate act as pro-oxidants that accelerate the photodegradation of LLDPE by generating free radicals on exposure to ultraviolet light.

The degradation and weathering of polymers affect the appearance and the physical properties of the materials, with some common effects being discoloration and embrittlement. Under extreme conditions, the release of volatile products or burning may occur. Infrared spectroscopy may be used to elucidate the degradation mechanisms [5, 22] of polymers.

Significant degradation mechanisms for polymers include photo-oxidation and thermo-oxidation. Such mechanisms result in the formation of carbonylated and hydroxylated compounds [8]. The role of infrared spectroscopy in polymer degradation is illustrated by its application to thermo- and photo-oxidized polyethylenes [8, 23]. During the thermal-oxidation process of PE, a range of carbonyl-containing compounds is formed.

4.2.4 Melt flow test

The melt flow indices (MFI) of the neat LLDPE and the LLDPE-prooxidant mixes were determined according to ASTM D-1238 [20]. The MFI of a polymer is related to its molecular weight distribution and is often used to characterize the processability [32].

The melt flow indices of neat LLDPE and the LLDPE-prooxidant mixes are shown in table 4.4. It is observed that the melt flow indices of all the mixes were slightly lower compared to neat LLDPE.

When solid particles (fillers) are present in the matrix of a polymer, they restrict the melt movement by increasing viscosity which implies a hardening effect [33-34]. This may be the reason for low melt indices observed in the case of LLDPE-prooxidant compositions

Table 4.4 Melt flow indices of LLDPE and LLDPE-prooxidant compositions

Sample	MFI (g/10 min)
LLDPE	1.09
LLDPE-0.25%Fe ₂ O ₃	0.92
LLDPE-0.5%Fe ₂ O ₃	0.89
LLDPE-0.75%Fe ₂ O ₃	0.87
LLDPE-1%Fe ₂ O ₃	0.85
LLDPE-0.25%MnO ₂	0.88
LLDPE-0.5%MnO ₂	0.86
LLDPE-0.75%MnO ₂	0.84
LLDPE-1%MnO ₂	0.78
LLDPE-0.25%TiO ₂ (Rutile)	0.9
LLDPE-0.5%TiO ₂ (Rutile)	0.86
LLDPE-0.75%TiO ₂ (Rutile)	0.83
LLDPE-1%TiO ₂ (Rutile)	0.79
LLDPE-0.25%TiO ₂ (Anatase)	0.89
LLDPE-0.5%TiO ₂ (Anatase)	0.87
LLDPE-0.75%TiO ₂ (Anatase)	0.85
LLDPE-1%TiO ₂ (Anatase)	0.83
LLDPE-0.25%Cobalt stearate	0.9
LLDPE-0.5%Cobalt stearate	0.87
LLDPE-0.75%Cobalt stearate	0.85
LLDPE-1%Cobalt stearate	0.74

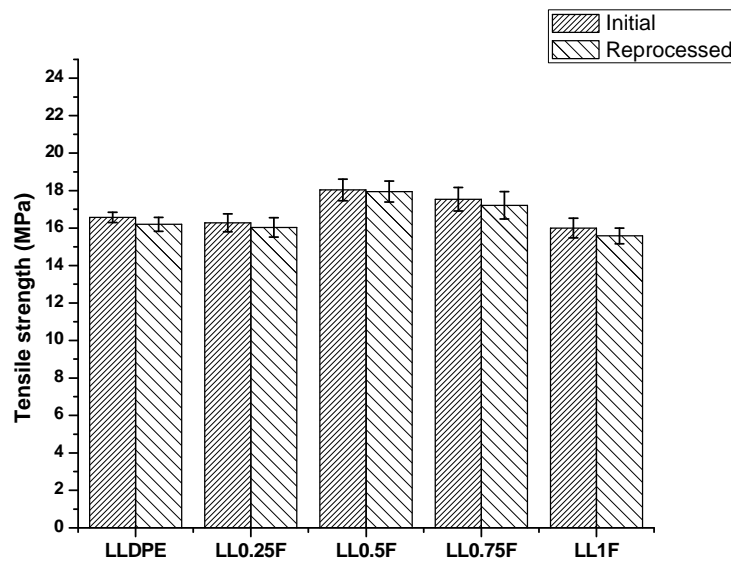
4.2.5 Water absorption studies

Table 4.5 Water absorption of LLDPE and LLDPE-prooxidant compositions

Sample	Initial weight (g)	Weight after 8 weeks (g)	% Water absorption
LLDPE	0.0394	0.0395	0.25
LLDPE-0.25%Fe ₂ O ₃	0.0865	0.0868	0.35
LLDPE-0.5%Fe ₂ O ₃	0.0643	0.0647	0.62
LLDPE-0.75%Fe ₂ O ₃	0.0627	0.0631	0.64
LLDPE-1%Fe ₂ O ₃	0.0753	0.0761	1.06
LLDPE-0.25%MnO ₂	0.0539	0.05405	0.28
LLDPE-0.5%MnO ₂	0.0842	0.0845	0.36
LLDPE-0.75%MnO ₂	0.0731	0.0737	0.82
LLDPE-1%MnO ₂	0.0817	0.0824	0.86
LLDPE-0.25%TiO ₂ (Rutile)	0.1046	0.1052	0.57
LLDPE-0.5%TiO ₂ (Rutile)	0.0792	0.08	1.01
LLDPE-0.75%TiO ₂ (Rutile)	0.0725	0.0734	1.24
LLDPE-1%TiO ₂ (Rutile)	0.0972	0.0985	1.34
LLDPE-0.25%TiO ₂ (Anatase)	0.0852	0.0855	0.35
LLDPE-0.5%TiO ₂ (Anatase)	0.0789	0.0793	0.51
LLDPE-0.75%TiO ₂ (Anatase)	0.0376	0.038	1.06
LLDPE-1%TiO ₂ (Anatase)	0.0649	0.0658	1.39
LLDPE-0.25%Cobalt stearate	0.1039	0.1043	0.38
LLDPE-0.5%Cobalt stearate	0.0919	0.0925	0.65
LLDPE-0.75%Cobalt stearate	0.0595	0.0599	0.67
LLDPE-1%Cobalt stearate	0.077	0.0777	0.91

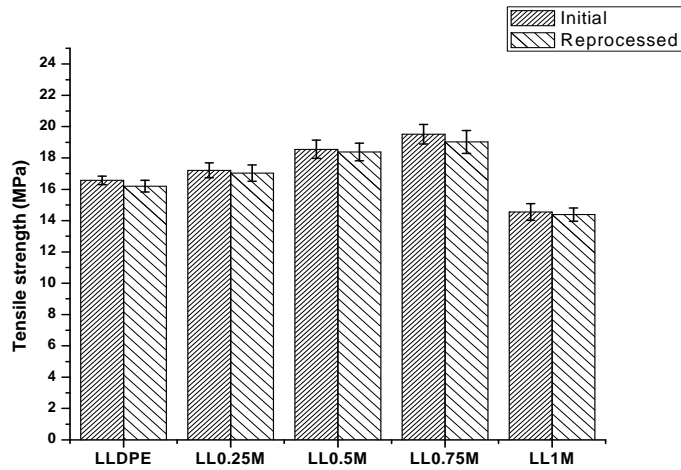
The water uptake of the neat LLDPE and LLDPE-prooxidant compositions are tabulated in table 4.5. The uptake of water by LLDPE-prooxidant compositions was determined according to ASTM D-570 [21]. The uptake of water by pure LLDPE was 0.25 % whereas for the mixes an enhancement in water uptake was observed. As the concentrations of pro-oxidants increased water absorption too increased. The higher water absorption shown by the LLDPE-prooxidant compositions may lead to higher susceptibility for microbial attack when the compositions are buried in soil.

4.2.6 Reprocessability



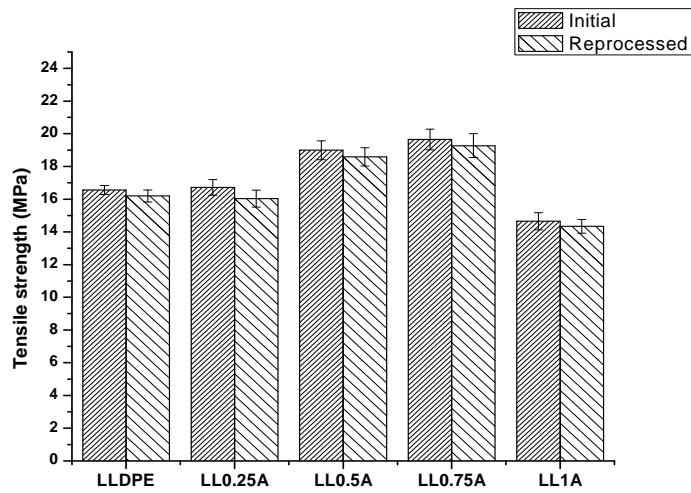
(LL0.25F = LLDPE-0.25% Fe₂O₃, LL0.5F = LLDPE-0.5% Fe₂O₃, LL0.75F = LLDPE-0.75% Fe₂O₃, LL1F = LLDPE-1% Fe₂O₃)

Figure 4.5a Reprocessability of LLDPE-Fe₂O₃ compositions



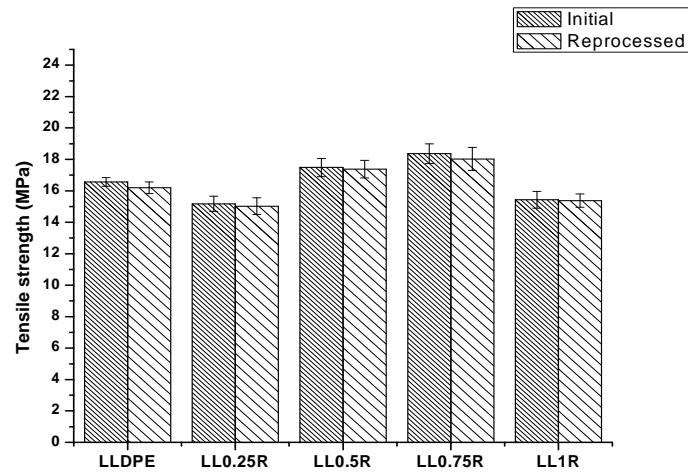
(LL0.25M = LLDPE-0.25% MnO₂, LL0.5M = LLDPE-0.5% MnO₂, LL0.75M = LLDPE-0.75% MnO₂, LL1M = LLDPE-1% MnO₂)

Figure 4.5b Reprocessability of LLDPE-MnO₂ compositions



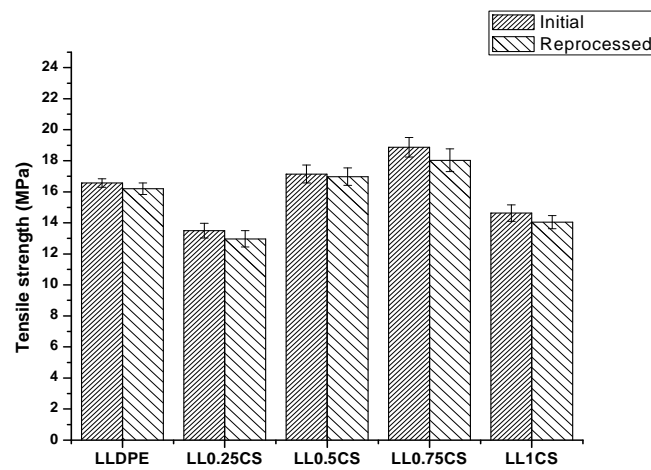
(LL0.25A = LLDPE-0.25% TiO₂ (Anatase), LL0.5A = LLDPE-0.5% TiO₂ (Anatase), LL0.75A = LLDPE-0.75% TiO₂ (Anatase), LL1A = LLDPE-1% TiO₂ (Anatase))

Figure 4.5c Reprocessability of LLDPE-TiO₂ (anatase) compositions



(LL0.25R = LLDPE-0.25% TiO₂ (Rutile), LL0.5R = LLDPE-0.5% TiO₂ (Rutile), LL0.75R = LLDPE-0.75% TiO₂ (Rutile), LL1R = LLDPE-1% TiO₂ (Rutile))

Figure 4.5d Reprocessability of LLDPE-TiO₂ (rutile) compositions



(LL0.25CS = LLDPE-0.25% Cobalt stearate, LL0.5CS = LLDPE-0.5% Cobalt stearate, LL0.75CS = LLDPE-0.75% Cobalt stearate, LL1CS = LLDPE-1% Cobalt stearate)

Figure 4.5e Reprocessability of LLDPE-cobalt stearate compositions

The reprocessability of LLDPE-prooxidant compositions were checked by repeatedly processing the neat LLDPE and LLDPE-prooxidant compositions in a Thermo HAAKE polylab system, moulding in an electrically heated hydraulic press and evaluating the mechanical properties. The process was repeated up to three cycles. It was observed that the change in tensile properties of the compositions was marginal suggesting that the compositions are reprocessable without sacrificing the mechanical properties.

4.3 Conclusion

The incorporation of low quantities of pro-oxidants [iron oxide, manganese dioxide, titanium dioxide (rutile and anatase grade) and cobalt stearate] causes only marginal changes in the mechanical properties of LLDPE. Results of the thermogravimetric analyses indicate that the pro-oxidant in the mix apparently accelerates the thermal oxidation of LLDPE and thus reduces its thermal stability. The differential scanning calorimetric studies show that the percentage crystallinity of the LLDPE and the LLDPE-prooxidant compositions are almost similar implying that the LLDPE and the pro-oxidants are incompatible. The photodegradation of LLDPE could be enhanced by the addition of pro-oxidants. The LLDPE-prooxidant compositions show low melt flow indices as compared to neat LLDPE apparently due to increased entanglement of the polymer chains of LLDPE and the pro-oxidants. The higher water absorption shown by the LLDPE-prooxidant compositions may lead to higher susceptibility for microbial attack when the compositions are buried in soil. The LLDPE-prooxidant compositions are reprocessable.

References

- [1] Richard CF, San Rafael C, US Patent 4197375, [1980].
- [2] Ranby B., Rabek JF, In “Photodegradation, Photo-oxidation and Photostabilization of Polymers”; John Wiley & Sons: New York, [1975], 120.
- [3] Jian Zhong BEI, Xing Zhou HU, Zhen Ming MA, Shen Guo Wang, *Chinese Chemical Letters*, **10(4)**, [1999], 327.
- [4] Andrady AL, *Journal of Applied Polymer Science*, **39**, [1990], 363.
- [5] Andrady AL, In: *Proceedings of the Symposium on Degradable Plastics*, Washington, DC, [1987], 22.
- [6] David C, Trojan M, Daro A, Demarteau W, *Polymer Degradation and Stability*, **37**, [1992], 233.
- [7] Gijnsman P, Meijers G, Vitarelli G, *Polymer Degradation and Stability*, **65**, [1999], 433.
- [8] Roy PK, Surekha P, Rajagopal C, Cahtterjee SN, Choudhary V, *Polymer Degradation and Stability*, **92**, [2007], 1151.
- [9] Chiellini E, Corti A, D’Antone S, Baciù R, *Polymer Degradation and Stability*, **91**, [2006], 2739.
- [10] Haines JR, Alexander M, *Applied Microbiology*, **28**, [1974], 1084.
- [11] Jin C, Christensen PA, Egerton TA, White JR, *Polymer*, **44**, [2003], 5969.
- [12] Scott G, Islam S, *Polymer Degradation and Stability*, **63**, [1999], 61.
- [13] Jakubowicz I, *Polymer Degradation and Stability*, **80**, [2003], 39.
- [14] Jakubowicz I, Yarahmadi N, Peterson H, *Polymer Degradation and Stability*, **91**, [2006], 1556.

- [15] Lin Y, *Journal of Applied Polymer Science*, **63**, [1997], 81.
- [16] Qin H, Zhao C, Zhang S, Chen G, Yang M, *Polymer Degradation and Stability*, **81**, [2003], 497.
- [17] Zhao X, Li Z, Chen Y, Shi L, Zhu Y, *Journal of Molecular Catalysis A: Chemical*, **268**, [2007], 101.
- [18] Wei S, Shiyi G, Changshui F, Dong X, Quan R, *J.Mater.Sci.*, **34**, [1999], 5995.
- [19] Annual Book of ASTM Standards, D 882, **08.01**, [2004].
- [20] Annual Book of ASTM Standards, D 1238, **08.01**, [2004].
- [21] Annual Book of ASTM Standards, D 570, **08.01**, [2004].
- [22] Guthrie JT, *Surface Coatings International Part B: Coatings Transactions*, **85(B1)**, [2002], 27.
- [23] Chapiro A, In: H.F. Mark, N.G. Gaylord (Eds.), *Encyclopaedia of Polymer Science & Technology*, John Wiley & Sons, New York, **11**, [1969], 702.
- [24] Vink P, In: *Degradation and Stabilisation of Polyolefins* (N. S. Allen (Ed.)), Applied Science Publishers, London and New York, [1983], 213.
- [25] Terence J. Kemp, Robin A, McIntyre; *Polymer Degradation and Stability*, **91(12)**, [2006], 3020.
- [26] Tibor K, In: *Polymer Degradation*; Van Nostrand Reinhold Company, New York, [1983], 10.
- [27] Albertsson AC, *Eighth Annual Conference on Advances in the Stabilization and Controlled Degradation of Polymers*, Lucerne, [1986].

- [28] Albertsson AC, Thesis, The Royal Institute of Technology, Stockholm, Sweden, [1977].
- [29] Wang HR, Chen KM, *Colloids and Surfaces A: Physicochemical and Engineering Aspects*, **281**, [2006], 190.
- [30] Lin SC, Bulkin BJ, Pearce EM, *Journal of Polymer Science Polymer Chemistry*, **17(10)**, [1979], 3121.
- [31] Coleman MM, Painter PC, In: Brame Jr EG (ed) Applications of Polymer Spectroscopy, Academic Press, New York, [1978], 135.
- [32] Bremner T, Rudin A and Cook DG, *Journal of Applied Polymer Science*, **41**, [1990], 1617.
- [33] Albano C, Karam A, Dominguez N, Sanchez Y, Gonzalez J, Aguirre O, Catano L, *Composite Structures*, **71**, [2005], 282.
- [34] Jang BC, Huh SY, Jang JG, Bae YC, *Journal of Applied Polymer Science*, **82**, [2001], 3313.

.....✪.....

COMBINED EFFECT OF BIO – FILLERS AND PRO-OXIDANTS ON THE DEGRADATION OF LLDPE

Contents	5.1 Introduction
	5.2 Results and Discussion
	5.3 Conclusion

.....

Linear low density polyethylene-biofiller [starch or dextrin (15 weight %, 300 mesh size)] blends were prepared by melt blending. Both the linear low density polyethylene-biofiller blends were mixed with various dosages (0.25, 0.5, 0.75 and 1 weight %) of pro-oxidants (iron oxide, manganese dioxide, titanium dioxide (anatase and rutile grades)). The combined effect of the bio-filler and the pro-oxidant in every composition was determined by evaluating the mechanical properties, thermal properties, melt flow indices and water absorption. The biodegradability of the compositions was established by subjecting the samples to biodegradation in a shake culture flask containing amylase producing vibrios and soil burial. The extent of biodegradability was established by measurement of mechanical properties, scanning electron microscopy (SEM) and fourier transform infrared spectroscopy (FTIR). The photodegradability of the linear low density polyethylene containing both the bio-filler and pro-oxidant was established by exposing the samples to ultraviolet (UV) radiation for 240 hours, and checking the mechanical properties and the FTIR spectra before and after UV irradiation. The combination of a bio-filler and a pro-oxidant improves the degradation of linear low density polyethylene.

.....

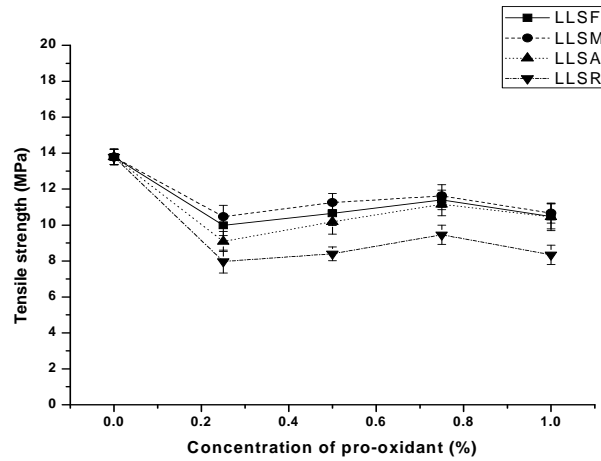
5.1 Introduction

Plastics have attained a unique position in packaging industry because of their favourable features such as high strength, water resistance, light weight, energy effectiveness and low cost [1]. It has been estimated that about 2% of all plastics eventually reach the environment, thus contributing considerably to a currently acute ecological problem. For this reason there have been several attempts towards the preparation of degradable natural or synthetic polymers or natural/synthetic polymer blends [2]. Linear low density polyethylene (LLDPE) is regarded as an inert bulk polymer and its degradability is very low compared to hydrolysable polymers such as thermoplastic polyesters [3]. One of the methods to accelerate the biodegradation of inert polymers is the incorporation of biopolymers to produce plastic films with a porous structure, which enhances the accessibility of the plastic to oxygen and micro-organisms [4-14]. Pro-oxidants too improve the degradability of plastics when exposed to sunlight [4-6,12].

In the previous chapters, it has been reported that the incorporation of bio-fillers such as starch and dextrin, and pro-oxidants (metal oxides and metal stearate) improve the biodegradation and photodegradation of LLDPE. This chapter reports the results of the studies on the combined effect of bio-fillers and pro-oxidants on the degradation of LLDPE.

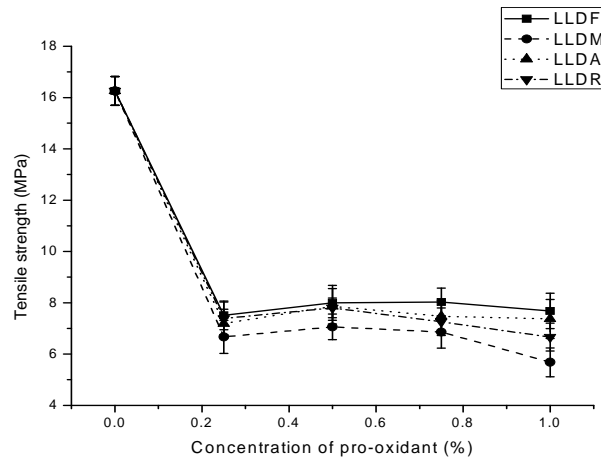
5.2 Results and Discussion

5.2.1 Mechanical properties



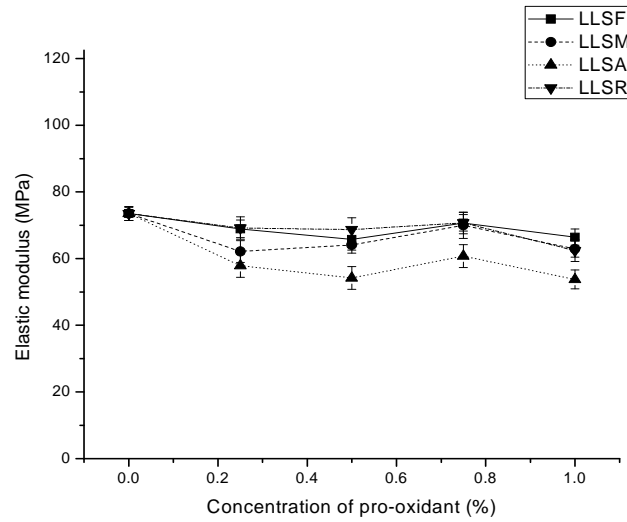
[LLSF = LLDPE-starch-Fe₂O₃, LLSM = LLDPE-starch-MnO₂, LLSA = LLDPE-starch-TiO₂ (anatase), LLSR = LLDPE-starch-TiO₂ (rutile)]

Figure 5.1a Variation of tensile strength with concentration of pro-oxidants in LLDPE-starch blends



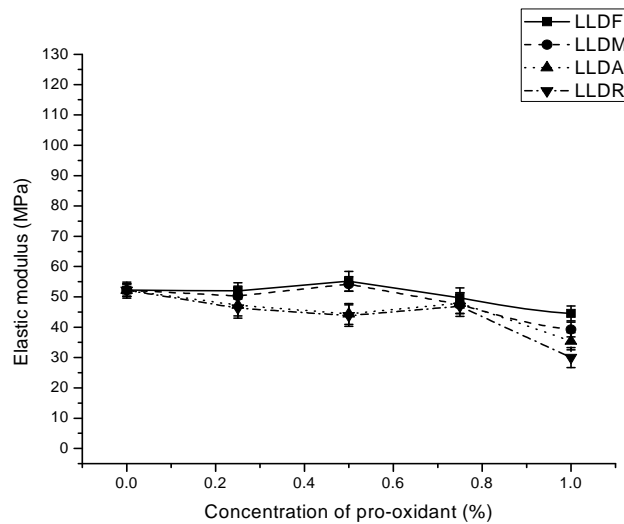
[LLDF = LLDPE-dextrin-Fe₂O₃, LLDM = LLDPE-dextrin-MnO₂, LLDA = LLDPE-dextrin-TiO₂ (anatase), LLDR = LLDPE-dextrin-TiO₂ (rutile)]

Figure 5.1b Variation of tensile strength with concentration of pro-oxidants in LLDPE-dextrin blends



[LLSF = LLDPE-starch-Fe₂O₃, LLSM = LLDPE-starch-MnO₂, LLSA = LLDPE-starch-TiO₂ (anatase), LLSR = LLDPE-starch-TiO₂ (rutile)]

Figure 5.1c Variation of elastic modulus with concentration of pro-oxidants in LLDPE-starch blends



[LLDF = LLDPE-dextrin-Fe₂O₃, LLDM = LLDPE-dextrin-MnO₂, LLDA = LLDPE-dextrin-TiO₂ (anatase), LLDR = LLDPE-dextrin-TiO₂ (rutile)]

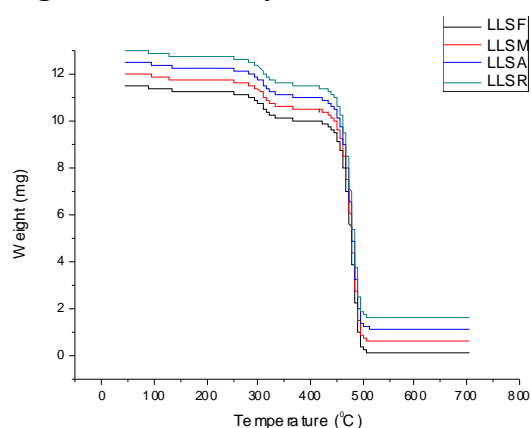
Figure 5.1d Variation of elastic modulus with concentration of pro-oxidants in LLDPE-dextrin blends

The variation of tensile strength and elastic modulus of LLDPE-starch-prooxidant compositions and LLDPE-dextrin-prooxidant compositions are shown in figures 5.1a, 5.1b, 5.1c and 5.1d. The tensile strength of all the compositions shows a decreasing tendency with the addition of pro-oxidants. The modulus of the LLDPE-dextrin-prooxidant compositions too showed similar results. In the case of LLDPE-starch-prooxidant compositions the elastic modulus values were lower as compared to LLDPE-starch blends. This suggests that the metal oxides have no significant reinforcing effect on the blends.

The bio-fillers used in this study are hydrophilic, as they have hydroxyl groups on their surface. Thus the formation of strong interfacial bonds like hydrogen bonds with LLDPE and the bio-fillers is not feasible due to the hydrophobicity of the polymer matrix [15-19].

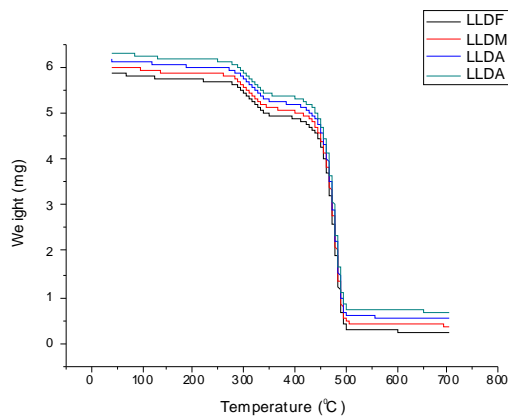
5.2.2 Thermal studies

5.2.2.1 Thermogravimetric analyses



[LLSF = LLDPE-starch-Fe₂O₃, LLSM = LLDPE-starch-MnO₂, LLSA = LLDPE-starch-TiO₂ (anatase), LLSR = LLDPE-starch-TiO₂ (rutile)]

Figure 5.2a TGA thermograms of LLDPE-starch blends containing various pro-oxidants



[LLDF = LLDPE-dextrin-Fe₂O₃, LLDM = LLDPE-dextrin-MnO₂, LLDA = LLDPE- dextrin-TiO₂ (anatase), LLDR = LLDPE-dextrin-TiO₂ (rutile)]

Figure 5.2b TGA thermograms of LLDPE-dextrin blends containing various pro-oxidants

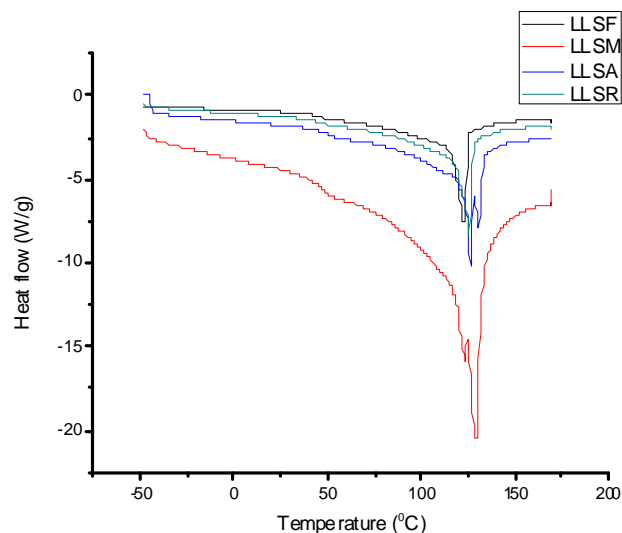
Table 5.1a Results from thermogravimetric analyses

Sample	T _{max} (°C)
LLDPE	482
LLS	481
LLSF	482
LLSM	483
LLSR	482
LLSA	482
LLD	482
LLDF	481
LLDM	486
LLDR	481
LLDA	478

[LLS = LLDPE-starch, LLSF = LLDPE-starch-Fe₂O₃, LLSM = LLDPE-starch-MnO₂, LLSA = LLDPE-starch-TiO₂ (anatase), LLSR = LLDPE-starch-TiO₂ (rutile), LLD = LLDPE-dextrin, LLDF = LLDPE-dextrin-Fe₂O₃, LLDM = LLDPE-dextrin-MnO₂, LLDA = LLDPE- dextrin-TiO₂ (anatase), LLDR = LLDPE-dextrin-TiO₂ (rutile)]

The thermograms of LLDPE-starch-prooxidant blends and LLDPE-dextrin-prooxidant blends are shown in figures 5.2a and 5.2b. The mass change during 250-350°C corresponds to the loss of bio-fillers, as this is the decomposition temperature for the bio-fillers. Above this temperature, a gradual loss in weight occurs due to the decomposition of LLDPE. The temperature at which the maximum degradation occurs (T_{max}) is given in table 5.1a. The T_{max} of LLDPE, LLDPE-starch and LLDPE-dextrin blends are also shown in the table. There is no significant decrease in T_{max} in presence of the bio-fillers, and also on addition of pro-oxidants which indicates that the presence of bio-fillers and pro-oxidants doesn't adversely affect the thermal stability of LLDPE.

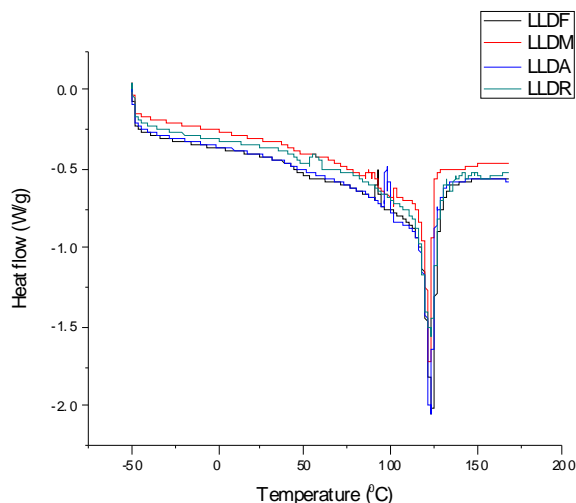
5.2.2.2 Differential scanning calorimetry



[LLSF = LLDPE-starch-Fe₂O₃, LLSM = LLDPE-starch-MnO₂, LLSA = LLDPE-starch-TiO₂ (anatase), LLSR = LLDPE-starch-TiO₂ (rutile)]

Figure 5.2c DSC thermograms of LLDPE-starch blends containing various pro-oxidants

The DSC thermograms of LLDPE-starch-prooxidant compositions are shown in figure 5.2c. The melting temperature, crystallisation temperature, heat of fusion, heat of crystallisation and degree of crystallinity of LLDPE, LLDPE-starch and LLDPE-starch-prooxidant compositions are shown in table 5.1b. The melting and crystallisation temperatures of the blends are similar to neat LLDPE. This suggests that the fillers and the polymer are incompatible and the filler-polymer interactions are weak.



[LLDF = LLDPE-dextrin-Fe₂O₃, LLDM = LLDPE-dextrin-MnO₂, LLDA = LLDPE-dextrin-TiO₂ (anatase), LLDR = LLDPE-dextrin-TiO₂ (rutile)]

Figure 5.2d DSC thermograms of LLDPE-dextrin blends containing various pro-oxidants

The DSC thermograms of LLDPE-dextrin-prooxidant compositions are shown in figure 5.2d. The melting temperature, crystallisation temperature, heat of fusion, heat of crystallisation and degree of crystallinity of LLDPE, LLDPE-dextrin and LLDPE-dextrin-prooxidant compositions are shown in table 5.1b. The melting and crystallisation

temperatures of the blends are similar to neat LLDPE. This suggests that the fillers and the polymer are incompatible and the filler-polymer interactions are weak. The degree of crystallinity of the blends is calculated by dividing heat of fusion of blends with heat of fusion of 100% pure crystalline polymer. The degree of crystallinity of the pro-oxidant containing blends was lower as compared to the neat polymer. This observation is in conformity with the lower tensile strength observed in presence of the pro-oxidants in the case of both LLDPE-starch and LLDPE-dextrin blends.

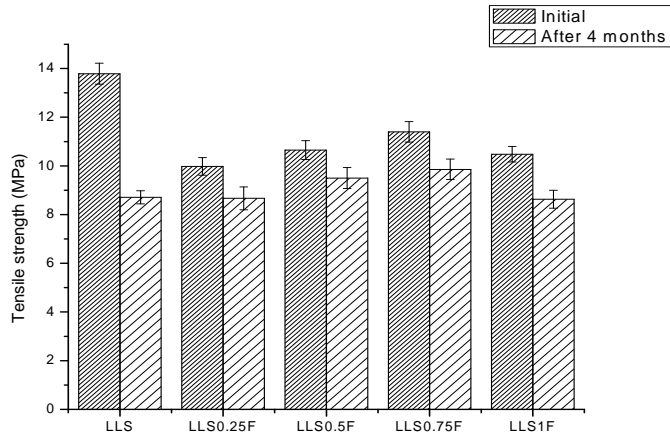
Table 5.1b Results from differential scanning calorimetry

Sample	T _m (°C)	ΔH _f (J/g)	T _c (°C)	ΔH _c (J/g)	% Crystallinity
LLDPE	126	58	106	59	20
LLS	125	57	107	53	19
LLSF	122	39	108	41	13
LLSM	128	40	107	46	14
LLSR	125	38	108	40	13
LLSA	123	36	108	42	12
LLD	126	55	107	48	19
LLDF	123	45	108	41	15
LLDM	122	30	108	32	10
LLDR	121	35	110	46	12
LLDA	123	38	108	39	13

[LLS = LLDPE-starch, LLSF = LLDPE-starch-Fe₂O₃, LLSM = LLDPE-starch-MnO₂, LLSA = LLDPE-starch-TiO₂ (anatase), LLSR = LLDPE-starch-TiO₂ (rutile), LLD = LLDPE-dextrin, LLDF = LLDPE-dextrin-Fe₂O₃, LLDM = LLDPE-dextrin-MnO₂, LLDA = LLDPE-dextrin-TiO₂ (anatase), LLDR = LLDPE-dextrin-TiO₂ (rutile)]

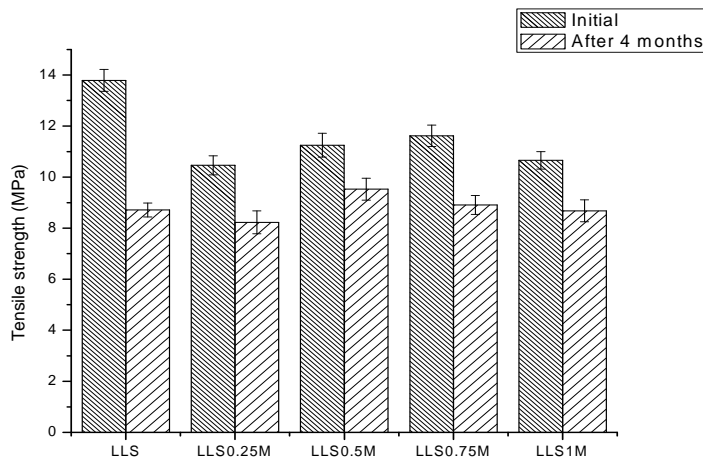
5.2.3 Biodegradation studies

5.2.3.1 In shake culture flask



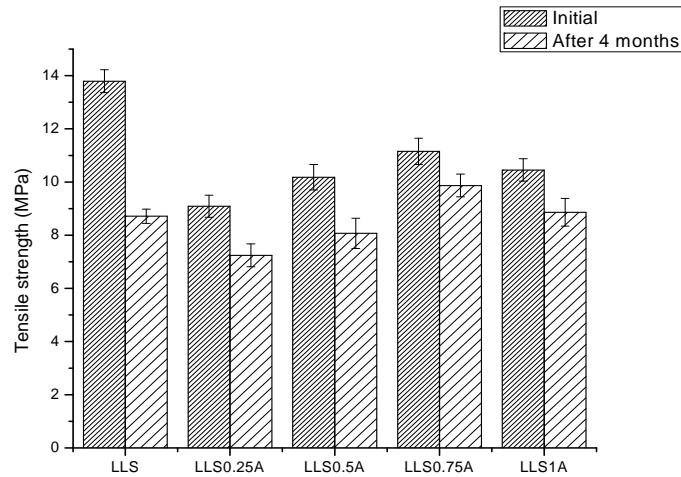
[LLS = LLDPE-starch300 (15%), LLS0.25F = LLDPE-starch-Fe₂O₃(0.25%), LLS0.5F = LLDPE-starch-Fe₂O₃(0.5%), LLS0.75F = LLDPE-starch-Fe₂O₃(0.75%), LLS1F = LLDPE-starch-Fe₂O₃(1%)]

Figure 5.3a Variation in tensile strength of LLDPE-starch-Fe₂O₃ blends after immersion of plastic strips in shake culture flask for 4 months



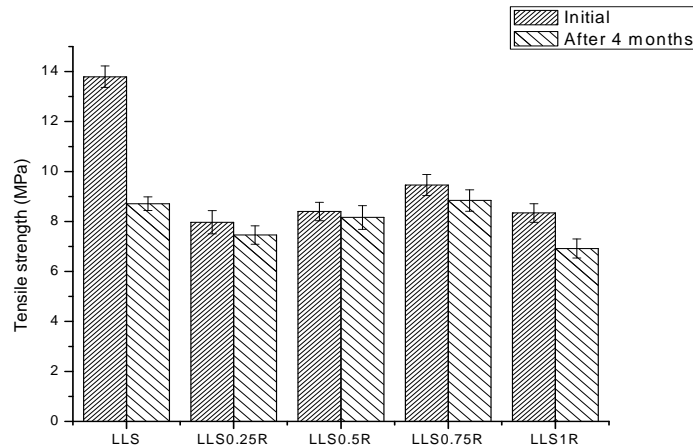
[LLS = LLDPE-starch300 (15%), LLS0.25M = LLDPE-starch-MnO₂(0.25%), LLS0.5M = LLDPE-starch-MnO₂(0.5%), LLS0.75M = LLDPE-starch-MnO₂(0.75%), LLS1M = LLDPE-starch-MnO₂(1%)]

Figure 5.3b Variation in tensile strength of LLDPE-starch-MnO₂ blends after immersion of plastic strips in shake culture flask for 4 months



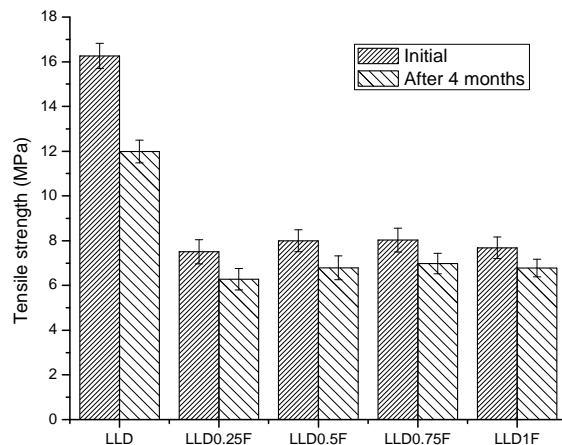
[LLS = LLDPE-starch300 (15%), LLS0.25A = LLDPE-starch-TiO₂(anatase-0.25%), LLS0.5A = LLDPE-starch-TiO₂(anatase-0.5%), LLS0.75A = LLDPE-starch-TiO₂(anatase-0.75%), LLS1A = LLDPE-starch-TiO₂(anatase-1%)]

Figure 5.3c Variation in tensile strength of LLDPE-starch-TiO₂ (anatase) blends after immersion of plastic strips in shake culture flask for 4 months



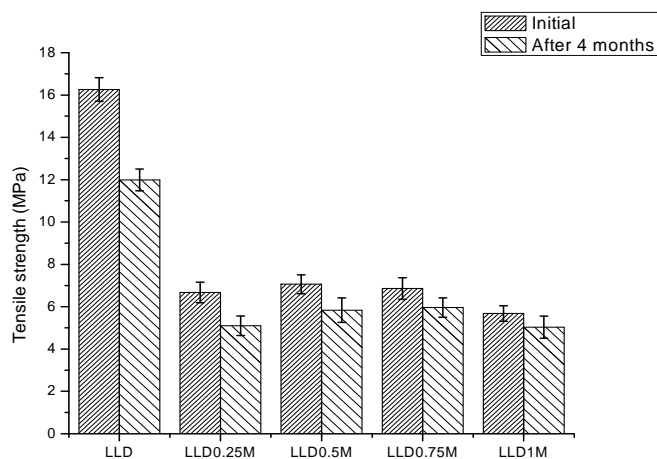
[LLS = LLDPE-starch300 (15%), LLS0.25R = LLDPE-starch-TiO₂(rutile-0.25%), LLS0.5R = LLDPE-starch-TiO₂(rutile-0.5%), LLS0.75R = LLDPE-starch-TiO₂(rutile-0.75%), LLS1R = LLDPE-starch-TiO₂(rutile-1%)]

Figure 5.3d Variation in tensile strength of LLDPE-starch- TiO₂ (rutile) blends after immersion of plastic strips in shake culture flask for 4 months



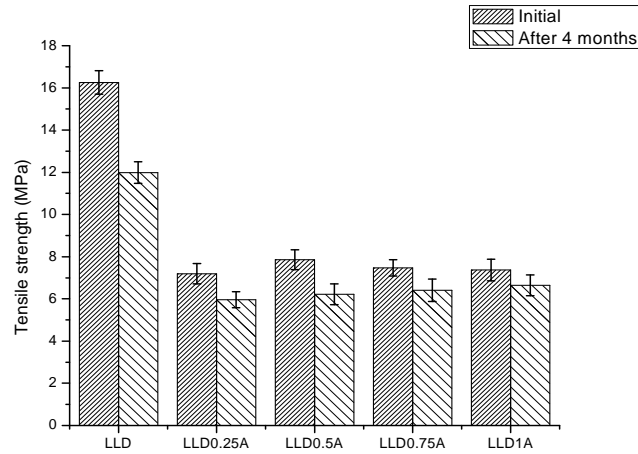
[LLD = LLDPE-dextrin300 (15%), LLD0.25F = LLDPE-dextrin-Fe₂O₃(0.25%), LLD0.5F = LLDPE-dextrin-Fe₂O₃(0.5%), LLD0.75F = LLDPE-dextrin-Fe₂O₃(0.75%), LLD1F = LLDPE-dextrin-Fe₂O₃(1%)]

Figure 5.3e Variation in tensile strength of LLDPE-dextrin-Fe₂O₃ blends after immersion of plastic strips in shake culture flask for 4 months



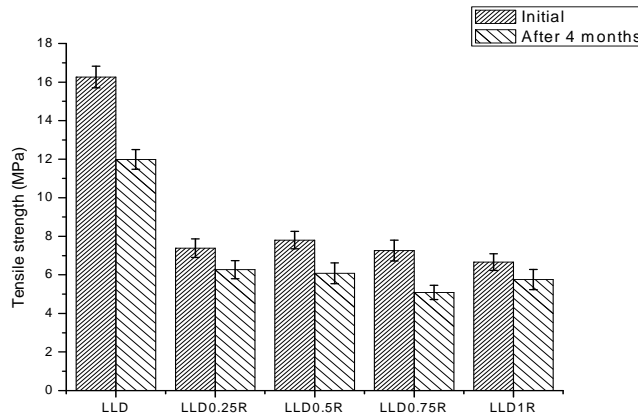
[LLD = LLDPE-dextrin300 (15%), LLD0.25M = LLDPE-dextrin-MnO₂(0.25%), LLD0.5M = LLDPE-dextrin-MnO₂(0.5%), LLD0.75M = LLDPE-dextrin-MnO₂(0.75%), LLD1M = LLDPE-dextrin-MnO₂(1%)]

Figure 5.3f Variation in tensile strength of LLDPE-dextrin-MnO₂ blends after immersion of plastic strips in shake culture flask for 4 months



[LLD = LLDPE-dextrin300 (15%), LLD0.25A = LLDPE-dextrin-TiO₂(anatase-0.25%), LLD0.5A = LLDPE-dextrin-TiO₂(anatase-0.5%), LLD0.75A = LLDPE-dextrin-TiO₂(anatase-0.75%), LLD1A = LLDPE-dextrin-TiO₂(anatase-1%)]

Figure 5.3g Variation in tensile strength of LLDPE-dextrin- TiO₂ (anatase) blends after immersion of plastic strips in shake culture flask for 4 months



[LLD = LLDPE-dextrin300 (15%), LLD0.25R = LLDPE-dextrin-TiO₂(rutile-0.25%), LLD0.5R = LLDPE-dextrin-TiO₂(rutile-0.5%), LLD0.75R = LLDPE-dextrin-TiO₂(rutile-0.75%), LLD1R = LLDPE-dextrin-TiO₂(rutile-1%)]

Figure 5.3h Variation in tensile strength of LLDPE-dextrin- TiO₂ (rutile) blends after immersion of plastic strips in shake culture flask for 4 months

Table 5.2 Variation in tensile strength of LLDPE-starch/dextrin-prooxidant (1%) blends after immersion of plastic strips in shake culture flask for 4 months

Composition	Initial tensile strength (MPa)	Tensile strength after 4 months (MPa)	Percentage loss in tensile strength
LLS	13.79	8.71	36.84
LLD	16.26	11.99	26.26
LLS1F	10.48	8.63	17.65
LLS1M	10.66	8.68	18.57
LLS1A	10.45	8.86	15.22
LLS1R	8.34	6.92	17.03
LLD1Fe	7.68	6.78	11.72
LLD1Mn	5.68	5.03	11.44
LLD1A	7.37	6.64	9.91
LLD1R	6.66	5.76	13.51

[LLS = LLDPE-starch300 (15%), LLD = LLDPE-dextrin300 (15%), LLS1F = LLDPE-starch-Fe₂O₃(1%), LLS1M = LLDPE-starch-MnO₂(1%), LLS1A = LLDPE-starch-TiO₂(anatase-1%), LLS1R = LLDPE-starch-TiO₂(rutile-1%), LLD1F = LLDPE-dextrin-Fe₂O₃(1%), LLD1M = LLDPE-dextrin-MnO₂(1%), LLD1A = LLDPE-dextrin-TiO₂(anatase-1%), LLD1R = LLDPE-dextrin-TiO₂(rutile-1%)]

The figures 5.3a, 5.3b, 5.3c, 5.3d, 5.3e, 5.3f, 5.3g and 5.3h show the variation in tensile strength of LLDPE-starch-prooxidant blends and LLDPE-dextrin-prooxidant blends after immersing the strips in shake culture flask containing amylase producing vibrios, which were isolated from marine benthic environment, for 4 months. After 4 months of immersion, the strips were retrieved and the tensile strength measurements were carried out for determining the extent of biodegradation. There is significant variation in tensile strength of the LLDPE sample containing either starch or dextrin alone as the bio-filler indicating higher degree of biodegradation as compared to neat

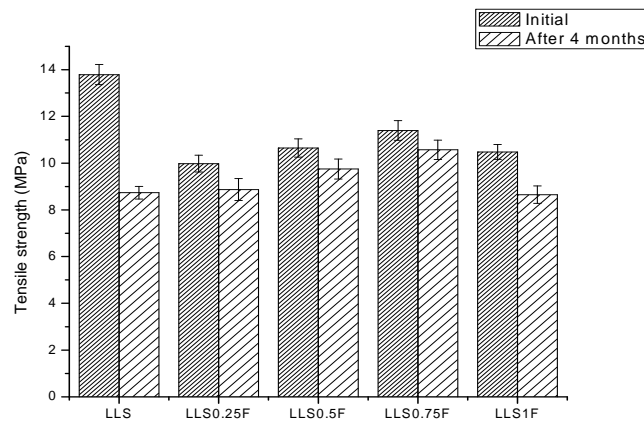
LLDPE. When pro-oxidants were incorporated in the LLDPE-biofiller blends and subjected to biodegradation in shake culture flask for 4 months, it was observed that the extent of biodegradation for the pro-oxidant containing blends were lower (table 5.2) as compared to the LLDPE containing either starch or dextrin alone as bio-filler. The mechanical damage of LLDPE macrochain might have caused by swelling and bursting of the growing cells of the invading micro-organisms or the micro-organisms in the shake culture flask [20-24].

Table 5.2 shows the percentage decrease in tensile strength of LLDPE-starch blends, LLDPE-dextrin blends, LLDPE-starch-prooxidant (1 weight %) blends and LLDPE-dextrin-prooxidant (1 weight %) blends after biodegradability test in shake culture flask for 4 months. Though the tensile strength of the LLDPE-starch and LLDPE-dextrin blends showed 36.84% and 26.26% loss in tensile strength after the biodegradation in shake culture flask for 4 months, the blends containing the pro-oxidants showed lower loss in tensile strength after the biodegradation. The results show that the pro-oxidants used in this study are effective in enhancing the rate of photodegradation of LLDPE, but they adversely affect the biodegradation of LLDPE.

5.2.3.2 Soil burial test

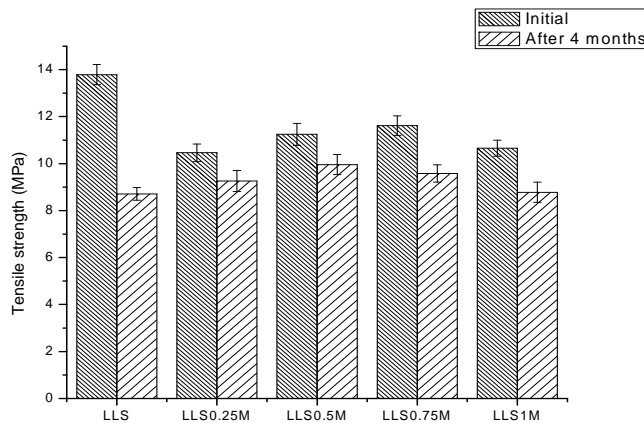
The tensile strength of the samples prepared from the blends after burial in soil for 4 months determined using a Shimadzu Autograph AG I series universal testing machine are shown in figures 5.4a, 5.4b, 5.4c, 5.4d, 5.4e, 5.4f, 5.4g and 5.4h. The tensile strength of

the blends decreased after burial in soil for 4 months. The results suggest that the blends are partially biodegradable.



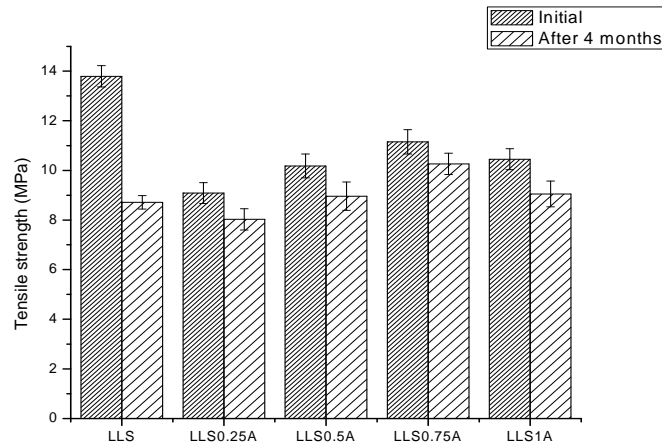
[LLS = LLDPE-starch300 (15%), LLS0.25F = LLDPE-starch-Fe₂O₃(0.25%), LLS0.5F = LLDPE-starch-Fe₂O₃(0.5%), LLS0.75F = LLDPE-starch-Fe₂O₃(0.75%), LLS1F = LLDPE-starch-Fe₂O₃(1%)]

Figure 5.4a Biodegradation of LLDPE-starch-Fe₂O₃ blends after soil burial test for 4 months as evident from the variation in tensile strength



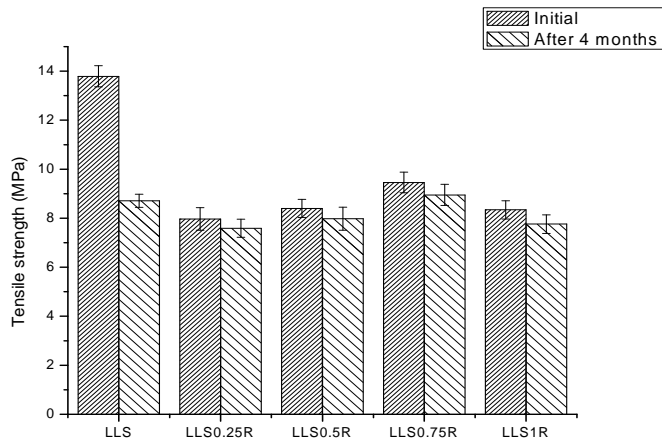
[LLS = LLDPE-starch300 (15%), LLS0.25M = LLDPE-starch-MnO₂(0.25%), LLS0.5M = LLDPE-starch-MnO₂(0.5%), LLS0.75M = LLDPE-starch-MnO₂(0.75%), LLS1M = LLDPE-starch-MnO₂(1%)]

Figure 5.4b Biodegradation of LLDPE-starch-MnO₂ blends after soil burial test for 4 months as evident from the variation in tensile strength



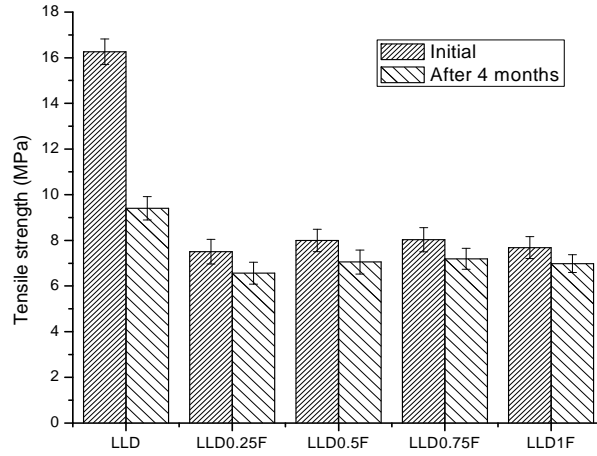
[LLS = LLDPE-starch300 (15%), LLS0.25A = LLDPE-starch-TiO₂(anatase-0.25%), LLS0.5A = LLDPE-starch-TiO₂(anatase-0.5%), LLS0.75A = LLDPE-starch-TiO₂(anatase-0.75%), LLS1A = LLDPE-starch-TiO₂(anatase-1%)]

Figure 5.4c Biodegradation of LLDPE-starch-TiO₂ (anatase) blends after soil burial test for 4 months as evident from the variation in tensile strength



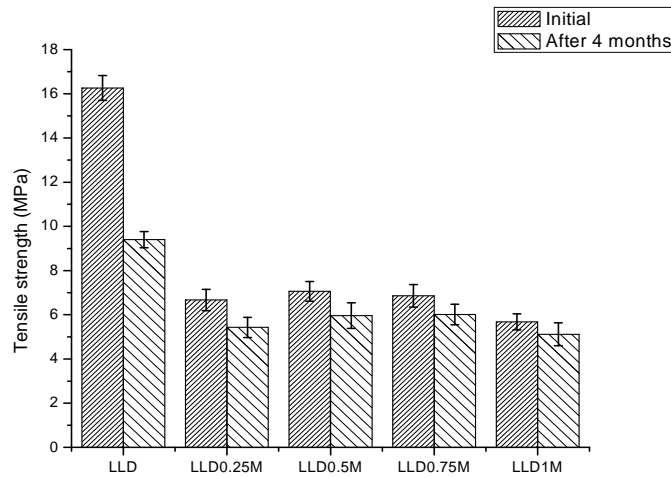
[LLS = LLDPE-starch300 (15%), LLS0.25R = LLDPE-starch-TiO₂(rutile-0.25%), LLS0.5R = LLDPE-starch-TiO₂(rutile-0.5%), LLS0.75R = LLDPE-starch-TiO₂(rutile-0.75%), LLS1R = LLDPE-starch-TiO₂(rutile-1%)]

Figure 5.4d Biodegradation of LLDPE-starch-TiO₂ (rutile) blends after soil burial test for 4 months as evident from the variation in tensile strength



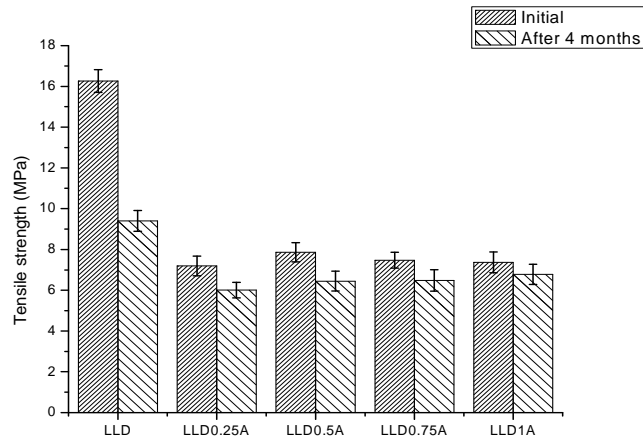
[LLD = LLDPE-dextrin300 (15%), LLD0.25F = LLDPE-dextrin-Fe₂O₃(0.25%), LLD0.5F = LLDPE-dextrin-Fe₂O₃(0.5%), LLD0.75F = LLDPE-dextrin-Fe₂O₃(0.75%), LLD1F = LLDPE-dextrin-Fe₂O₃(1%)]

Figure 5.4e Biodegradation of LLDPE-dextrin-Fe₂O₃ blends after soil burial test for 4 months as evident from the variation in tensile strength



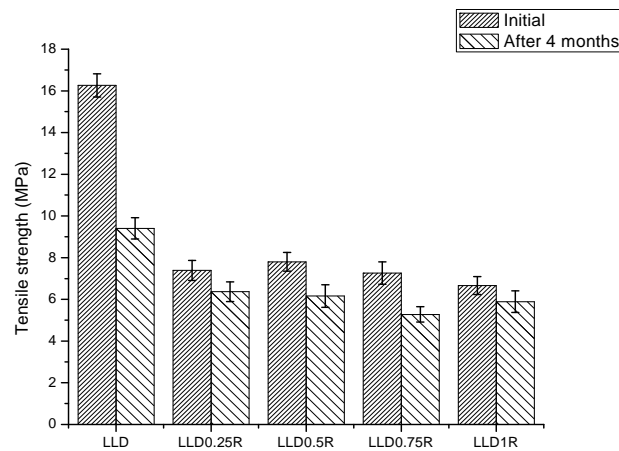
[LLD = LLDPE-dextrin300 (15%), LLD0.25M = LLDPE-dextrin-MnO₂(0.25%), LLD0.5M = LLDPE-dextrin-MnO₂(0.5%), LLD0.75M = LLDPE-dextrin-MnO₂(0.75%), LLD1M = LLDPE-dextrin-MnO₂(1%)]

Figure 5.4f Biodegradation of LLDPE-dextrin-MnO₂ blends after soil burial test for 4 months as evident from the variation in tensile strength



[LLD = LLDPE-dextrin300 (15%), LLD0.25A = LLDPE-dextrin-TiO₂(anatase-0.25%), LLD0.5A = LLDPE-dextrin-TiO₂(anatase-0.5%), LLD0.75A = LLDPE-dextrin-TiO₂(anatase-0.75%), LLD1A = LLDPE-dextrin-TiO₂(anatase-1%)]

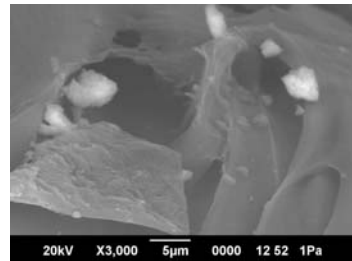
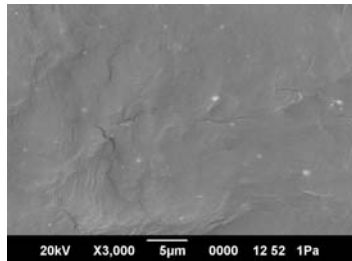
Figure 5.4g Biodegradation of LLDPE-dextrin- TiO₂ (anatase) blends after soil burial test for 4 months as evident from the variation in tensile strength



[LLD = LLDPE-dextrin300 (15%), LLD0.25R = LLDPE-dextrin-TiO₂(rutile-0.25%), LLD0.5R = LLDPE-dextrin-TiO₂(rutile-0.5%), LLD0.75R = LLDPE-dextrin-TiO₂(rutile-0.75%), LLD1R = LLDPE-dextrin-TiO₂(rutile-1%)]

Figure 5.4h Biodegradation of LLDPE-dextrin- TiO₂ (rutile) blends after soil burial test for 4 months as evident from the variation in tensile strength

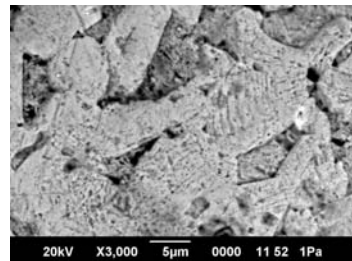
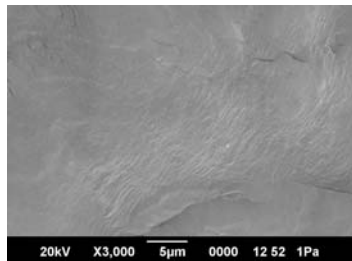
5.2.3.3 Scanning electron microscopic analyses



(a)

(b)

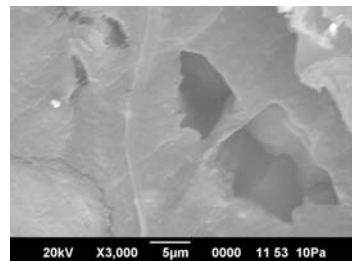
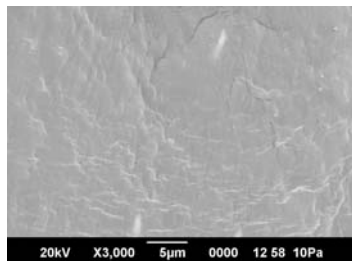
LLDPE-starch- Fe_2O_3 blends



(a)

(b)

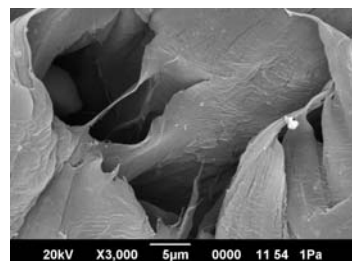
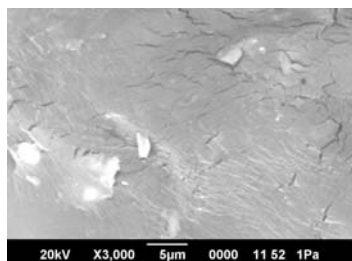
LLDPE-starch- MnO_2 blends



(a)

(b)

LLDPE-starch- TiO_2 (anatase) blends



(a)

(b)

LLDPE-starch- TiO_2 (rutile) blends

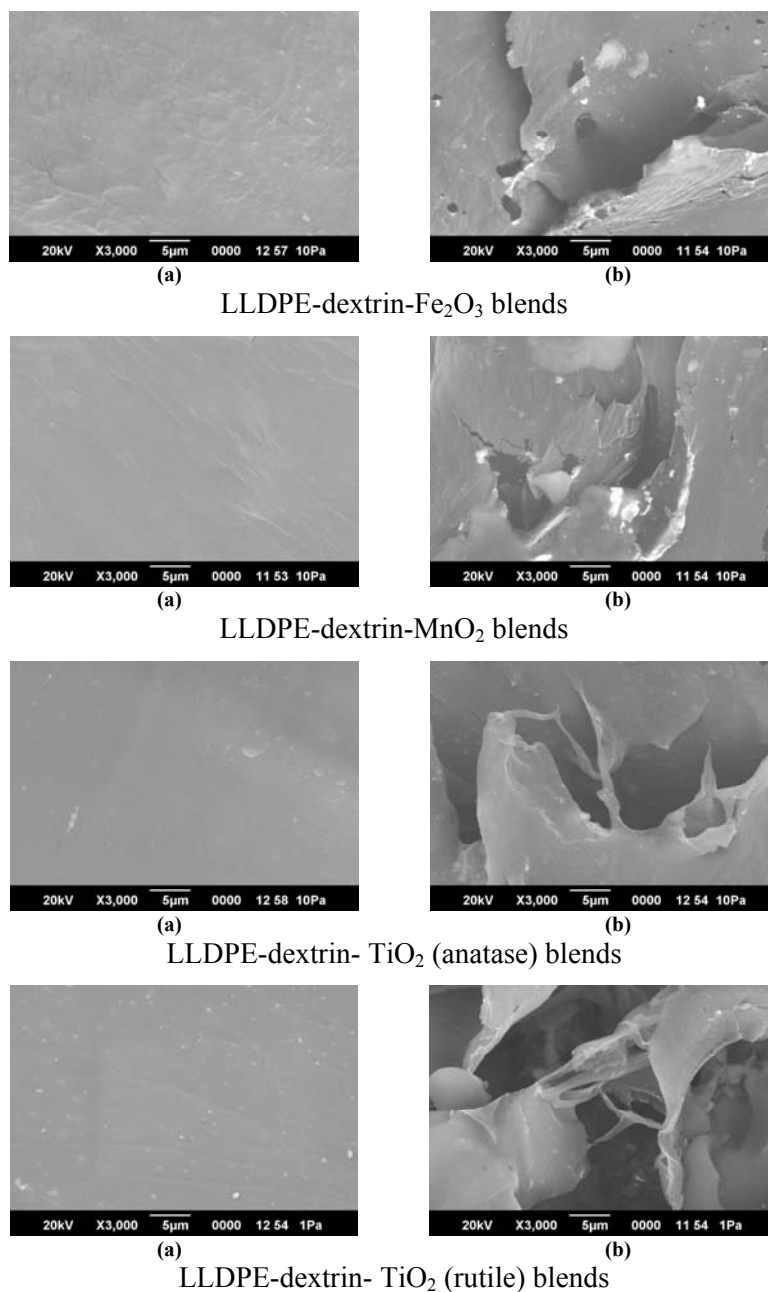


Figure 5.5 Scanning electron photomicrographs: (a) before biodegradation, (b) after biodegradation in shake culture flask for 4 months

The scanning electron photomicrographs of LLDPE-starch-prooxidant compositions and LLDPE-dextrin-prooxidant compositions, before and after biodegradation in shake culture flask for 4 months, are shown in figure 5.5. The surface of nondegraded LLDPE (Chapter 3, figure 3.6a) was smooth, without cracks and defects. Smooth surfaces were observed in the case of the scanning electron photomicrographs of the samples prepared from LLDPE-starch-prooxidant and LLDPE-dextrin-prooxidant blends too, before biodegradation. During the incubation period, the degradation of LLDPE-starch-prooxidant and LLDPE-dextrin-prooxidant blends occurred and the characteristic change in morphology was observed in the scanning electron photomicrographs. The formation of cavities in the blends after biodegradation is attributed to the removal of bio-fillers by the microorganisms. It shows that the bio-fillers in the blends favour the microbial accumulation throughout the surface [25]. Apparently the micro-organism in the shake culture flask attacks the plastic strips as their nutritional source and the bio-fillers were removed from the surface. As the concentration of pro-oxidant in the blends increased, a decrease in the rate of biodegradation was observed. The scanning electron photomicrographs also give evidence for the dispersion of filler particles in the LLDPE matrix.

5.2.3.4 Infrared spectroscopic analyses

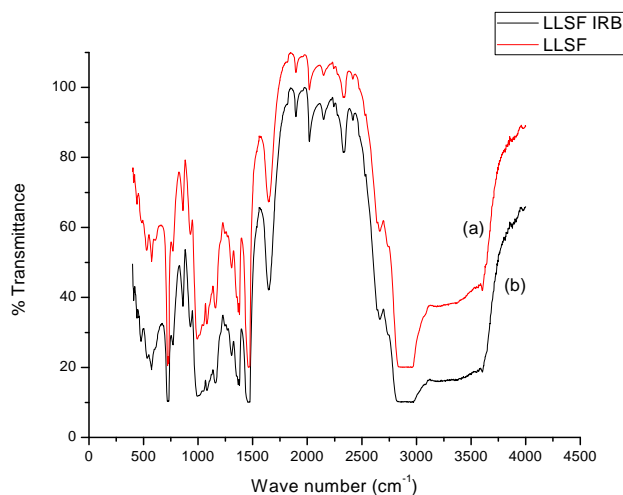


Figure 5.6a FTIR spectra of LLDPE-starch-Fe₂O₃ blends (a)before biodegradation (LLSF), and (b)after biodegradation studies in shake culture flask for 4 months (LLSF IRB)

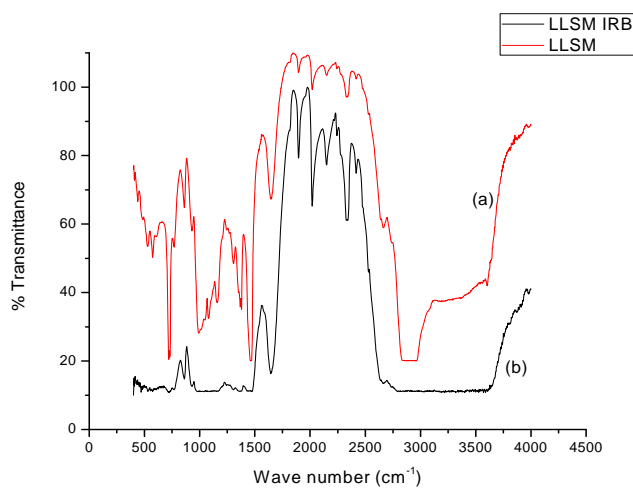


Figure 5.6b FTIR spectra of LLDPE-starch-MnO₂ blends (a)before biodegradation (LLSM), and (b)after biodegradation studies in shake culture flask for 4 months (LLSM IRB)

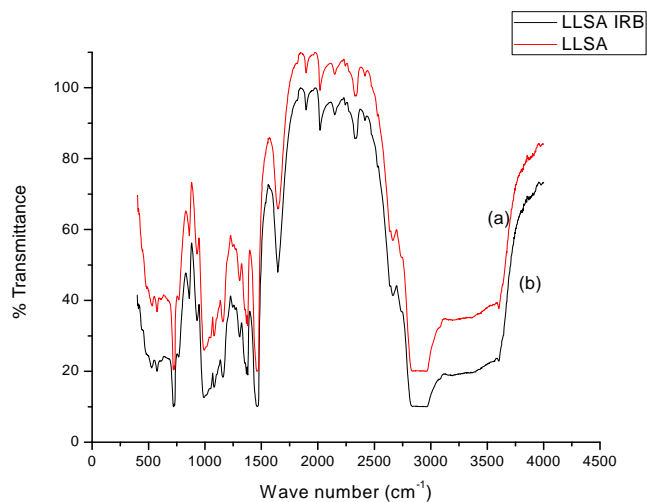


Figure 5.6c FTIR spectra of LLDPE-starch- TiO₂ (anatase) blends (a)before biodegradation (LLSA), and (b)after biodegradation studies in shake culture flask for 4 months (LLSA IRB)

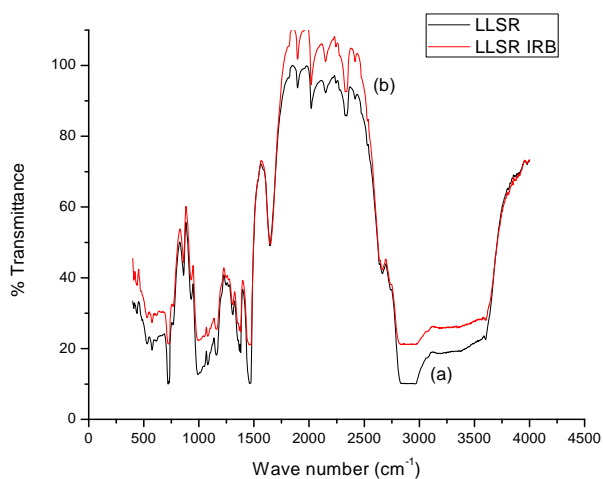


Figure 5.6d FTIR spectra of LLDPE-starch- TiO₂ (rutile) blends (a)before biodegradation (LLSR), and (b)after biodegradation studies in shake culture flask for 4 months (LLSR IRB)

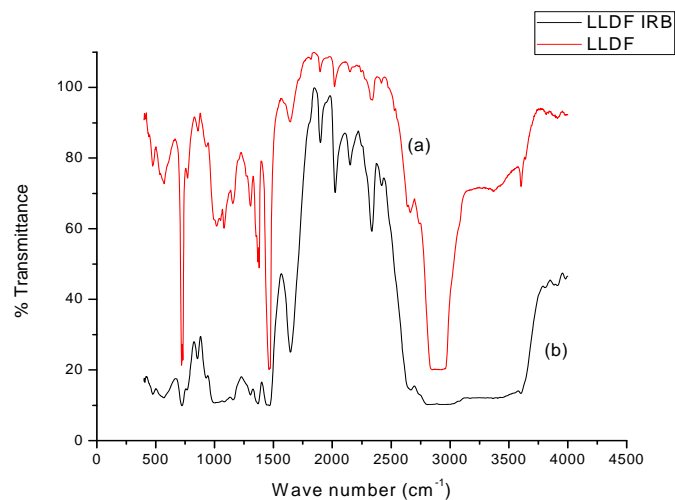


Figure 5.6e FTIR spectra of LLDPE-dextrin-Fe₂O₃ blends (a)before biodegradation (LLDF), and (b)after biodegradation studies in shake culture flask for 4 months (LLDF IRB)

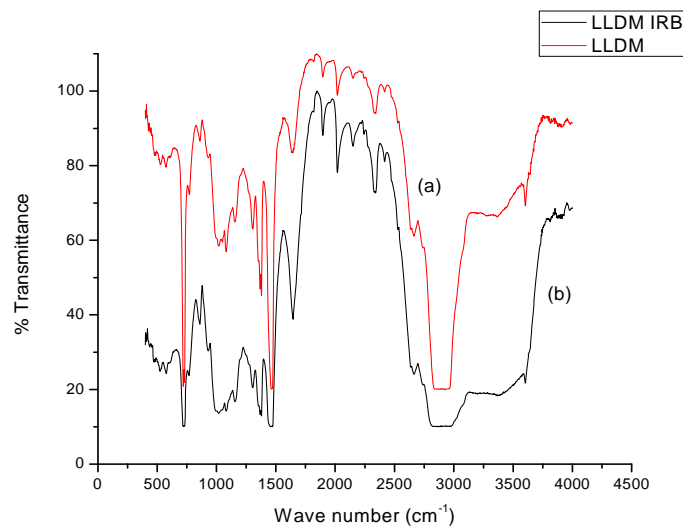


Figure 5.6f FTIR spectra of LLDPE-dextrin-MnO₂ blends (a)before biodegradation (LLDM), and (b)after biodegradation studies in shake culture flask for 4 months (LLDM IRB)

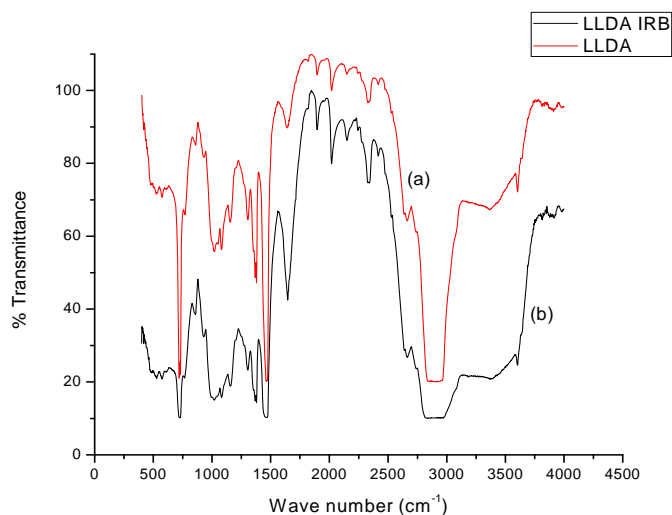


Figure 5.6g FTIR spectra of LLDPE-dextrin-TiO₂ (anatase) blends (a)before biodegradation (LLDA), and (b)after biodegradation studies in shake culture flask for 4 months (LLDA IRB)

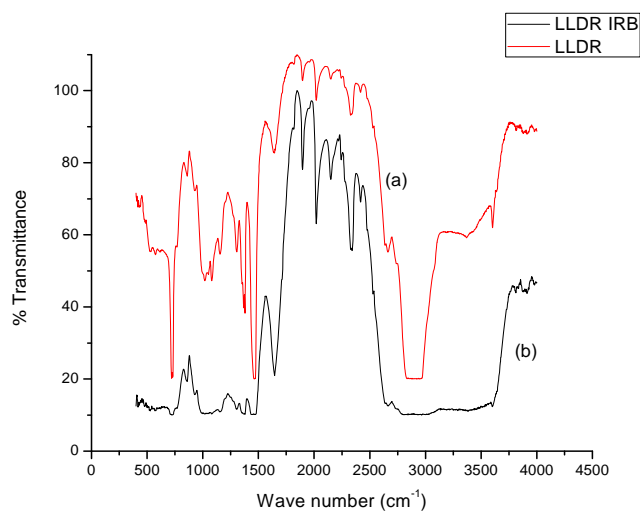


Figure 5.6h FTIR spectra of LLDPE-dextrin- TiO₂ (rutile) blends (a)before biodegradation (LLDR), and (b)after biodegradation studies in shake culture flask for 4 months (LLDR IRB)

The FTIR spectra of starch, dextrin and neat LLDPE are shown in Chapter 3 (figures 3.10a, 3.10b and 3.10c). The figures 5.6a, 5.6b, 5.6c, 5.6d, 5.6e, 5.6f, 5.6g and 5.6h show the spectra of LLDPE-starch-prooxidant and LLDPE-dextrin-prooxidant blends before and after biodegradation in shake culture flask. The characteristic peak assignments are shown in tables 5.3a and 5.3b. For starch three peaks corresponding to C-O stretching and O-H deformation were observed. For dextrin the peaks obtained correspond to O-H stretching, C-H bending, C-O stretching and O-H deformation. All the characteristics peaks of the neat polymers and the fillers can be seen in the spectra of LLDPE-starch-prooxidant and LLDPE-dextrin-prooxidant blends indicating that the spectra of the blends are the superposition of the spectra of pure polymers. This shows that IR spectral bands are not affected by the compositions of blends. The results of the FTIR analyses indicate that there is no specific interaction between LLDPE and the fillers. Thus the incompatibility of LLDPE and the fillers is evident from the FTIR spectra of the neat polymers and the blends.

Two peaks at 3317 cm^{-1} and 999 or 1000 cm^{-1} were observed which correspond to the O-H stretching vibrations of starch and dextrin. A typical IR spectrum of the dextrin presents bands at 3365 cm^{-1} (O-H), $2851\text{-}2940\text{ cm}^{-1}$ (CH), $1040\text{-}1110\text{ cm}^{-1}$ (C-O) [25].

Table 5.3a Data obtained from FTIR spectra of LLDPE-starch-prooxidant blends after biodegradation

	Peak position (cm ⁻¹)	Characteristic group
Starch	1149	C-O stretching
	1077	C-O stretching
	998	O-H deformation
LLDPE	1644	δ (O-H) band of absorbed water
	1470	CH ₂ bending
	720	skeletal vibration of CH ₂
LLDPE-starch-Fe ₂ O ₃	2901	C-H stretching
	1459	CH ₂ bending
	720	skeletal vibration CH ₂
LLDPE-starch-MnO ₂	2889	C-H stretching
	1459	CH ₂ bending
	998	O-H deformation
	721	skeletal vibration of CH ₂
LLDPE-starch-TiO ₂ (anatase)	2903	C-H stretching
	1460	CH ₂ bending
	722	skeletal vibration of CH ₂
LLDPE-starch-TiO ₂ (rutile)	2880	C-H stretching
	720	skeletal vibration of CH ₂

Comparison of spectra of LLDPE-starch-Fe₂O₃ blends before and after biodegradation shows notable differences in intensities at 2901 cm⁻¹ (C-H stretching), 1459 cm⁻¹ and 720 cm⁻¹ (CH₂ vibration). In case of LLDPE-starch-MnO₂ blends, the differences in the peak intensities are observed at 2889 cm⁻¹, 1459 cm⁻¹, 998 cm⁻¹ and 721 cm⁻¹ corresponding to the variations in C-H stretching, CH₂ bending, O-H deformation and CH₂ vibrations. Similar observations were obtained in case of LLDPE-starch-TiO₂ (anatase) and LLDPE-starch-TiO₂ (rutile) blends also. The difference in peak intensities in the region

1450-1490 cm^{-1} reveals the removal of starch by the microorganism. There is slight difference in the intensity of the peaks at 2869 cm^{-1} and 720 cm^{-1} in the case of the LLDPE-starch-prooxidant blends which could be due to the removal of LLDPE also from the blends. The pores generated by the removal of starch may be acting as a feasible sites for oxygen and microbes to enhance the degradation process.

Table 5.3b Data obtained from FTIR spectra of LLDPE-dextrin-prooxidant blends after biodegradation

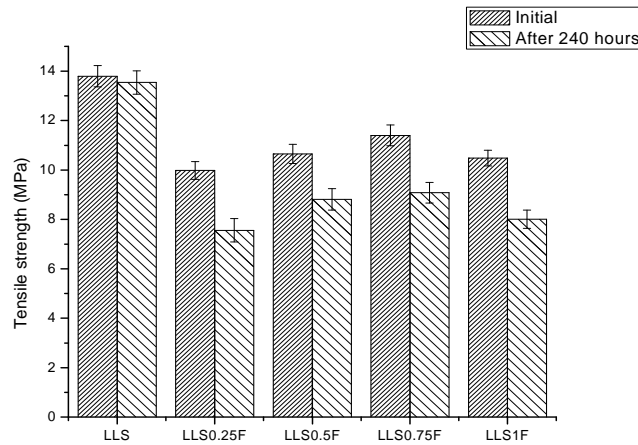
	Peak position (cm^{-1})	Characteristic group
Dextrin	3317	O-H stretching
	1352	C-H bending
	1147	C-O stretching
	1076	C-O stretching
	999	O-H deformation
LLDPE	1644	δ (O-H) band of absorbed water
	1470	CH_2 bending
	720	skeletal vibration of CH_2
	473	O-H deformation (broadening by water, C-O-C ring vibration)
LLDPE-dextrin- Fe_2O_3	2914	C-H stretching
	1460	CH_2 bending
	722	skeletal vibration of CH_2
LLDPE-dextrin- MnO_2	2889	C-H stretching
	1459	CH_2 bending
	720	skeletal vibration of CH_2
LLDPE-dextrin- TiO_2 (anatase)	2889	C-H stretching
	1459	CH_2 bending
	721	skeletal vibration of CH_2
LLDPE-dextrin- TiO_2 (rutile)	2891	C-H stretching
	1460	CH_2 bending
	1370	CH_3 bending
	722	skeletal vibration of CH_2

Information about different stages of degradation can be obtained by subtracting the spectrum of the pure polymer from the spectrum of the degraded sample [26, 27].

Comparison of spectra of LLDPE-dextrin-Fe₂O₃ blends before and after biodegradation shows notable differences in intensities at 2914 cm⁻¹ (C-H stretching), 1450-1460 cm⁻¹(CH₂ bending) and 720 cm⁻¹ (CH₂ vibration). In all the cases, the differences were observed in the same frequency regions. The difference in peak intensities in the region 1450-1490 cm⁻¹ reveals the removal of dextrin by the microorganism. In the case of LLDPE-dextrin-prooxidant blends too slight difference in the intensity of peaks at 2869 cm⁻¹ and 720 cm⁻¹ was observed which could be due to the removal of LLDPE also from the blends. Here too the pores generated by the removal of dextrin may be acting as feasible sites for oxygen and microbes to enhance the degradation process.

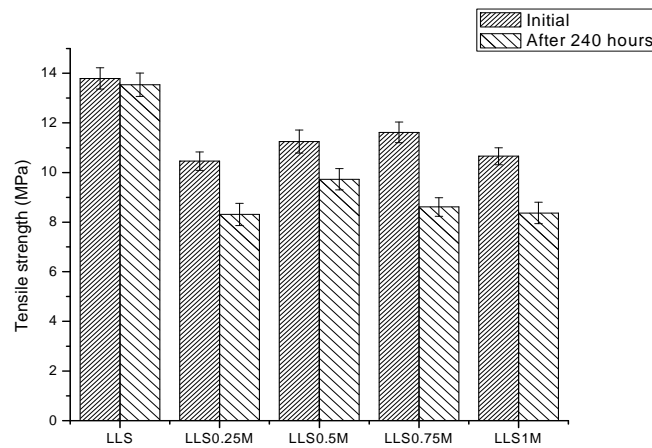
5.2.4 Photodegradability studies

5.2.4.1 Variation in tensile strength



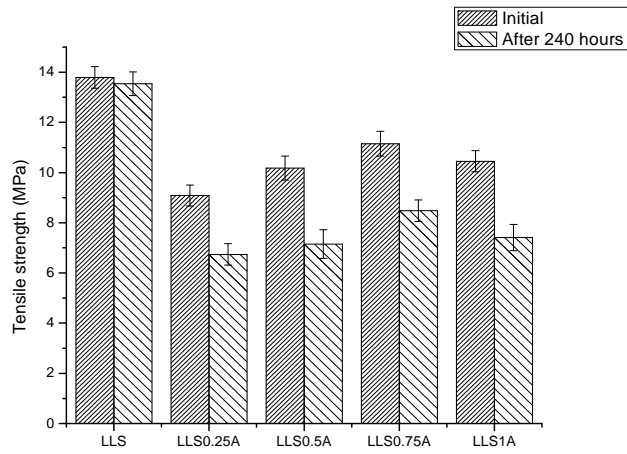
[LLS = LLDPE-starch, LLS0.25F = LLDPE-starch-Fe₂O₃(0.25%), LLS0.5F = LLDPE-starch-Fe₂O₃(0.5%), LLS0.75F = LLDPE-starch-Fe₂O₃(0.75%), LLS1F = LLDPE-starch-Fe₂O₃(1%)]

Figure 5.7a Photodegradation of LLDPE-starch-Fe₂O₃ blends after UV irradiation for 240 hours as evident from variation in tensile strength



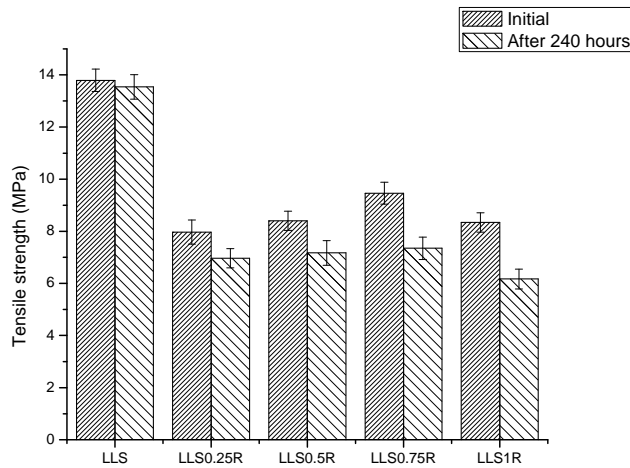
[LLS = LLDPE-starch, LLS0.25M = LLDPE-starch-MnO₂(0.25%), LLS0.5M = LLDPE-starch-MnO₂(0.5%), LLS0.75M = LLDPE-starch-MnO₂(0.75%), LLS1M = LLDPE-starch-MnO₂(1%)]

Figure 5.7b Photodegradation of LLDPE-starch-MnO₂ blends after UV irradiation for 240 hours as evident from variation in tensile strength



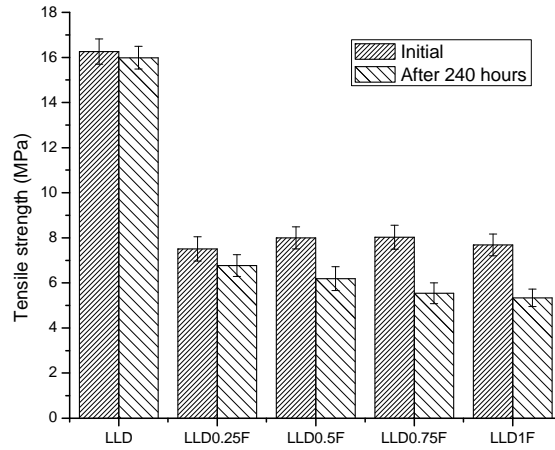
[LLS = LLDPE-starch, LLS0.25A = LLDPE-starch-TiO₂(anatase-0.25%), LLS0.5A = LLDPE-starch-TiO₂(anatase-0.5%), LLS0.75A = LLDPE-starch-TiO₂(anatase-0.75%), LLS1A = LLDPE-starch-TiO₂(anatase-1%)]

Figure 5.7c Photodegradation of LLDPE-starch-TiO₂(anatase) blends after UV irradiation for 240 hours as evident from variation in tensile strength



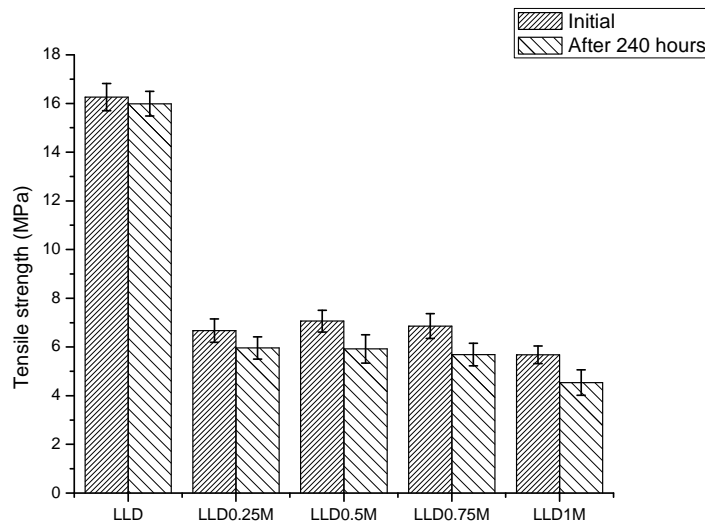
[LLS = LLDPE-starch, LLS0.25R = LLDPE-starch-TiO₂(rutile-0.25%), LLS0.5R = LLDPE-starch-TiO₂(rutile-0.5%), LLS0.75R = LLDPE-starch-TiO₂(rutile-0.75%), LLS1R = LLDPE-starch-TiO₂(rutile-1%)]

Figure 5.7d Photodegradation of LLDPE-starch-TiO₂(rutile) blends after UV irradiation for 240 hours as evident from variation in tensile strength



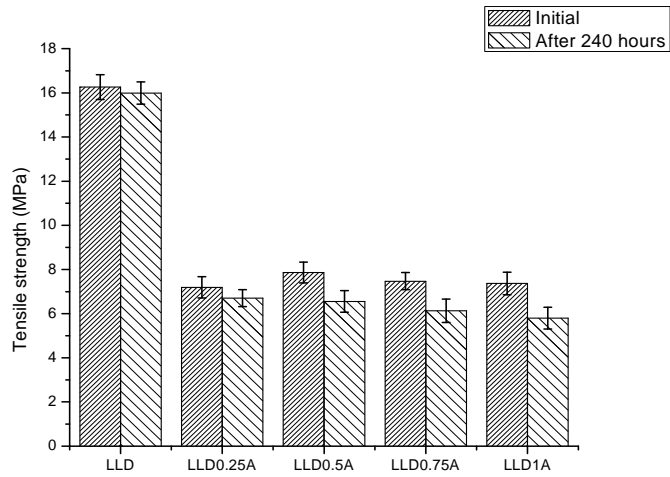
[LLD = LLDPE-dextrin, LLD0.25F = LLDPE-dextrin-Fe₂O₃(0.25%), LLD0.5F = LLDPE-dextrin-Fe₂O₃(0.5%), LLD0.75F = LLDPE-dextrin-Fe₂O₃(0.75%), LLD1F = LLDPE-dextrin-Fe₂O₃(1%)]

Figure 5.7e Photodegradation of LLDPE-dextrin-Fe₂O₃ blends after UV irradiation for 240 hours as evident from variation in tensile strength



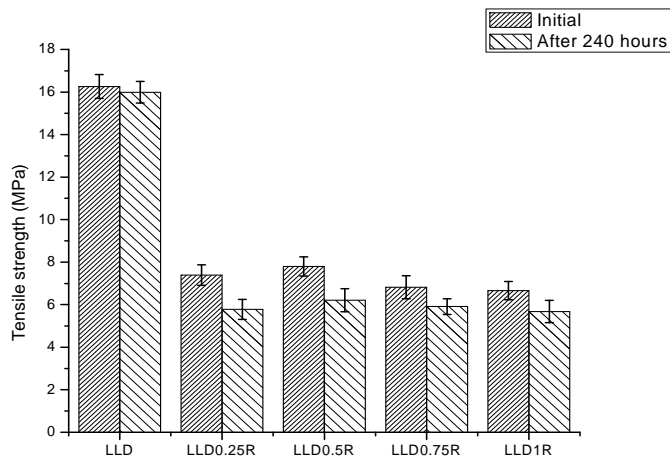
[LLD = LLDPE-dextrin, LLD0.25M = LLDPE-dextrin-MnO₂(0.25%), LLD0.5M = LLDPE-dextrin-MnO₂(0.5%), LLD0.75M = LLDPE-dextrin-MnO₂(0.75%), LLD1M = LLDPE-dextrin-MnO₂(1%)]

Figure 5.7f Photodegradation of LLDPE-dextrin-MnO₂ blends after UV irradiation for 240 hours (Evident from tensile strength)



[LLD = LLDPE-dextrin, LLD0.25A = LLDPE-dextrin-TiO₂(anatase-0.25%), LLD0.5A = LLDPE-dextrin-TiO₂(anatase-0.5%), LLD0.75A = LLDPE-dextrin-TiO₂(anatase-0.75%), LLD1A = LLDPE-dextrin-TiO₂(anatase-1%)]

Figure 5.7g Photodegradation of LLDPE-dextrin- TiO₂ (anatase) blends after UV irradiation for 240 hours as evident from variation in tensile strength



[LLD = LLDPE-dextrin, LLD0.25R = LLDPE-dextrin-TiO₂(rutile-0.25%), LLD0.5R = LLDPE-dextrin-TiO₂(rutile-0.5%), LLD0.75R = LLDPE-dextrin-TiO₂(rutile-0.75%), LLD1R = LLDPE-dextrin-TiO₂(rutile-1%)]

Figure 5.7h Photodegradation of LLDPE-dextrin- TiO₂ (rutile) blends after UV irradiation for 240 hours as evident from variation in tensile strength

Table 5.4 Variation in tensile strength of LLDPE-starch/dextrin-prooxidant (1%) blends after UV irradiation for 240 hours

Composition	Initial tensile strength (MPa)	Tensile strength after 4 months (MPa)	Percentage loss in tensile strength
LLS	13.79	12.98	5.87
LLD	16.26	15.58	4.18
LLS1F	9.88	8.1	18.01
LLS1M	9.66	8.37	13.35
LLS1A	8.34	6.75	19.06
LLS1R	10.45	8.54	18.27
LLD1F	7.96	6.59	17.21
LLD1M	5.68	4.54	20.07
LLD1A	7.37	5.8	21.3
LLD1R	6.66	5.38	19.21

[LLS = LLDPE-starch300 (15%), LLD = LLDPE-dextrin300 (15%),
 LLS1F = LLDPE-starch-Fe₂O₃(1%), LLS1M = LLDPE-starch-MnO₂(1%),
 LLS1A = LLDPE-starch-TiO₂(anatase-1%),
 LLS1R = LLDPE-starch-TiO₂(rutile-1%), LLD1F = LLDPE-dextrin-Fe₂O₃(1%),
 LLD1M = LLDPE-dextrin-MnO₂(1%), LLD1A = LLDPE-dextrin-TiO₂(anatase-1%),
 LLD1R = LLDPE-dextrin-TiO₂(rutile-1%)]

The reduction in tensile strength after placing the samples under ultraviolet radiation for 240 hours are shown in figures 5.7a, 5.7b, 5.7c, 5.7d, 5.7e, 5.7f, 5.7g and 5.7h. The percentage decrease in tensile strength of LLDPE-starch/dextrin-prooxidant (1%) compositions after UV exposure for 240 hours is shown in table 5.4. There is considerable decrease in tensile strength after 240 hours of UV exposure in all the samples. The samples containing metal oxides as pro-oxidants show more variation in tensile strength after UV irradiation as compared to the LLDPE-starch blends and LLDPE-dextrin blends. It was observed that the decrease in tensile strength was higher for blends containing

more amount of pro-oxidant. The results suggest that the metal oxide content in the blends accelerates the photo-oxidation of linear low density polyethylene by generating free radicals which in turn may be accelerating the degradation process.

It has been reported that the polyester films used in the packaging industry undergo degradation on exposure to UV light without an induction period and therefore UV stabilisers have to be added to minimize the photodegradation [26]. The polyester films are more expensive as compared to the LLDPE films for packaging applications. Hence LLDPE blended with bio-fillers and pro-oxidants is an economic alternative for polyester films in packaging applications [27-29].

5.2.4.2 FTIR

The FTIR spectra of LLDPE-starch-prooxidant compositions and LLDPE-dextrin-prooxidant compositions are presented in figures 5.8a, 5.8b, 5.8c, 5.8d, 5.8e, 5.8f, 5.8g and 5.8h. The characteristic peak assignments are shown in tables 5.5a and 5.5b. The FTIR spectra of these compositions show all the characteristic peaks of the neat starch, dextrin and LLDPE (Chapter 3, figures 3.10a, 3.10b and 3.10c) which shows that the spectra of LLDPE-starch/dextrin-prooxidant blends are the superposition of the spectra of pure polymers. This reveals that IR spectral bands are not affected by the compositions of blends, which indicates that there is no specific interaction between LLDPE and the fillers.

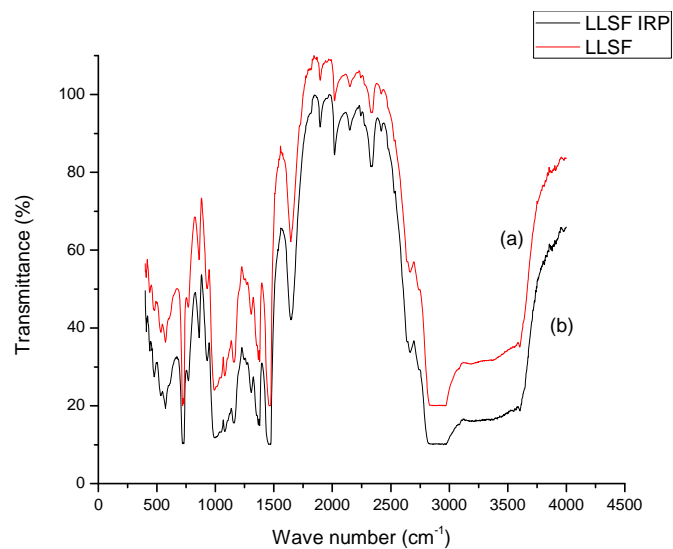


Figure 5.8a FTIR spectra of LLDPE-starch-Fe₂O₃ blends [LLSF]: (a) before UV irradiation [LLSF], and (b) after UV irradiation for 240 hours [LLSF IRP]

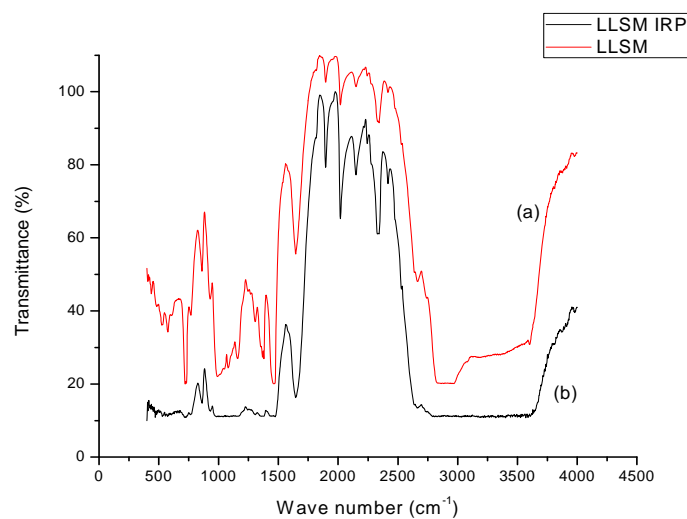


Figure 5.8b FTIR spectra of LLDPE-starch-MnO₂ blends [LLSM]: (a) before UV irradiation [LLSM], and (b) after UV irradiation for 240 hours [LLSM IRP]

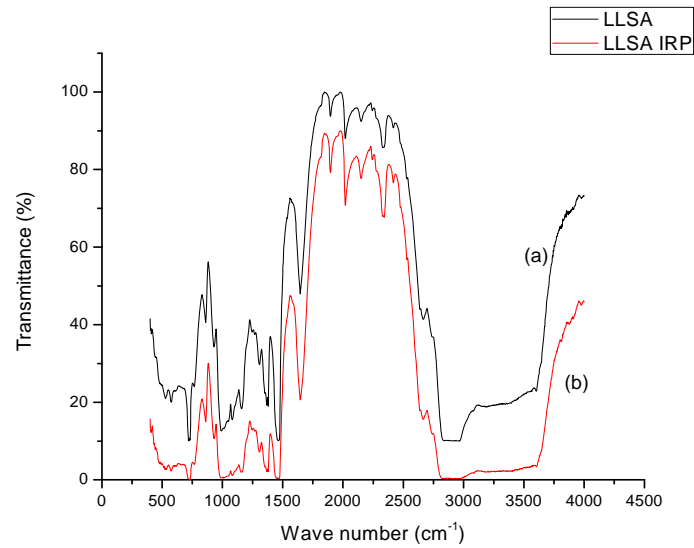


Figure 5.8c FTIR spectra of LLDPE-starch- TiO₂ (anatase) blends [LLSA]: (a)before UV irradiation [LLSA], and (b)after UV irradiation for 240 hours [LLSA IRP]

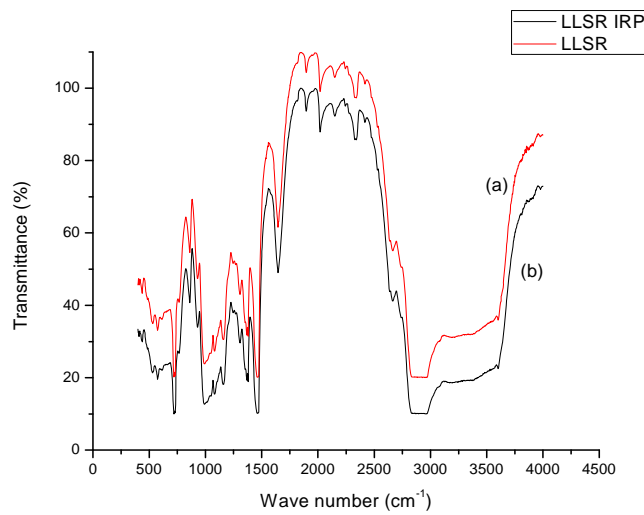


Figure 5.8d FTIR spectra of LLDPE-starch- TiO₂ (rutile) blends [LLSR]: (a)before UV irradiation [LLSR], and (b)after UV irradiation for 240 hours [LLSR IRP]

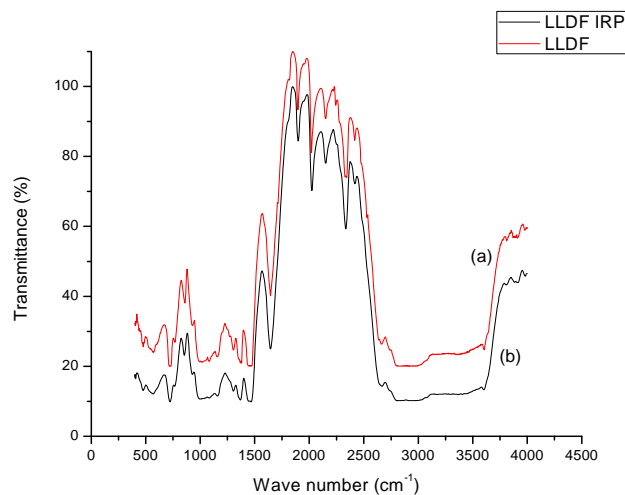


Figure 5.8e FTIR spectra of LLDPE-dextrin-Fe₂O₃ blends [LLDF]: (a)before UV irradiation [LLDF], and (b)after UV irradiation for 240 hours [LLDF IRP]

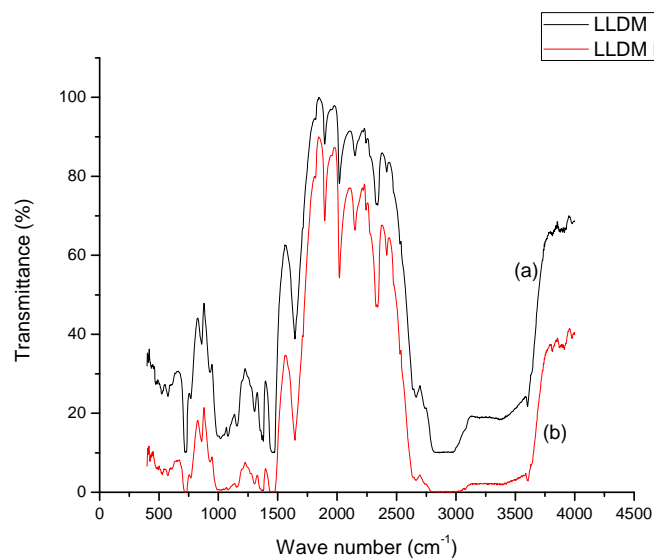


Figure 5.8f FTIR spectra of LLDPE-dextrin-MnO₂ blends [LLDM]: (a)before UV irradiation [LLDM], and (b)after UV irradiation for 240 hours [LLDM IRP]

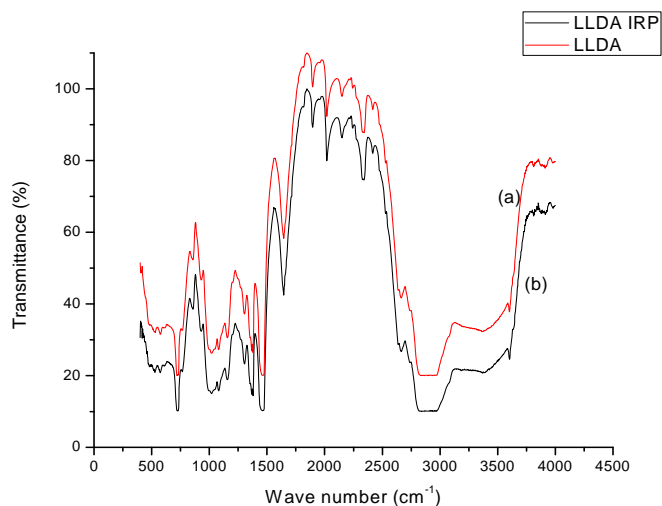


Figure 5.8g FTIR spectra of LLDPE-dextrin- TiO_2 (anatase) blends [LLDA]: (a) before UV irradiation [LLDA], and (b) after UV irradiation for 240 hours [LLDA IRP]

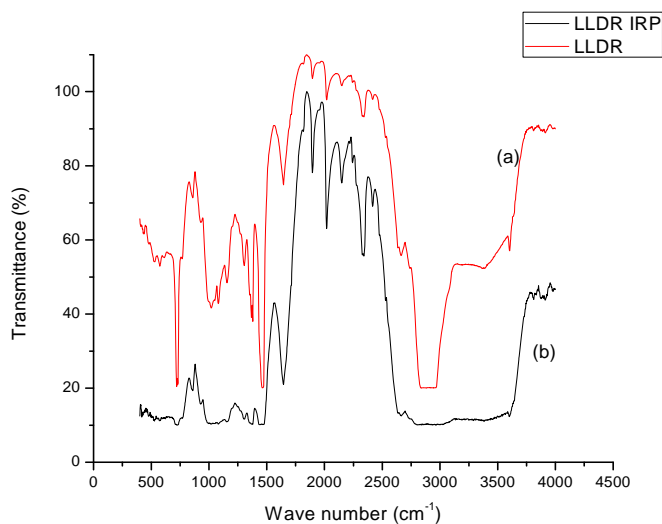


Figure 5.8h FTIR spectra of LLDPE-dextrin- TiO_2 (rutile) blends [LLDR]: (a) before UV irradiation [LLDR], and (b) after UV irradiation for 240 hours [LLDR IRP]

Table 5.5a Data obtained from FTIR spectra of LLDPE-starch-prooxidant blends after UV exposure

	Peak position (cm ⁻¹)	Characteristic group
Starch	1149	C-O stretching
	1077	C-O stretching
	998	O-H deformation
LLDPE	1644	δ (O-H) band of absorbed water
	1470	CH ₂ bending
	720	skeletal vibration CH ₂
	473	O-H deformation (broadening by water, C-O-C ring vibration)
LLDPE-starch-Fe ₂ O ₃	2901	C-H stretching
	1459	CH ₂ bending
	721	skeletal vibration CH ₂
LLDPE-starch-MnO ₂	2889	C-H stretching
	1459	CH ₂ bending
	721	skeletal vibration CH ₂
LLDPE-starch-TiO ₂ (anatase)	2891	C-H stretching
	1460	CH ₂ bending
	722	skeletal vibration CH ₂
LLDPE-starch-TiO ₂ (rutile)	2903	C-H stretching
	1460	CH ₂ bending
	722	skeletal vibration CH ₂

Comparison of spectra of LLDPE-starch-Fe₂O₃ blends before and after UV exposure shows notable differences in intensities at 2901 cm⁻¹, 1459 cm⁻¹ and 721 cm⁻¹ which corresponds to the C-H stretching, CH₂ bending and skeletal vibrations of CH₂. In the case of LLDPE-starch-MnO₂, LLDPE-starch-TiO₂ (anatase) and LLDPE-

starch-TiO₂ (rutile) blends too, similar results were observed. There is slight difference in the intensity of the peak at 2869 cm⁻¹ and 720 cm⁻¹ which could be due to the changes in vibrational frequencies of the groups in LLDPE also.

Table 5.5b Data obtained from FTIR spectra of LLDPE-dextrin-prooxidant blends after UV exposure

	Peak position (cm ⁻¹)	Characteristic group
Dextrin	3317	O-H stretching
	1352	C-H bending
	1147	C-O stretching
	1076	C-O stretching
	999	O-H deformation
LLDPE	1644	δ (O-H) band of absorbed water
	1470	CH ₂ bending
	720	skeletal vibration CH ₂
LLDPE-dextrin-Fe ₂ O ₃	2880	C-H stretching
	722	skeletal vibration CH ₂
LLDPE-dextrin-MnO ₂	2878	C-H stretching
	1459	CH ₂ bending
	721	skeletal vibration CH ₂
LLDPE-dextrin-TiO ₂ (anatase)	2878	C-H stretching
	1459	CH ₂ bending
	721	skeletal vibration CH ₂
LLDPE-dextrin-TiO ₂ (rutile)	2901	C-H stretching
	1459	CH ₂ bending
	1379	CH ₃ bending
	721	skeletal vibration CH ₂

Comparison of spectra of LLDPE-dextrin-Fe₂O₃ blends before and after UV exposure shows notable differences in intensities at 2880 cm⁻¹ (O-H band of absorbed water) and 722 cm⁻¹ (CH₂ vibration). In case of LLDPE-dextrin-MnO₂ blends, the differences in peak intensities are observed at 1648 cm⁻¹, 1459 cm⁻¹ and 720 cm⁻¹ which correspond to the variations in O-H band of absorbed water, CH₂ bending and CH₂ vibrations. Similar observations were obtained in case of LLDPE-dextrin-TiO₂ (anatase) and LLDPE-dextrin-TiO₂ (rutile). There is slight difference in the intensity of the peaks at 2869 cm⁻¹ and 720 cm⁻¹ which could be due to the changes in the vibrational frequency of the groups in LLDPE.

5.2.5 Melt flow test

The melt flow indices (MFI) of all the blends were determined according to ASTM D- 1238 [30]. The melt flow index has been widely used as a common measure for judging the processability of polymers [31]. It is an indirect measure of viscosity [32]. In tables 5.6a and 5.6b, the melt flow indices of LLDPE-starch-prooxidant and LLDPE-dextrin-prooxidant blends are compared with those of neat LLDPE, LLDPE-starch and LLDPE-dextrin blends.

On comparing the melt flow indices of neat LLDPE, LLDPE-starch and LLDPE-starch-prooxidant blends, it was observed that the blends containing pro-oxidants have lower melt flow indices as compared to the neat LLDPE and the LLDPE-starch blends. The incorporation of starch into neat LLDPE also decreased the melt flow rate of LLDPE.

This may be due to the increased entanglement of the polymer chains of LLDPE and the starch [32-35].

Table 5.6a Melt flow indices of LLDPE-starch-prooxidant blends

Sample	MFI (g/10 min)
LLDPE	1.09
LLDPE-starch*	0.75
LLDPE-starch-0.25%Fe ₂ O ₃	0.71
LLDPE-starch-0.5%Fe ₂ O ₃	0.65
LLDPE-starch-0.75%Fe ₂ O ₃	0.62
LLDPE-starch-1%Fe ₂ O ₃	0.58
LLDPE-starch-0.25%MnO ₂	0.75
LLDPE-starch-0.5%MnO ₂	0.70
LLDPE-starch-0.75%MnO ₂	0.66
LLDPE-starch-1%MnO ₂	0.61
LLDPE-starch-0.25%TiO ₂ (rutile)	0.72
LLDPE-starch-0.5%TiO ₂ (rutile)	0.66
LLDPE-starch-0.75%TiO ₂ (rutile)	0.62
LLDPE-starch-1%TiO ₂ (rutile)	0.57
LLDPE-starch-0.25%TiO ₂ (anatase)	0.69
LLDPE-starch-0.5%TiO ₂ (anatase)	0.67
LLDPE-starch-0.75%TiO ₂ (anatase)	0.65
LLDPE-starch-1%TiO ₂ (anatase)	0.61

*starch 300 mesh, 15 weight %

The addition of metal oxides as pro-oxidants to the LLDPE-starch blend might have decreased the movement of the polymer chain by increasing the viscosity of the blend, which eventually decreased the melt

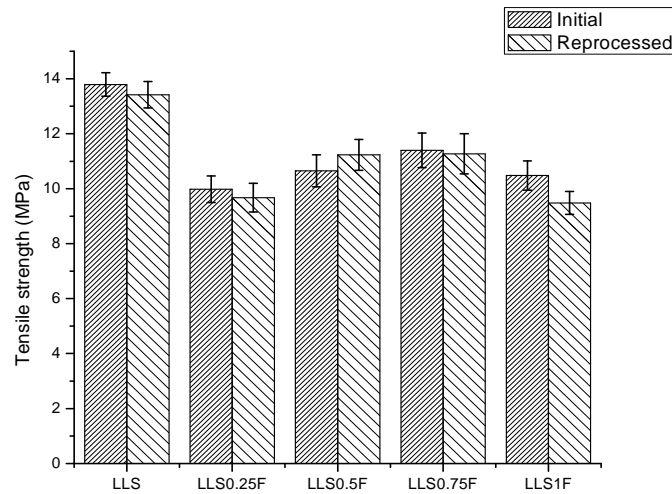
flow rate of the blends containing the pro-oxidants. In the case of LLDPE-dextrin-prooxidant blends also the melt flow indices were lower compared to the neat LLDPE and the LLDPE-dextrin blends. The presence of bio-fillers and the pro-oxidants in LLDPE matrix apparently restricts the melt movement by increasing viscosity, which implies a hardening effect of the fillers [34].

Table 5.6b Melt flow indices of LLDPE-dextrin-prooxidant blends

Sample	MFI
LLDPE	1.09
LLDPE-dextrin*	0.95
LLDPE-dextrin-0.25%Fe ₂ O ₃	0.73
LLDPE-dextrin-0.5%Fe ₂ O ₃	0.64
LLDPE-dextrin-0.75%Fe ₂ O ₃	0.55
LLDPE-dextrin-1%Fe ₂ O ₃	0.51
LLDPE-dextrin-0.25%MnO ₂	0.84
LLDPE-dextrin-0.5%MnO ₂	0.73
LLDPE-dextrin-0.75%MnO ₂	0.65
LLDPE-dextrin-1%MnO ₂	0.57
LLDPE-dextrin-0.25%TiO ₂ (rutile)	0.83
LLDPE-dextrin-0.5%TiO ₂ (rutile)	0.76
LLDPE-dextrin-0.75%TiO ₂ (rutile)	0.52
LLDPE-dextrin-1%TiO ₂ (rutile)	0.45
LLDPE-dextrin-0.25%TiO ₂ (anatase)	0.86
LLDPE-dextrin-0.5%TiO ₂ (anatase)	0.79
LLDPE-dextrin-0.75%TiO ₂ (anatase)	0.77
LLDPE-dextrin-1%TiO ₂ (anatase)	0.72

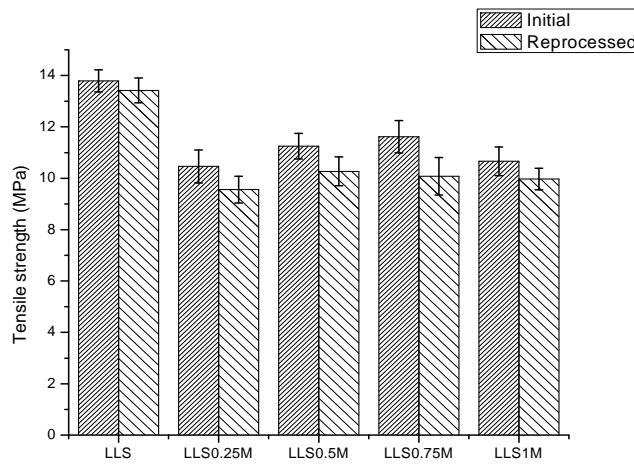
*dextrin 300 mesh, 15 weight %

5.2.6 Reprocessability



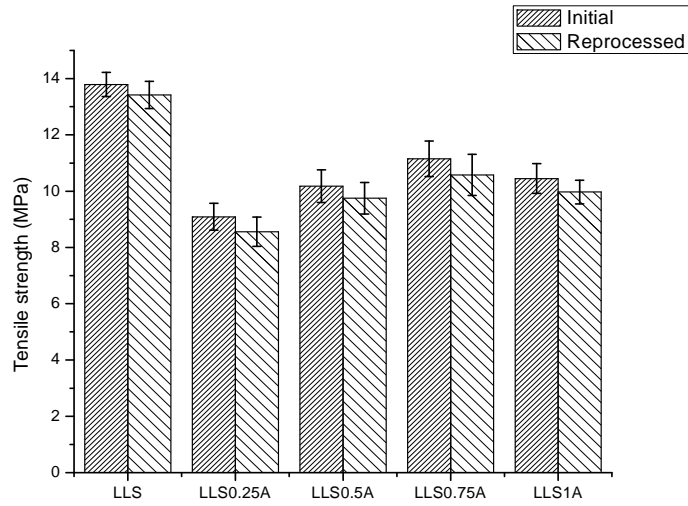
[LLS = LLDPE-starch300 (15%), LLS0.25F = LLDPE-starch-Fe₂O₃(0.25%), LLS0.5F = LLDPE-starch-Fe₂O₃(0.5%), LLS0.75F = LLDPE-starch-Fe₂O₃(0.75%), LLS1F = LLDPE-starch-Fe₂O₃(1%)]

Figure 5.9a Reprocessability of LLDPE-starch-Fe₂O₃ blends



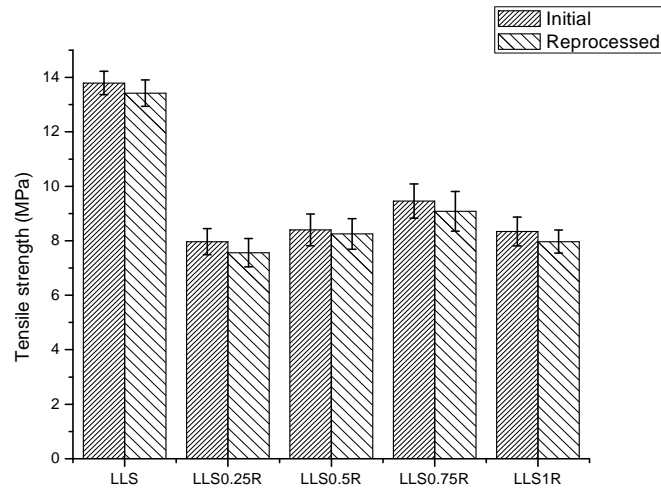
[LLS = LLDPE-starch300 (15%), LLS0.25M = LLDPE-starch-MnO₂(0.25%), LLS0.5M = LLDPE-starch-MnO₂(0.5%), LLS0.75M = LLDPE-starch-MnO₂(0.75%), LLS1M = LLDPE-starch-MnO₂(1%)]

Figure 5.9b Reprocessability of LLDPE-starch-MnO₂ blends



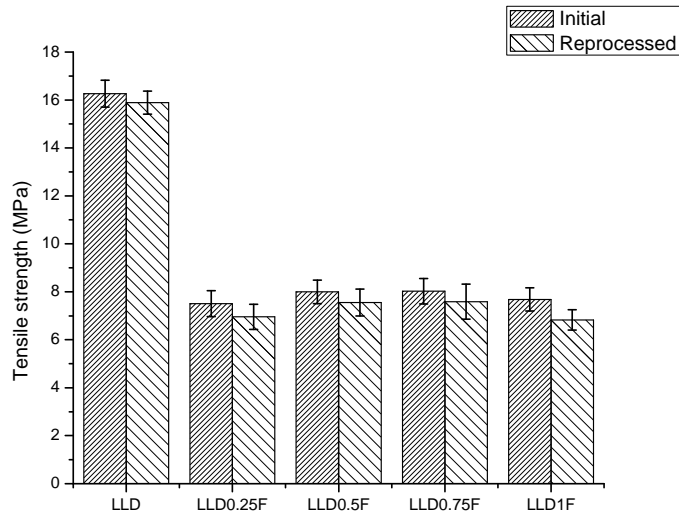
[LLS = LLDPE-starch300 (15%), LLS0.25A = LLDPE-starch-TiO₂(anatase-0.25%), LLS0.5A = LLDPE-starch-TiO₂(anatase-0.5%), LLS0.75A = LLDPE-starch-TiO₂(anatase-0.75%), LLS1A = LLDPE-starch-TiO₂(anatase-1%)]

Figure 5.9c Reprocessability of LLDPE-starch- TiO₂ (anatase) blends



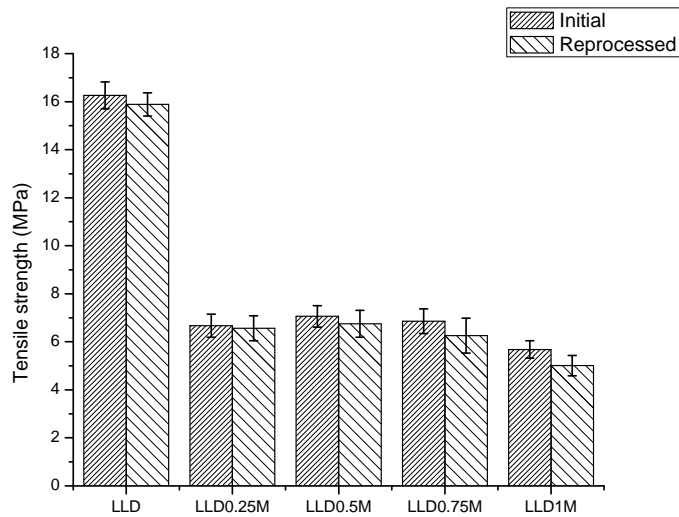
[LLS = LLDPE-starch300 (15%), LLS0.25R = LLDPE-starch-TiO₂(rutile-0.25%), LLS0.5R = LLDPE-starch-TiO₂(rutile-0.5%), LLS0.75R = LLDPE-starch-TiO₂(rutile-0.75%), LLS1R = LLDPE-starch-TiO₂(rutile-1%)]

Figure 5.9d Reprocessability of LLDPE-starch- TiO₂ (rutile) blends



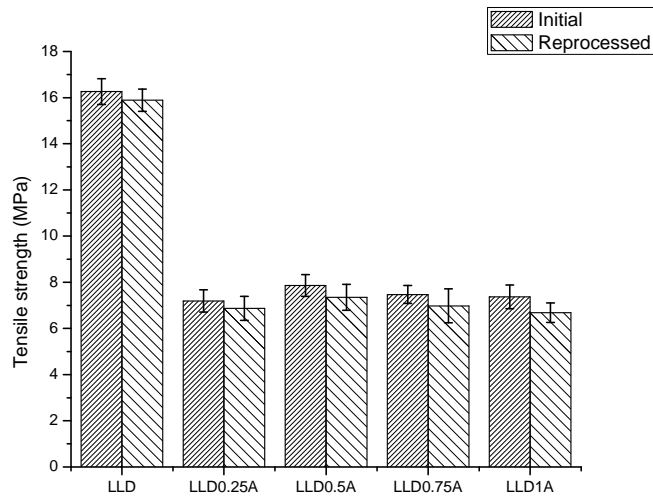
[LLD = LLDPE-dextrin300 (15%), LLD0.25F = LLDPE-dextrin-Fe₂O₃(0.25%), LLD0.5F = LLDPE-dextrin- Fe₂O₃(0.5%), LLD0.75F = LLDPE-dextrin-Fe₂O₃(0.75%), LLD1F = LLDPE-dextrin-Fe₂O₃(1%)]

Figure 5.9e Reprocessability of LLDPE-dextrin-Fe₂O₃ blends



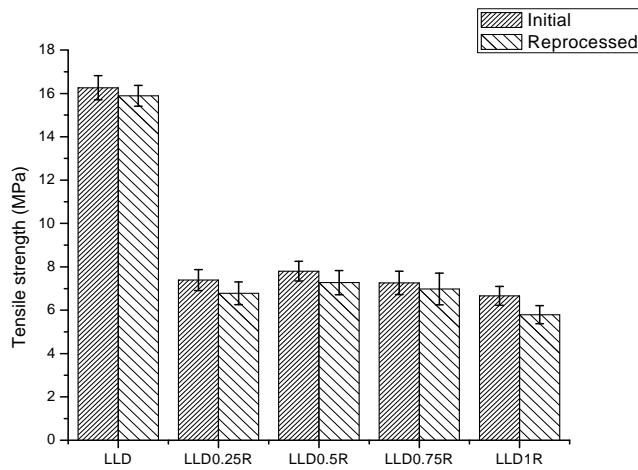
[LLD = LLDPE-dextrin300 (15%), LLD0.25M = LLDPE-dextrin-MnO₂(0.25%), LLD0.5M = LLDPE-dextrin-MnO₂(0.5%), LLD0.75M = LLDPE-dextrin-MnO₂(0.75%), LLD1M = LLDPE-dextrin-MnO₂(1%)]

Figure 5.9f Reprocessability of LLDPE-dextrin-MnO₂ blends



[LLD = LLDPE-dextrin300 (15%), LLD0.25A = LLDPE-dextrin-TiO₂(anatase-0.25%), LLD0.5A = LLDPE-dextrin-TiO₂(anatase-0.5%), LLD0.75A = LLDPE-dextrin-TiO₂(anatase-0.75%), LLD1A = LLDPE-dextrin-TiO₂(anatase-1%)]

Figure 5.9g Reprocessability of LLDPE-dextrin- TiO₂ (anatase) blends



[LLD = LLDPE-dextrin300 (15%), LLD0.25R = LLDPE-dextrin-TiO₂(rutile-0.25%), LLD0.5R = LLDPE-dextrin-TiO₂(rutile-0.5%), LLD0.75R = LLDPE-dextrin-TiO₂(rutile-0.75%), LLD1R = LLDPE-dextrin-TiO₂(rutile-1%)]

Figure 5.9h Reprocessability of LLDPE-dextrin- TiO₂ (rutile) blends

The figures 5.9a, 5.9b, 5.9c, 5.9d, 5.9e, 5.9f, 5.9g and 5.9h show the variation of tensile strength of LLDPE-starch-prooxidant and LLDPE-dextrin-prooxidant blends after reprocessing the samples in Thermo HAAKE polylab system and moulding in an electrically heated hydraulic press. The tensile strength measurements were carried out after three cycles of reprocessing the samples. It was observed that the tensile strength of the blends remained more or less unchanged after reprocessing the samples up to three cycles which implies that the blends are reprocessable.

5.3 Conclusion

The mechanical properties of LLDPE-biofiller blends containing pro-oxidants suggest that the metal oxides used as pro-oxidants have no significant reinforcing effect on the blends. The results of thermogravimetric analyses suggest that there is no significant decrease in T_{max} in presence of the pro-oxidants which indicates that the presence of pro-oxidants doesn't adversely affect the thermal stability of LLDPE. The differential scanning calorimetric analyses show that the degree of crystallinity of the pro-oxidant containing blends was lower as compared to the LLDPE-biofiller blends. The biodegradation of the samples in shake culture flask and in soil for 4 months suggest that the LLDPE-biofiller blends containing the pro-oxidants show lower extent of biodegradation as compared to the LLDPE-biofiller blends. The results show that the metal oxides used as pro-oxidants in this study adversely affect the biodegradation of LLDPE. The photodegradability studies show that the pro-oxidants are

effective in enhancing the rate of photodegradation of LLDPE. The scanning electron microscopic analyses reveal that the bio-fillers in the blends favour the microbial accumulation throughout the surface of the blends. The results of the FTIR analyses indicate that there is no specific interaction between LLDPE, bio-fillers and the pro-oxidants. The melt flow indices of the LLDPE-biofiller blends decreased on incorporating the pro-oxidants, and the values decreased as the concentration of the pro-oxidant increased suggesting that the pro-oxidants in LLDPE-biofiller matrix apparently restricts the melt movement by increasing the melt viscosity. The reprocessability studies established that the LLDPE-biofiller blends containing the pro-oxidants are reprocessable.

References

- [1] Guilbert S. Technology and application of edible protective films. In: Mathlouthi M, Editor. Food packaging and preservation., Elsevier Applied Science, London, [1986], 371.
- [2] Psomiadou E, Awanitoyannis I, Biliaderis CG, Ogawa H, Kawasaki N, *Carbohydrate Polymers*, **33**, [1997], 227.
- [3] Albertsson AC, Karlsson S, *Journal of Applied Polymer Science*, **35**, [1988], 1289.
- [4] Omichi H, In: Allen N, editor. Degradation and stabilization of polyolefins. Applied Science Publishers, London, [1983].
- [5] Gilead GS, US Patent 4,519,161, [1978].
- [6] Griffin GJL, U.S. Patent 4,016, 117 [1977]
- [7] Carlsson DJ, Garton A & Wiles DM, *Macromolecules*, **9**, [1976], 695.

- [8] Lenz RW, *Advances in Polymer Science*, **107**, [1993], 1.
- [9] Otey FH, Mark AM, Mehlretter CL, Russell CR, *Industrial Engineering Chemistry Production Research and Development*, **13(1)**, [1974], 90.
- [10] Willet JL, *Journal of Applied Polymer Science*, **54**, [1994], 1685.
- [11] Nikolov ZL, Evangeslista RL, Wung W, Jane JL, Gelina RJ, *Industrial Engineering Chemistry and Research*, **30**, [1991], 1841.
- [12] Kabbaz F, *Photo and thermo-oxidation of polyethylene with enhanced degradability*, Royal Institute of Technology, Sweden, [1998].
- [13] Carioca, Arora, Selvam, Tavares, & Kennedy, *Starch*, **48**, [1996], 322.
- [14] Chandra R and Rustgi R, *Progress in Polymer Science*, **23**, [1998], 1273.
- [15] Mascia L, *The role of additives in plastics*, Edward Arnold Publication, [1974].
- [16] Albertsson AC, Benenstedt C, Karlsson S, *Journal of Applied Polymer Science*, **51**, [1994], 1097.
- [17] Carlsson DJ, Wiles DM, *Macromolecules*, **4**, [1971], 179.
- [18] Mellor DC, Moir AB, Scott G, *European Polymer Journal*, **9**, [1973], 219.
- [19] Scott G, Wiles DM, *Biomacromolecules*, **2**, [2001], 615.
- [20] Annual Book of ASTM Standards, D 6691, **08.03**, [2004].
- [21] Buchanan RE and Gibbons NE, *Bergey's manual of systematic bacteriology*, (Eighth edition), The Williams and Wilkins Co., Baltimore, [1974], 747.
- [22] Furniss BS, Hannaford AJ, Rogersm V, Smith PWG and Tatchell AR (eds), *Vogel's textbook of practical organic chemistry*, Longman publications, England, 4 Ed, [1978], 497.

- [23] Bernfed PC, Enzymes of Starch degradation and synthesis. *Advanced Enzymology*, **12**, [1951], 379.
- [24] Rutkowska M, Heimowska A, Krasowska K, Janik H, *Polish Journal of Environmental Studies*, **11(3)**, [2002], 267.
- [25] Pratheep Kumar A, Jitendra K. Pandey, Bijendra Kumar, Singh RP, *Journal of Polymers and the Environment*, **14**, [2006], 203.
- [26] Amin MU and Scott G, *European Polymer Journal*, **10**, [1974], 1019.
- [27] Mellor DC, Moir AB and Scott G, *European Polymer Journal*, **9**, [1973], 219.
- [28] Osawa Z, In: Developments in Polymer Stabilisation-7, Ed. Scott G, Elsevier Applied Science, 1984, 193.
- [29] Al-Malaika, S., Chakraborty, K. B. & Scott, G., In Developments in Polymer Stabilisation--6, ed. G. Scott, Elsevier Applied Science, [1983], 73.
- [30] Annual Book of ASTM Standards, D 1238, **08.01**, [2004].
- [31] Furumiya A, Akana Y, Ushida Y, Masuda T and Nakajima A, *Pure and Applied Chemistry*, **57(6)**, [1985], 823.
- [32] Nielsen LE, Mechanical properties of polymers and composites, Marcel Dekker, New York, [1974].
- [33] Kawai F., Shibata M., Yokoyama S., Maeda S., Tada K., Hayashi S., *Macromolecular Symposia*, **144**, [1999], 73.
- [34] Albano C, Karam A, Dominguez N, Sanchez Y, Gonzalez J, Aguirre O, Catano L, *Composite Structures*, **71**, [2005], 282.
- [35] Jang BC, Huh SY, Jang JG, Bae YC, *Journal of Applied Polymer Science*, **82**, [2001], 3313.



EFFECT OF MALEATION ON THE COMPATIBILITY OF LLDPE–BIOFILLER BLENDS AND THE PHOTODEGRADABILITY OF THE COMPATIBILISED BLENDS IN PRESENCE OF PRO–OXIDANTS

<i>Contents</i>	6.1 Introduction
	Part A
	EFFECT OF MALEATION ON THE COMPATIBILITY OF LLDPE AND BIO-FILLERS
	6A.1 Results and Discussion
	Part B
	PHOTODEGRADABILITY OF THE COMPATIBILISED BLENDS
	6B.1 Results and Discussion
6.2 Conclusion	

.....

The process of maleation introduces polar groups onto the non-polar backbone of linear low density polyethylene (LLDPE). Maleic anhydride (1%) was grafted onto linear low-density polyethylene using dicumyl peroxide (0.25%) as the initiator. LLDPE grafted with maleic anhydride (LLDPE-g-MA) was blended with the bio-fillers (starch or dextrin - 5, 10 and 15 weight %). Various compositions (0.25, 0.5, 0.75 and 1 weight %) of the pro-oxidants (iron oxide, manganese dioxide, titanium dioxide (anatase and rutile grades)) were incorporated to the LLDPE-g-MA-biofiller blends to evaluate the effect of the pro-oxidants on the photodegradability of the blends. The studies include the evaluation of mechanical properties, thermal properties, biodegradability, SEM, FTIR spectra and water absorption. The maleation of LLDPE improves the compatibility of the blend components and the pro-oxidants enhances the photodegradability of the blends.

.....

6.1 Introduction

Several means [1-9] have been used to achieve the biodegradability /photo-biodegradability in polymers and composites. Scott et al. [1-4] developed a photo-biodegradable film which can be used to reduce the polymer waste. The effect of starch and dextrin as bio-fillers and the role of various metal oxides as pro-oxidants for photodegradation of LLDPE has been reported in the previous chapters. However, the poor compatibility of non-polar LLDPE with the polar bio-fillers limits their use in polymer blends for use in practical applications. To overcome this deficiency and to facilitate the compatibilization with polar bio-fillers, polyethylenes have been chemically modified through functionalization or grafting. This process introduces polar groups onto the polymer main chain as pendant units or short-chain branching [10]. Grafting is an important method for preparation of polymers with suitable functional groups [11].

This chapter reports the results of the studies on the effects of maleation of LLDPE on the compatibility of LLDPE and the bio-fillers, and the role of pro-oxidants on the photodegradation of the compatibilised blends.

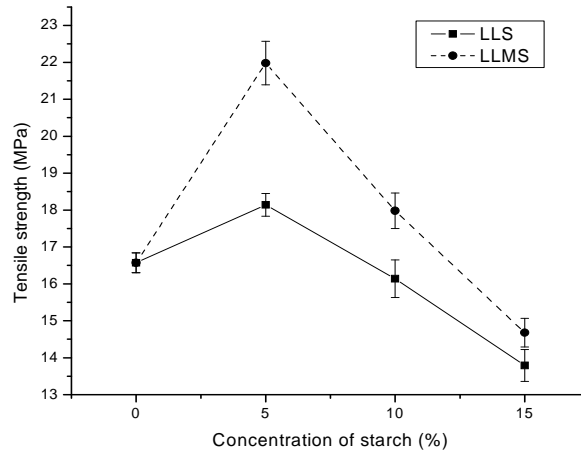
Part A

**EFFECT OF MALEATION ON THE COMPATIBILITY OF
LLDPE AND BIO-FILLERS**

6A.1 Results and Discussion

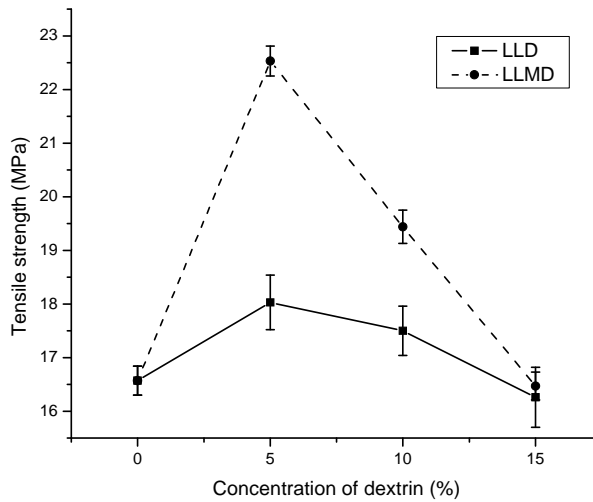
6A.1.1 Mechanical properties

The tensile strength and elastic modulus of LLDPE-g-MA-starch and LLDPE-g-MA-dextrin blends were evaluated according to ASTM D 882. Figures 6A.1a and 6A.1b show the variation of tensile strength of LLDPE-starch and LLDPE-dextrin blends with and without compatibilisation. On increasing the bio-filler (starch or dextrin, 300 mesh size) content, the tensile strength of LLDPE-starch and LLDPE-dextrin blends decreased, presumably because of incompatibility of LLDPE with bio-fillers. It is possible that the addition of starch or dextrin in LLDPE matrix would cause very significant stress concentration. Therefore, fracture would be initiated from the weak interface of the blend due to the poor interfacial adhesion, thus resulting in reduced tensile properties. The LLDPE-g-MA-biofiller blends show improved tensile strength as compared to the blend containing unmodified LLDPE. It is believed that the grafting of maleic anhydride to LLDPE increased adhesion between the LLDPE matrix and the starch or dextrin filler. The improved interfacial adhesion between LLDPE and starch as well as LLDPE and dextrin has a positive impact on the stress transfer, thus reducing the chance of interfacial debonding leading to improved tensile properties [12].



[LLS= LLDPE-starch (300 mesh), LLMS = LLDPE-g-MA-starch (300 mesh)]

Figure 6A.1a Variation of tensile strength with concentration of starch in LLDPE-starch and LLDPE-g-MA-starch blends

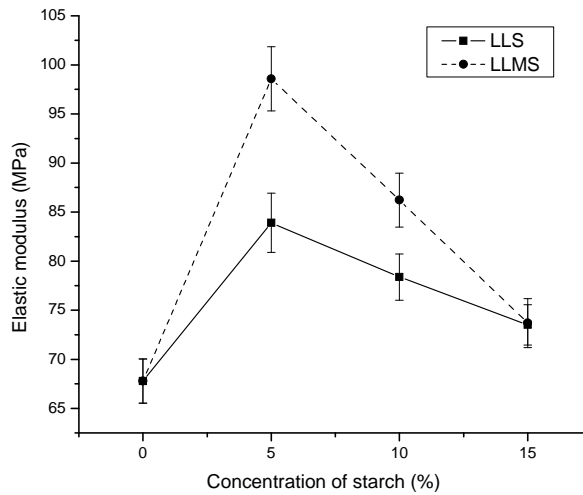


[LLD= LLDPE-dextrin (300 mesh), LLMD = LLDPE-g-MA-dextrin (300 mesh)]

Figure 6A.1b Variation of tensile strength with concentration of dextrin in LLDPE-dextrin and LLDPE-g-MA-dextrin blends

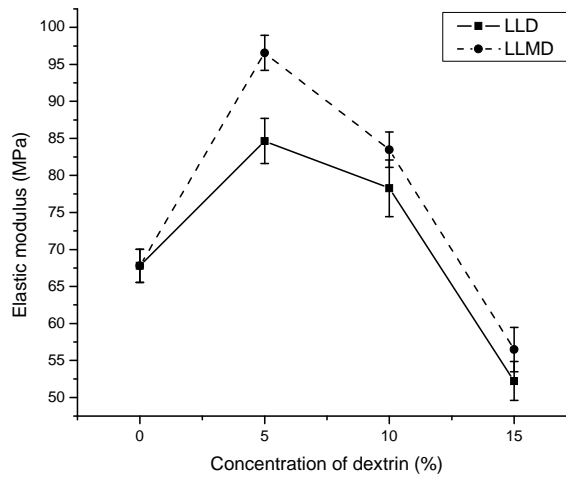
The variation in elastic modulus of LLDPE-starch and LLDPE-dextrin blends with and without compatibilisation are shown in figures

6A.1c and 6A.1d. The compatibilisation improved the elastic modulus of LLDPE-starch and LLDPE-dextrin blends.



[LLS= LLDPE-starch (300 mesh), LLMS = LLDPE-g-MA-starch (300 mesh)]

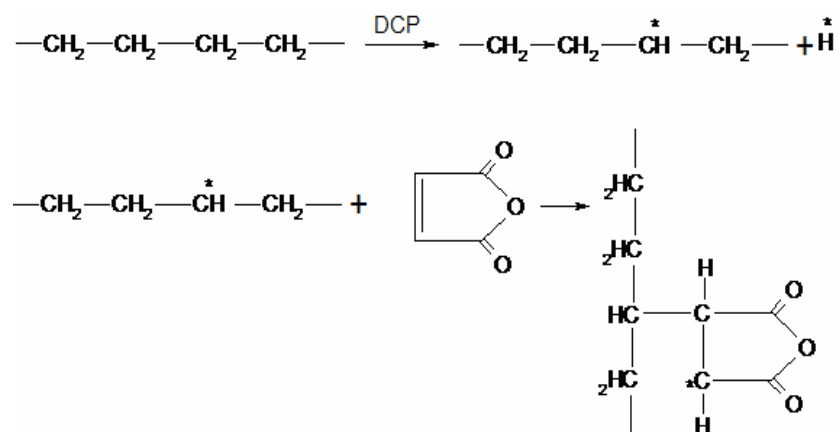
Figure 6A.1c Variation of elastic modulus with concentration of starch in LLDPE-starch and LLDPE-g-MA-starch blends



[LLD= LLDPE-dextrin (300 mesh), LLMD = LLDPE-g-MA-dextrin (300 mesh)]

Figure 6A.1d Variation of elastic modulus with concentration of dextrin in LLDPE-dextrin and LLDPE-g-MA-dextrin blends

On maleation of LLDPE, apparently the interfacial adhesion between LLDPE and starch as well as LLDPE and dextrin improved. In addition, these results also support the assumption that a chemical reaction occurs between bio-fillers and LLDPE-g-MA through the hydroxyl groups in starch or dextrin and anhydride groups in LLDPE-g-MA [13], as proposed in scheme 6.1.

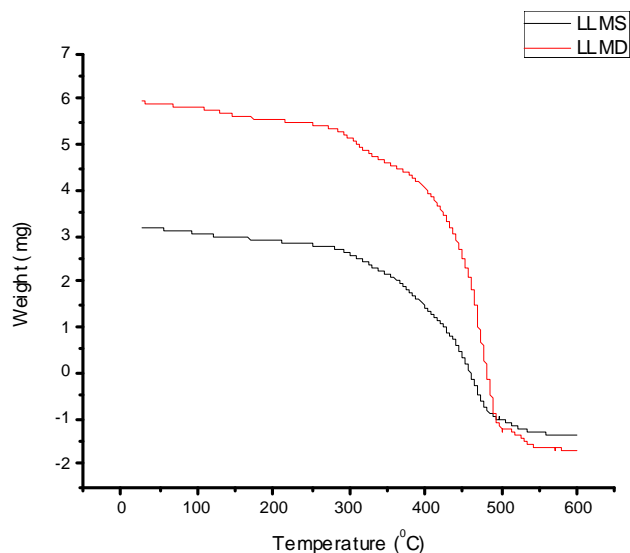


Scheme 6.1 Mechanism of maleic anhydride grafting on polyethylene

6A.1.2 Thermal studies

6A.1.2.1 Thermogravimetric analyses

The thermogravimetric analyses of the blends were carried out using Perkin Elmer, Diamond TG/DTA from room temperature to 600 °C under nitrogen atmosphere. The TGA thermograms of LLDPE-starch and LLDPE-dextrin blends are shown in figures 3.2a and 3.2b in Chapter 3.



[LLMS = LLDPE-g-MA-starch (15 weight%, 300 mesh),
 LLMD = LLDPE-g-MA-dextrin (15 weight%, 300 mesh)]

Figure 6A.2a TGA thermogram of LLDPE-g-MA-starch and LLDPE-g-MA-dextrin blends

Table 6A.1a Results from thermogravimetric analyses

Sample	T _{max} (°C)
LLDPE*	482
LLDPE-starch*	481
LLDPE-dextrin*	482
LLDPE-g-MA-starch	483
LLDPE-g-MA-dextrin	483

(* Ref: Chapter 3, Table 3.1)

For LLDPE-starch, there is considerable decrease in weight during the temperature range 250-350°C (Chapter 3, figure 3.2a). For LLDPE-dextrin blend also similar weight loss was observed during

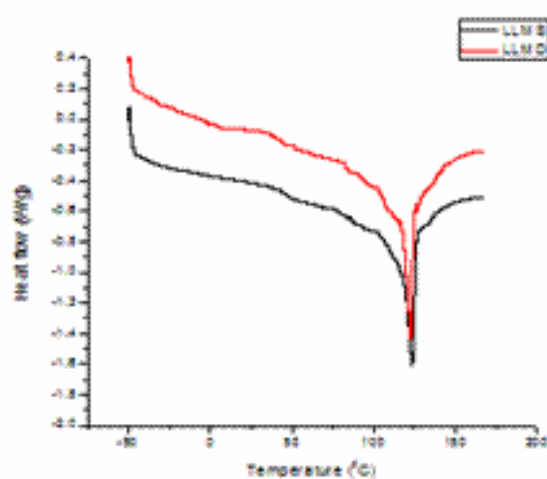
the same temperature range (Chapter 3, figure 3.2b). This corresponds to the loss of starch and dextrin from the blends as this is the decomposition temperature for these fillers. As reported in Chapter 3, the LLDPE and bio-fillers are incompatible to each other.

The thermograms of LLDPE-g-MA-starch and LLDPE-g-MA-dextrin are shown in figure 6A.2a. The weight change during the temperature range of 250-350°C is very low for these blends as compared to the blends without the compatibiliser, which suggests that the adhesion between LLDPE and starch or dextrin was improved on grafting LLDPE with maleic anhydride.

Table 6A.1a shows the results obtained from thermogravimetric analyses. The temperature at which maximum degradation occurs for all the blends and neat LLDPE are almost similar which is an indication that the thermal stability of LLDPE is unaltered on compatibilisation.

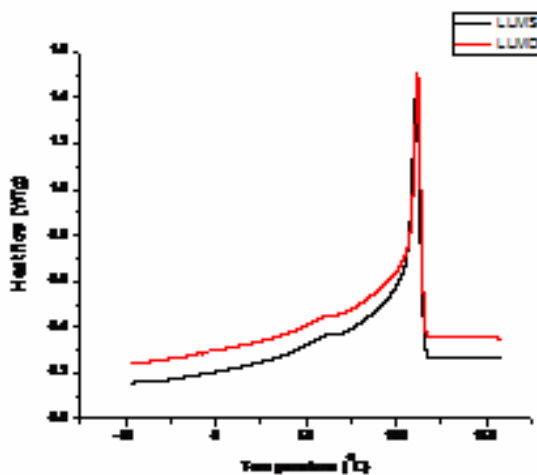
6A.1.2.2 Differential scanning calorimetry

As polymers are heated, they undergo a number of phase changes such as the glass transition (T_g), crystallization transition (T_c) and melting (T_m). Locations of these transitions are used to identify the polymers whereas the heat of fusion ΔH_f determined from the heat flux versus temperature curves in DSC are used to quantify the polymers [14].



[LLMS = LLDPE-g-MA-starch (15 weight%, 300 mesh)
LLMD = LLDPE-g-MA-dextrin (15 weight%, 300 mesh)]

Figure 6A.2b DSC thermograms (heating) of LLDPE-g-MA-starch and LLDPE-g-MA-dextrin blends



[LLMS = LLDPE-g-MA-starch (15 weight%, 300 mesh)
LLMD = LLDPE-g-MA-dextrin (15 weight%, 300 mesh)]

Figure 6A.2c DSC thermograms (cooling) of LLDPE-g-MA-starch and LLDPE-g-MA-dextrin blends

The DSC heating and cooling thermograms of LLDPE-g-MA-starch and LLDPE-g-MA-dextrin blends are shown in figures 6A.2b and 6A.2c. The melting temperature, crystallisation temperature, heat of fusion, heat of crystallisation and percentage crystallinity of LLDPE, and the blends are shown in table 6A.1b. It was observed that the melting temperature of LLDPE-g-MA-starch and LLDPE-g-MA-dextrin blends tend to decrease as compared to the neat LLDPE.

The crystallization temperature (T_c) of LLDPE-g-MA-starch and LLDPE-g-MA-dextrin blends increased as compared to LLDPE and the blends without compatibiliser apparently due to the nucleation of LLDPE-g-MA [15]. However, the percentage crystallinity values of LLDPE-g-MA-starch and LLDPE-g-MA-dextrin blends are lower than that of neat LLDPE. This may be due to the grafting of maleic anhydride onto LLDPE and cross-link formation in LLDPE-g-MA leading to more defects in the crystals of LLDPE-g-MA and starch as well as LLDPE-g-MA and dextrin blends [15].

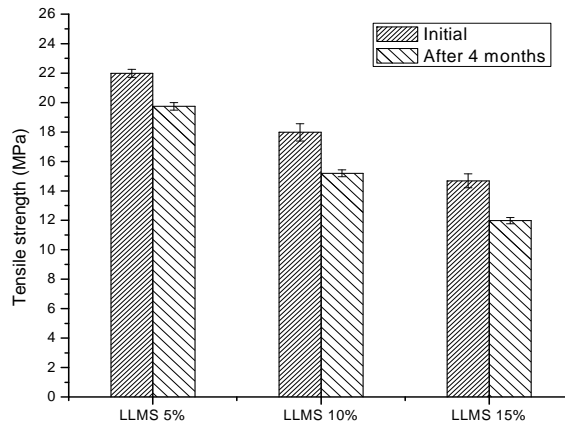
Table 6A.1b Results from differential scanning calorimetry

Sample	T_m (°C)	ΔH_f (J/g)	T_c (°C)	ΔH_c (J/g)	% Crystallinity
LLDPE*	126	58	106	59	20
LLDPE-starch*	125	57	107	53	19
LLDPE-dextrin*	126	55	107	48	19
LLDPE-g-MA-starch	123	26	111	30	9
LLDPE-g-MA-dextrin	122	25	111	27	8

(* Ref: Chapter 3, Table 3.2)

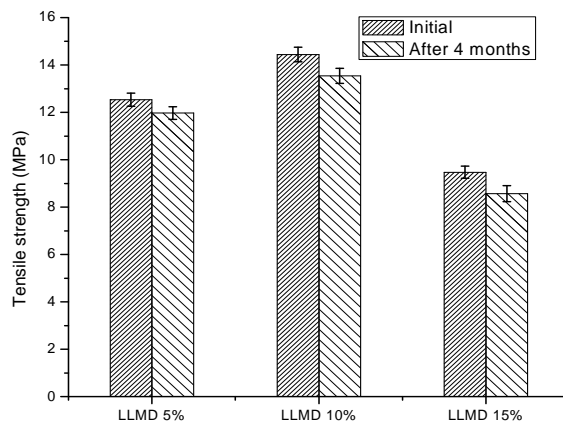
6A.1.3 Biodegradation studies

6A.1.3.1 In shake culture flask



[LLMS5% = LLDPE-g-MA-starch 5%, LLMS10% = LLDPE-g-MA-starch 10%, LLMS15% = LLDPE-g-MA-starch 15%]

Figure 6A.3a Biodegradation of LLDPE-g-MA-starch blends after immersion of plastic strips in shake culture flask for 4 months as evident from tensile strength



[LLMD5% = LLDPE-g-MA-dextrin 5%, LLMD10% = LLDPE-g-MA-dextrin 10%, LLMD15% = LLDPE-g-MA-dextrin 15%]

Figure 6A.3b Biodegradation of LLDPE-g-MA-dextrin blends after immersion of plastic strips in shake culture flask for 4 months as evident from tensile strength

Table 6A.2a Percentage decrease in tensile strength of LLDPE-g-MA-starch and LLDPE-g-MA-dextrin blends after immersion of plastic strips in shake culture flask for 4 months

Composition	Initial tensile strength (MPa)	Tensile strength after 4 months (MPa)	% decrease in tensile strength
LLMS5	11.98	11.74	2
LLMS10	14.98	14.19	5.27
LLMS15	13.68	12.48	8.77
LLMD5	12.53	11.97	4.47
LLMD10	14.44	13.54	6.23
LLMD15	9.47	8.57	9.5

[LLMS5 = LLDPE-g-MA-starch 5%, LLMS10 = LLDPE-g-MA-starch 10%, LLMS15 = LLDPE-g-MA-starch 15%, LLMD5 = LLDPE-g-MA-dextrin 5%, LLMD10 = LLDPE-g-MA-dextrin 10%, LLMD15 = LLDPE-g-MA-dextrin 15%]

The variation in tensile strength of LLDPE-g-MA-starch and LLDPE-g-MA-dextrin blends after biodegradability studies for 4 months in shake culture flask containing amylase producing vibrios which were isolated from marine benthic environment are shown in figure 6A.3a and 6A.3b. The tensile strength of the blends decreased after biodegradation in shake culture flask suggesting that the blends are partially biodegradable.

The percentage decrease in tensile strength and % weight loss of LLDPE-g-MA-starch and LLDPE-g-MA-dextrin blends after biodegradability tests in shake culture flask are shown in table 6A.2a and 6a.2b. As the starch and dextrin content increased the percentage decrease in tensile strength and percentage weight loss of the blends increased. Though the compatibility of LLDPE and the bio-filler was improved by grafting LLDPE with maleic anhydride as reported in the

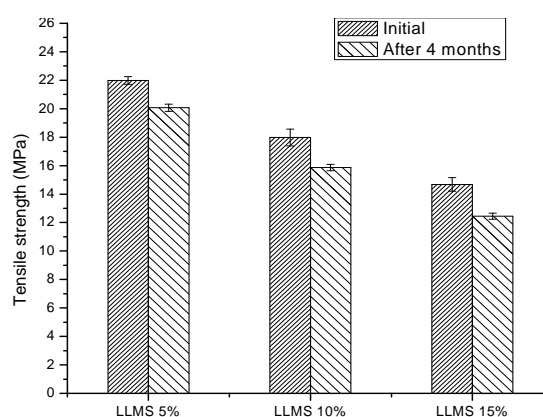
previous section of this chapter, it appears that the microorganisms could attack the plastic strips [16]. The extent of biodegradation of the newly prepared blends is lower as compared to the unmodified LLDPE-biofiller blends of similar compositions.

Table 6A.2b Percentage weight loss of LLDPE-g-MA-starch and LLDPE-g-MA-dextrin blends after immersion of plastic strips in shake culture flask for 4 months

Sample	Initial weight (g)	Weight after 4 months (g)	% weight loss
LLDPE	0.1467	0.1465	0.14
LLMS5	0.2619	0.258	1.49
LLMS10	0.2744	0.2677	2.44
LLMS15	0.2828	0.2726	3.61
LLMD5	0.2803	0.2674	4.6
LLMD10	0.3239	0.3023	6.67
LLMD15	0.2858	0.2676	6.37

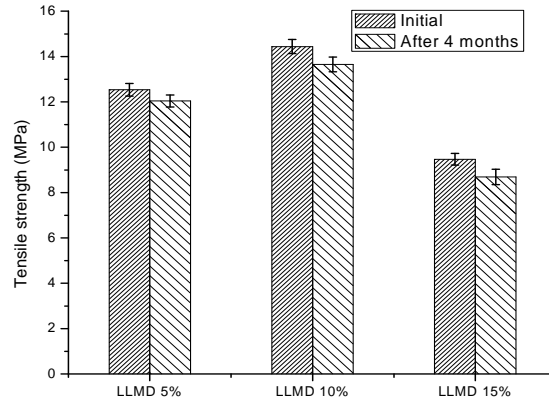
[LLMS5 = LLDPE-g-MA-starch 5%, LLMS10 = LLDPE-g-MA-starch 10%, LLMS15 = LLDPE-g-MA-starch 15%, LLMD5 = LLDPE-g-MA-dextrin 5%, LLMD10 = LLDPE-g-MA-dextrin 10%, LLMD15 = LLDPE-g-MA-dextrin 15%]

6A.1.3.2 Soil burial test



[LLMS5% = LLDPE-g-MA-starch 5%, LLMS10% = LLDPE-g-MA-starch 10%, LLMS15% = LLDPE-g-MA-starch 15%]

Figure 6A.4a Variation of tensile strength after soil burial test for 4 months of LLDPE-g-MA-starch blends



[LLMD5% = LLDPE-g-MA-dextrin 5%, LLMD10% = LLDPE-g-MA-dextrin 10%, LLMD15% = LLDPE-g-MA-dextrin 15%]

Figure 6A.4b Variation of tensile strength after soil burial test for 4 months of LLDPE-g-MA-dextrin blends

The variation of tensile strength of LLDPE-g-MA-starch and LLDPE-g-MA-dextrin blends after soil burial test are shown in figure 6A.4a and 6A.4b. As in the case of biodegradation in shake culture flask, here too the percentage decrease in tensile strength of the newly prepared blends is considerable suggesting that the blends are partially biodegradable.

6A.1.3.3 Scanning electron microscopic analyses

Scanning electron microscopic analysis was used to study the morphology of the surface degradation of LLDPE-g-MA-starch and LLDPE-g-MA-dextrin blends, before and after biodegradability studies in shake culture flask. The photomicrographs were obtained using a JEOL Model JSM - 6390LV scanning electron microscope before and after the biodegradation of the specimens in shake culture flask for 4 months. The specimens were coated with platinum before taking the SEM images.

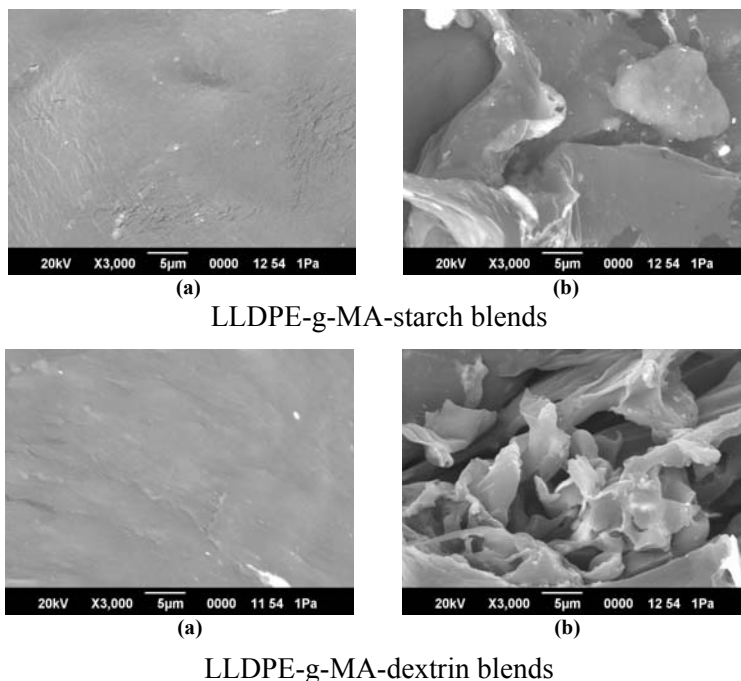


Figure 6A.5 Scanning electron photomicrographs: (a) before biodegradation, (b) after biodegradation in shake culture flask for 4 months

Incorporation of the bio-fillers in unmodified LLDPE results in a two phase morphology indicating that the filler and the polymer are immiscible as discussed in Chapter 3. This observation supports the lower tensile strength shown by the LLDPE-biofiller blends, apparently due to large interfacial tension and low interfacial adhesion [17-19].

The morphology of LLDPE-g-MA-starch and LLDPE-g-MA-dextrin blends before and after biodegradability studies are shown in figure 6A.5. As compared to the SEM photomicrographs of unmodified LLDPE-biofiller blends (Ref. Chapter 3, figures 3.7a, 3.7b, 3.8a and 3.8b), the photomicrographs of the LLDPE-g-MA-

starch and LLDPE-g-MA-dextrin blends show better compatibility between the polymer and the bio-filler. This may be due to the better interaction between the polar bio-filler (starch/dextrin) and the maleated LLDPE [19]. The scanning electron microscopic analyses confirms the results of the differential scanning calorimetry and explains the reason for the reduction in crystallinity in LLDPE-g-MA-starch and LLDPE-g-MA-dextrin blends. The possible interaction between the hydroxyl groups in starch and dextrin with anhydride groups in LLDPE-g-MA is proposed in scheme 6.1.

6A.1.3.4 Infrared spectroscopic analyses

FTIR spectra ($4000\text{-}400\text{ cm}^{-1}$) of LLDPE-g-MA-starch and LLDPE-g-MA-dextrin blends (before and after biodegradability studies in shake culture flask) are shown in figures 6A.6a and 6A.6b.

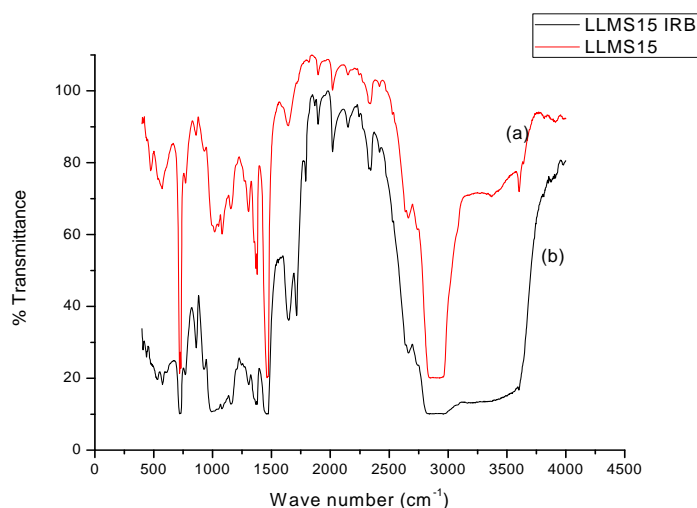


Figure 6A.6a FTIR spectra of LLDPE-g-MA-starch blends (a) before biodegradation (LLMS15), and (b) after biodegradation in shake culture flask for 4 months (LLMS15 IRB)

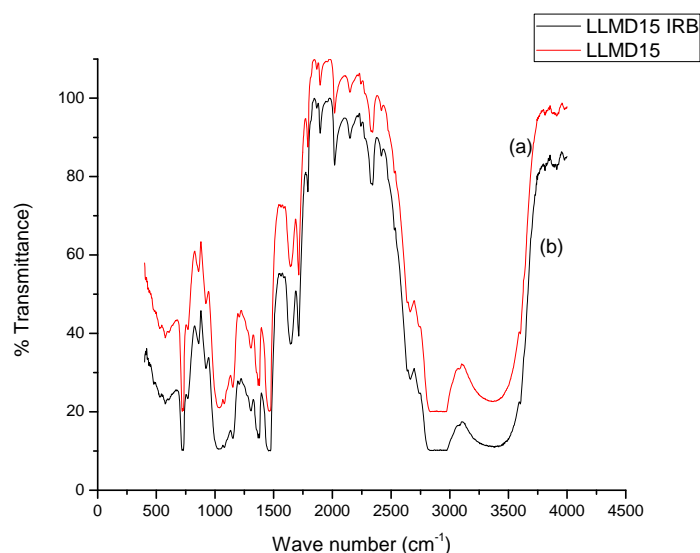


Figure 6A.6b FTIR spectra of LLDPE-g-MA-dextrin blends (a) before biodegradation (LLMD15), and (b) after biodegradation in shake culture flask for 4 months (LLMD15 IRB)

The characteristic peak assignments are shown in table 6A.3. As discussed in Chapter 3 (figure 3.10a and 3.10b), for starch three peaks corresponding to C-O stretching and O-H deformation were observed. For dextrin the peaks obtained correspond to O-H stretching, C-H bending, C-O stretching and O-H deformation. Two peaks at 3317 cm⁻¹ and 999 or 1000 cm⁻¹ were observed which correspond to the O-H stretching vibrations of starch and dextrin [20].

In the case of LLDPE-g-MA-starch and LLDPE-g-MA-dextrin, the characteristic peaks obtained include the peaks in the region 2885-2895cm⁻¹, 1450-1460 cm⁻¹, and 719 cm⁻¹ corresponding to C-H stretching, C-H bending and CH₂ skeletal vibration respectively.

Table 6A.3 Data obtained from FTIR spectra of LLDPE-g-MA-starch and LLDPE-g-MA-dextrin blends after biodegradation in shake culture flask

	Peak position (cm ⁻¹)	Characteristic group
LLDPE-g-MA-starch	2886	C-H stretching
	1454	C-H bending
	719	Skeletal vibration of CH ₂
LLDPE-g-MA-dextrin	2894	C-H stretching
	1455	C-H bending
	719	Skeletal vibration of CH ₂

Comparison of spectra of LLDPE-g-MA-starch and LLDPE-g-MA-dextrin, before and after biodegradation in shake culture flask for 4 months, shows notable differences in intensities at 2886 cm⁻¹ (C-H stretching), 1454 cm⁻¹ (C-H bending), and 719 cm⁻¹ (Skeletal vibration of CH₂). These differences in peak intensities at 2886 cm⁻¹, 1454 cm⁻¹ and 719 cm⁻¹ reveal the removal of bio-fillers and LLDPE from the blends. The infrared spectroscopic studies provide evidence for the biodegradation of the LLDPE-g-MA-starch and LLDPE-g-MA-dextrin blends after the biodegradation in shake culture flask for 4 months.

6A.1.4 Water absorption studies

Table 6A.4 Water absorption of LLDPE-g-MA-starch and LLDPE-g-MA-dextrin blends

Sample	Initial weight (g)	Weight after 8 weeks (g)	% Water absorption
LLDPE	0.0394	0.0395	0.25
LLDPE-g-MA-S300 5%	0.1618	0.1654	2.22
LLDPE-g-MA-S300 10%	0.0422	0.0432	2.4
LLDPE-g-MA-S300 15%	0.0463	0.0476	2.81
LLDPE-g-MA-D300 5%	0.0695	0.0703	1.15
LLDPE-g-MA-D300 10%	0.1271	0.1289	1.41
LLDPE-g-MA-D300 15%	0.0694	0.0721	3.89

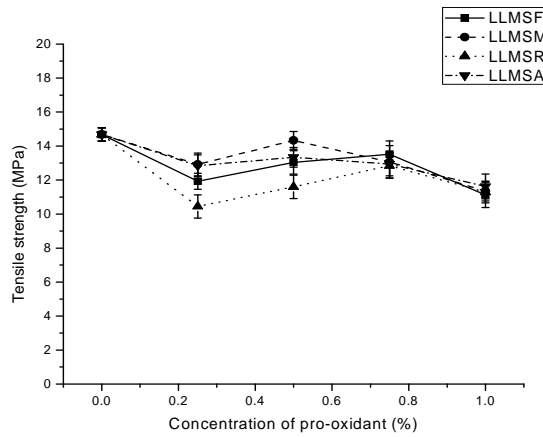
The uptake of water by LLDPE-g-MA-starch and LLDPE-g-MA-dextrin blends were determined according to ASTM D-570 [21]. Table 6A.4 shows the percentage water absorption of the blends and the neat LLDPE. The uptake of water by neat LLDPE was 0.25 % whereas for blends an enhancement in water uptake was observed. As the concentration of the bio-filler increased, the water absorption also increased. However, as compared to the unmodified LLDPE-biofiller blends, the compatibilised (maleated LLDPE) blends showed decreased tendency for water uptake. This observation is in agreement with the lower extent of biodegradation of the maleated blends in shake culture flask.

Part B

PHOTODEGRADABILITY OF THE COMPATIBILISED BLENDS

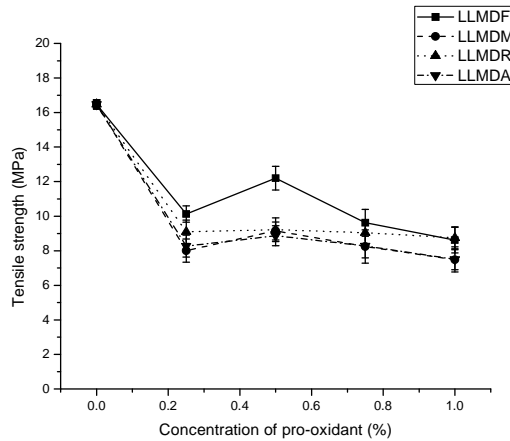
6B.1 Results and Discussion

6B.1.1 Mechanical properties



[LLMSF = LLDPE-g-MA-starch-Fe₂O₃, LLMSM = LLDPE-g-MA-starch-MnO₂, LLMSR= LLDPE-g-MA-starch-TiO₂ (rutile), LLMSA = LLDPE-g-MA-starch-TiO₂ (anatase)]

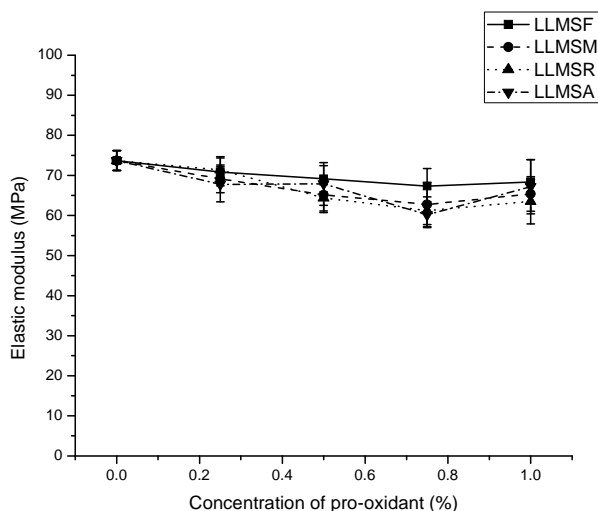
Figure 6B.1a Variation of tensile strength with concentration of pro-oxidants in LLDPE-g-MA-starch blends



[LLMDF = LLDPE-g-MA-dextrin-Fe₂O₃, LLMDM = LLDPE-g-MA-dextrin-MnO₂, LLMDR= LLDPE-g-MA-dextrin-TiO₂ (rutile), LLMDA = LLDPE-g-MA-dextrin-TiO₂ (anatase)]

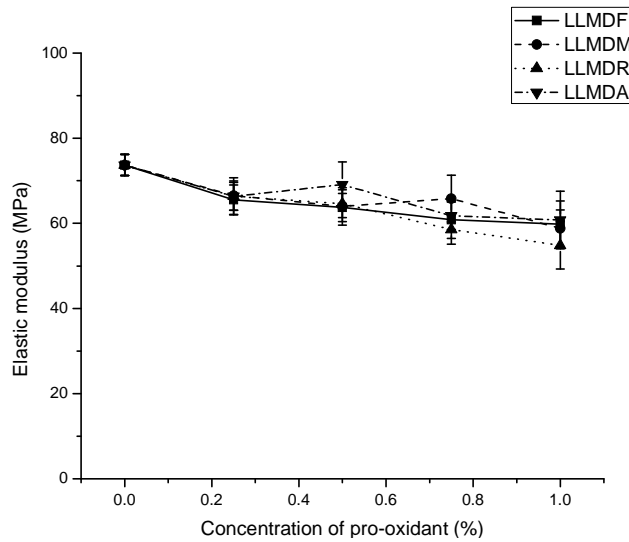
Figure 6B.1b Variation of tensile strength with concentration of pro-oxidants in LLDPE-g-MA-dextrin blends

The effect of pro-oxidants (metal oxides) on the tensile strength of LLDPE-g-MA-starch and LLDPE-g-MA-dextrin blends are shown in figures 6B.1a and 6B.1b. For all the compositions, the tensile strength decreased on addition of pro-oxidants. For LLDPE-g-MA-starch-Fe₂O₃ and LLDPE-g-MA-starch-rutile blends, the maximum tensile strength was obtained for the composition containing 0.75% of metal oxide. For LLDPE-g-MA-starch-MnO₂ and LLDPE-g-MA-starch-anatase blends, the maximum tensile strength was observed for the composition containing 0.5% of metal oxide. But for LLDPE-g-MA-dextrin-metal oxide blends the maximum tensile strength was obtained for the composition containing 0.5% of metal oxide, in all the cases. Further addition of metal oxides reduced the tensile strength of the blends.



[LLMSF = LLDPE-g-MA-starch-Fe₂O₃, LLMSM = LLDPE-g-MA-starch-MnO₂, LLMSR = LLDPE-g-MA-starch-TiO₂ (rutile), LLMSA = LLDPE-g-MA-starch-TiO₂ (anatase)]

Figure 6B.1c Variation of elastic modulus with concentration of pro-oxidants in LLDPE-g-MA-starch blends



[LLMDf = LLDPE-g-MA-dextrin-Fe₂O₃, LLMDM = LLDPE-g-MA-dextrin-MnO₂, LLMDR = LLDPE-g-MA-dextrin-TiO₂ (rutile), LLMDA = LLDPE-g-MA-dextrin-TiO₂ (anatase)]

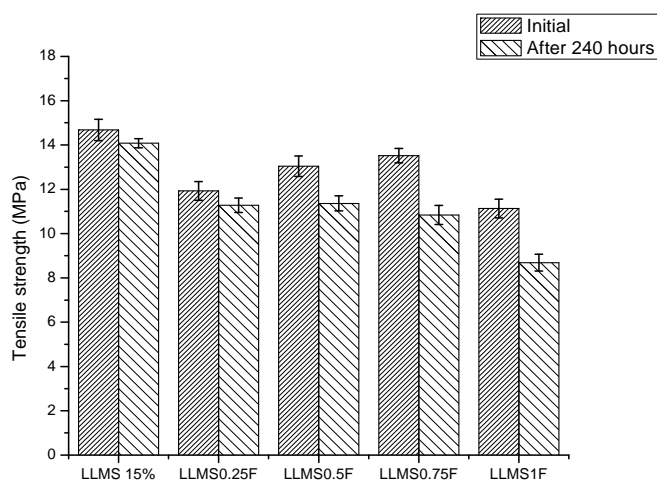
Figure 6B.1d Variation of elastic modulus with concentration of pro-oxidants in LLDPE-g-MA-dextrin blends

The variation in elastic modulus of LLDPE-g-MA-starch-prooxidant and LLDPE-g-MA-dextrin-prooxidant are shown in figures 6B.1c and 6B.1d. The elastic modulus of the blends showed a decreasing tendency on incorporation of metal oxide to the compatibilised blends.

In general, the starch and dextrin containing hydroxyl groups on their surface are hydrophilic, whereas LLDPE is non-polar and therefore hydrophobic. Therefore, the strong interfacial bonds such as hydrogen bonds between starch/dextrin and LLDPE are not formed. This may be the reason for the lower mechanical properties of the unmodified LLDPE-biofiller blends. However, the blends of maleated LLDPE with bio-fillers showed improved mechanical properties. In

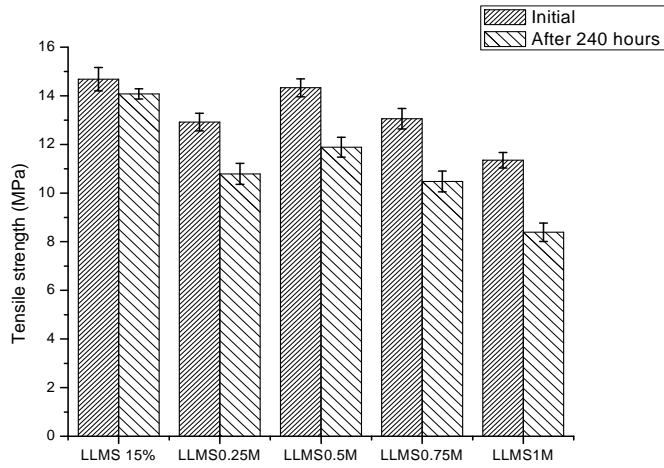
the presence of DCP, the introduction of maleic anhydride into the LLDPE-biofiller blends, at elevated temperature during mixing, is believed to strengthen the interfacial adhesion between LLDPE and bio-fillers. The addition of metal oxide to LLDPE-g-MA-starch and LLDPE-g-MA-dextrin matrix decreased the tensile strength and elastic modulus of the blends. This may be due to less interfacial adhesion of metal oxide to the matrix. The reduction in tensile strength of the blends on incorporation of the pro-oxidants suggests that the addition of pro-oxidants doesn't reinforce LLDPE-g-MA-starch and LLDPE-g-MA-dextrin blends.

6B.1.2 Photodegradability studies



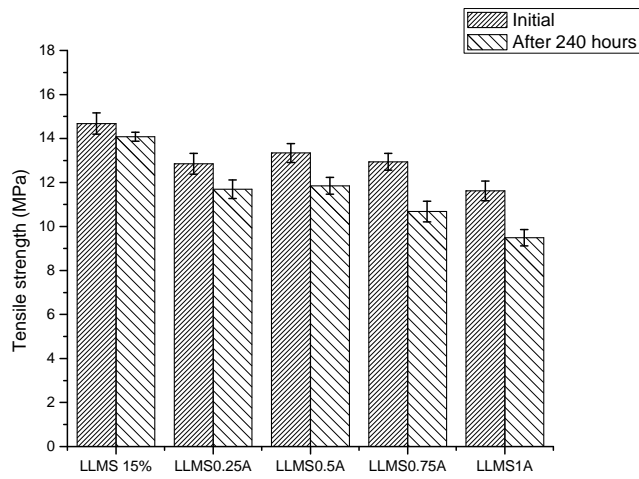
[LLMS15% = LLDPE-g-MA-15%starch, LLMS0.25F = LLDPE-g-MA-starch-0.25%Fe₂O₃, LLMS0.5F = LLDPE-g-MA-starch-0.5%Fe₂O₃, LLMS0.75F = LLDPE-g-MA-starch-0.75%Fe₂O₃, LLMS1F = LLDPE-g-MA-starch-1%Fe₂O₃]

Figure 6B.2a Variation in tensile strength of LLDPE-g-MA-starch-Fe₂O₃ blends after UV irradiation for 240 hours



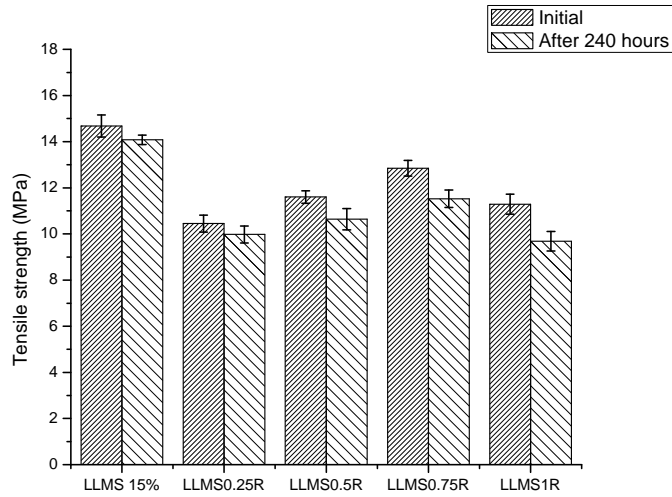
[LLMS15% = LLDPE-g-MA-15%starch, LLMS0.25M = LLDPE-g-MA-starch-0.25%MnO₂, LLMS0.5M = LLDPE-g-MA-starch-0.5%MnO₂, LLMS0.75M = LLDPE-g-MA-starch-0.75%MnO₂, LLMS1M = LLDPE-g-MA-starch-1%MnO₂]

Figure 6B.2b Variation in tensile strength of LLDPE-g-MA-starch-MnO₂ blends after UV irradiation for 240 hours



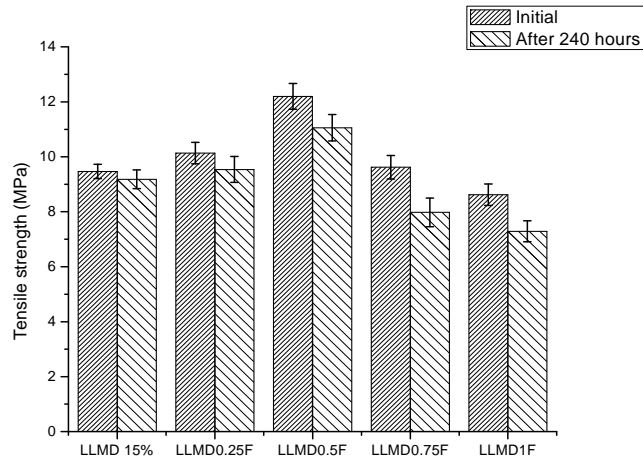
[LLMS15% = LLDPE-g-MA-15%starch, LLMS0.25A = LLDPE-g-MA-starch-0.25%TiO₂(anatase), LLMS0.5A = LLDPE-g-MA-starch-0.5%TiO₂(anatase), LLMS0.75A = LLDPE-g-MA-starch-0.75%TiO₂(anatase), LLMS1A = LLDPE-g-MA-starch-1% TiO₂(anatase)]

Figure 6B.2c Variation in tensile strength of LLDPE-g-MA-starch-TiO₂(anatase) blends after UV irradiation for 240 hours



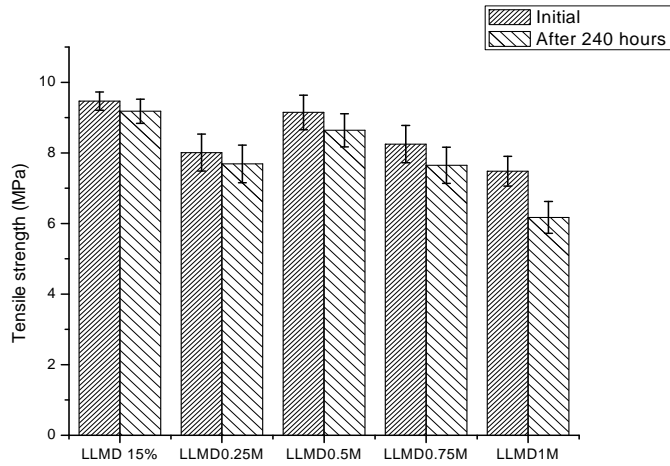
[LLMS15% = LLDPE-g-MA-15%starch, LLMS0.25R = LLDPE-g-MA-starch-0.25%TiO₂(rutile), LLMS0.5R = LLDPE-g-MA-starch-0.5%TiO₂(rutile), LLMS0.75R = LLDPE-g-MA-starch-0.75%TiO₂(rutile), LLMS1R= LLDPE-g-MA-starch-1% TiO₂(rutile)]

Figure 6B.2d Variation in tensile strength of LLDPE-g-MA-starch-TiO₂(rutile) blends after UV irradiation for 240 hours



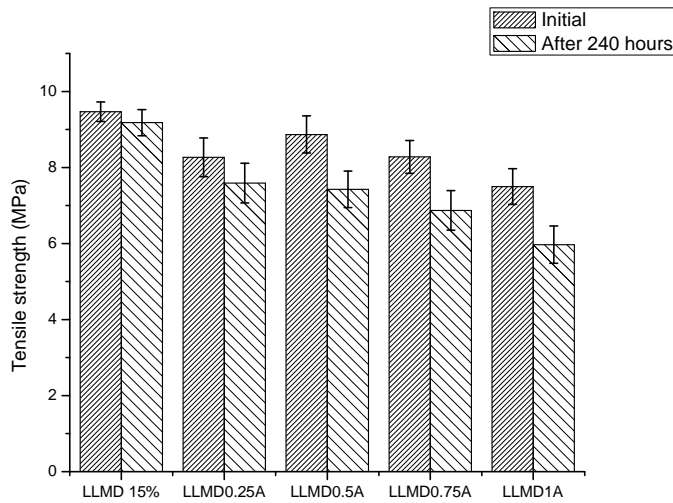
[LLMD15% = LLDPE-g-MA-15%dextrin, LLMD0.25F = LLDPE-g-MA-dextrin-0.25%Fe₂O₃, LLMD0.5F = LLDPE-g-MA-dextrin-0.5%Fe₂O₃, LLMD0.75F = LLDPE-g-MA-dextrin-0.75%Fe₂O₃, LLMD1F = LLDPE-g-MA-dextrin-1%Fe₂O₃]

Figure 6B.2e Variation in tensile strength of LLDPE-g-MA-dextrin-Fe₂O₃ blends after UV irradiation for 240 hours



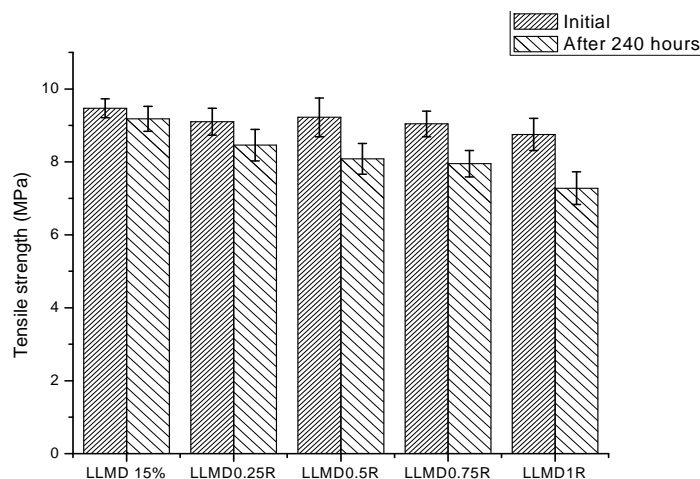
[LLMD15% = LLDPE-g-MA-15%dextrin, LLMD0.25M = LLDPE-g-MA-dextrin-0.25%MnO₂, LLMD0.5M = LLDPE-g-MA-dextrin-0.5%MnO₂, LLMD0.75M = LLDPE-g-MA-dextrin-0.75%MnO₂, LLMD1M = LLDPE-g-MA-dextrin-1%MnO₂]

Figure 6B.2f Variation in tensile strength of LLDPE-g-MA-dextrin-MnO₂ blends after UV irradiation for 240 hours



[LLMD15% = LLDPE-g-MA-15%dextrin, LLMD0.25A = LLDPE-g-MA-dextrin-0.25%TiO₂(anatase), LLMD0.5A = LLDPE-g-MA-dextrin-0.5%TiO₂(anatase), LLMD0.75A = LLDPE-g-MA-dextrin-0.75%TiO₂(anatase), LLMD1A = LLDPE-g-MA-dextrin-1% TiO₂(anatase)]

Figure 6B.2g Variation in tensile strength of LLDPE-g-MA-dextrin-TiO₂ (anatase) blends after UV irradiation for 240 hours



[LLMD15% = LLDPE-g-MA-15%dextrin, LLMD0.25R = LLDPE-g-MA-dextrin-0.25%TiO₂(rutile), LLMD0.5R = LLDPE-g-MA-dextrin-0.5%TiO₂(rutile), LLMD0.75R = LLDPE-g-MA-dextrin-0.75%TiO₂(rutile), LLMD1R= LLDPE-g-MA-dextrin-1% TiO₂(rutile)]

Figure 6B.2h Variation in tensile strength of LLDPE-g-MA-dextrin-TiO₂ (rutile) blends after UV irradiation for 240 hours

The variation of tensile strength after exposing the samples to ultraviolet radiation for 240 hours are shown in figures 6B.2a, 6B.2b, 6B.2c, 6B.2d, 6B.2e, 6B.2f, 6B.2g and 6B.2h. After UV exposure the tensile strengths of the blends decreased considerably. The decrease in mechanical properties is a significant tool for determining the extent of degradation of the blends. The presence of metal oxide in the blends may be functioning as pro-oxidant which enhances the photodegradation of LLDPE by generating free radicals when exposed to ultraviolet light. Several metal complexes, dithiocarbamates and metal oxides have been reported to be capable of functioning both as compatibilizers and also as autoxidants [22].

The mechanism of the transition metal-catalyzed degradation of LLDPE has been described in the literature as a free radical chain

mechanism proceeding from the formation of hydroperoxides along the polymer back bone through reaction of the polymer with molecular oxygen [23-25]. According to Albertsson [22], in presence of a metal catalyst, these peroxides readily decompose to form reactive intermediates. The catalytic activity of the metal was reported to correlate with the redox potential of the metal and requires several oxidation states of comparable energy for the metal. The peroxide decomposition products react further to yield volatile low molecular weight fragments. The percentage decrease in tensile strength of the blends containing 1% of the pro-oxidants are shown in table 6B.1.

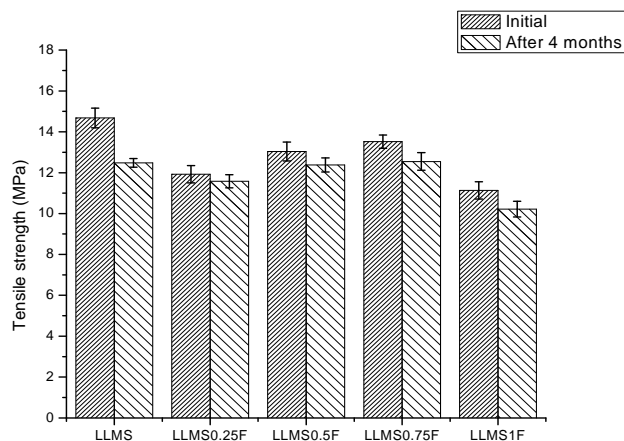
Table 6B.1 Percentage decrease in tensile strength of LLDPE-g-MA-starch/dextrin-prooxidant (1%) blends after UV irradiation for 240 hours

Composition	Initial tensile strength (MPa)	Tensile strength after 240 hours (MPa)	% decrease in tensile strength
LLMS15	14.68	14.08	4.09
LLMD15	9.47	9.18	3.06
LLMS1F	11.13	8.69	21.92
LLMS1M	11.35	8.39	26.08
LLMS1A	11.62	9.49	18.33
LLMS1R	11.29	9.69	14.17
LLMD1F	8.62	7.29	15.43
LLMD1M	7.48	6.17	17.51
LLMD1A	7.5	5.97	20.4
LLMD1R	8.75	7.28	16.8

[LLMS15 = LLDPE-g-MA-15%starch, LLMD15 = LLDPE-g-MA-15%dextrin, LLMS1F = LLDPE-g-MA-starch-1% Fe₂O₃, LLMS1M = LLDPE-g-MA-starch-1% MnO₂, LLMS1A = LLDPE-g-MA-starch-1% TiO₂(anatase), LLMS1R = LLDPE-g-MA-starch-1% TiO₂(rutile), LLMD1F = LLDPE-g-MA-dextrin-1% Fe₂O₃, LLMD1M = LLDPE-g-MA-dextrin-1% MnO₂, LLMD1A = LLDPE-g-MA-dextrin-1% TiO₂(anatase), LLMD1R = LLDPE-g-MA-dextrin-1% TiO₂(rutile)]

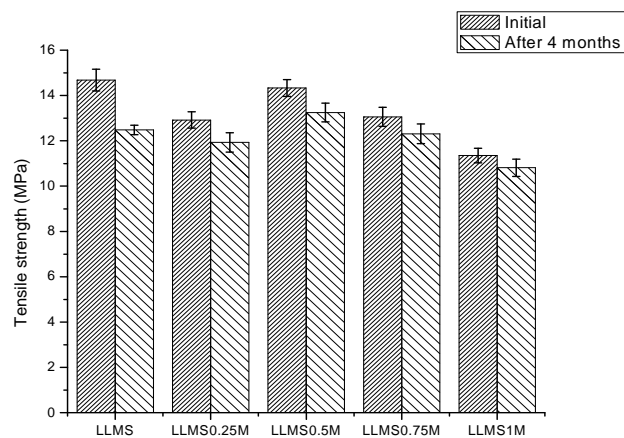
6B.1.3 Biodegradation studies

6B.1.3.1 In shake culture flask



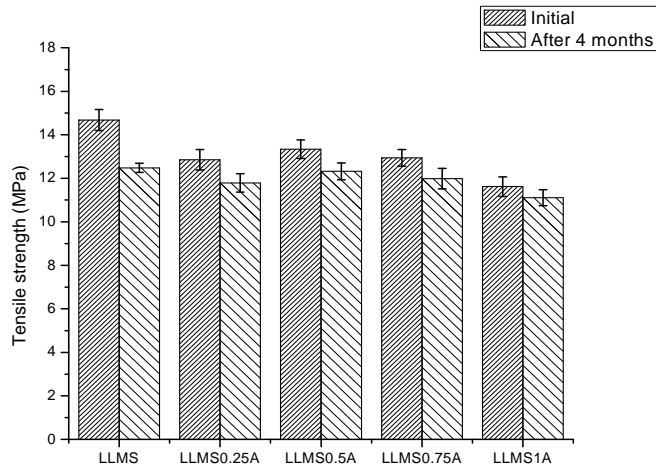
[LLMS = LLDPE-g-MA-15%starch, LLMS0.25F = LLDPE-g-MA-starch-0.25%Fe₂O₃, LLMS0.5F = LLDPE-g-MA-starch-0.5%Fe₂O₃, LLMS0.75F = LLDPE-g-MA-starch-0.75%Fe₂O₃, LLMS1F = LLDPE-g-MA-starch-1%Fe₂O₃]

Figure 6B.3a Variation in tensile strength of LLDPE-g-MA-starch-Fe₂O₃ blends after immersion of plastic strips in shake culture flask for 4 months



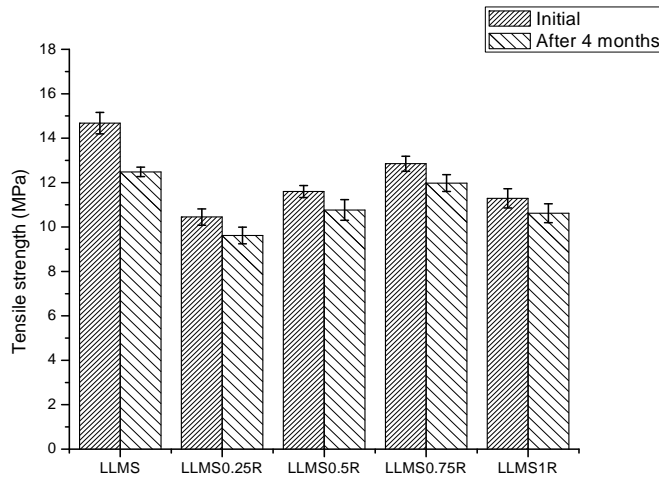
[LLMS = LLDPE-g-MA-15%starch, LLMS0.25M = LLDPE-g-MA-starch-0.25%MnO₂, LLMS0.5M = LLDPE-g-MA-starch-0.5%MnO₂, LLMS0.75M = LLDPE-g-MA-starch-0.75%MnO₂, LLMS1M = LLDPE-g-MA-starch-1%MnO₂]

Figure 6B.3b Variation in tensile strength of LLDPE-g-MA-starch-MnO₂ blends after immersion of plastic strips in shake culture flask for 4 months



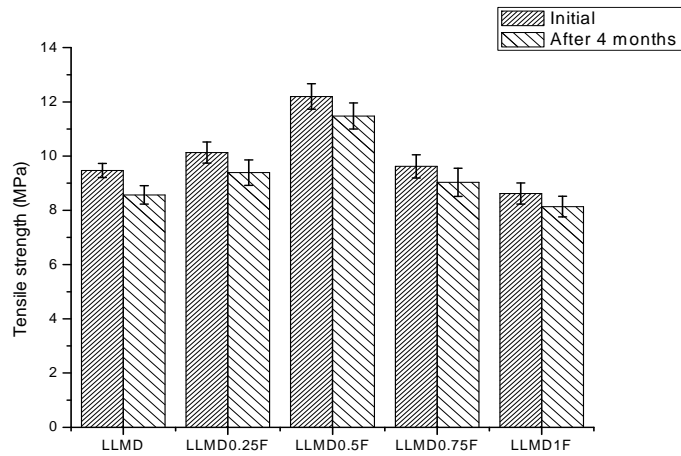
[LLMS = LLDPE-g-MA-15%starch, LLMS0.25A = LLDPE-g-MA-starch-0.25%TiO₂(anatase), LLMS0.5A = LLDPE-g-MA-starch-0.5%TiO₂(anatase), LLMS0.75A = LLDPE-g-MA-starch-0.75%TiO₂(anatase), LLMS1A = LLDPE-g-MA-starch-1% TiO₂(anatase)]

Figure 6B.3c Variation in tensile strength of LLDPE-g-MA-starch-TiO₂(anatase) blends after immersion of plastic strips in shake culture flask for 4 months



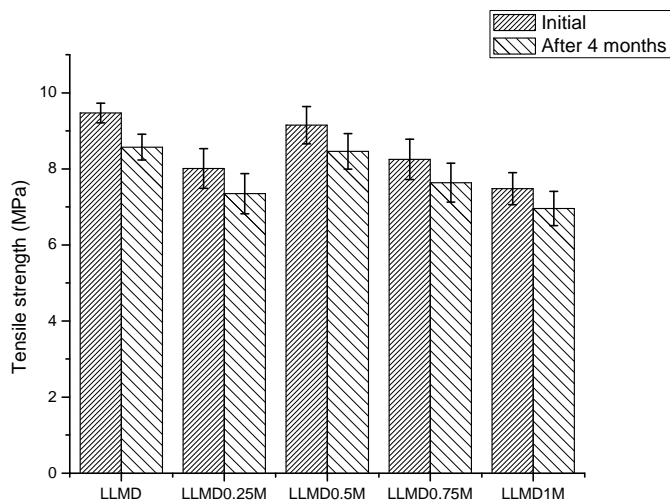
[LLMS = LLDPE-g-MA-15%starch, LLMS0.25R = LLDPE-g-MA-starch-0.25%TiO₂(rutile), LLMS0.5R = LLDPE-g-MA-starch-0.5%TiO₂(rutile), LLMS0.75R = LLDPE-g-MA-starch-0.75%TiO₂(rutile), LLMS1R = LLDPE-g-MA-starch-1% TiO₂(rutile)]

Figure 6B.3d Variation in tensile strength of LLDPE-g-MA-starch-TiO₂(rutile) blends after immersion of plastic strips in shake culture flask for 4 months



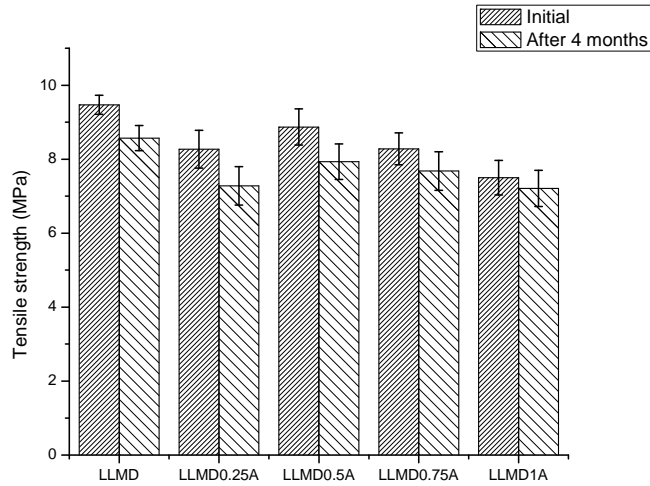
[LLMD = LLDPE-g-MA-15%dextrin, LLMD0.25F = LLDPE-g-MA-dextrin-0.25%Fe₂O₃, LLMD0.5F = LLDPE-g-MA-dextrin-0.5%Fe₂O₃, LLMD0.75F = LLDPE-g-MA-dextrin-0.75%Fe₂O₃, LLMD1F = LLDPE-g-MA-dextrin-1%Fe₂O₃]

Figure 6B.3e Variation in tensile strength of LLDPE-g-MA-dextrin-Fe₂O₃ blends after immersion of plastic strips in shake culture flask for 4 months



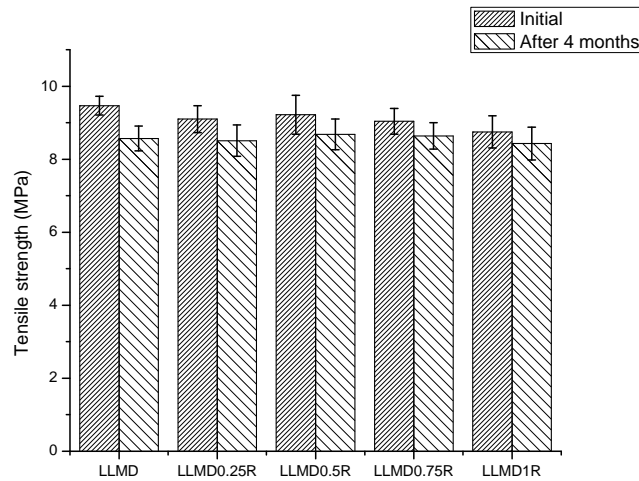
[LLMD = LLDPE-g-MA-15%dextrin, LLMD0.25M = LLDPE-g-MA-dextrin-0.25%MnO₂, LLMD0.5M = LLDPE-g-MA-dextrin-0.5%MnO₂, LLMD0.75M = LLDPE-g-MA-dextrin-0.75%MnO₂, LLMD1M = LLDPE-g-MA-dextrin-1%MnO₂]

Figure 6B.3f Variation in tensile strength of LLDPE-g-MA-dextrin-MnO₂ blends after immersion of plastic strips in shake culture flask for 4 months



[LLMD = LLDPE-g-MA-15%dextrin, LLMD0.25A = LLDPE-g-MA-dextrin-0.25%TiO₂(anatase), LLMD0.5A = LLDPE-g-MA-dextrin-0.5%TiO₂(anatase), LLMD0.75A = LLDPE-g-MA-dextrin-0.75%TiO₂(anatase), LLMD1A = LLDPE-g-MA-dextrin-1% TiO₂(anatase)]

Figure 6B.3g Variation in tensile strength of LLDPE-g-MA-dextrin-TiO₂(anatase) blends after immersion of plastic strips in shake culture flask for 4 months



[LLMD = LLDPE-g-MA-15%dextrin, LLMD0.25R = LLDPE-g-MA-dextrin-0.25%TiO₂(rutile), LLMD0.5R = LLDPE-g-MA-dextrin-0.5%TiO₂(rutile), LLMD0.75R = LLDPE-g-MA-dextrin-0.75%TiO₂(rutile), LLMD1R = LLDPE-g-MA-dextrin-1% TiO₂(rutile)]

Figure 6B.3h Variation in tensile strength of LLDPE-g-MA-dextrin-TiO₂(rutile) blends after immersion of plastic strips in shake culture flask for 4 months

The figures 6B.3a, 6B.3b, 6B.3c, 6B.3d, 6B.3e, 6B.3f, 6B.3g and 6B.3h show the variation in tensile strength of LLDPE-g-MA-starch-prooxidant blends and LLDPE-g-MA-dextrin-prooxidant blends after immersing the strips in shake culture flask containing amylase producing vibrios, which were isolated from marine benthic environment, for 4 months [26-28]. After 4 months of immersion, the strips were retrieved and the tensile strength measurements were carried out for determining the extent of biodegradation. There is significant variation in tensile strength of the samples indicating higher degree of biodegradation. The decrease in tensile strength of the blends may be due to the mechanical damage of LLDPE macrochain caused by swelling and bursting of the growing cells of the invading micro-organisms or micro-organisms in the shake culture flask [29].

Tables 6B.2a and 6B.2b show the percentage loss in tensile strength and percentage loss of weight of LLDPE-g-MA-starch-prooxidant (1%) blends and LLDPE-g-MA-dextrin-prooxidant (1%) blends after biodegradability test in shake culture flask for 4 months. The tensile strength of these blends decreased after immersing the samples in shake culture flask for 4 months. The samples show considerable loss of weight too. The results show that the maleated LLDPE-biofiller blends undergo biodegradation in presence of pro-oxidants.

Table 6B.2a Variation in tensile strength of LLDPE-g-MA-starch /dextrin-prooxidant (1%) blends after immersion of plastic strips in shake culture flask for 4 months

Composition	Initial tensile strength (MPa)	Tensile strength after 4 months (MPa)	% decrease in tensile strength
LLMS15	13.68	12.48	8.77
LLMD15	9.47	8.57	9.5
LLMS1F	12.04	11.38	5.48
LLMS1M	11.35	10.81	4.76
LLMS1A	11.62	11.11	4.39
LLMS1R	11.29	10.62	5.93
LLMD1F	8.62	8.14	5.57
LLMD1M	7.48	6.96	6.95
LLMD1A	7.5	7.21	3.87
LLMD1R	8.75	8.43	3.66

[LLMS15 = LLDPE-g-MA-15%starch, LLMD15 = LLDPE-g-MA-15%dextrin, LLMS1F = LLDPE-g-MA-starch-1% Fe₂O₃, LLMS1M = LLDPE-g-MA-starch-1% MnO₂, LLMS1A = LLDPE-g-MA-starch-1% TiO₂(anatase), LLMS1R = LLDPE-g-MA-starch-1% TiO₂(rutile), LLMD1F = LLDPE-g-MA-dextrin-1% Fe₂O₃, LLMD1M = LLDPE-g-MA-dextrin-1% MnO₂, LLMD1A = LLDPE-g-MA-dextrin-1% TiO₂(anatase), LLMD1R = LLDPE-g-MA-dextrin-1% TiO₂(rutile)]

Table 6B.2b Percentage weight loss of LLDPE-g-MA-starch/dextrin-prooxidant (1%) blends after immersion of plastic strips in shake culture flask for 4 months

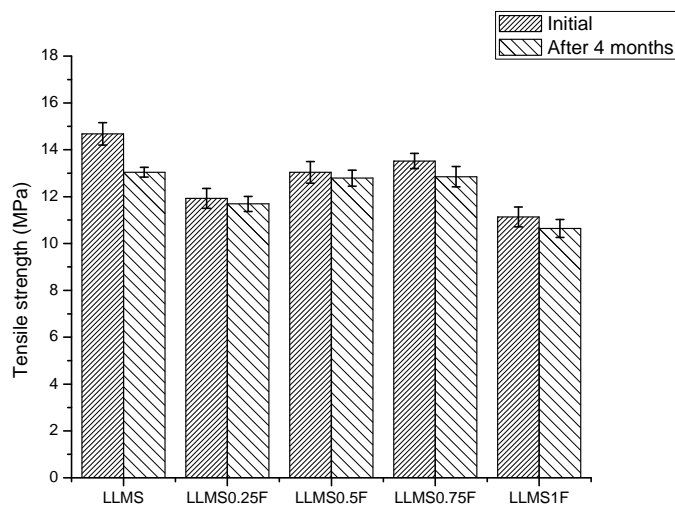
Sample	Initial weight (g)	Weight after 4 months (g)	% weight loss
LLMS15	0.2798	0.2601	7.04
LLMD15	0.3452	0.3202	7.24
LLMS1F	0.3964	0.3589	9.46
LLMS1M	0.2634	0.2553	3.08
LLMS1A	0.4031	0.3916	2.85
LLMS1R	0.3153	0.3079	2.35
LLMD1F	0.2448	0.2326	4.98
LLMD1M	0.3388	0.3282	3.13
LLMD1A	0.2743	0.2611	4.81
LLMD1R	0.2001	0.1868	6.65

[LLMS15 = LLDPE-g-MA-15%starch, LLMD15 = LLDPE-g-MA-15%dextrin, LLMS1F = LLDPE-g-MA-starch-1% Fe₂O₃, LLMS1M = LLDPE-g-MA-starch-1% MnO₂, LLMS1A = LLDPE-g-MA-starch-1% TiO₂(anatase), LLMS1R = LLDPE-g-MA-starch-1% TiO₂(rutile), LLMD1F = LLDPE-g-MA-dextrin-1% Fe₂O₃, LLMD1M = LLDPE-g-MA-dextrin-1% MnO₂, LLMD1A = LLDPE-g-MA-dextrin-1% TiO₂(anatase), LLMD1R = LLDPE-g-MA-dextrin-1% TiO₂(rutile)]

6B.1.3.2 Soil burial test

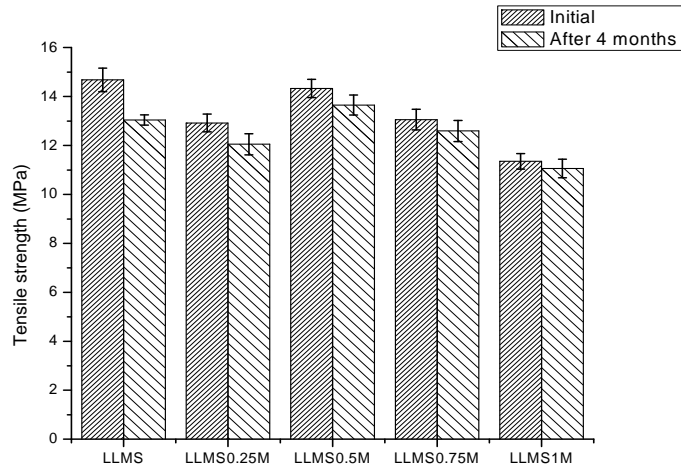
Soil burial is probably the most appropriate test to determine the biodegradability of plastic-biofiller blends. Under suitable conditions, microorganisms in the soil can remove the bio-fillers embedded in the polymer matrix by enzymatic action.

Figures 6B.4a, 6B.4b, 6B.4c, 6B.4d, 6B.4e, 6B.4f, 6B.4g and 6B.4h show the loss in tensile strength of LLDPE-g-MA-starch-prooxidant and LLDPE-g-MA-dextrin-prooxidant blends after burial in soil for 4 months. After 4 months of soil burial, all the compositions showed drop in tensile strength. This suggests that the blends are partially biodegradable.



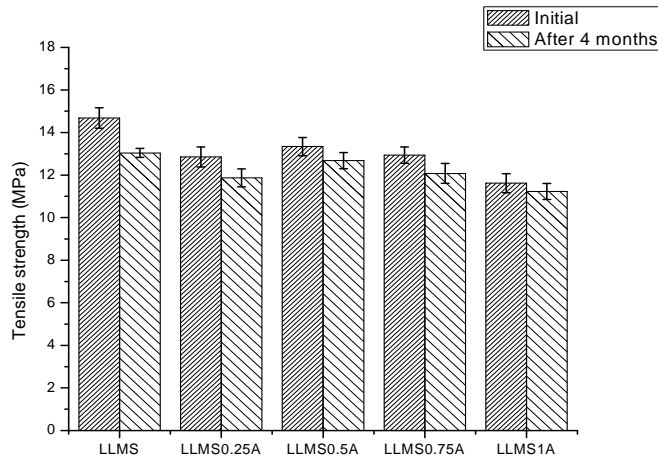
[LLMS = LLDPE-g-MA-15%starch, LLMS0.25F = LLDPE-g-MA-starch-0.25%Fe₂O₃, LLMS0.5F = LLDPE-g-MA-starch-0.5%Fe₂O₃, LLMS0.75F = LLDPE-g-MA-starch-0.75%Fe₂O₃, LLMS1F = LLDPE-g-MA-starch-1%Fe₂O₃]

Figure 6B.4a Variation in tensile strength of LLDPE-g-MA-starch-Fe₂O₃ blends after soil burial test for 4 months



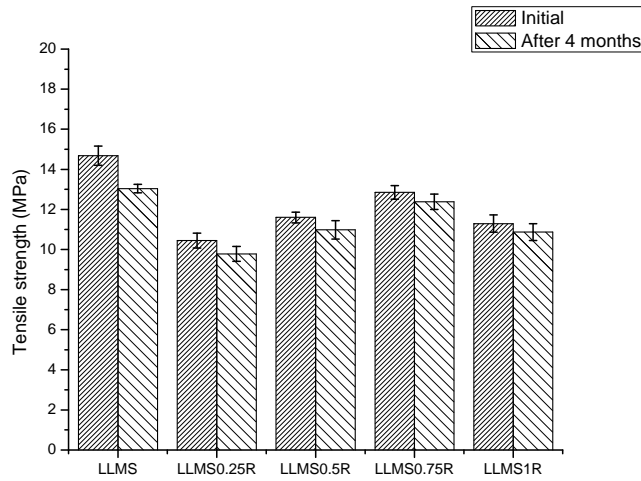
[LLMS = LLDPE-g-MA-15%starch, LLMS0.25M = LLDPE-g-MA-starch-0.25%MnO₂, LLMS0.5M = LLDPE-g-MA-starch-0.5%MnO₂, LLMS0.75M = LLDPE-g-MA-starch-0.75%MnO₂, LLMS1M = LLDPE-g-MA-starch-1%MnO₂]

Figure 6B.4b Variation in tensile strength of LLDPE-g-MA-starch-MnO₂ blends after soil burial test for 4 months



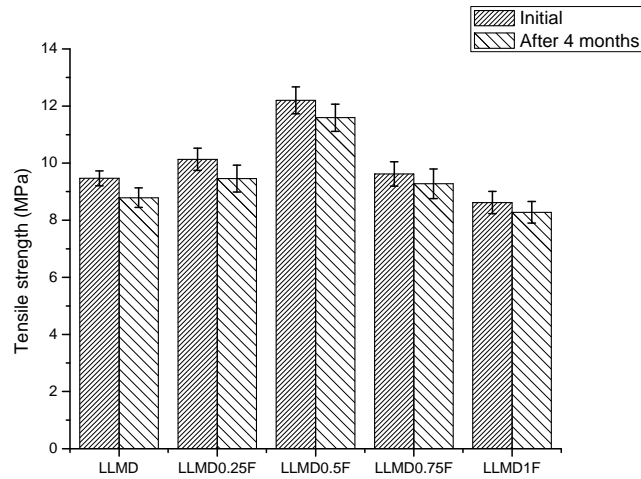
[LLMS = LLDPE-g-MA-15%starch, LLMS0.25A = LLDPE-g-MA-starch-0.25%TiO₂(anatase), LLMS0.5A = LLDPE-g-MA-starch-0.5%TiO₂(anatase), LLMS0.75A = LLDPE-g-MA-starch-0.75%TiO₂(anatase), LLMS1A = LLDPE-g-MA-starch-1% TiO₂(anatase)]

Figure 6B.4c Variation in tensile strength of LLDPE-g-MA-starch-TiO₂(anatase) blends after soil burial test for 4 months



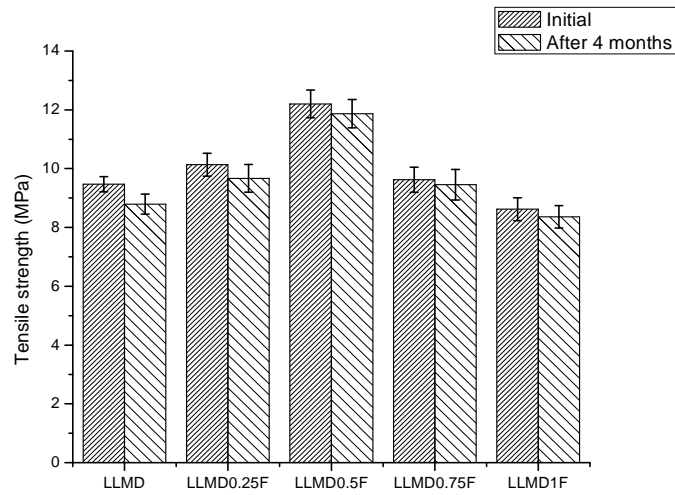
[LLMS = LLDPE-g-MA-15%starch, LLMS0.25R = LLDPE-g-MA-starch-0.25%TiO₂(rutile), LLMS0.5R = LLDPE-g-MA-starch-0.5%TiO₂(rutile), LLMS0.75R = LLDPE-g-MA-starch-0.75%TiO₂(rutile), LLMS1R= LLDPE-g-MA-starch-1% TiO₂(rutile)]

Figure 6B.4d Variation in tensile strength of LLDPE-g-MA-starch-TiO₂(rutile) blends after soil burial test for 4 months



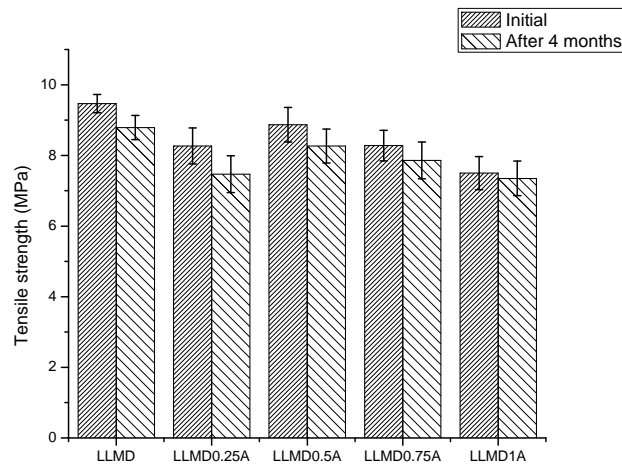
[LLMS = LLDPE-g-MA-15%starch, LLMS0.25F = LLDPE-g-MA-starch-0.25%Fe₂O₃, LLMS0.5F = LLDPE-g-MA-starch-0.5%Fe₂O₃, LLMS0.75F = LLDPE-g-MA-starch-0.75%Fe₂O₃, LLMS1F = LLDPE-g-MA-starch-1%Fe₂O₃]

Figure 6B.4e Variation in tensile strength of LLDPE-g-MA-dextrin-Fe₂O₃ blends after soil burial test for 4 months



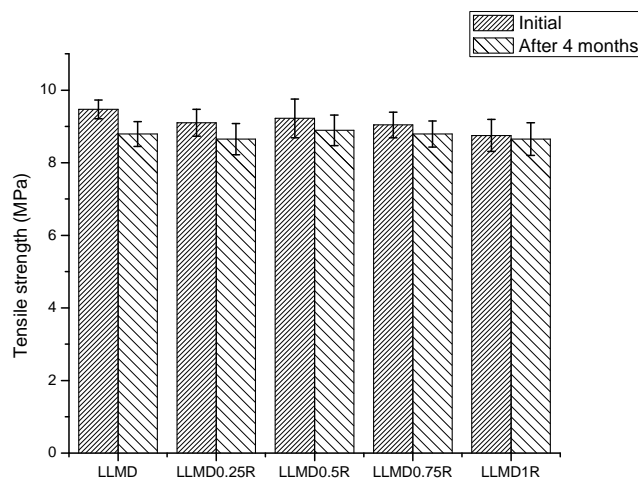
[LLMS = LLDPE-g-MA-15%starch, LLMS0.25M = LLDPE-g-MA-starch-0.25%MnO₂, LLMS0.5M = LLDPE-g-MA-starch-0.5%MnO₂, LLMS0.75M = LLDPE-g-MA-starch-0.75%MnO₂, LLMS1M = LLDPE-g-MA-starch-1%MnO₂]

Figure 6B.4f Variation in tensile strength of LLDPE-g-MA-dextrin-MnO₂ blends after soil burial test for 4 months



[LLMD = LLDPE-g-MA-15%dextrin, LLMD0.25A = LLDPE-g-MA-dextrin-0.25%TiO₂(anatase), LLMD0.5A = LLDPE-g-MA-dextrin-0.5%TiO₂(anatase), LLMD0.75A = LLDPE-g-MA-dextrin-0.75%TiO₂(anatase), LLMD1A = LLDPE-g-MA-dextrin-1% TiO₂(anatase)]

Figure 6B.4g Variation in tensile strength of LLDPE-g-MA-dextrin-TiO₂(anatase) blends after soil burial test for 4 months

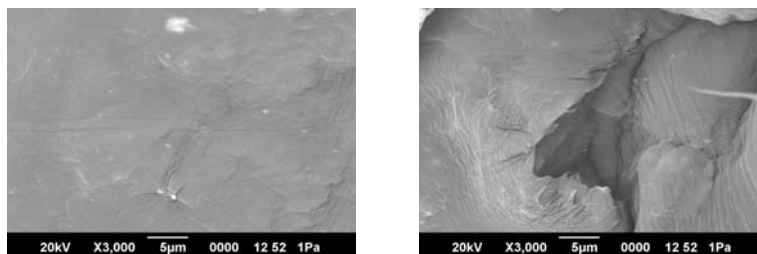


[LLMD = LLDPE-g-MA-15%dextrin, LLMD0.25R = LLDPE-g-MA-dextrin-0.25%TiO₂(rutile), LLMD0.5R = LLDPE-g-MA-dextrin-0.5%TiO₂(rutile), LLMD0.75R = LLDPE-g-MA-dextrin-0.75%TiO₂(rutile), LLMD1R= LLDPE-g-MA-dextrin-1% TiO₂(rutile)]

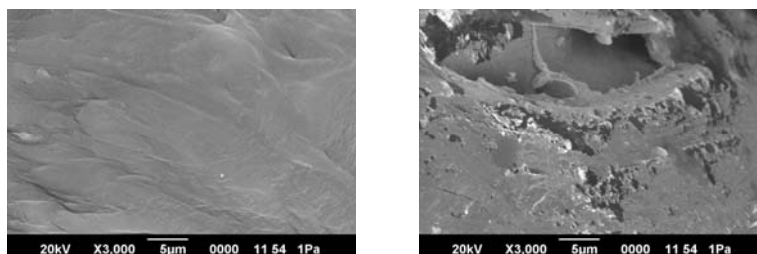
Figure 6B.4h Variation in tensile strength of LLDPE-g-MA-dextrin-TiO₂(rutile) blends after soil burial test for 4 months

6B.1.4 Scanning electron microscopic analyses

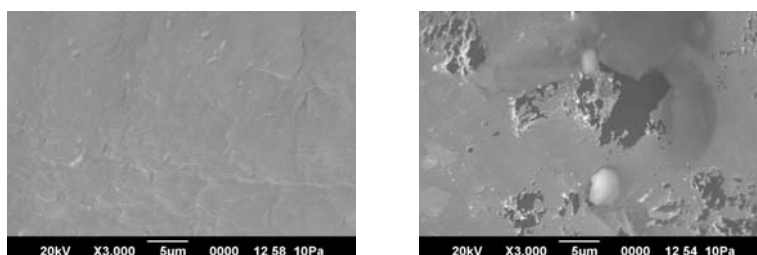
Morphology of the polymer blends plays an important role in the properties of the final product, especially their mechanical properties depend on it. The SEM images of the blends, before and after biodegradation in shake culture flask for 4 months were taken and compared for establishing the extent of biodegradation. The scanning electron images of LLDPE-g-MA-starch/dextrin-prooxidant blends, before and after biodegradation in shake culture flask for 4 months, are shown in figure 6B.5.



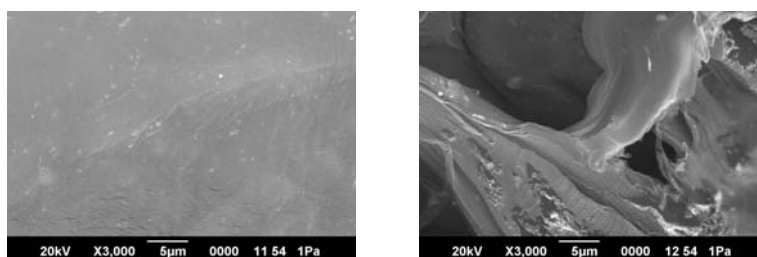
(a) (b)
LLDPE-g-MA-starch-Fe₂O₃ blend



(a) (b)
LLDPE-g-MA-starch-MnO₂ blend



(a) (b)
LLDPE-g-MA-starch-TiO₂(anatase) blend



(a) (b)
LLDPE-g-MA-starch-TiO₂(rutile) blend

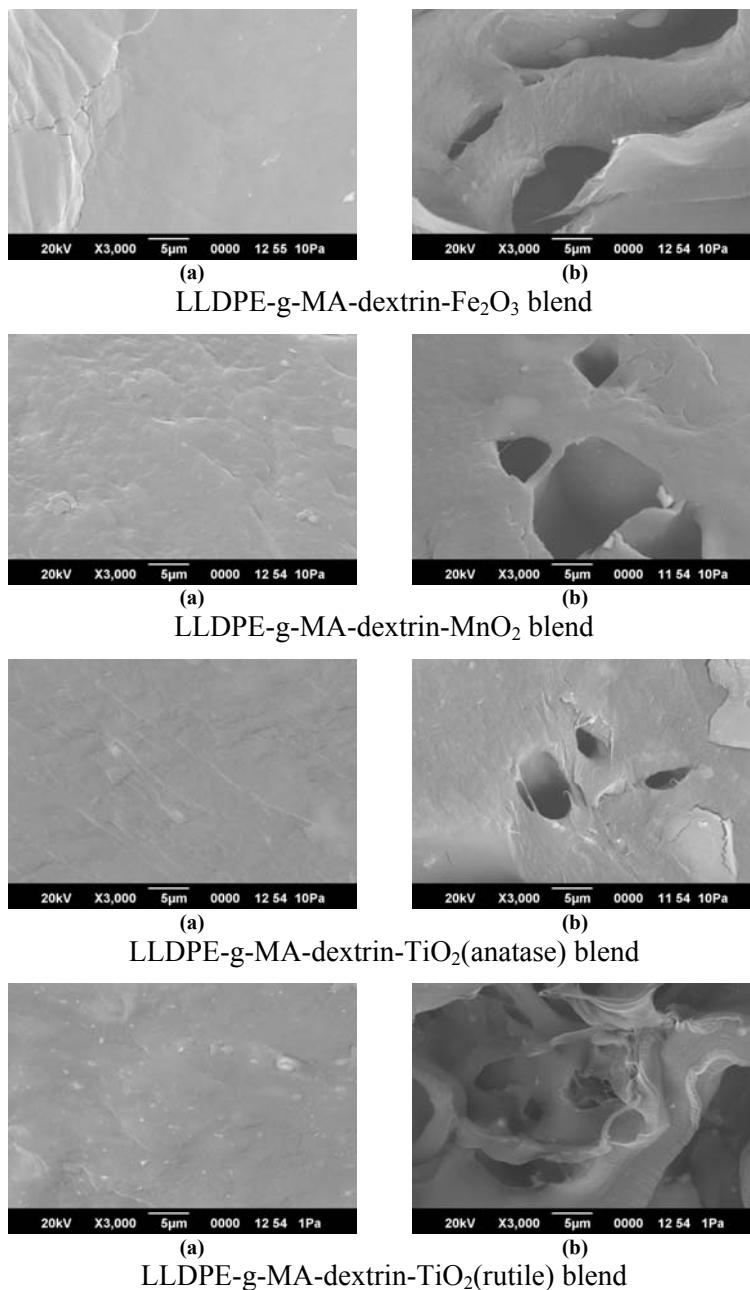


Figure 6B.5 Scanning electron photomicrographs: (a) before biodegradation, (b) after biodegradation in shake culture flask for 4 months

Before biodegradation the images of the samples show uniform phase distribution. There was also no apparent phase separation between the LLDPE and the fillers. The images of the samples after the biodegradation in shake culture flask for 4 months show cavities. The formation of cavities after the biodegradation indicates the removal of bio-fillers from the surface of the blends.

In the case of the samples containing dextrin too, the scanning electron photomicrographs show evidence for biodegradation. It shows that the presence of bio-fillers in the blends favours the microbial accumulation throughout the surface of the samples [30]. The LLDPE acts as the continuous phase and the filler as the dispersed phase. The maleation of LLDPE improves the compatibility between LLDPE and the bio-fillers. From the scanning electron microphotographs, it can be seen that the dispersion of filler particles in the LLDPE matrix is almost uniform. The micro-organism in the shake culture flask are believed to attack the plastic strips as their nutritional source after the bio-fillers are removed from the surface. The pores created as a result of the removal of bio-fillers provides habitat for nurturing the microorganisms and act as channels for the oxygen supply for oxidation.

6.2 Conclusion

The grafting of maleic anhydride on LLDPE improves the compatibility between LLDPE and bio-fillers and improves the mechanical properties of the blends. Addition of pro-oxidants to the compatibilised blends results in the reduction of tensile strength

suggesting that the pro-oxidants do not reinforce the compatibilised blends. The thermogravimetric studies on the compatibilised blends indicate that the thermal stability of LLDPE and the blends are unaltered by compatibilisation. The results of the differential scanning calorimetry show that the percentage crystallinity of LLDPE-g-MA-starch and LLDPE-g-MA-dextrin blends are lower than that of neat LLDPE as a result of grafting. A slight increase in water absorption of the compatibilised blends suggests that the maleic anhydride grafting makes the blends conducive for biodegradation. The results of the photodegradation studies on the pro-oxidant added blends suggest that the metal oxide present in the blends accelerates the photodegradation of LLDPE. The reduction in tensile strength and the weight of all the samples after biodegradation in shake culture flask and after burial in soil for 4 months suggests that the blends are partially biodegradable. The infrared spectroscopic analyses and the scanning electron photomicrographs of LLDPE-g-MA-starch and LLDPE-g-MA-dextrin blends confirm the biodegradability of the blends in shake culture flask.

References

- [1] Scott G, In: Scott G, Gilead D (eds) Degradable Polymers Principles and Applications. Chapman and Hall, London, [1995].
- [2] Gilead D, Scott G, British Patent 1,586,344, [1978].
- [3] Gilead D, Scott G, In: Scott G (ed) Developments in polymer stabilization, Vol. 5. Applied Science, London, [1995], 71.
- [4] Gilead D, In: Scott G, Gilead D (eds) Degradable Polymers Principles and Applications. Chapman and Hall, London, [1995]

- [5] Griffin GJL, US Patent 40,16,117, [1997].
- [6] Griffin GJL, *Pure and Applied Chemistry*, 52, [1980], 399.
- [7] Bastioli, Catia, In: Scott G, Gilead D (eds) *Degradable Polymers Principles and Applications*, Chapman and Hall, London, [1980].
- [8] Evans JD, Sikdar SK, *Chemtech*, **20**, [1990], 38.
- [9] Johnson R, In: *Proceedings of symposium on Degradable Plastics*. Society of Plastics Industry, Washington DC, [1987], 6.
- [10] Villarreal N, Pastor JM, Perera R, Rosales C, Merino JC, *Macromolecular Chemistry and Physics*, **203(1)**, [2002], 238.
- [11] Guthrie J.T., *Surface Coatings International Part B: Coatings Transactions*, **85 (B1)**, [2002], 27.
- [12] Heinen W, Rosenmoler CH, Wenzel CB, Groot HJM, Lugtenburg J, *Macromolecules*, **29**, [1996], 1151.
- [13] Sailaja RRN, Chanda M, *Journal of Applied Polymer Science*, **80**, [2001], 863.
- [14] Sailaja RRN, Chanda M, *Journal of Polymer Materials*, **17**, [2000], 165.
- [15] Bikiaris D, Panayiotou C, *Journal of Applied Polymer Science*, **70**, [1998], 1503
- [16] Pierre NS, Davis BD, Ramsay BA, Verhoogt H, *Polymer*, **38**, [1997], 647.
- [17] Ojeda T, Dalmolin E, Forte M, Jacques R, Bento F, Camargo F., *Polymer Degradation and Stability*, **94**, [2009], 965.
- [18] Olabisi O, Robeson LM, Shaw MT, *Polymer – Polymer Miscibility*, Academic Press, New York, [1979].

- [19] Mohanty AK, Misra M, Hinrichsen G, *Macromolecular Materials and Engineering*, **266/277**, [2000], 1.
- [20] Paul DR, Newman S, *Polymer Blends*, Volume 1, Academic Press, New York, [1978].
- [21] Annual Book of ASTM Standards, D 570, **08.01**, [2004].
- [22] Albertsson AC, Benenstedt C, Karlsson S, *Journal of Applied Polymer Science*, **51**, [1994], 1097.
- [23] Carlsson DJ, Wiles DM, *Macromolecules*, **4**, [1971], 179.
- [24] Amin MU, Scott G, *European Polymer Journal*, **9**, [1973], 219.
- [25] Scott G., *Polymer Age*, **6**, [1975], 54.
- [26] Annual Book of ASTM Standards, D 6691, **08.03**, [2004].
- [27] Buchanan RE and Gibbons NE, *Bergey's Manual of Systematic Bacteriology* (Eighth edition), The Williams and Wilkins Co., Baltimore, [1974], 747.
- [28] Furniss BS, Hannaford AJ, Rogersm V, Smith PWG and Tatchell AR (eds), *Vogel's Textbook of Practical Organic Chemistry*, Longman publishing, England, **4**, [1978], 497.
- [29] Rutkowska M, Heimowska A, Krasowska K, Janik H, *Polish Journal of Environmental Studies*, **11**, [2002], 267.
- [30] Pratheep Kumar A, Jitendra K. Pandey, Bijendra Kumar, R. P. Singh, *Journal of Polymers and the Environment*, **14**, [2006], 203.

..........

The present study is an effort to investigate the biodegradability of linear low density polyethylene (LLDPE) in presence of the bio-fillers (starch and dextrin) using a shake culture flask containing amylase producing vibrios isolated from marine benthic environment and by soil burial test. Maleic anhydride grafting on LLDPE was used to improve the compatibility between the non-polar LLDPE and the polar bio-fillers. The role of metal oxides [iron oxide, manganese dioxide, titanium dioxide (rutile and anatase grades)] and metal stearate (cobalt stearate) as pro-oxidants to enhance the photodegradability of LLDPE was also studied by exposing the samples to ultraviolet light.

The mechanical properties of neat LLDPE, the LLDPE-biofiller blends, and the LLDPE-biofiller blends containing pro-oxidants suggest that the additives have no significant reinforcing effect on LLDPE. The grafting of maleic anhydride on LLDPE improves the compatibility between LLDPE and bio-fillers and improves the mechanical properties of the blends. Addition of pro-oxidants to the compatibilised blends reduces the tensile strength suggesting that the pro-oxidants do not reinforce the compatibilised blends.

The thermogravimetric analyses on all the blends indicate that the thermal stability of the blends are unaffected by the addition of the

bio-fillers and the pro-oxidants. The results of differential scanning calorimetry show that the percentage crystallinity of the neat LLDPE and the blends are almost similar suggesting that the LLDPE and the additives are incompatible to each other. The results of FTIR studies also support the incompatibility of LLDPE and the bio-fillers.

In the case of compatibilised blends the results of the differential scanning calorimetry show that the percentage crystallinity of LLDPE-g-MA-starch and LLDPE-g-MA-dextrin blends are lower than that of neat LLDPE as a result of grafting.

The samples after biodegradation in the shake culture flask containing amylase producing vibrios, which were isolated from marine benthic environment, and also after soil burial test for 4 months show reduction in tensile strength and loss of weight indicating that the blends are partially biodegradable.

A comparison of the scanning electron photomicrographs of the newly prepared blends containing bio-filler before and after biodegradation in shake culture flask confirm the biodegradability of the blends. The differences in the characteristic FTIR peak intensities of the blends before and after biodegradation in shake culture flask also reveal the biodegradation of the samples in presence of amylase producing vibrios.

The biodegradation of the samples prepared from LLDPE-biofiller blends containing pro-oxidants in shake culture flask and in soil for 4 months suggest that these blends show lower extent of

biodegradation as compared to the LLDPE-biofiller blends. The results show that the metal oxides used as pro-oxidants in this study adversely affect the biodegradation of LLDPE.

Photodegradability studies on samples of LLDPE, LLDPE-biofiller blends, and compatibilised blends with and without pro-oxidants by exposing the samples to ultraviolet light show that the pro-oxidants are effective in enhancing the rate of photodegradation.

All the blends show lower melt flow indices as compared to neat LLDPE apparently due to increased entanglement of the polymer chains and the additives. The water absorption values of the blends containing bio-filler were higher indicating the enhanced affinity of the blends for microbial attack as compared to neat LLDPE.

The reprocessability studies on LLDPE and the partially biodegradable blends investigated in this study suggest that the LLDPE and the blends are reprocessable without deterioration in mechanical properties.

Suggestion for further work

It is expected that the results of the present investigation will encourage research in the area of biodegradable and photodegradable polymers. There is ample scope for research into the use of these affordable polymers in commercial applications. Development of commercially acceptable compatibilised blends of popular commodity plastics such as polyethylenes and bio-fillers is another potential area for further research.

.....&OQ.....

List of Symbols and Abbreviations

ASTM	- American Society for Testing and Materials
C	- Carbon
Ca	- Calcium
cm	- Centimetre
cm ⁻¹	- Centimetre inverse
cm ³	- Cubic centimetre
CO ₂	- Carbon dioxide
C _p	- Heat flow rate
C-T	- Charge-Transfer
DCP	- Dicumyl peroxide
DSC	- Differential Scanning Calorimetry
DTG	- Derivative Thermogravimetry
EAA	- Poly(ethylene- <i>co</i> -acrylic acid)
ESC	- Environmental Stress Cracking
Fe	- Iron
FTIR	- Fourier Transform Infrared Spectroscopy
g/cm ³	- Gram per cubic centimeter
H	- Hydrogen
HDPE	- High Density Polythethylene
J/g	- Joules per gram
K	- Pottassium
kcal/mol	- Kilocalories per mol
KCl	- Pottassium chloride
kg	- Kilogram
kN	- Kilonewton
L	- Litre
LCB	- Long Chain Branching
LDPE	- Low Density Polythethylene

LLDPE	-	Linear Low Density Polythethylene
MA	-	Maleic Anhydride
MFI	-	Melt Flow Index
Mg	-	Magnesium
mg	-	Milligram
MgSO ₄	-	Magnesium sulphate
min	-	Minute
mL	-	Millilitre
mL/min	-	Millilitre per minute
mm	-	Millimetre
MPa	-	Mega Pascal
MWD	-	Molecular Weight Distribution
N	-	Nitrogen
NaCl	-	Sodium Chloride
nm	-	Nanometre
Nm	-	Newton meter
O	-	Oxygen
OD	-	Optical Density
P	-	Phosphorous
PE	-	Polyethylene
PEEK	-	Poly ether ether ketone
PP	-	Polypropylene
PTFE	-	Poly tetrafluoroethylene
PVA	-	Polyvinylalcohol
rpm	-	Rotations per minute
S	-	Sulphur
SEM	-	Scanning Electron Microscope
T _c	-	Crystallisation temperature
TCBS	-	Thiosulphate Citrate Bile salt Sucrose
TGA	-	Thermogravimetric Analysis
T _m	-	Melting Temperature

T_{\max}	-	Temperature at which maximum degradation occurs
UV	-	Ultraviolet
X	-	Crystallinity
α	-	Alpha
β	-	Beta
%	-	Percentage
ΔH_c	-	Heat of crystallisation
ΔH_f	-	Heat of fusion
$^{\circ}\text{C}$	-	Degree celcius
$^{\circ}\text{C}/\text{min}$	-	Degree celcius per minute
^{13}C	-	Carbon 13
4-MP-1	-	4-methyl-1-pentene

.....

A. LIST OF RESEARCH PAPERS PUBLISHED IN INTERNATIONAL JOURNALS

- 1) Effect of amylase producing vibrios from the benthic environment on the biodegradation of low density polyethylene-dextrin blends, **Anna Dilfi K. F.**, Zeena P. Hamza, Thomas Kurian and Saritha G. Bhat, *Polymer-Plastics Technology and Engineering*, 48 (6), 602-606, 2009.
- 2) Studies on biodegradability of linear low density polyethylene-dextrin blends using vibrios from benthic environment, Zeena P. Hamza, **Anna Dilfi K. F.**, Thomas Kurian and Saritha G. Bhat, *Progress in Rubber, Plastics and Recycling Technology*, 25 (3),129-139, 2009.
- 3) Biodegradability studies on LDPE-starch blends using amylase-producing vibrios, Zeena P. Hamza, **Anna Dilfi K. F.**, Thomas Kurian and Saritha G. Bhat, *International Journal of Polymeric Materials*, 58 (5), 257-266, 2009.
- 4) Biodegradability of LLDPE-starch blends using vibrios from benthic environment, **Anna Dilfi K. F.**, Zeena P. Hamza, Thomas Kurian and Saritha G. Bhat, *International Journal of Plastics Technology*, 12, 1021-1030, 2008.
- 5) Combined effect of bio-filler and pro-oxidant on the degradation of linear low density polyethylene, **Anna Dilfi K. F.**, Raghul Subin S., Thomas Kurian and Saritha G. Bhat, *Indian Journal of Engineering and Materials Sciences* (Communicated).
- 6) Effect of iron oxide on the photodegradation of linear low density polyethylene-dextrin blend, **Anna Dilfi K. F.**, Raghul Subin S., Thomas Kurian and Saritha G. Bhat, *International Journal of Materials Research* (Communicated).

- 7) Effect of maleation on the mechanical properties and biodegradation of linear low density polyethylene-starch blends, **Anna Dilfi K. F.**, Raghul Subin S., Thomas Kurian and Saritha G. Bhat, *International Journal of Polymeric Materials* (Communicated).

B. LIST OF RESEARCH PAPERS PRESENTED AT NATIONAL AND INTERNATIONAL CONFERENCES

- 1) Influence of starch on the mechanical properties, morphology and biodegradation of low density polyethylene, Zeena P. Hamza, Anna Dilfi K. F., Raghul Subin S., Thomas Kurian and Saritha G. Bhat, **Polycon-2011, 5th National Conference on Plastics & Rubber Technology (NCPRT)**, Sri Jayachamarajendra College of Engineering, Mysore, April 25-26, 2011.
- 2) Influence of dextrin on the tensile properties, morphology and biodegradation of low density polyethylene, Zeena P. Hamza, Anna Dilfi K. F., Raghul Subin S., Thomas Kurian and Saritha G. Bhat, **International Conference on Advancements in Polymeric Materials (APM 2011)**, CIPET, Chennai, March 25-27, 2011.
- 3) Dextrin filled low density polyethylene films: Mechanical properties, melt flow indices and water absorption, Zeena P. Hamza, Anna Dilfi K. F., Raghul Subin S., Thomas Kurian and Saritha G. Bhat, **International Conference on Materials for the Future**, Govt. Engineering College, Thrissur, Kerala, India, February 23-25, 2011.
- 4) Investigations on tapioca starch filled low density polyethylene films, Zeena P. Hamza, Anna Dilfi K. F., Raghul Subin S., Thomas Kurian and Saritha G. Bhat, **International Conference on Functional Polymers**, NIT Calicut, Kerala, India, January 28-30, 2011.

- 5) Biodegradation of environment-friendly low density polyethylene-dextrin blends, Zeena P. Hamza, Anna Dilfi K. F., Raghul Subin S., Thomas Kurian and Saritha G. Bhat, **International Conference on Polymer Science and Engineering: Emerging Dimensions**, Chandigarh, November 26-27, 2010.
- 6) Thermal properties of partially biodegradable LDPE/Dextrin blends, Zeena P. Hamza, Anna Dilfi K. F., Julie Jose, Raghul Subin S., Thomas Kurian and Saritha G. Bhat, **International Conference on Advances in Polymer Technology**, Kochi, India, February 26-27, 2010.
- 7) Partially biodegradable LLDPE-starch blends, Anna Dilfi K. F., Zeena P. Hamza, Raghul Subin S., Thomas Kurian and Saritha G. Bhat, **International Conference on Advances in Polymer Technology**, Kochi, India, February 26-27, 2010.
- 8) Thermal properties of partially biodegradable LDPE/Starch blends, Zeena P. Hamza, Anna Dilfi K. F., Julie Jose, Thomas Kurian and Saritha G. Bhat, **International Conference on Advancements in Polymeric Materials (APM '10)**, CIPET, Bhubaneswar, February 20-22, 2010.
- 9) Biodegradable Plastics based on Linear Low Density Polyethylene, Anna Dilfi K. F., Thomas Kurian, and Saritha G. Bhat, **Kerala Science Congress**, Peechi, Thrissur, January 28-31, 2010.
- 10) Mechanical, thermal and morphological studies on partially biodegradable LLDPE-dextrin blends*, Anna Dilfi K. F., Zeena P. Hamza, Julie Jose, Thomas Kurian and Saritha G. Bhat, **97th Indian Science Congress**, Thiruvananthapuram, India, January 3-7, 2010. (*Awarded the *BEST POSTER PRESENTATION AWARD* in the *Materials Science* section)

- 11) Role of benthic vibrios on the biodegradability of LLDPE, Anna Dilfi K. F., Zeena P. Hamza, Thomas Kurian and Saritha G. Bhat, **CHEMREFERENCE 09**, IIT Chennai, August 23-24, 2009.
- 12) Novel biodegradable plastics based on LDPE and LLDPE, Anna Dilfi K. F., Zeena P. Hamza, Thomas Kurian and Saritha G. Bhat, **POLYCHAR 16 World Forum on Advanced Materials**, Lucknow, India, February 17-21, 2008.

.....❧.....

RESUME

ANNA DILFI K. F.

Surya City
MIG-4, House No:110
Anekkal Road, Chandapura
Bangalore-560081
Karnataka
Ph: +91-8086479840
E-mail: anndilff@gmail.com



CARRIER OBJECTIVES

To build career in the research and development oriented activities, utilizing technological skills and awareness.

ACADEMIC QUALIFICATION

- M.Sc. Polymer Chemistry... (71.5%, May 2005, Mahatma Gandhi University, Kottayam)
- B.Sc. Chemistry... (80.4%, April 2003, Mahatma Gandhi University, Kottayam)
- HSC... (73.0%, May 2000, Board of Higher Secondary Education, Kerala State)
- S.S.L.C... (82.8%, March 1998, Board of Public Examinations, Kerala State)

PROJECT WORK DURING M.Sc.

Novel method for the preparation of exfoliable clay; Studies on the preparation and properties of clay-LDPE nanocomposites. (Done at Regional Research Laboratory, Trivandrum)

EXPERIENCE

1. Worked as trainee in the "Technical Consultancy Division" (Latex Wing) of Rubber Research Institute of India, Kottayam for 6 months, March-August 2006. During the training period I acquired:

- Experience in testing of medical gloves for Physical properties, Protein content & Powder content.
 - Experience in testing of Latex Foam & Adhesives.
 - Experiences in Compounding of NR Latex, Pre vulcanization & Dipping.
 - Experience in Operation of equipments like Tensile machine (Instron), UV Spectrophotometer, pH meter, MST tester, Brookfield Viscometer, etc.
2. Worked as Laboratory Assistant in the Department of Polymer Science and Rubber Technology for 10 months, October 2006-August 2007. During that period I acquired skills in operating sophisticated processing and testing equipments.

AWARDS AND HONOURS

Won BEST POSTER PRESENTATION AWARD in the Materials Science section in 97th Indian Science Congress held at Thiruvananthapuram during January 3-7, 2010.

PERSONAL DETAILS

▪ Father's name	:	K. M. Francis
▪ Mothers name	:	P. V. Sabeth
▪ Date of birth	:	30-05-1983
▪ Sex	:	Female
▪ Marital status	:	Married
▪ Husband's name	:	Rijo Mathew
▪ Languages Known	:	English, Malayalam, Hindi

REFERENCE

Dr. Thomas Kurian
Professor
Department of Polymer Science and Rubber Technology
Cochin University of Science and Technology
Kochi-22.
Tel: +91-484-2575723
Email: drtkurian@gmail.com

.....✍.....